

Georgia Institute of Technology
State Engineering Experiment Station
Atlanta, Georgia

FINAL REPORT
(No. 11)

PROJECT NO. 131-45

HIGH FREQUENCY CRYSTAL-CONTROLLED
OSCILLATOR CIRCUITS

By

WILLIAM A. EDSON,
WILLIAM T. CLARY,
JAMES C. HOGG, JR.

PREPARED FOR

U. S. ARMY, SIGNAL CORPS ENGINEERING LABORATORIES
FORT MONMOUTH, NEW JERSEY

CONTRACT NO. W36-039-sc-36841

DEPARTMENT OF THE ARMY PROJECT: 3-99-11-022
SIGNAL CORPS PROJECT: 142B

1 MAY 1948 to 31 DECEMBER 1950

APPROVED

Gerald A. Rosselot, Director
State Engineering Experiment Station

William A. Edson
Project Director

TABLE OF CONTENTS

PART ONE

	Page
I. INTRODUCTION	1
A. History of the Contract.	1
B. The Problem.	1
C. State of the Art in Spring of 1948	2
D. Objectives and Methods of Approach	2
E. Orientation and General Information.	5
II. QUARTZ CRYSTAL RESONATORS.	7
A. General Properties of Crystals	7
B. Types of Mounts.	7
C. Equivalent Circuit of a Quartz Resonator	9
D. Overtone Crystals.	14
E. Use of Inductance with Crystals.	16
III. BASIC MATERIAL ON OSCILLATOR CIRCUITS.	27
A. General Circuit Requirements	27
B. Nonlinear and U.H.F. Effects	34
C. Intermittent Oscillation	36
IV. CONVENTIONAL CRYSTAL OSCILLATORS	39
A. General Properties	39
B. The Pierce Circuit	39
C. The Miller Circuit	41
D. Loop Gain Considerations	41
E. Loop Gain in the Miller Oscillator	41
F. Loop Gain in the Pierce Oscillator	44
G. Frequency Stability of the Pierce Oscillator	45
H. Frequency Stability of the Miller Oscillator	47
V. SERIES-RESONANT CRYSTAL-CONTROLLED OSCILLATORS	49
A. Introduction	49
B. Circuit Arrangements	49
C. Advantages and Disadvantages of Series-Resonant Operation. . .	54

TABLE OF CONTENTS (CONTINUED)

	Page
VI. FREQUENCY STABILITY CONSIDERATIONS IN SERIES-MODE OSCILLATORS . . .	57
A. Introduction	57
B. Rate of Phase Change with Frequency for Crystal Series Arm Alone.	59
C. Effect of Shunt Resistance on the Rate of Change of Phase Shift of a Crystal Operated in the Series Mode	60
D. Crystal with Shunt Capacitance	63
E. Crystal Driven in the Series Mode Between Pure Resistance. . .	65
F. Crystal Driven by an Impedance Inverting Network	66
G. Effects of Capacity Variations on the Phase Shift of Impedance Inverting Networks	68
H. Effect of Capacity Variations on the Phase Shift of Transformer networks.	69
I. Evaluation of the Frequency Stability of Oscillator Circuits to Capacity Variations	70
VII. POWER CONSIDERATIONS IN CRYSTAL OSCILLATORS	73
A. Introduction	73
B. Everitt's Approximate Method of Nonlinear Calculation.	73
C. Relation Between Power Output and Power Dissipation in the Crystal.	86
VIII. NETWORKS FOR USE IN OSCILLATORS	98
A. Introduction	98
B. Wide-Band Low-Phase Two-Terminal Networks.	100
C. Synthesis of a Specified Phase Characteristic.	103
D. Four-Terminal Networks Having Low Transfer Phase Shifts. . . .	104
E. Four-Terminal Networks	106
F. Four-Terminal Transformer Networks Using Two-Terminal Phase Correctors	108
G. Low-Side Two-Terminal Phase Corrector.	109
H. High-Side Two-Terminal Phase Corrector	111
I. Phase Shift Due to Electron Transit Time	116

TABLE OF CONTENTS (CONTINUED)

PART TWO

	Page
IX. CATHODE-COUPLED OSCILLATOR	118
A. Introduction	118
B. Gain Requirements.	118
C. Phase Requirements	120
D. Crystal Operation and Compensation	122
E. Degradation of the Crystal Q	124
F. Range of Element Values.	125
G. Load and Power Considerations.	125
H. Experimental Data.	127
I. Advantage and Disadvantages.	128
X. THE TRANSFORMER-COUPLED OSCILLATOR	130
A. Introduction	130
B. Impedance Levels and Loop Gain Considerations.	130
C. Frequency Stability Considerations	133
D. Phase Considerations and Crystal Compensation.	135
E. Balance Between Tube and Crystal Capacitance	136
F. Design Procedure	137
G. Conclusions.	140
H. Typical Designs and Experimental Results	141
I. Advantages and Disadvantages	148
XI. THE GROUNDED-GRID OSCILLATOR	149
A. Introduction	149
B. Impedance Levels and Loop Gain Considerations.	149
C. Frequency Stability Considerations	153
D. Phase Considerations and Crystal Compensation.	160
E. Design Procedures and Experimental Results	163
F. Advantages and Disadvantages	174
XII. IMPEDANCE-INVERTING OSCILLATORS.	175
A. General Theory	175

TABLE OF CONTENTS (CONTINUED)

	Page
B. Impedance-Inverting Pierce Oscillator	177
C. The Miller Impedance Inverting Oscillator	182
D. Impedance Inverting Transitron Oscillator	185
E. Conclusions	188
XIII. THE GROUNDED-PLATE OSCILLATOR	189
A. Circuit Description	189
B. Linear Analysis	189
C. Analysis and Design of a Triode Grounded-Plate Oscillator . .	191
D. Analysis and Design of Class C Electron-Coupled Grounded-Plate Oscillator.	193
E. Conclusions	194
XIV. MULTIPLE FEEDBACK OSCILLATORS	195
A. Introduction.	195
B. Cathode-Degenerative Oscillator	195
C. Analysis.	195
D. Experimental Results.	199
E. Conclusions	200
XV. STABILIZATION OF A FREE-RUNNING OSCILLATOR.	201
A. Introduction.	201
B. Principles of Automatic Frequency Control	202
C. Quartz Crystal Discriminators	204
D. Control Circuits.	206
E. Experimental Work	207
F. Conclusions	208
XVI. MISCELLANEOUS OSCILLATOR CIRCUITS	210
A. Line-Coupled Oscillator	210
B. Parallel Mode Overtone Oscillator	213
C. The Negative Transconductance Oscillator.	215
XVII. ELECTRON COUPLING AND FREQUENCY MULTIPLICATION.	218
A. Introduction.	218
B. Cathode-Coupled Oscillator for Frequency Multiplication . . .	218

TABLE OF CONTENTS (CONTINUED)

	Page
C. Electron-Coupled Impedance-Inverting Pierce Oscillator . . .	220
D. Electron-Coupled Grounded-Screen Oscillator.	221
E. Conclusions.	223
XVIII. COMPONENTS AND ADJUSTMENT PROCEDURES	226
A. Components	226
B. Transformers	230
C. Layout	242
D. Adjustment Procedures.	242
XIX. CONCLUSIONS AND RECOMMENDATIONS.	247
A. Summary of Results Achieved.	247
B. State of the Art	247
C. Preferred Circuits and Their Properties.	248
D. Choice of Circuits	251
E. Remaining Problems	252
XX. IDENTIFICATION OF TECHNICIANS.	254
XXI. APPENDICES	256
A. Stability of Crystal-Controlled Oscillators Methods of Determining.	256
B. Conservation of Band Width and Low Pass to Band Pass Transformation.	259

LIST OF SYMBOLS

- A = Magnitude of self or transfer impedance.
B = Phase angle of self or transfer impedance.
C = Capacitance.
 C_o = Holder capacitance of crystal.
 C_1 = Series arm capacitance of crystal.
 C_n = Input capacitance of amplifier.
D = Q degradation factor.
E = E.M.F.
F = Function of coil diameter to length ratio.
G = Power gain.
 G_p = Power gain of grounded-plate amplifier.
 G_k = Power gain of grounded-cathode amplifier.
 G_g = Power gain of grounded-grid amplifier.
I = Peak value of current.
K = A constant.
L = Inductance.
 L_1 = Inductance of crystal series arm.
M = Mutual inductance.
N = Transformer voltage ratio.
P = Power.
 P_n = Input power.
 P_L = Useful output power.
 P_x = Power dissipated in crystal.
Q = Quality factor of resonator.
R = Resistance.
 R_1 = Series arm resistance of crystal.
 R_g = Grid leak resistance.
 R_L = Load resistance.
 R_x = Input resistance of impedance-inverting network.
 S_f = Frequency stability of circuit.
 S_r = Frequency stability of resonator.

LIST OF SYMBOLS

- V - Voltage.
X - Reactance.
Y - Admittance.
Z - Impedance.
 Z_o - Characteristic impedance.
d - Mean diameter of inductor winding.
e - Total instantaneous voltage.
f - Frequency (cycles per second).
 g_m - Transconductance of vacuum tube.
h - Excitation ratio.
i - Total instantaneous current.
k - Coefficient of coupling.
 λ - Length.
n - Transformer turns ratio.
r - Capacitance ratio of crystal (C_o/C_1).
 r_g - Positive grid resistance of vacuum tube.
 r_p - Dynamic plate resistance of vacuum tube.
 β_p - Function of plate conduction angle.
 β_g - Function of grid conduction angle.
 Δf - Frequency deviation.
 e - 2.71828... Base of natural logarithms.
 θ_p - Half angle of plate conduction.
 θ_g - Half angle of grid conduction.
 μ - Amplification factor.
 μ - Prefix micro.
 π - 3.1416...
 ϕ^2 - Impedance ratio of ideal transformer.
 ω - Angular frequency.
 ω_o - Resonant frequency of crystal series arm ($1/\sqrt{L_1 C_1}$)
 ω_r - Series resonant frequency of crystal.
 ω_a - Antiresonant frequency of crystal.

PURPOSE

The purpose of this work was to investigate the operation and fundamental limitations of oscillator circuits for use with high-frequency quartz crystals, with a view to developing circuits having improved characteristics. Because existing information on crystal oscillator circuits in general, and high-frequency crystal oscillator circuits in particular, was widely scattered, part of the problem was to collect, integrate, and evaluate this material.

In typical situations the engineer who is faced with the problems of designing an oscillator for a particular application has no time for research, and little familiarity with oscillator theory; one objective of the work was to develop simple rules for choosing a tube and circuit for a particular application and for adjusting the circuit to give the desired performance.

ABSTRACT

This report presents the results of an extended investigation of the properties and limitations of oscillator circuits for the operation of high-frequency quartz crystal resonators. The frequency region of principal interest is 50 to 150 Mc, but most of the results are applicable with minor variation at lower frequencies, and some of the circuits are capable of operation at somewhat higher frequencies.

The present report includes everything of importance which appeared in the ten previous progress reports; and coordinates many topics which previously appeared isolated or detached. Moreover, it presents a considerable amount of new and useful material. Because the existing literature on crystal oscillators is somewhat scattered, the present report includes several sections devoted to an orderly presentation of old material. It is believed that the inclusion of this material adds to the usefulness of the document.

The first portion of the report is general in nature and presents background information applicable to all types of circuits and in all frequency ranges. The latter portion of the report is much more specific. It discusses the properties, advantages, and limitations of the more important circuits, and presents criteria for selecting a circuit and adjusting the elements so as to realize the design conditions.

I INTRODUCTION

A. History of the Contract.

This project, entitled "High Frequency Crystal-Controlled Oscillator Circuits", was sponsored by the Signal Corps, U. S. Army, through the Squier Signal Laboratories, Fort Monmouth, New Jersey. The initial contract, numbered W36-039-sc-36841, for the period 1 May, 1948 through the 28 February, 1949, was signed and forwarded to this station on 10 June, 1948. The number 131-45 was assigned to this project by the Georgia Institute of Technology.

Two extensions of the initial contract were granted. The first covered the ten month period, 1 March, 1949 through 31 December, 1949; the second covered the twelve month period, 1 January, 1950 through 31 December, 1950.

B. The Problem.

The expanded requirements of the Armed Forces necessitate a more efficient use of the available high frequency spectrum with channel bandwidths as small as possible. The required bandwidth of a communication channel is largely dependent on the frequency stability of the transmitter. Thus, the desirability of frequency control by crystals is evident. In the past, satisfactory operation at high frequencies has been achieved by multiplying the output of a low-frequency crystal controlled oscillator. This method does provide a high degree of frequency stability but, from the standpoint of overall efficiency and conservation of space, direct crystal control of the transmitter frequency is preferred. Moreover, in military equipment, it is particularly desirable that the number of adjustments required during operation be reduced to a minimum. In communication equipment where frequency changes are required, the number of associated adjustments must be minimized. In the oscillator itself, the crystal at least must be changed, and it is desirable that no other change in this circuit should be necessary. At low and moderate frequencies, the Pierce oscillator provides this type of operation. One objective of this project was to find a counterpart of the Pierce oscillator to operate satisfactorily at high frequencies. The broad-band untuned oscillators, described in later chapters of this report, were found to be the satisfactory counterparts.

C. State of the Art in Spring of 1948.

As part of the initial work on this project, a thorough search of the existing literature was made. This search was directed toward accumulating and evaluating information pertinent to the direct crystal control of high frequency oscillators. It was found that few authors have treated this subject.

Three papers that reflect the state of the art at the beginning of this project are listed in the Bibliography at the end of this chapter. The first of these, by Mason and Fair¹, describes a crystal-controlled oscillator capable of operating at 197 megacycles using the 23rd overtone of an AT-cut crystal, and experimental evidence is given to show that at 130 megacycles the fractional stability is comparable to that of ordinary crystal oscillators. The circuits described utilize a capacitance-bridge network to balance out the shunt capacity of the resonator in order to provide a purely resistive coupling. In addition, this paper presents a good survey of the properties of high frequency crystals with particular reference to overtone operation. The favorable performance of these circuits is partly attributed to the excellence the resonators used.

The second paper, by Goldberg and Crosby², describes a cathode-coupled oscillator which operates at 118 megacycles using the 11th overtone of a crystal. Various factors which influence frequency stability are considered, and it is concluded that broad-band, or low Q, circuits external to the resonator are desirable. Many variations of the cathode-coupled oscillator are presented, but little detailed design information is given.

The third paper, by Butler³, describes three basic circuits which are variations of the familiar Hartley oscillator. Although all the experimental work presented was done below 10 megacycles, at least two of the circuits can be used at higher frequencies: the grounded-grid and grounded-plate oscillators. This paper is concerned largely with series-resonant operation at the fundamental frequency to achieve a higher degree of frequency stability.

D. Objectives and Methods of Approach.

The principal objective of this study was the evaluation of the factors relating the frequency of an oscillator to the overtone-shear vibrations of a

quartz resonator.

In any given oscillator it may be assumed that the operating frequency is, to some extent, a function of the value of every circuit element. Thus, the maintenance of a precisely constant operating frequency requires that all circuit elements remain constant or vary in such a manner that equal and opposing tendencies toward frequency change are produced. In practice, it is not possible to maintain ordinary circuit elements constant over a wide range of temperature, humidity, etc. Where a constant frequency is desired, quartz resonators which may be made highly stable with respect to these factors, are used. Therefore, it is necessary to investigate circuit arrangements which will minimize the effect of uncontrolled variations on the frequency of crystal-controlled oscillators by utilizing the high intrinsic stability of the quartz resonator.

In the present study the circuit frequency stability is defined in terms of loop phase shift, as the rate of change of phase shift with frequency. The various methods of driving the resonator are compared by using as a reference the rate of phase change of the series-arm self-impedance of the crystal. Since this latter quantity is directly proportional to the intrinsic Q of the crystal, the comparison may be expressed as the ratio of the resonator Q alone to that of the resonator and associated circuit elements. For all circuits considered in this report, this ratio exceeds one which indicates that, with regard to frequency stability, the performance of the resonator is degraded by its association with the circuit.

While this ratio indicates quantitatively the degree to which the inherent stability of the resonator is utilized, it alone is not sufficient to specify completely desirable network configurations. Therefore, further analysis is necessary. In particular, it is desirable to know the frequency change which will result from a change in a given circuit element. Since one of the major causes of short-term frequency instability is due to capacity variations, the rate of phase shift with capacity is determined for various network configurations. This is then combined with the previously developed rate of phase change with frequency for the corresponding networks to give the rate of frequency change with capacity. By choosing the network elements so as to minimize this latter rate, good frequency stability with respect to capacity variations

may be obtained.

Available quartz resonators suitable for use in high frequency oscillators have fundamental frequencies up to about 20 Mc and operate at mechanical overtones of the thickness-shear mode. These units are necessarily quite thin and can not dissipate power in excess of about 0.1 watt without suffering damage or permanent frequency change. In fact, experience on a somewhat limited number of resonators indicates that dissipation should be kept below 0.05 watt if the best frequency stability is to be obtained. The low power-handling capability of overtone crystals results in much lower useful power outputs than are commonly obtained for crystal oscillators at low frequencies.

The suitability of a circuit for use as a power oscillator may be studied in terms of the ratio of its useful power output to the power dissipated in the crystal. Expressions for this ratio are developed for each circuit considered in this report. These expressions are similar in form and show that the power output may be increased by using tubes and circuit configurations which give high values of power gain, and by increasing the amount by which the Q of the resonator is degraded by the circuit. If the latter method of increasing the power output is used, the frequency stability of the oscillator is reduced. In practice, however, power output up to about two watts may be obtained from a single-tube circuit with only a moderate sacrifice in frequency stability.

If an oscillator is to be capable of operating over a broad band of frequencies by simply changing the resonator, and without recourse to retuning, the circuit must have low loop phase shift external to the resonator. The loop gain, including the resonator loss, must also exceed one over the desired band of frequencies. In operation, the crystal must correct for the circuit phase shift so as to reduce the total loop phase to zero; therefore, the amount of phase shift for which the crystal can correct without excessive frequency shift sets a limit on the allowable phase shift of the circuit alone.

In practice, phase shift results from finite electron transit time in the vacuum tube, and from unavoidable or necessary reactive elements in the

circuit. Transit-time phase shift is directly proportional to frequency; in tubes designed for use at high frequencies this constant of proportionality is small. Therefore, if the fractional bandwidth is not too great, this phase shift may be assumed to be constant over the band of interest and may be corrected for by using simple networks which do not seriously alter the circuit impedance levels. Correction for the phase shift due to the reactive elements, however, is considerably more difficult. The performance of networks for oscillators is limited primarily by parasitic capacitance in the same manner as for broad-band amplifiers, with the important added restriction that the phase shift be nearly zero or 360° throughout the band of interest. In this report both two-terminal and four-terminal networks are considered, and, design procedures based on network synthesis and inspection of available curves of impedance and phase angle are discussed.

E. Orientation and General Information.

Part One of this report presents background information and theoretical developments used in the analysis and design of various oscillator circuits which are considered in this report. Since some of the readers of this report, while technically trained, may not be familiar with the vocabulary and analytical details employed in oscillator work, a chapter covering basic material on oscillator circuits is included. This chapter is intended to present a compact summary of material obtained from a number of sources.

While no effort has been made to obtain high-frequency operation using conventional crystal controlled oscillators, a review of the characteristics of these circuits is appropriate to provide a point of departure for the discussion of less familiar arrangements. Also, as is shown later, some of the same equations may be applied to both conventional and overtone oscillators. This study is also important because a whole class of high frequency oscillators, the impedance inverting circuits, may be treated in essentially the same manner as conventional oscillators.

Part Two of this report describes the detailed analysis and design of oscillators. Experimental results are presented for each type of circuit, and consideration is given to those factors which influence power output and frequency stability. Since the units were constructed primarily to test the

validity of the design procedure, adjustments were limited to those required to assure the realization of the design conditions. In most cases this resulted in performance agreeing quite closely with that predicted by theory. Commercially available miniature tubes and components were used in all experimental work, and the requirements of good engineering practice were observed in the construction of circuits. In most of the circuits investigated, it was desirable to minimize shunt capacity, so permeability-tuned coils and transformers were used.

Type CR-23/U crystal units and similar units which were supplied by various companies engaged in crystal manufacture and development, were used in all experimental work. These units are designed to operate at particular orders of overtone; however, use was made of other overtones in order to obtain a more complete frequency coverage with available resonators. Although this procedure is not recommended for general use, it was found to be satisfactory for experimental purposes.

In the course of this project, considerable experience was obtained on the construction and adjustment of oscillator circuits, and it is believed that the inclusion of practical information on this subject is justified. Groups of oscillator circuits may be adjusted by similar procedures. Material concerning adjustment is collected for reference in Chapter XVIII. The equipment used in all adjustment procedures is commercially available, and the recommended procedures are sufficiently simple to be suitable for use by moderately skilled personnel.

BIBLIOGRAPHY

1. Mason, W. P. and Fair, I. E., "A New Direct Crystal-Controlled Oscillator for Ultra-Short-Wave Frequencies." Proc. I. R. E., 30, Oct., (1942).
2. Goldberg, H., and Crosby, E. L., "Series Mode Crystal Circuits." Tel-Tech, 1, No. 5, (1948).
3. Butler, F., "Series Resonant Crystal Oscillators," Wireless Engineer 23, June (1946).

II QUARTZ CRYSTAL RESONATORS

A. General Properties of Crystals.

The frequency stability of an oscillator can not be superior to that of the frequency determining element or resonator; it approaches that of the resonator only if the latter has a high value of selectivity Q. In electronic equipment for military applications, excellent frequency stability must be maintained over long intervals of time and in spite of adverse operating conditions. At the present time, no practical resonator is known which is superior to the quartz crystal resonator which employs the piezoelectric effect to control electric oscillations by means of mechanical vibrations.

The properties of quartz which make it so admirably suited for use as a electromechanical resonator are a high degree of secular stability, fairly high piezoelectric coefficient, high stability of elastic coefficients, and mechanical dimensions with respect to temperature and its low internal viscosity. Also, some of the elastic constants of quartz are positive while others are negative; therefore, the temperature coefficient of frequency may be either positive, negative, or zero according to the orientation of the crystal plate, the shape of the plate, and the mode of oscillation. These properties, along with good mechanical strength, permit the construction of a wide variety of quartz resonators suitable for the range from several kilocycles per second to above one hundred megacycles per second.

Although certain synthetic crystals such as ammonium dihydrogen phosphate (ADP), ethylene diamine tartrate (EDT) and barium titanate have properties which make them useful in electro-mechanical transducers and wave filters,¹ they are substantially inferior to quartz for the precise control of frequency. They are therefore ignored in the following discussions.

B. Types of Mounts.

A complete resonator consists of the quartz plate and its associated mount. The functions of the mount are to support the plate in such a manner that it will be protected from vibrations and mechanical shock, to provide electrical connection to the driving source, and to protect the crystal from

dust and corrosion. In a good design², these functions are accomplished with a minimum disturbing effect on the inherent characteristics of the quartz plate.

In all known types of mechanical vibration, there are nodal points on the crystal surface where no motion occurs. An obvious type of mounting is, therefore, one which clamps the crystal at these points for mechanical support, and utilizes a conductive plating on the surface of the crystal for the electrodes. Since the area of the nodes is small compared to the total area of the crystal, this type of mount has been used only at relatively low frequencies with plates which vibrate in extensional or face-shear modes. A mount of this type, as used with GT, CT, and DT crystals, is shown in Figure 2.1.

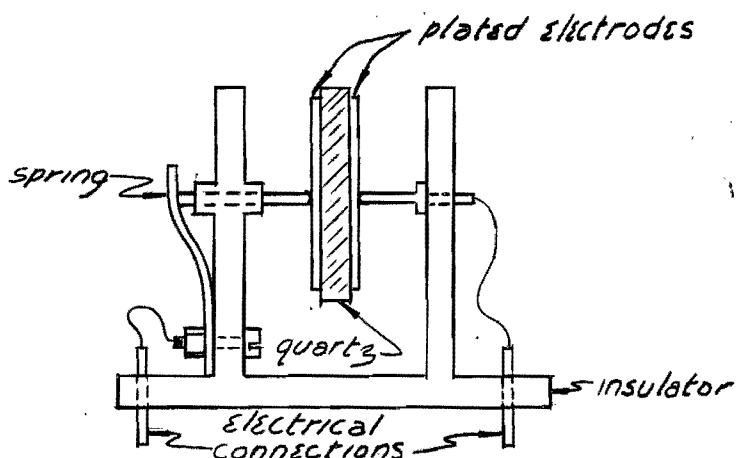


Figure 2.1 - Clamp Type Mount

The simple clamp mount just described is unsuitable for use with high frequency AT or BT type crystals, which vibrate in thickness shear. For plates of this kind, the air gap mounting shown in Figure 2.2 is appropriate.

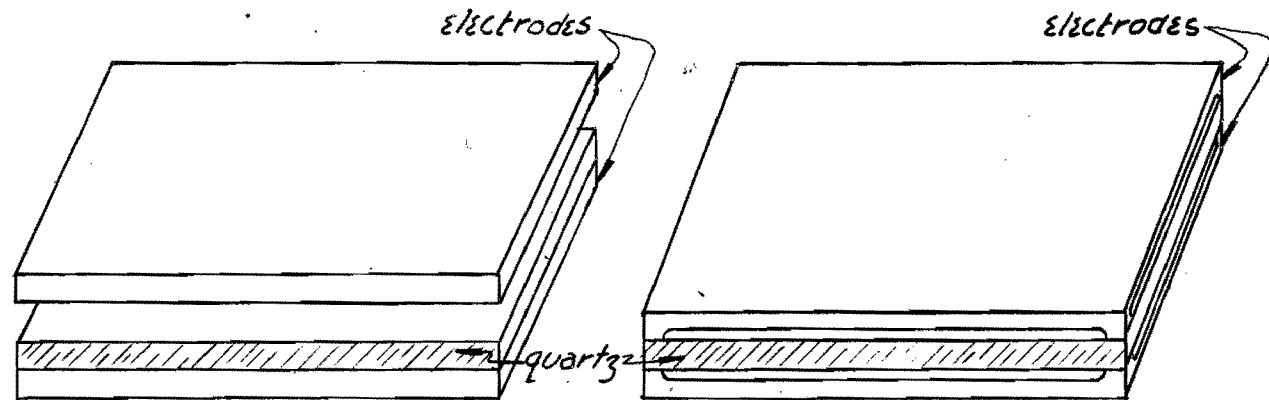


Figure 2.2 - Air Gap Type Mounting

In crystals designed for frequencies upwards of about 3 Mc, the thickness of the plate is so small compared to the other dimensions that the vibration is not appreciably affected if the corners are clamped, as shown in Figure 2.2b. Such clamping is desirable because it minimizes the effect of external shock and because it reduces the effect of many unwanted modes of vibration. For crystals in which the length to thickness ratio is less than about 20, clamping interferes excessively with the desired vibration, and the unrestricted mounting of Figure 2.2a is preferred.

Because the air gap mounting is somewhat bulky, the wire-mounted plated-crystal construction shown in Figure 2.3 has become nearly universal.

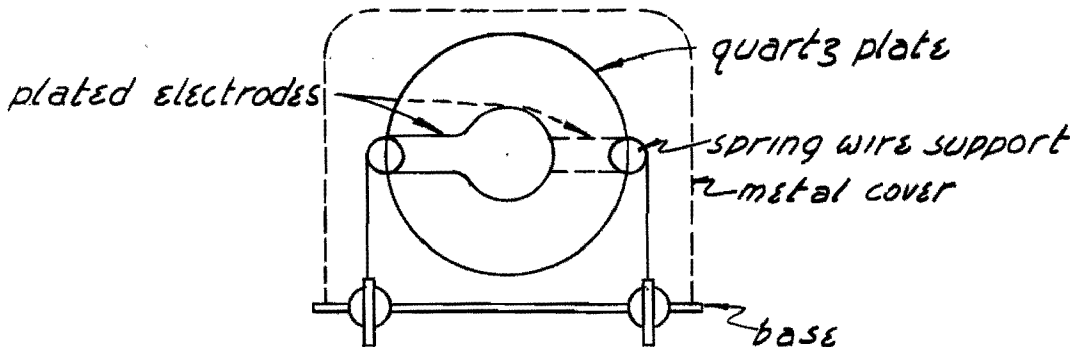


Figure 2.3 - Wire Mounted Crystal, Type HC-6 Holder

The support wires have spring clips which grip the edges of the quartz plate, and are electrically bonded to the plated electrodes by means of conducting paste or solder. Since the electrodes overlap only at the center of the plate, the tendency to produce spurious responses is reduced. Connection to the external circuit is made through metal-to-glass seals, and the metal cover is soldered to the base to produce a hermetically sealed unit.

Resonators using this type of mount are now constructed with fundamental frequencies from about 1 to 30 Mc, and work is being done to extend both limits³. By operating these resonators at overtone frequencies, direct crystal control may be obtained at frequencies well above 100 Mc.

C. Equivalent Circuit of a Quartz Resonator.

The electrical equivalent of a quartz resonator with plated electrodes

is shown in Figure 2.4. Circuits of this type were first developed by Van Dyke⁴ some time after crystals were used to control the frequency of oscillators.

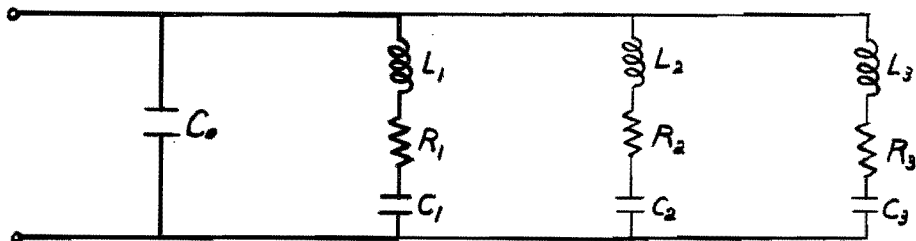


Figure 2.4 - Equivalent Circuit of a Quartz Resonator
With Plated Electrodes

In Figure 2.4, the portion of the circuit in heavy lines represents the principal response, and is all that need be considered in most cases. The other elements represent spurious responses, which are relatively small in the units of present interest. These responses may be due to coupling with overtones of various low frequency modes, or to manufacturing deviations which result in irregular dimensions or electrical properties. In either case, it is possible for two responses of about equal amplitude to occur in such a narrow frequency range that minor changes in the oscillator circuit external to the resonator will cause the frequency to shift from one response to another. This, of course, makes the resonator useless for precise frequency control. Good design requires that all spurious modes be separated in frequency from the desired response, and it is desirable that their action be well damped.

The parameters L_1 , R_1 , and C_1 , associated with the principal response, represent respectively the mass, the internal and mounting losses, and the stiffness of the crystal transformed into electrical terms by the piezoelectric properties of the quartz. The shunt capacity, C_o , represents the static capacity of the resonator, which may be measured at a frequency differing somewhat from any of the mechanical response frequencies. For quartz, values of L_1 vary from about 0.1 henry for high frequency crystals, to 100 henries for low frequency crystals. Correspondingly, values of C_1 range from about one thousandth to about one tenth of a micromicrofarad. Because the value of R_1 is normally relatively low, very high values of selectivity are obtained. It

is this property which allows quartz resonators to perform so well as frequency controlling elements and in selective filters. Commonly, the ratio of $\omega L_1/R_1$ exceeds ten thousand in commercial units, and a value of 6×10^6 has been obtained under laboratory conditions¹.

For resonators using the air gap type of mounting, the equivalent circuit of Figure 2.5a is applicable. In this circuit, C_a represents the series capacitance due to the separation of the quartz from the electrodes.

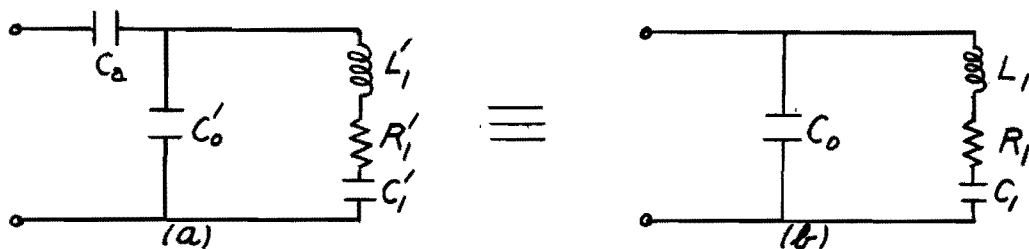


Figure 2.5 - Equivalent Circuit of Air Gap Mounted Crystal

For simplicity in analysis, this circuit, in which only a single response is considered, may be reduced to that of Figure 2.5b by using the following expressions⁵:

$$C_o/C_o' = C_a/(C_a + C_o') \quad (2.1)$$

$$C_1/C_1' = C_a^2/(C_a + C_o')(C_a + C_1' + C_o') \quad (2.2)$$

$$L_1/L_1' = R_1/R_1' = (C_o' + C_a)^2/C_a^2 \quad (2.3)$$

From these equations, it is seen that the principal effects of the air gap are to increase the impedance level of the resonator without affecting the selectivity, and to increase the ratio of the holder to crystal capacity.

Considering only the main response of the resonator, the reactance versus frequency characteristic has the general form shown in Figure 2.6.

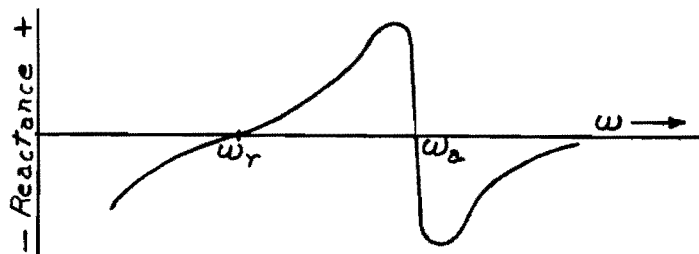


Figure 2.6 - Reactance Frequency Characteristic of Quartz Resonator

Conditions of zero reactance and respectively low and high resistance are obtained at the two frequencies ω_r and ω_a . The first is commonly known as series resonance, and the second as parallel resonance. The operating frequency will normally lie between ω_r and ω_a because conventional oscillator circuits require the crystal to exhibit an inductive reactance. Due to the high ratio of C_0 to C_1 , the separation between these two frequencies is only a fraction of one per cent. It is this rapidly varying reactance characteristic that makes the quartz resonator such an excellent frequency stabilizing element.

A more complete picture of the resonator performance may be had by the use of an admittance diagram⁵, such as that of Figure 2.7. It is well known that the plot of the admittance versus frequency of a series R, L, and C circuit results in a circle having a radius of $1/2R$ with its center on the real axis $1/2R$ units from the origin. If the susceptance of a shunt capacitor is added to this circle, the admittance of the resonator as a whole is obtained. Since the R_1 , L_1 , C_1 branch has a very high Q, the susceptance of the shunt capacity may be considered to be constant over the frequency range of interest.

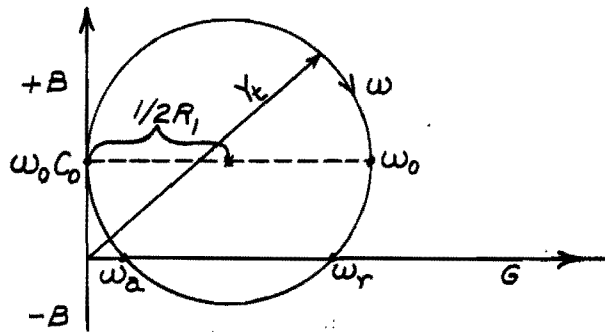


Figure 2.7 - Admittance Diagram of Quartz Resonator

In Figure 2.7, the total admittance of the resonator is Y_t , and the frequency scale on the circle increases in a clockwise direction. There are three frequencies of particular interest. The first, ω_0 , is given by

$$\omega_0^2 = 1 / L_1 C_1 \quad (2.4)$$

and is the resonant frequency of the series arm of the resonator. At this frequency, the resonator appears as a low resistance, R_1 , shunted by the

holder capacity C_o .

The second frequency at which the resonator appears as a pure low resistance is, as shown by Cady⁵, given to a close approximation by

$$\omega_r^2 = \frac{1}{L_1 C_1} + \frac{R_1^2 C_o}{L_1^2 C_1}. \quad (2.5)$$

The frequency given by this expression differs very slightly from ω_o , and is commonly called the series resonant frequency of the resonator. For many applications which use the resonator as a low impedance element, the frequency difference between ω_o and ω_r is insignificant. However, if $\omega_o C_o$ is nearly as large as $1/R_1$, the admittance at these two frequencies will be significantly different.

The frequency ω_a , at which the resonator appears as a pure high resistance, is known as the parallel resonant frequency. It may be seen from Figure 2.7 that the value of this frequency for a given quartz plate decreases as the shunt capacity is increased. The magnitude of the parallel resonant resistance, in conjunction with the capacity which the crystal faces, is referred to as the Performance Index (P.I.), which is a very useful design parameter.

If it is considered for the moment that the value of R_1 is so small that it may be neglected, the value of the reactance of the series arm at ω_a is given by $\omega_a L_1 - 1/\omega_a C_1$. Since this is equal in magnitude to the reactance of the shunt capacity as shown in Figure 2.7, the following expression is valid:

$$\omega_a L_1 - 1/\omega_a C_1 = 1/\omega_a C_o. \quad (2.6)$$

Defining the capacitance ratio r as

$$r = C_o/C_1, \quad (2.7)$$

and combining 2.6 and 2.7 we have

$$\omega_a^2 = (r + 1)/L_1 C_1 \doteq \omega_o^2(1 + 1/2r)^2. \quad (2.8)$$

One of the properties of quartz is that each type of cut has a fixed value of r , of which the smallest obtainable value is 125. Using this value

of r in equation 2.8, the ratio ω_a/ω_0 is found to be 1.004. This is the largest ratio that may be obtained in quartz. For the AT cut which is commonly used for high frequencies, r equals 200, and ω_a/ω_0 has a still smaller ratio of 1.0025. Because the intrinsic shunt capacitance of the crystal is always considerably increased by the holder and circuit, the actual value of r is usually in excess of 1000, and the ratio ω_a/ω_0 is less than 1.0005.

Since most of the conventional oscillator circuits operate with the resonator inductive, it is important to examine the resonator characteristics to determine under what conditions it is possible to obtain this type of performance. From Figure 2.7, it is seen that if $\omega_0 C_0$ is made equal to $1/2R$, the circle is tangent to the real axis, and no inductive susceptance is possible. From this condition and the definition of Q below

$$Q = \omega_0 L_1 / R_1 = 1 / \omega_0 C_0 R_1 , \quad (2.9)$$

the following is obtained as the limiting condition

$$r = C_0 / C_1 = Q/2 . \quad (2.10)$$

Therefore, if the resonator is to exhibit an inductive susceptance, the following inequality must be satisfied:

$$r < Q/2 . \quad (2.11)$$

Since in a physical circuit, the resonator must face some capacity in addition to its holder capacity, and from stability considerations, this capacity must be fairly large, the intrinsic r must be from two to ten times smaller than the maximum value specified by equation 2.11.

D. Overtone Crystals.

At the present time, it is impractical to produce crystals having a fundamental frequency in excess of about 30 Mc; and frequencies of this order are universally obtained by use of thickness shear vibration in an AT or BT plate. Of these, the AT has a substantially better temperature characteristic, but the BT has a 54 per cent higher frequency for a given thickness. For a thickness of $0.005'' = 0.0127$ cm, an AT plate has a frequency of 13.0 Mc, and a BT plate has a frequency of 20.1 Mc.

Still higher frequencies may be obtained by operating AT or BT plates

on mechanical overtones of the fundamental thickness shear mode. This is desirable, not only because the arrangement is simpler than those which employ electrical frequency multipliers, but also because it is free from other frequencies inevitably produced in the alternative arrangement. Although the crystal is capable of vibrating in all orders of overtones, only the odd orders may be excited by piezoelectric action. Therefore, the frequencies that may be obtained from a given crystal are very nearly equal to the odd multiples of the fundamental frequency. However, the departure of the overtone frequencies from exact integral relationship to the fundamental may be in the order of 0.1 per cent. For this reason, the resonator must be constructed for a specific overtone if an exact operating frequency is required.

For analytical purposes, the equivalent circuit of the resonator operated in a harmonic mode has the same form as Figure 2.4, but the element values must be modified. In general, the capacitance ratio(r) will increase as the square of the order of overtone, and the inductance of the series arm will remain substantially constant. Data by Mason and Fair⁶ indicate that in carefully prepared resonators the increase in R_1 with order of overtone is less than proportional. Since the reactance of the series arm is directly proportional to the order of overtone, the Q of these resonators was found to increase. However, for resonators typical of production units, the increase in R_1 is generally greater than proportional, resulting in a reduced Q . This fact has been verified by measurements made at this project and by other investigators³. Because of the reduction in Q , and the increase in capacitance ratio, the resonator is not capable of exhibiting an inductive reactance at the higher overtones, and is not satisfactory for use in circuits such as the Miller and Pierce. For these reasons, the series mode of operation is favored for high frequencies.

In addition to the above effects, an increase in the order of overtone is usually accompanied by an increase in the number of spurious responses located near the main response. These responses increase the difficulty of circuit tuning and result in a tendency for the frequency to shift from one value to another with slight changes in circuit constants. By carefully

controlling the flatness of the quartz plate, it is possible to obtain resonators that may be operated as high as the 23rd overtone. However, few of the units used on this project perform satisfactorily above the 11th overtone, and good operation is usually obtained only up to the 7th or 9th.

Another factor which, particularly when accompanied with spurious response near the main response, may seriously degrade the performance of the resonator is the ohmic resistance of the plated electrodes. To a first order approximation, this resistance (R_f) may be represented as in Figure 2.8.

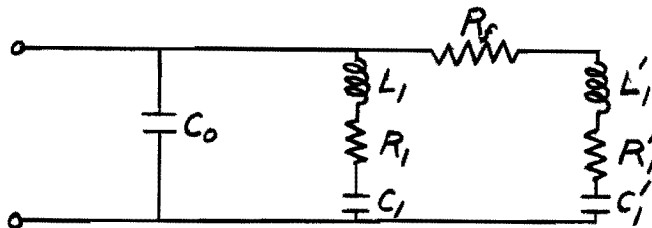


Figure 2.8 - Equivalent Circuit of Quartz Resonator
With Appreciable Losses in the Plated Electrodes

If the frequency of the spurious response is near that of the principal response, circulating currents will flow through R_f , thus increasing the resonator losses. It is not feasible to decrease the magnitude of R_f by increasing the thickness of the plated electrodes, because the added mass tends to load the vibrating crystal and reduce its Q. It does appear, however, that by using the air gap type of mount with the supports made of some stable non-conducting material, the electrodes may be plated on the mount in sufficient thickness to reduce this resistance to a negligible value. This type of mount has been investigated by R.C.A.³ and Philco⁷.

E. Use of Inductance With Crystals.

The shunt capacity (C_o) of the resonator plays an important part in the operation of oscillators at frequencies above 100 Mc. At these frequencies, the admittance of the shunt capacity becomes comparable to the maximum admittance of the series arm, and compensation of the shunt capacity is necessary if reliable crystal control is to be obtained. At frequencies up to 150 Mc, satisfactory compensation has been achieved by shunting the

resonator with a coil (L_o) which antiresonates the holder capacitance at the operating frequency. This results in negligible transmission through the shunt capacity, and allows the series arm to control the frequency of oscillation. The Q of this antiresonant circuit is lowered, usually by shunting the coil with an appropriate resistor, so that its maximum impedance is from five to ten times the value of R_1 . The presence of the shunting resistor simplifies the adjustment of L_o and permits operation over a substantial band of frequencies.

In a typical crystal, the resistance R_1 increases with the order of overtone, whereas, the reactance of the shunt capacity decreases. Therefore, the Q required of the compensating circuit increases rapidly with the order of overtone to the point where satisfactory operation is difficult to obtain. This situation is made worse by the presence of losses in the crystal mounting. These are represented by R_o in Figure 2.9.

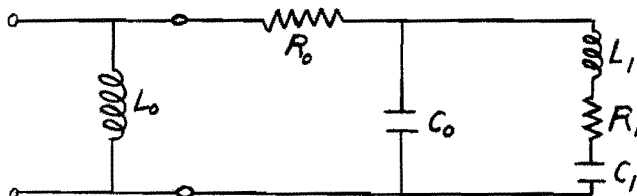


Figure 2.9 - Compensated Crystal
with
Appreciable Lead or Electrode Losses

Because the terminals connected directly to C_o are inaccessible, the Q of the compensating circuit is degraded by R_o . Moreover, the series arm of the resonator is no longer effectively connected to the terminals.

Measurements made on typical crystals from stock show values of R_o between 6 and 15 ohms at frequencies near 150 Mc. These measurements were made on a high frequency Q-Meter, at frequencies far from the resonant frequencies of the crystal. Other measurements on holders with the quartz removed indicate that about half the value of R_o is contributed by the pins and support wires, the remaining half being contributed by the soldered connections, and the plated surfaces of the crystal.

It is concluded that crystals designed for operation at very high

frequencies must have low values of R_o , as well as low values of R_1 and C_o . Properly constructed air gap type pressure mountings are likely to lead to this result.

Because there is considerable design information and a wide background of experience available on oscillator circuits which operate the resonator in the parallel mode, it is advantageous to study the use of networks that invert the low impedance obtained when the resonator is operated in the series mode. A network suitable for this purpose is shown in Figure 2.10.

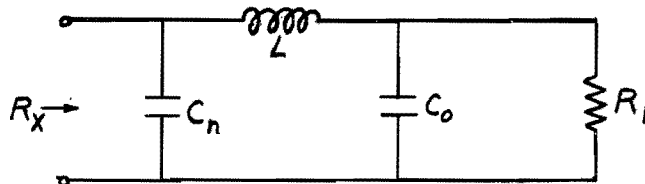


Figure 2.10 - Impedance Inverting Network

If the resonator is operated at the resonant frequency of the series arm (ω_o , Figure 2.7), it appears as a pure resistance, R_1 , shunted by the holder capacitance C_o . By associating the shunt capacity of the resonator with values of L and C_n given by equation 2.12

$$\omega_o^2 = 1/LC_o = 1/LC_n , \quad (2.12)$$

the network becomes the lumped-constant equivalent of the quarter-wave line, and has the desired property of impedance inversion. For this condition, the resistance at the input of the line is given by

$$R_x = Z_o^2/R_1 \quad (2.13)$$

where

$$Z_o = \omega_o L = 1/\omega_o C_o . \quad (2.14)$$

When this network is incorporated into a circuit, the input capacity is largely supplied by the tube and wiring strays. However, it seldom occurs that the tube capacity is equal to the holder capacity, so padding capacity must be added to obtain the equality of reactances required by equation 2.12.

It might be pointed out here that for cases in which the holder capacity

is larger than the tube capacity, no advantage is obtained by using a capacitor in series with the resonator to reduce the effective holder capacity as indicated by equation 2.1. This procedure causes an increase in the effective R_1 which is proportional to the increase in Z_o^2 , resulting in the same value of R_x that would be obtained by padding the tube capacity to equality with C_o . Furthermore, as is shown in following paragraphs, the impedance inverting property of the line is not lost when C_o and C_n are unequal, so padding is rarely necessary.

Near ω_o , the rate of change of Z_o with frequency is small compared to the phase change of the series arm of the crystal; therefore, the input impedance of the line is essentially the inverse of the series arm impedance. At frequencies quite different from ω_o , the input impedance is essentially that of an L C circuit, antiresonant at $\omega_o\sqrt{2}$. To damp this response, the effect of this resistor on the performance of the resonator is considered in Chapter VI, and it is shown that if Z_o is a few times larger than R_1 there is only a small loss in frequency stability.

Since the network in Figure 2.10 will exhibit a resistive input at or near ω_o , with constants other than those specified by equations 2.12, some questions arise as to the fundamental nature of the quarter-wave line concept. Moreover, it has been pointed out by Mr. A. C. Prichard of S.C.E.L. that values of R_x greater than that produced by the quarter-wave line may be obtained by a suitable choice of L and C_n . A more general analysis is therefore desirable. For this purpose the use of impedance and admittance diagrams is convenient and advantageous in that the performance of the network over a range of frequencies is clearly indicated. Adequate accuracy may be obtained by calculating points of interest. This procedure is greatly simplified by normalizing the resonator admittance with respect to R_1 , as done in Figure 2.11.

Starting with the admittance diagram in Figure 2.11a which is typical of a resonator with C_o equal to 10mmf, R_1 equal to 100 ohms, and f_o approximately 125 Mc, the impedance diagram in Figure 2.11b is obtained. Since the frequency scales in the two diagrams are not the same, the admittance

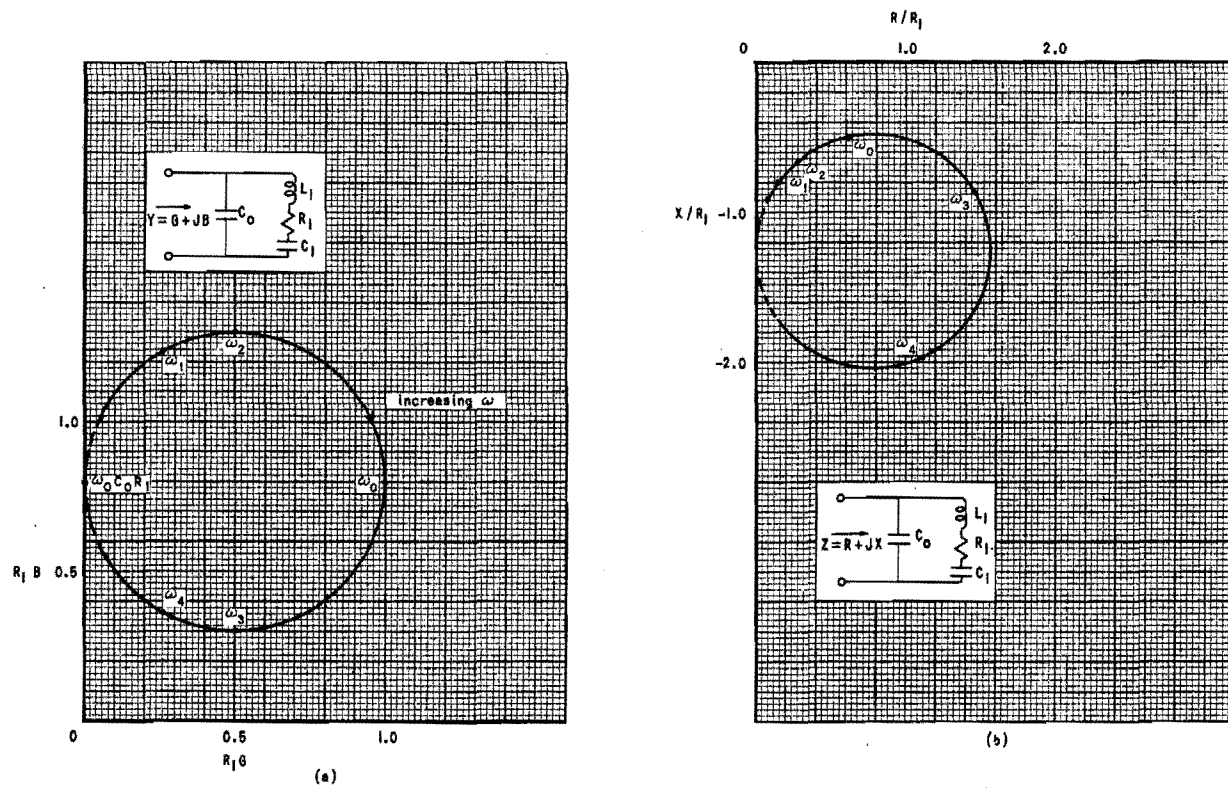


Figure 2.11. Admittance and Impedance Plot for a Crystal ($\omega_0 C_0 R_1 = 0.8$).

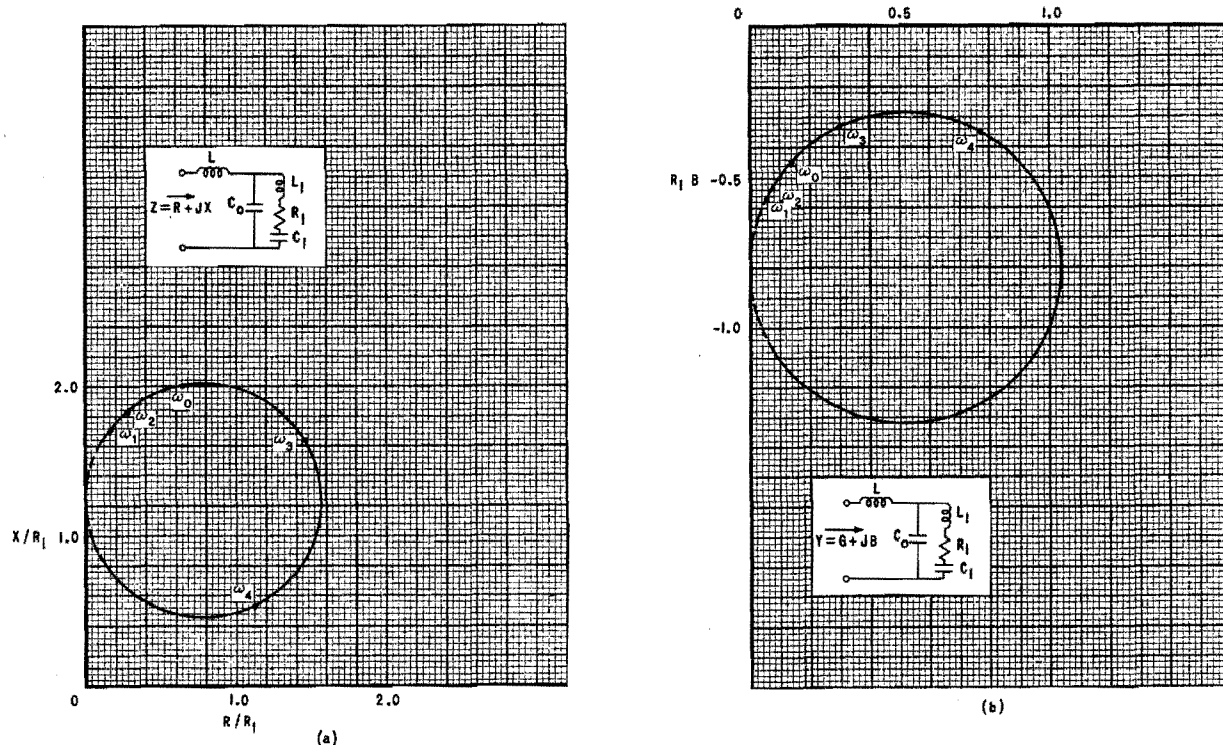


Figure 2.12. Impedance and Admittance Plot of a Crystal in Series With a Coil.

and impedance values for five frequencies are calculated. This process facilitates an estimate of the rate of change of phase for various element values to be considered. At the frequencies ω_1 and ω_4 , the impedance of the series arm of the resonator has a 60° phase angle while at ω_2 and ω_3 the phase angle is 45° .

From Figure 2.11b, it is seen that unity power factor may be obtained by adding sufficient inductance in series with the resonator to bring the point ω_0 up to the real axis. The resistance represented by this condition is, however, too low and a larger inductance is added, giving Figure 2.12a. Inverting this diagram gives the admittance of the series combination of L and the resonator (Figure 2.12b) and shows at once the magnitude of the shunt susceptance that must be added to give antiresonance at ω_0 , as well as the value of R_x that will be obtained. By repeating this process for different values of L, and adding in each case sufficient shunt susceptance to give antiresonance at ω_0 , Figure 2.13 is obtained. The numbered points represent discrete values of admittance for the frequencies ω_2 , ω_0 , and ω_3 corresponding to the values of L and C_n in Table I.

TABLE 2.1

Point No	Ratio of L to That of Quarter-wave Line	C_n/C_0	Ratio of R_x to That of Quarter-wave Line
1	2.00	0.569	4.64
2	1.84	0.620	3.83
3	1.68	0.679	3.12
4	1.50	0.755	2.41
5	1.12	0.947	1.26
6	1.00	1.00	1.00
7	0.80	1.009	0.665

For the special case of the quarter-wave line, L as shown in Figure 2.12a is just sufficient to bring the center of the impedance circle to the real axis. The inversion of this impedance circle and the addition of shunt susceptance to bring ω_0 to the real axis in Figure 2.12b located ω_2 and ω_3

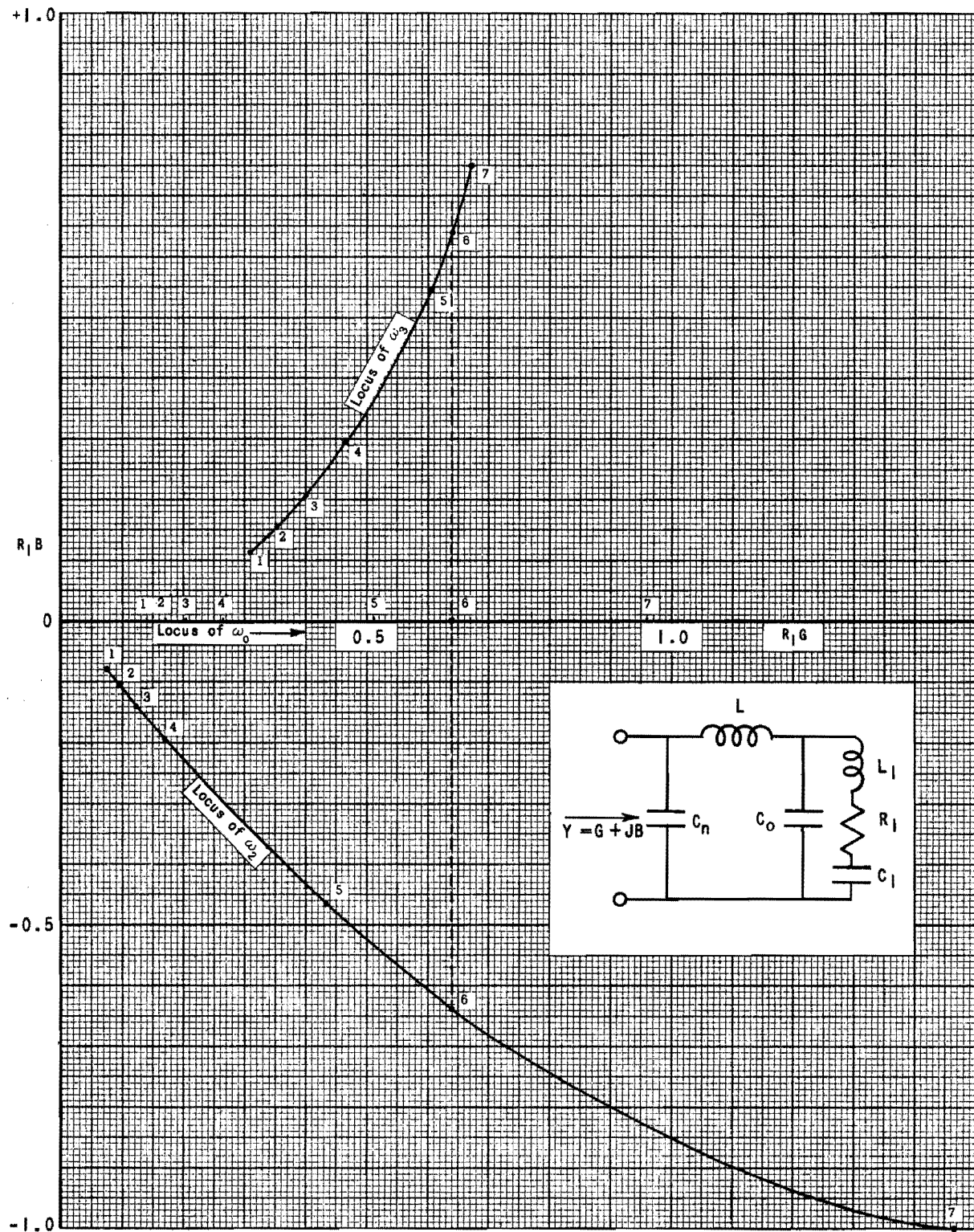


Figure 12.13. Effect of Variation of L and Readjustment of C.

symmetrically about the real axis, and results in phase angles ($\pm 45^\circ$) for these two frequencies that are the same as the series arm of the resonator alone. This conclusion holds for any values of R_1 and C_o and is accurate to the extent that Z_o remains constant over the interval between ω_2 and ω_3 . It follows that resonators having relative values of R_1 and $\omega_o C_o$ which differ from those in Figure 2.11a will, when associated with appropriate values of L and C, exhibit characteristics similar to those shown in Figure 2.13. This figure indicates that an antiresonant resistance of any reasonable value may be obtained by reducing C_n . A high value of antiresonant resistance can be obtained, however, only at the expense of frequency stability, as shown by the decreasing angle between ω_2 and ω_3 . Moreover, the final capacity C_n must be identified with that of the tube, which is rarely appreciably less than C_o . Another aspect of this type of operation may prove troublesome; viz., a decrease in C_n causes the resonant frequency ω_n of the network itself, as given by the expression

$$\omega_n^2 = \frac{C_n + C_o}{C_n C_o L} \quad (2.15)$$

to approach ω_o , and the degree of control exerted by the crystal decreases.

The case in which C_n is greater than C_o is yet to be considered. It may be conveniently approached through a study of the admittance of the series combination of L and the resonator as L is varied at a fixed frequency. Figures 2.11b and 2.12a indicate that the addition of an inductor in series with the resonator shifts the impedance circle vertically with no change in diameter or frequency scale. Therefore at constant frequency the locus of the impedance as a function of L is a vertical line in the impedance plane. This locus, for ω equal to ω_o , is shown in Figure 2.14a. The inversion of this straight line gives the locus of the admittance of the resonator and series inductor as a function of L as shown in Figure 2.14b. As before, the network is completed by adding a shunt capacitor to antiresonate the equivalent inductance of the remainder of the network. Figure 2.14b shows that for each value of L, a different value of input capacitance is required to obtain anti-resonance, and that the required capacitance is maximum if L is adjusted so that the admittance of the series combination of L and the resonator has a

-45° phase angle at the desired operating frequency. It is also evident that for a given resonator and operating frequency there is a maximum fixed input capacitance which may be tolerated.

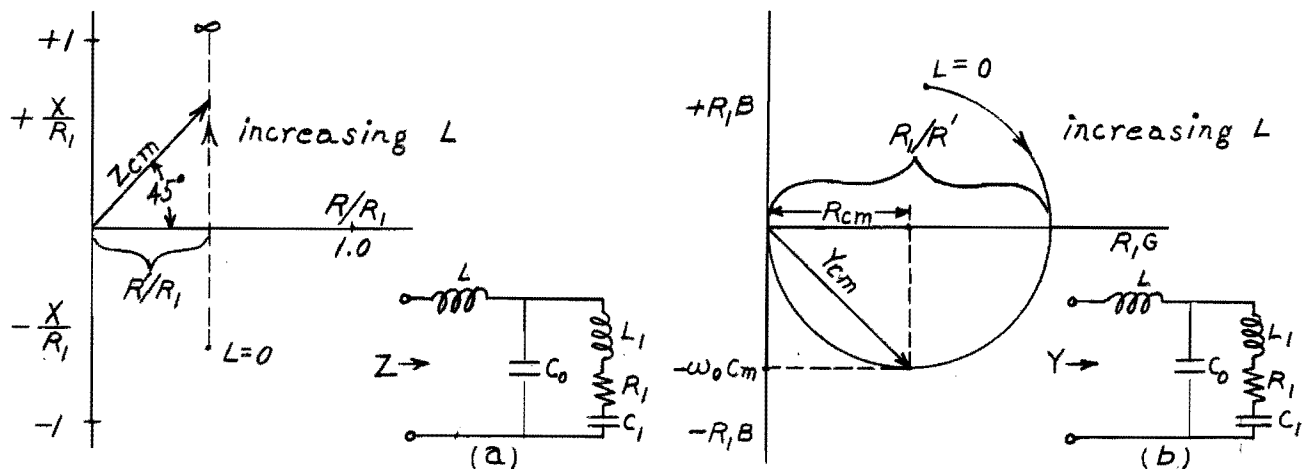


Figure 2.14 - Single Frequency Impedance and Admittance Plots
As a Function of the Series Inductance

Since the magnitude of the phase angle is not changed by the inversion process, the value of L which permits the use of the largest possible input capacity for a given operating frequency is the same value of L which produces a $+45^\circ$ phase angle in Figure 2.14a. From this fact, expressions relating the value of inductance consistent with maximum input capacitance to the resonator parameters may be obtained. The chosen operating frequency is ω_0 ; however, other operating frequencies within the range of crystal response may be selected by using different values of L or C_n without altering the analytical procedure.

The admittance of the resonator alone at ω_0 may be written as

$$Y' = G_o + j\omega_o C_o \quad (2.16)$$

where

$$G_o = 1/R_1. \quad (2.17)$$

Inverting this and adding the series L gives

$$Z' = \frac{G_o}{G_o^2 + (\omega_o C_o)^2} - j \frac{\omega_o C_o}{G_o^2 + (\omega_o C_o)^2} + j\omega_o L. \quad (2.18)$$

Since the maximum value of input capacity occurs for $Z' = Z' \angle +45^\circ$, it follows that

$$\omega_0 L_{Cm} - \frac{\omega_0 C_0}{G_0^2 + (\omega_0 C_0)^2} = \frac{G_0}{G_0^2 + (\omega_0 C_0)^2} . \quad (2.19)$$

From which

$$L_{Cm} = \frac{1}{\omega_0} \frac{G_0 + \omega_0 C_0}{G_0^2 + (\omega_0 C_0)^2} , \quad (2.20)$$

where L_{Cm} is the value of L required to give operation at ω_0 with a maximum value of input capacity. The value of this capacity (C_m) as well as the antiresonant resistance (R_{Cm}) obtained under these conditions are given by

$$\omega_0 C_m = \frac{1}{R_{Cm}} = \frac{G_0^2 + (\omega_0 C_0)^2}{2G_0} . \quad (2.21)$$

Equation 2.21 shows that for a resonator in which G_0 equals $\omega_0 C_0$, the maximum input capacity for operation at ω_0 is equal to C_0 , and the configuration is that of the quarter-wave line. It is of interest to compare the antiresonant resistance of a network composed of C_m , L_{Cm} , and C_0 with that of a quarter-wave line with both capacitors equal to C_m and having a particular value of inductance L_4 equal to $1/\omega_0^2 C_m$. This latter resistance is given by

$$R_4 = Z_0^2/R_1 = G_0/(\omega_0 C_m)^2 . \quad (2.22)$$

From equations 2.21 and 2.22 we may obtain the ratio

$$\frac{R_4}{R_{Cm}} = \frac{2G_0^2}{G_0^2 + (\omega_0 C_0)^2} = \frac{2}{1 + a^2} , \quad (2.23)$$

where

$$a = \omega_0 C_0 / G_0 . \quad (2.24)$$

Also from equation 2.21

$$\frac{C_m}{C_0} = \frac{G_0^2 + (\omega_0 C_0)^2}{2G_0 \omega_0 C_0} = \frac{1 + a^2}{2a} . \quad (2.25)$$

From equation 2.20 and the relation between L_4 and $\omega_o^2 C_m$, the following may be obtained:

$$\frac{L_{Cm}}{L_4} = \frac{G_o + \omega_o C_o}{2G_o} = \frac{1+a}{2} \quad (2.26)$$

From these it may be seen that for all values of a except unity, C_m , will be greater than C_o . However, R_4 will be greater than R_{Cm} for a less than one and smaller for larger values of a.

The foregoing treatment, while not completely general, indicates the conditions for obtaining the most advantageous impedance level. While the development of these relations assumes that the operating frequency is ω_o , the method of analysis applies to circuits that operate at other frequencies. For example, sufficient susceptance may be added in Figure 2.12b to give unity power factor at ω_2 . This results in an increased value of the resistance looking into the impedance inverting network and a decreased range of phase variation for which the crystal can compensate. The restrictions imposed by these relations show that for a given resonator, there is an overtone and a frequency above which efficient operation can not be obtained.

BIBLIOGRAPHY

- (1) Mason, W. P., Piezoelectric Crystals and Their Application to Ultrasonics. D. van Nostrand Co., Inc., New York, 1950.
- (2) Heising, R. A., Quartz Crystals for Electrical Circuits. D. Van Nostrand Co. Inc., New York, 1950.
- (3) Washburn, E. M., Investigation of Mechanical Overtone Crystals, 50 Mc to 150 Mc or Higher. R. G. A., Contract No. W30-039-sc-38265, Progress Reports Nos. 1 through 4, 1949, 1950.
- (4) Van Dyke, K. S., "The Piezoelectric Resonator and Its Equivalent Network." PROC. I.R.E., 16, June, (1928).
- (5) Cady, W. G., Piezoelectricity, McGraw Hill Book Co., Inc., New York, 1946.
- (6) Mason, W. P. and Fair, I. E. "A New Direct Crystal-Controlled Oscillator for Ultra-Short-Wave Frequencies." PROC I.R.E., 30, Oct., (1942).
- (7) "H. F. Harmonic Crystal Investigations 1 and 2." Philco Radio Corp., Contract No. W33-038-ac-14172, Final Report, April 1947.

III BASIC MATERIAL ON OSCILLATOR CIRCUITS

A. General Circuit Requirements.

An oscillator is essentially a vacuum-tube amplifier, in which a portion of the output having a suitable phase and magnitude is used as the input. From a dc power source such an arrangement can produce an ac output with a period which may be made highly stable. For this reason, oscillators, particularly those using quartz resonators, constitute one of the most accurate standards of time and frequency now known.

1. Feedback Oscillators.

Most oscillators may be represented by the functional diagram of Figure 3.1. The elements herein may not exist as separate items, but each function is essential to the performance of the oscillator.

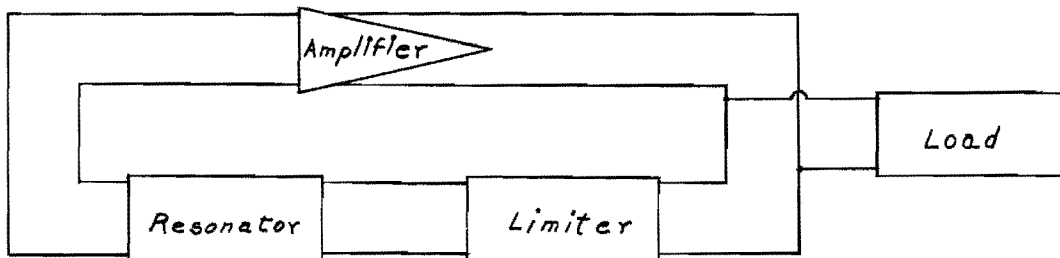


Figure 3.1 - Block Diagram of Feedback Oscillator

The amplifier serves to produce a power gain, the resonator controls the frequency of oscillation, and the limiter stabilizes the amplitude of oscillation. These elements are common to all oscillators, but their relative proportions may change. In some arrangements, a high efficiency of conversion of dc into ac energy is desired. In this case, the load should be adjusted to absorb nearly all the power which the amplifier can deliver, and the amount of power diverted into the feedback path should be as small as possible. In other oscillators, where the primary concern is constancy of frequency, the proportions will be quite different. Here the feedback circuit takes nearly all the output of the amplifier and the load is decoupled so as to have little effect on the behavior.

Ideally, the amplifier gain is independent of both frequency and amplitude, the resonator characteristic is dependant on frequency but independent

of amplitude, and the limiter output is dependent on its input amplitude but is independent of frequency. Practically, these ideals are not attained. However, the gain versus frequency characteristic of the amplifier need approximate the ideal only over a moderate frequency range. Also available resonators are quite selective and reasonably linear. Although a separate limiter is used in a few special circuits such as the Meacham¹, the function is ordinarily obtained by operating the amplifier in class C, with grid-leak bias.

Resonators may be constructed with characteristics which are essentially independent of applied potentials. In LC resonators, this result is achieved by use of air-core coils and air-dielectric capacitors. If coils with magnetic cores or capacitors with certain ceramic dielectrics are used, considerable nonlinearity (variation of element values) with respect to applied potentials may be encountered. From many viewpoints, quartz resonators are most desirable for high frequency stability; however, they do have a slight degree of nonlinearity with respect to applied potentials.

Good frequency stability may be obtained by using resonators which produce a high rate of change of loop phase with frequency; such resonators are able to compensate for phase changes elsewhere in the circuit with a minimum frequency change. Also the resonant frequency of the resonator should be, as nearly as possible, independent of the effects of such variables as time, temperature, and humidity.

Amplitude stability is achieved by including the limiter in the system. This device, which may have a number of different configurations, counteracts changes in loop gain so as to maintain the output amplitude very nearly constant. In conventional class C oscillators, limiting is usually obtained by grid rectification of the input voltage. The bias voltage so developed is proportional to the amplitude of oscillation and varies the tube gain in such a manner as to limit the amplitude. Here, the time constant of the grid leak resistor and condenser determines the rapidity with which the limiter corrects for amplitude variations. In oscillators where the greatest possible frequency stability is desired, class A operating conditions are used. In such a case limiting is obtained either by using a separate rectifier and filter to produce a gain control bias for the amplifier, or by inserting in the

feedback loop an attenuator having thermistor elements which cause an increase in attenuation as the level of oscillations increase. An outstanding example of this type of operation is the Meacham¹ oscillator, which is one of the most stable circuits now known.

The system of Figure 3.1 can be conveniently analyzed by opening the loop as shown in Figure 3.2. It should be noted that the limiter may be located either in the feedback path or at the amplifier input without altering the method of analysis. A current is fed from an auxiliary generator into the amplifier, and a detecting device is connected across the open terminals. The impedance of the test generator and the detector are chosen as indicated to avoid upsetting the behavior of the system. This analysis is based on feedback theory and may be accomplished by either experimental or analytical methods.

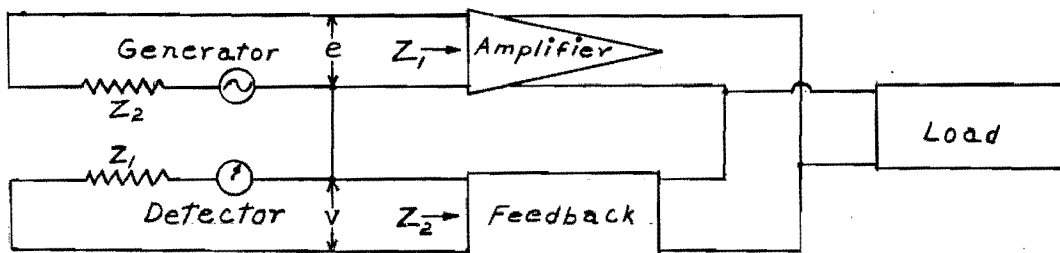


Figure 3.2 - Test to Determine Behavior of a Feedback System

To determine experimentally whether or not a circuit such as that in Figure 3.2 can oscillate, the phasor ratio of v to e is observed for a wide range of frequencies. Theoretically, this range should extend from zero to infinity, but in practice, the presence of coupling capacitors, transformers, and shunt capacities, limits the frequency range that need be considered. The voltage e is maintained at a small value so as not to over-load the circuit. For each frequency, the return voltage, v , bears some definite phase and magnitude relationship to e . Thus, the phasor ratio v/e , i.e. the loop transmission, has a definite value at each frequency. The results of this test may be represented as in Figure 3.3. This plot, which has a total loop phase of $\pm 90^\circ$, is representative of a system having a single-tuned circuit, and shows that for very small values of e the feedback

voltage v may be in phase with and considerably larger than e .

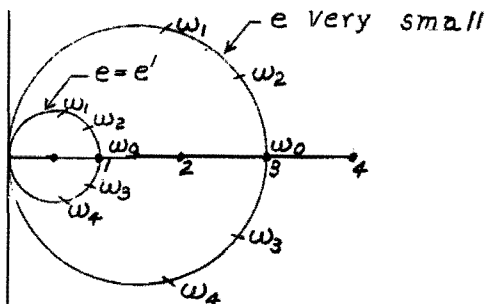


Figure 3.3 - Phasor Ratio of v to e or Nyquist Diagram

Now as the amplitude of e is increased, the limiter begins to function, and at each frequency the ratio v/e is decreased. For some particular frequency and amplitude, say ω_0 and e' , v and e' are identical, and their ratio becomes equal to $1 + j0$. From this it may be concluded that if the circuit connections are restored to their original form, oscillations will begin and that e' is the amplitude of the input voltage for which the stable amplitude of oscillation is reached. The foregoing facts lead to an important general conclusion: if, for a sufficiently small value of e , the plot of the loop transmission v/e encircles the point $1,0$ as the frequency is varied from zero to infinity, the system will oscillate; if the point $1,0$ is not encircled, the system will not oscillate. This is a statement of Nyquist's criterion of stability. This criterion is general and is used in both oscillator and feedback amplifier analysis. However, a more specific criterion of oscillation is that the loop transmission be just equal to $1 + j0$. This is referred to as Barkhausen's condition for oscillation.

While the experimental approach serves well to illustrate some details of operation, an analytical approach provides a better foundation for oscillator design. Since small values of e may be assumed, the conventional linear equivalent circuits for the amplifier may be used. Also, simplifying assumptions may be made as to the operation of the limiter, or its existence may be ignored. If the circuit is not too complicated, it is often possible to determine by inspection the general shape of the Nyquist diagram. Then, it is only necessary to determine whether the loop transmission exceeds unity at the frequency for which its phase angle is zero, or 2π radians. The general shape of the Nyquist diagram must be determined because non-oscillatory

systems do exist that have real intercepts of loop transmission greater than unity. The Nyquist diagram of such a system is shown in Figure 3.4.

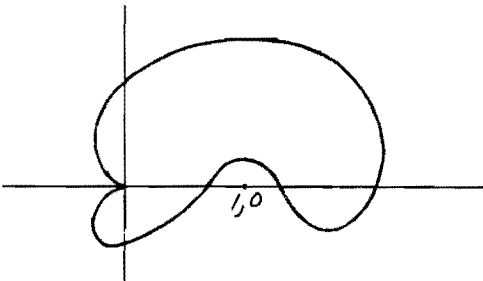


Figure 3.4 - Nyquist Diagram of Conditionally Stable System

In this case the loop transmission is real and exceeds unity for two frequencies. However, the point 1,0 is not encircled, so the system is actually stable.

An analytical demonstration that the point 1,0 is encircled proves that oscillations will exist, but it gives no information as to the final amplitude of oscillation. However, if the encirclement is by a generous margin, the oscillations will build up rapidly; and often a careful examination of the limiter will enable one to estimate the final amplitude.

The frequency of oscillation may be determined with good accuracy from the requirement that the total loop phase be zero for a small signal input. This method is possible because normal limiting action causes the Nyquist diagram to shrink radially with little or no relative change in the frequency scale.

The frequency stability of the system may be studied by examining the frequency scale on the Nyquist diagram. If a phase change occurs due to any variation of circuit elements, the frequency of operation will change enough to restore the total loop phase to zero. In general, a change in amplitude will also occur, but if the phase change is small, this variation may be neglected. In order that the frequency change be small, it is desirable that the rate of change of loop phase with frequency be large. This condition is indicated by an open frequency scale near ω_0 on the Nyquist diagram. Conversely, poor frequency stability is indicated if in Figure 3.3 the frequency interval between ω_1 and ω_4 is large.

Analytically, the frequency stability of the circuit may be expressed as

$$S_f = \frac{dB}{d\omega/\omega} \quad (3.1)$$

where B is the phase angle of the loop transmission. In the ideal system, the resonator is the only element which can cause a phase variation with frequency; therefore, the frequency stability of the system equals that of the resonator. In most oscillators, the Q of the resonator is degraded by its association with the rest of the system. The degree of this degradation may be expressed as the ratio of the resonator to system stability, or

$$D = S_r/S_f, \quad (3.2)$$

where S_r , the resonator stability has the same form as equation 3.1. This relation is useful in comparing the relative frequency stability of circuits which employ similar resonators.

2. Negative Resistance Analysis.

In addition to the foregoing method of analysis, oscillators may be studied from the negative resistance viewpoint. If the resonator is assumed to be a two terminal device, which includes the circuit capacities to the right and left of $a'---a$, the ideal circuit may be drawn as in Figure 3.5.

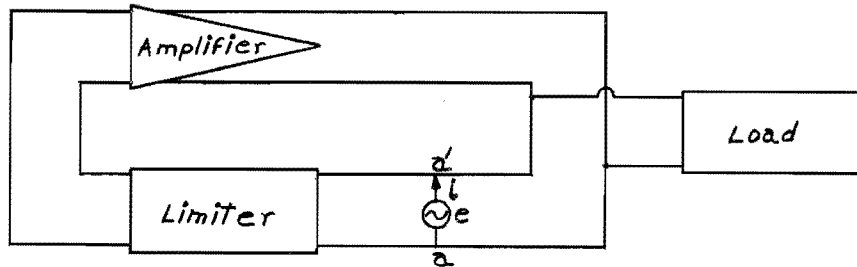


Figure 3.5 - Ideal Oscillator Circuit for Negative Resistance Analysis
Here, the resonator is replaced by a voltage generator. If the voltage e is small, the ratio of e to i may be calculated using the usual linear equivalent circuits for the amplifier. This ratio defines the impedance across the generator terminals. Since the ideal amplifier, limiter, and load have characteristics which are independent of frequency, there is no reactive component to this impedance, and ideally the frequency of oscillation for

small signals is determined by the resonator alone. In physical systems, this impedance may have a reactive component which will influence the frequency of operation.

If the system is to be capable of oscillating, the impedance across the generator terminals must have a negative real component for small values of e . The circuit with the resonator restored to its proper location then reduces to Figure 3.6. In this figure L and C constitute the resonator, R represents the resonator loss, and $-r$ represents the negative resistance developed by the system.

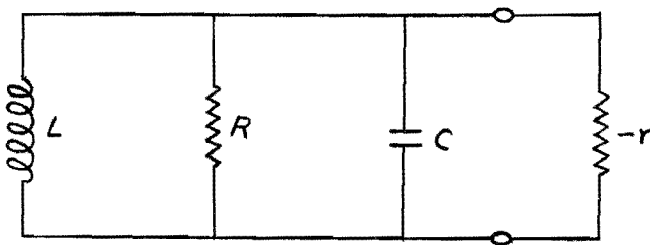


Figure 3.6 - Analysis of Negative Resistance Oscillator

The total resistance across the resonator is given by

$$R' = \frac{-rR}{R - r}, \quad (3.3)$$

and if R equals $|r|$, R' becomes infinite. This reflects the fact that the oscillator system then constitutes a source of power sufficient to supply the resonator losses. For this condition, oscillations once started in the LC circuit will persist at a constant amplitude. If R exceeds $|r|$ the total resistance is negative, indicating that the power supplied by the amplifier exceeds that dissipated by the load and resonator. For this condition the oscillations will increase in amplitude. Therefore the criterion of oscillation for the negative resistance analysis is that, for small voltages, R be equal to or greater than $|r|$.

Due to the limiting action in the system, any tendency for the amplitude of oscillation to increase or decrease is met by a corresponding increase or decrease in the magnitude of the negative resistance. Thus, the amplitude of oscillation is stabilized.

The negative resistance analysis is not so flexible nor so informative

as that based on feedback. However, almost any kind of oscillator may be interpreted from this viewpoint. In some negative-resistance or two-terminal oscillators, there is no physical feedback loop that may be broken for analysis and the negative resistance approach must be used.

B. Nonlinear and U.H.F. Effects.

If an oscillator is to possess amplitude stability, some element in the system must be nonlinear with respect to applied potentials; in the discussion of ideal systems this element was assumed to have no effect on the frequency of oscillation. In practical systems, however, it is often found that the frequency of oscillation differs from the resonant frequency of the resonator and is to some extent dependent on the exact nature of the nonlinear element. Some idea as to how this occurs may be obtained from a study of the Dynatron oscillator^{3,4}. The equivalent circuit of this device is the same as that in Figure 3.6, and again the resonator includes the shunt capacity contributed by the circuit. The negative resistance in this case is obtained directly from a screen grid tube which has a plate characteristic as shown in Figure 3.7.

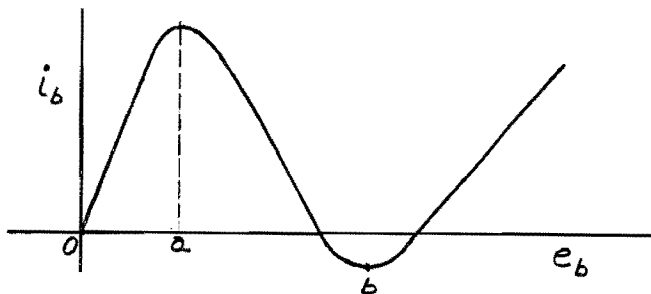


Figure 3.7 - Dynatron Characteristic

In the plate voltage range $a \rightarrow b$, an increase in plate voltage results in a decrease in plate current. Therefore, the dynamic plate resistance of the tube is negative, and oscillations will result if some kind of resonator having a shunt resistance greater than the negative plate resistance is connected from plate to ground. The amplitude of these oscillations will increase until the voltage swing into the positive-resistance regions of the characteristic reduces the average value of the negative resistance to equality with the shunt resistance of the resonator. Thus, limiting occurs due to the nonlinear character of the negative resistance.

If convenient values of ac and dc plate voltages are assumed, the corresponding plate current may be obtained from Figure 3.7. Assuming the tube is biased to a point about midway between a and b, and that the voltage excursions extend considerably outside the negative resistance region, it is clear that the plate current will contain large harmonic components, even though the voltage be substantially sinusoidal. A Fourier analysis may be made of the actual plate current to determine the harmonic content. If the assumed ac plate voltage is a pure sine wave, it will be found that the fundamental component of plate current is exactly 180 degrees out of phase with the voltage. Therefore, for a sinusoidal plate voltage the tube appears as a pure negative resistance. The frequency of operation, i.e. the resonant frequency of the resonator, is independent of amplitude and of the shape of the negative resistance characteristic.

Experiments show, however, that the circuit does not operate at the exact resonant frequency of the resonator, and that the operating frequency depends to some extent on the electrode potentials. This situation may be explained by noting that the voltage wave cannot be exactly sinusoidal when the current wave is markedly distorted. Consideration of a distorted voltage wave shows that the fundamental component of current is no longer 180 degrees out of phase with the fundamental component of voltage, and the tube appears as a negative resistance shunted by a reactance. Since the shape of the tube characteristic varies with applied potentials, the shape of the current wave depends upon the amplitude of oscillation. Therefore, the reactive component of the tube impedance varies with both, and the operating frequency depends upon applied potentials and amplitude of oscillation.

For sinusoidal plate voltages the frequency of operation is independent of the tube characteristic; accordingly, the frequency variation may be attributed to the presence of harmonics in the plate voltage. It follows that a reduction of harmonic content will improve the frequency stability. Such a reduction may be made by simultaneously decreasing the resonator reactances and increasing the resonator Q to maintain the shunt resistance at the value required for oscillations. Alternately, or in addition, the amplitude of oscillation may be restricted to the most linear portion of the negative

resistance characteristic by using an auxiliary limiter. In this case, the amplitude of oscillation is held constant by changing the slope of the characteristic (magnitude of the negative resistance) rather than by over-loading, thereby minimizing the production of harmonics.

At very high frequencies tube and circuit losses reduce the obtainable value of Q, making larger resonator reactances necessary. The impedance of the resonator to harmonic frequencies is thereby increased and the frequency stability is degraded. Also the tube capacitance becomes all or a large part of the resonator capacitance. This situation is serious because the tube capacitance has a higher temperature coefficient than a good fixed or variable capacitor. Transit-time phase-shift phenomena also contribute to the difficulty of obtaining stable oscillators at ultra-high frequencies. In this region the time required for the electrons to travel from cathode to plate is an appreciable fraction of the oscillation period; consequently, the plate voltage, with a resistive load, is not 180° out of phase with the driving voltage. From the negative resistance viewpoint, this situation results in the association of a reactance with the negative resistance; from the feedback viewpoint, the loop phase is altered. Since transit time depends on electrode potentials and spacing, frequency changes will result if either is changed.

In the microwave region suitable oscillators and good resonators are separately available, but good amplifiers are not. For this reason, automatic-frequency-control systems (which maintain the oscillator frequency at a reference frequency determined by the resonator) are used. Results obtained with the best of these systems are comparable to those obtained by conventional means at lower frequencies⁵.

C. Intermittent Oscillation.

While some form of limiter is necessary if amplitude stability is to be obtained, experiments show that under certain conditions limiting devices can cause amplitude modulation or intermittent oscillations. This behavior may be studied by extending the feedback analysis⁶ previously presented. Reference to Figure 3.2 indicates that if the system can oscillate there will be some frequency and some value of e for which the loop transmission is unity. In applying the test for self modulation, the test generator is first adjusted.

to supply the aforementioned frequency and voltage, and is then amplitude modulated at a frequency which may be varied. For each modulating frequency, the envelope of the return voltage, v , bears a definite phase and amplitude relationship to the envelope of e so a plot similar to Figure 3.3 may be obtained from the ratio of the two envelopes. If this plot encircles the point 1,0 it again follows that the system output can supply the input, and that, if the loop is closed, oscillations will occur which have essentially the same character as the modulated input. This test, however, supplies no information as to the degree of modulation that will result when the loop is closed.

Oscillators which operate at moderate frequencies and use grid leak bias seldom tend toward intermittent operation. When such operation does occur, it is usually due to such excessively large values of grid resistance and capacitance that the large grid time constant prevents the bias from changing rapidly; any sudden decrease in feedback voltage is not accompanied by a correspondingly rapid increase in gain. If the resonator has a relatively low Q , a condition conducive to sudden changes in feedback voltage, it is possible for the loop transmission to decrease more rapidly than the gain increases, and oscillations will cease. Then, as the grid capacitor discharges the bias decreases until oscillations again start. When the original amplitude of oscillation is reached, this cycle repeats itself. The result is a series of bursts of high frequency oscillations that are interrupted at a rate determined by the grid time constant. While operation of this type is occasionally useful it is to be avoided where frequency stability is desired.

BIBLIOGRAPHY

1. Meacham, L. B., "The Bridge Stabilized Oscillator", Proc. I.R.E., 26 1278, (October, 1938).
2. Nyquist, H., "Regeneration Theory". Bell System Technical Journal, 11 126-147 (January, 1932).
3. Arguimbau, L. B., Vacuum Tube Circuits, John Wiley & Sons, Inc., New York 1948.
4. Groszkowski, J., "The Interdependance of Frequency Variation and Harmonic Content, and the Problem of Constant Frequency Oscillators". I.R.E., 21, 958-981, (1933).

Final Report Project No. 131-45

5. Hershberger, W. D. and Norton, L. E., "Frequency Stabilization with Microwave Spectral Lines." RCA Review, 9, 38-49 (1948).
6. Edson, W. A., "Intermittent Behavior in Oscillators," B.S.T.J., 24, 1, (January 1945).

IV CONVENTIONAL CRYSTAL OSCILLATORS

A. General Properties.

A review of the general characteristics and circuit configurations of conventional crystal oscillators is appropriate here to provide a point of departure for the discussion of oscillators which operate in a less familiar manner. The importance of this inclusion is enhanced by the fact that later sections show that the same equations often apply to both conventional and overtone oscillators.

Conventional crystal oscillators are characterized by the fact that the crystal operates as an equivalent inductance in effective antiresonance with the capacitance provided by the remainder of the circuit. The antiresonant resistance so produced is referred to as the Performance Index (PI) of the crystal; it is ordinarily rather high, in the order of 10,000 ohms. Usually, but not necessarily, the crystal vibrates at its fundamental frequency rather than at a mechanical overtone. It is usually possible and desirable to arrange the circuit so that no oscillation of any kind is produced unless a suitable crystal is present in the circuit.

B. The Pierce Circuit.

The circuit which is now commonly referred to as the Pierce crystal oscillator is shown in Figure 4.1. It is characterized by extreme simplicity and economy of parts, and has the desirable property of oscillating over a very wide frequency range with no change except substitution of suitable crystal units. In the arrangement shown the average plate voltage, and hence the amplitude of oscillation, is greatly reduced by the flow of plate current through the resistor R_L , which must be relatively high in order to produce conditions suitable for oscillation. Where a larger amplitude of oscillation is desirable, a high-inductance low-resistance choke may be substituted for R_L . Moreover, if operation is desired over only a moderate frequency range, the choke may have smaller inductance, and C_p may be increased somewhat to produce the desired net susceptance. This arrangement is desirable when a crystal must be forced to operate at a mechanical overtone or when the plate voltage wave should have a nearly sinusoidal form.

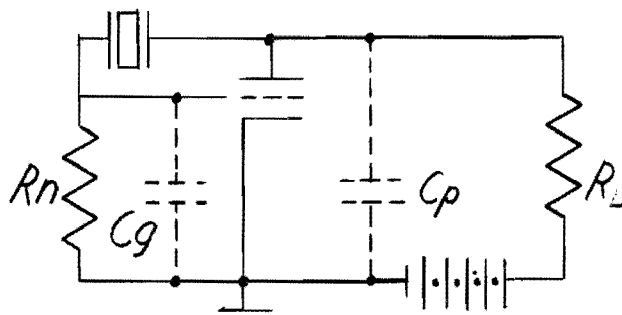


Figure 4.1 - The Pierce Crystal Oscillator

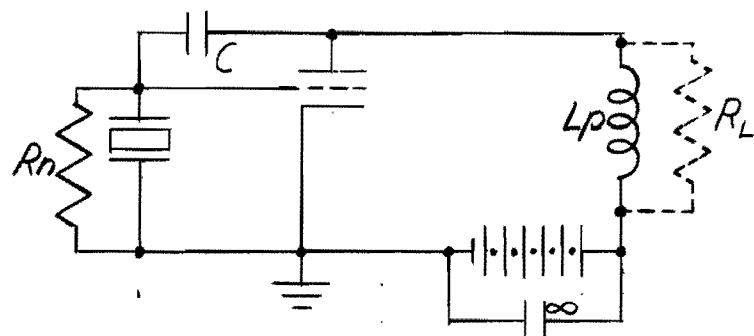


Figure 4.2 - The Miller Crystal Oscillator

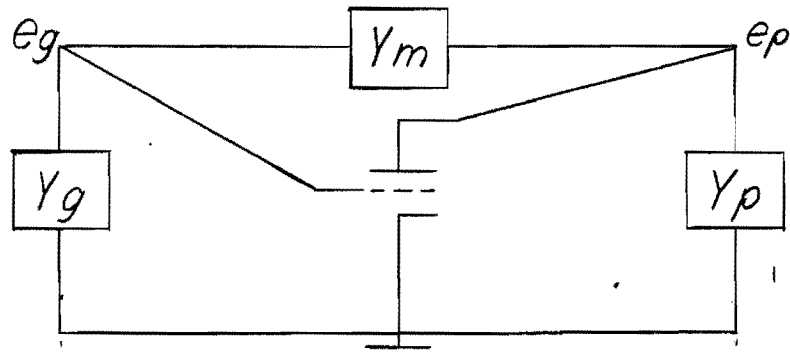


Figure 4.3 - General Circuit for Analysis

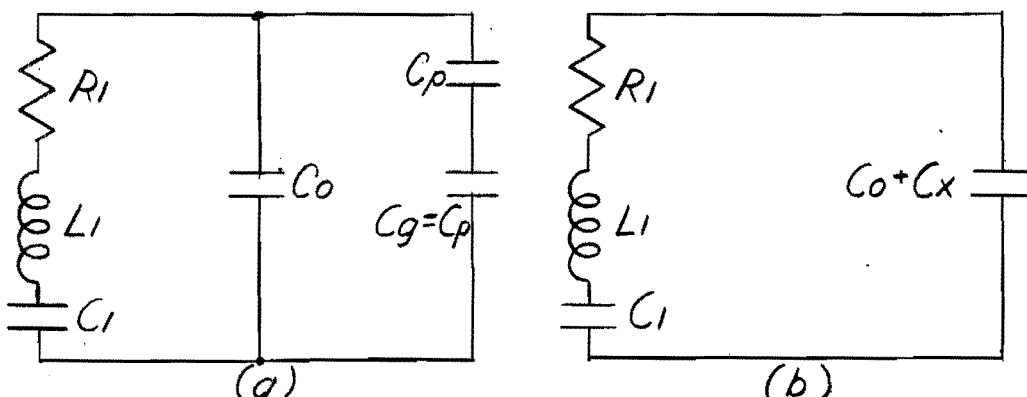


Figure 4.4 - Calculation of Frequency Stability

C. The Miller Circuit.

Another widely used crystal oscillator circuit is referred to as the Miller and is shown in Figure 4.2. The feedback capacitance C is ordinarily provided by the tube interelectrode capacitance, so that no external capacitor is necessary. Moreover, because a relatively large value of the plate inductance L_p is commonly required, a capacitance is often added in shunt with L_p to increase the effective inductive reactance produced. As in the Pierce oscillator, the use of a suitable tuned plate circuit improves the output wave form and insures that oscillation will be produced only at a frequency near that of the tuned circuit. Compared to the Pierce, the Miller circuit can produce a considerably greater power output without damaging the crystal, but its initial adjustment is somewhat more critical and the circuit must be readjusted if a crystal of appreciably different frequency is to be substituted.

D. Loop Gain Considerations.

The operating frequency and the relationships required between transconductance and circuit resistances for both the Pierce and Miller circuits is conveniently studied in terms of Figure 4.3. There is economy of thought and effort in treating both circuits by a common analysis. Using e_p and e_g for the alternating components of the plate and grid voltages respectively, and including any dynamic plate and grid conductance in Y_p and Y_g respectively, we may write

$$e_g(Y_g + Y_m) - e_p(Y_m) = 0 \quad (4.1)$$

and

$$-e_g(Y_m) + e_p(Y_p + Y_m) = -e_g g_m \quad (4.2)$$

where g_m represents the effective transconductance of the tube. The voltage variables may be eliminated to obtain

$$(Y_g + Y_m)(Y_p + Y_m) = Y_m(Y_m - g_m), \quad (4.3)$$

or

$$-g_m = -Y_m + (Y_g + Y_m)(Y_p + Y_m)/Y_m = Y_p + Y_g + Y_p Y_g/Y_m. \quad (4.4)$$

E. Loop Gain in the Miller Oscillator.

The general loop gain equation given by 4.4 appears very simple, and

one might suppose that it would remain simple when actual circuit parameters were substituted. Unfortunately this is not true, and unmanageably complicated expressions result unless a number of simplifying assumptions are made. These are most conveniently made at the beginning.

In the Miller oscillator we have quite accurately

$$Y_m = j\omega C . \quad (4.5)$$

Moreover, we may write

$$Y_p = 1/R_L + 1/j\omega L_p \quad (4.6)$$

where R_L accounts for any useful load, the dynamic resistance of the tube, and any losses in the coil. Finally, at the operating frequency

$$Y_g = 1/R_g + 1/j\omega L_x \quad (4.7)$$

where R_g accounts for the losses of the grid and crystal, and L_x is the equivalent inductance of the crystal. This representation is legitimate because crystal units are designed to operate at a specific frequency in conjunction with a specified load capacitance, C_x , consistent with the equation

$$\omega^2 = 1/L_x C_x . \quad (4.8)$$

Substitution of these several equations in 4.4 yields

$$-g_m = 1/R_L + 1/R_g + 1/j\omega L_p + 1/j\omega L_x + j \frac{(R_L + j\omega L_p)(R_g + j\omega L_x)}{\omega^3 R_g R_L L_p L_x C} . \quad (4.9)$$

Separation of real and imaginary components yields

$$-g_m = 1/R_L + 1/R_g - \frac{L_p R_g + L_x R_L}{\omega^2 R_g R_L L_p L_x C} , \quad (4.10)$$

and

$$L_p + L_x = \frac{R_L R_g - \omega^2 L_x L_p}{\omega^2 R_g R_L C} . \quad (4.11)$$

In the usual case $R_L R_g \gg \omega^2 L_x L_p$, and the latter equation reduces to the form

$$\omega^2 = 1/C(L_x + L_p) , \quad (4.12)$$

which indicates that oscillation occurs at the frequency of series resonance

between C and L_x and L_p. The substitution of this value in 4.10 yields

$$g_m = \frac{(L_p R_g + L_x R_L)(L_p + L_x) - R_g L_x p - R_L L_x p}{R_g R_L L_x p} = \frac{R_g L_p^2 + R_L L_x^2}{R_g R_L L_x p}. \quad (4.13)$$

From 4.12 we see that the main oscillation current flows through C, L_p, and L_x; therefore, the excitation ratio h may be written

$$h = e_p / e_g = L_p / L_x. \quad (4.14)$$

Use of the excitation ratio reduces 4.13 to the form

$$g_m = \frac{h^2 R_g + R_L}{h R_g R_L}. \quad (4.15)$$

For prescribed values of R_g and R_L it is readily shown that a minimum value of g_m corresponds to the condition

$$h^2 R_g = R_L. \quad (4.16)$$

Provided R_L is sufficiently large, it is possible to secure oscillation by making h large, even with a relatively poor crystal and a very low value of g_m.

Use of 4.14 with 4.8 and 4.12 yields

$$C = C_x / (1 + h). \quad (4.17)$$

It is seen that C may become quite small if the excitation ratio h is large. The Miller oscillator is well adapted to producing relatively large values of power output without damage to the crystal. To show this, let us consider a pentode tube with a high internal plate resistance and a plate coil with negligible losses so that all the power produced is useful and is consumed in the load. Under these conditions, the output power may be written

$$P_L = e_p^2 / R_L. \quad (4.18)$$

If in addition we assume that the conductance of the grid and grid leak is negligible, the power dissipated in the crystal is

$$P_x = e_g^2 / R_g. \quad (4.19)$$

The ratio of these powers is

$$\frac{P_L}{P_X} = h^2 \frac{R_g}{R_L} . \quad (4.20)$$

It is feasible to obtain values of h near 5 and ratios of R_g/R_L as high as 4; consequently, it is possible to obtain power ratios near 100.

F. Loop Gain in the Pierce Oscillator.

One might suppose that the loop gain equations governing the Pierce oscillator would be simpler than those applying to the Miller. Unfortunately the reverse is true, and we must make several simplifying assumptions to obtain equations capable of useful interpretation. It is essentially correct to assume that the grid-plate capacitance and grid conductance are negligible, so that we may write

$$Y_g = j\omega C_g , \quad (4.21)$$

$$Y_p = j\omega C_p + 1/R_L ,$$

and

$$Y_m = 1/R_x + 1/j\omega L_x$$

where R_x and L_x represent respectively the parallel resistance and inductance of the crystal unit at the specified operating frequency. Substituting these values in 4.4 yields

$$-g_m = j\omega(C_g + C_p) + 1/R_L - \frac{\omega^2 L_x C_g R_x (1 + j\omega R_x C_p)}{(R_x + j\omega L_x) R_L} . \quad (4.22)$$

Rationalizing and separating real and imaginary components on the basis that $\omega^2 L_x^2 \ll R_x^2$, yields

$$-g_m = 1/R_L - \frac{\omega^2 L_x C_g}{R_x R_L} (R_x + R_L \omega^2 C_p L_x) , \quad (4.23)$$

and

$$0 = C_g + C_p - \frac{\omega^2 L_x C_g}{R_x R_L} (L_x + R_x R_L C_p) . \quad (4.24)$$

Because $R_x \gg \omega L_x$ and $R_L \gg 1/\omega C_p$, the last term in the final parenthesis is controlling, and the frequency is given to a very close approximation by

$$\omega^2 = \frac{C_g + C_p}{L_x C_g C_p} . \quad (4.25)$$

That is, the oscillation occurs at the frequency of resonance between the crystal inductance and the series combination of C_g and C_p . This series combination should correspond to the specified load capacitance C_x for operation of the proper frequency. Substituting this value of ω in 4.23 and using the excitation ratio $h = e_p/e_g = C_g/C_p$, one has

$$-g_m = 1/R_L - \frac{h+1}{R_x R_L} (R_x + R_L + R_L/h), \quad (4.26)$$

or

$$g_m = h/R_L + \frac{2+h+1/h}{R_x}. \quad (4.27)$$

In particular, if R_L is very large, the smallest value of transconductance for which oscillation can occur is

$$(\text{min}) g_m = 4/R_x, \quad (4.28)$$

which occurs when

$$h = 1. \quad (4.29)$$

The useful power output is given by

$$P_L = e_p^2/R_L \quad (4.30)$$

while the power dissipated in the crystal is

$$P_x = (e_p + e_g)^2/R_x. \quad (4.31)$$

The ratio is

$$P_L/P_x = h^2 R_x / R_L (h+1)^2. \quad (4.32)$$

The ratio R_x/R_L and the excitation ratio h should both be large if a large power output is desired. However, the ratios which may be obtained with practical tubes and crystals are seriously limited. If, for example, $R_x = 10,000$ ohms, $R_L = 5,000$ ohms, and $h = 2$, we have $P_L/P_x = 4$. The required transconductance is, by 4.27, $g_m = 2/5,000 + 4.5/10,000$ or 950 micromhos, a typical value for the effective transconductance of a modern tube operating in class C.

G. Frequency Stability of the Pierce Oscillator.

The frequency of any oscillator changes somewhat when the circuit

parameters or applied voltages change. In crystal oscillators, the frequency variation is quite small because of the high Q value characteristic of quartz resonators. Because the total variation is small, it is sufficient to consider only first-order terms in the mathematical expressions. The following discussion is limited to the frequency change produced by a small change in the tube or circuit capacitance. It is known that frequency changes also result from changes of the resistances of the tube and circuit elements, and that additional changes result from the effective reactances produced by non-linearity through intermodulation effects. However, these latter effects are difficult to evaluate and it is probable that they are approximately proportional to the one calculated.

When the maximum possible frequency stability is required of a Pierce oscillator, it is customary and desirable to make $C_g = C_p = 2C_x$ so that $h = 1$, and to make R_L as well as R_n as large as possible. These choices permit oscillation with the lowest possible value of transconductance and result in the smallest possible frequency deviations due to random small variations in C_g or C_p . Subject to these choices, we may readily evaluate the frequency change which results from an increment in either C_g or C_p . The relations

$$C_x = C_g/2 = C_p/2 , \quad (4.33)$$

show that an increment, dC_p , in either capacitance changes the total capacitance to

$$1/(C_x + dC_x) = 1/C_p + 1/(C_p + dC_p) . \quad (4.34)$$

Using the approximation valid for small values of x

$$1 + x \approx 1/(1 - x) \quad (4.35)$$

together with 4.33, one has

$$2(1 - dC_x/C_x) = 1 + 1 - dC_p/C_p , \quad (4.36)$$

or

$$dC_x/C_x = dC_p/2C_p = dC_p/4C_x . \quad (4.37)$$

The reference or normal frequency is given by

$$\omega L_1 = 1/\omega C_1 + 1/\omega(C_o + C_x) = \frac{C_o + C_1 + C_x}{\omega(C_o + C_x)} \quad (4.38)$$

The frequency which exists when C_x is incrementally increased is

$$(\omega + d\omega)^2 L_1 = \frac{C_o + C_1 + C_x + dC_x}{C_o + C_x + dC_x} . \quad (4.39)$$

Division of 4.39 by 4.38 yields

$$(1 + 2d\omega/\omega) = \frac{(C_o + C_1 + C_x + dC_x)(C_o + C_x)}{(C_o + C_1 + C_x)(C_o + C_x + dC_x)} . \quad (4.40)$$

If we again use 4.35 and neglect certain small terms we obtain

$$2d\omega/\omega = \frac{dC_x}{(C_o + C_1 + C_x)} - \frac{dC_x}{(C_o + C_x)} = \frac{-C_1 dC_x}{(C_o + C_1 + C_x)(C_o + C_x)} . \quad (4.41)$$

Because C_1 is very small compared to C_o , this reduces to

$$d\omega/\omega \doteq -C_1 dC_x / 2(C_o + C_x)^2 . \quad (4.42)$$

Finally using 4.37,

$$d\omega/\omega \doteq -C_1 dC_p / 8(C_o + C_x)^2 . \quad (4.43)$$

The desirability of a small value of C_1 (that is, a stiff crystal) is clear from this equation. However, the extent to which C_1 may be reduced is limited by considerations of crystal Q and power dissipation, available transconductance, etc. An evaluation of these relationships is quite complicated and exceeds the purpose of the present treatment.

H. Frequency Stability of the Miller Oscillator.

The development of 4.42 is entirely independent of the oscillator circuit; therefore, we may use this relationship to evaluate the frequency stability of the Miller oscillator. Figure 4.2 indicates that an increment of grid-cathode capacitance corresponds directly to an increment in C_x so that 4.42 is directly applicable.

To find the frequency change produced by an increment in the grid-plate capacitance C we use the frequency equation 4.12 and also 4.8 to obtain

$$1/\omega^2 C - L_p = 1/\omega^2 C_x , \text{ or, } C_x = C/(1 - \omega^2 CL_p) . \quad (4.44)$$

Differentiation yields

$$dC_x = \frac{(1 - \omega^2 C L_p) dC + \omega^2 C L_p dC + 2\omega C^2 L_p d\omega}{(1 - \omega^2 C L_p)^2} \doteq C_x^2 dC/C^2 , \quad (4.45)$$

where the term in $d\omega$ may be shown to be small compared to the others and so is neglected. Substituting 4.45 in 4.42 yields

$$d\omega/\omega \doteq -C_1 C_x^2 dC/2C^2(C_o + C_x)^2 . \quad (4.46)$$

It is seen that frequency stability is enhanced by use of a stiff crystal ($\text{low } C_1$) and by making C as large as practical. Unfortunately, the efficiency and power output suffer when C is increased, so a compromise is necessary.

The effect of a change in L_p is obtained by differentiating 4.44 with respect to L_p , again neglecting differentials in ω to obtain

$$dC_x \doteq \omega^2 C^2 dL_p / (1 - \omega^2 C L_p)^2 = \omega^2 C_x^2 dL_p . \quad (4.47)$$

Again substituting in 4.42, one has

$$d\omega/\omega \doteq -\omega^2 C_1 C_x^2 dL_p / 2(C_o + C_x)^2 = -C_1 C_x (C_x - C) dL_p / 2CL_p (C_o + C_x)^2 . \quad (4.48)$$

From this equation, it is seen that a fractional change in L_p produces the least possible frequency change when C is nearly as large as C_x . Unfortunately, this is again a condition of low power output.

V SERIES-RESONANT CRYSTAL-CONTROLLED OSCILLATORS

A. Introduction.

Up to about 20 Mc, conventional crystal-controlled oscillator circuits are simple and quite satisfactory. Above these frequencies, however, crystals ground for fundamental operation would be too thin for economical production, so overtone operation is desirable. It is possible to operate crystals at mechanical overtones in parallel-resonant circuits, but the capacitance ratio increases as the square of the order of overtone; consequently, the maximum order of overtone that may be excited will be low unless the crystal has an exceptionally large Q. Furthermore, circuit operation and adjustment is difficult because the resonant and antiresonant frequencies are quite close. These frequencies may be separated somewhat by shunting the crystal with an appropriate inductance to reduce the effective capacitance ratio¹. The shunting, however, reduces the range of phase angle for which the crystal can compensate. Moreover, the tube capacity assumes a larger role in determining the operating frequency, and since the frequency stability is adversely affected, this parameter will vary with changes in electrode potentials and tube aging.

High-frequency crystal-controlled signals may be obtained by using a parallel-mode oscillator in conjunction with suitable frequency multiplying circuits. By this means, stable signals have been obtained in the microwave region. However, the efficiency of harmonic generators is low, and many stages of multiplication are required to obtain even moderately high frequencies. Moreover, it is difficult to avoid the production of undesired frequencies.

With presently available components, series-resonant oscillators may be constructed up to 150 Mc using overtones up to the seventh or ninth. At the high frequency limit, these circuits have reasonable stability and power output, and below 100 Mc their performance is at least comparable to that of parallel-resonant oscillators at much lower frequencies. The series-resonant circuits are reasonably simple to design, adjust and operate. For these reasons, series-resonant operation is favored for high frequencies.

B. Circuit Arrangements.

The overtone oscillator circuits described herein may be classified in

two groups on the basis of the number of feedback loops. The first group, the single feedback-loop circuits, may be divided into two sub-classes by the manner in which the crystal controls the feedback. These two sub-classes are the impedance-inverting circuits, and the circuits having the crystal in series with the feedback loop. The circuits representing this latter sub-class are presented in Figures 5.1 through 5.5. These circuits may all be regarded as variations of the transformer-coupled circuit. In each, the inductances antiresonate the associated capacitances at the series resonant frequency of the crystal and the value of the resistors (R_2 , R_3) are selected so as not to degrade seriously the crystal Q. The loop gain is adjusted so that sufficient feedback to sustain oscillation can occur only when the crystal exhibits a relatively low impedance. Oscillations, therefore, occur near the series resonant frequency of the crystal. Proper phase relations are obtained in the transformer-coupled circuit by a polarity reversal in one of the transformers and in the transition oscillator by virtue of the negative suppressor-to-screen transconductance. Because the plate and cathode voltages of any grounded-grid amplifier are in phase, as are the grid and cathode voltages in a cathode follower, no polarity reversing transformer is required in the other three circuits.

The transformer-coupled, grounded-grid and cathode-coupled oscillators are satisfactory for broad-band low-power operation, as well as single-frequency high-power operation. The grounded-plate oscillator using a pentode tube is useful for frequency multiplication in electron-coupled circuits, and the transitron oscillator is capable of operating with crystals having unusually high series-resonant resistance.

Several impedance-inverting oscillators are shown in Figures 5.6 through 5.9.

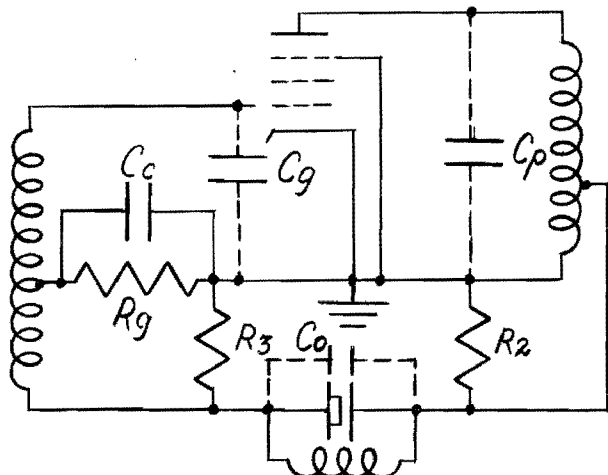


Figure 5.1 - Transformer Coupled
Oscillator

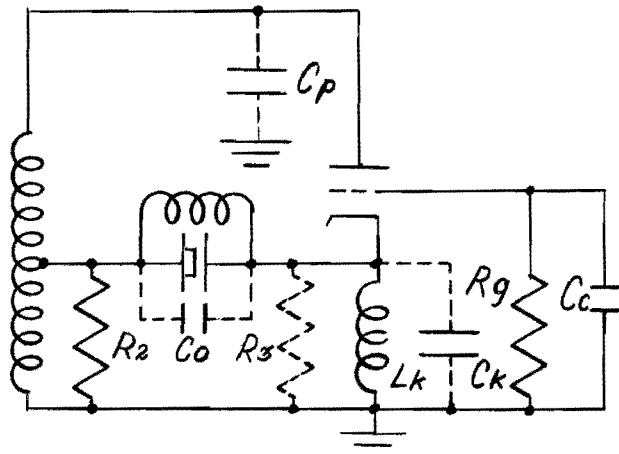


Figure 5.2 - Grounded-Grid
Oscillator

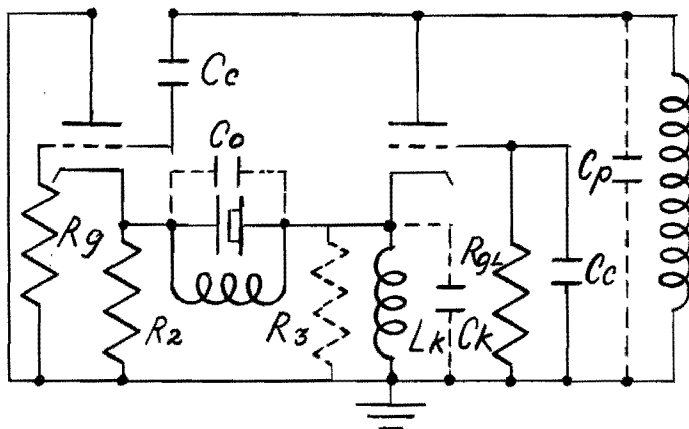


Figure 5.3 - Cathode-Coupled
Oscillator

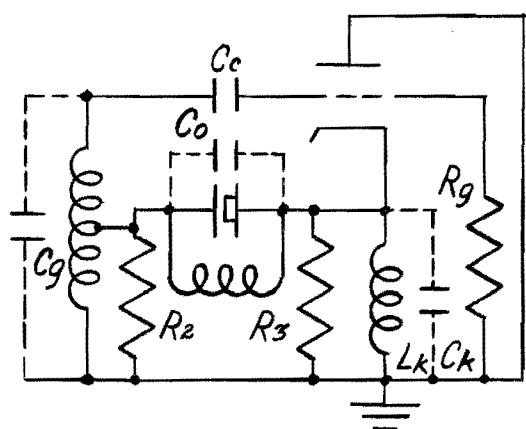


Figure 5.4 - Grounded-Plate
Oscillator

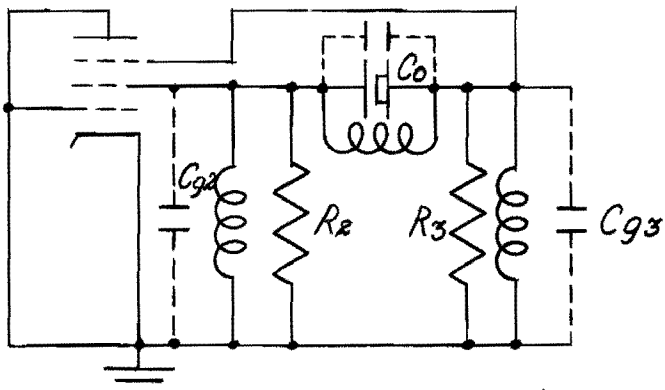


Figure 5.5 - Transitron Oscillator

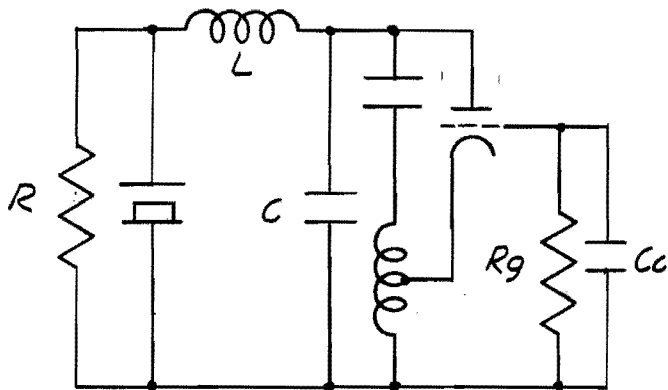


Figure 5.6 - Impedance Inverting Hartley Oscillator

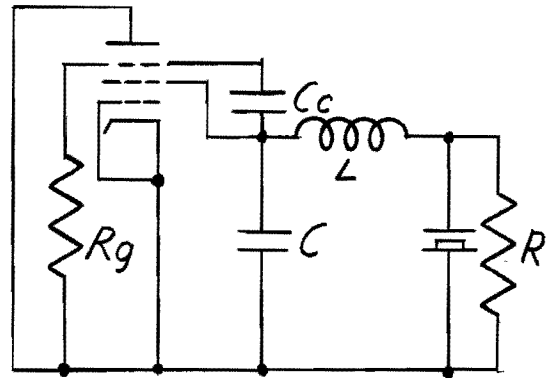


Figure 5.7 - Impedance Inverting Transitron Oscillator

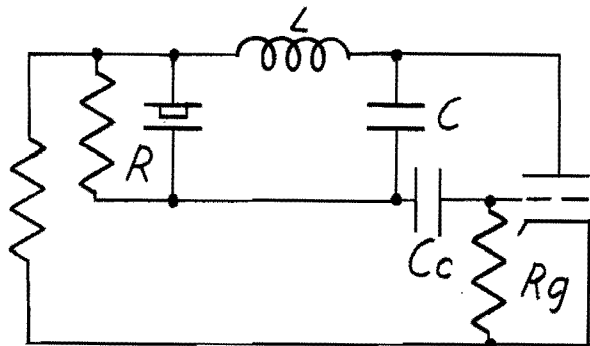


Figure 5.8 - Impedance Inverting Pierce Oscillator

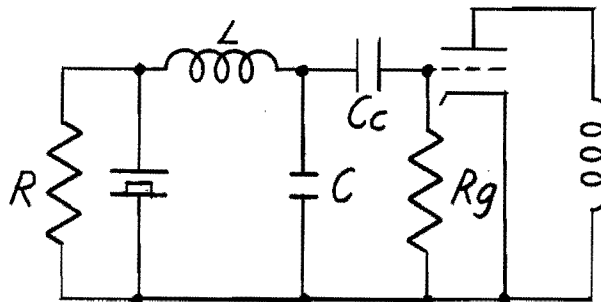


Figure 5.9 - Impedance Inverting Miller Oscillator

These circuits are characterized by moderate to low power output, good frequency stability, simplicity, and economy of components. The input capacity of the network, which is usually supplied by tube and stray capacities, limits the impedance that may be obtained from the network at high frequencies, and it is difficult to obtain satisfactory operation above 100 Mc. Since the impedance inverting network exhibits the desired properties only in a narrow band of frequencies, these circuits are not satisfactory for broadband operation.

Two circuits representative of the multiple feedback loop oscillators are shown in Figures 5.10 and 5.11.

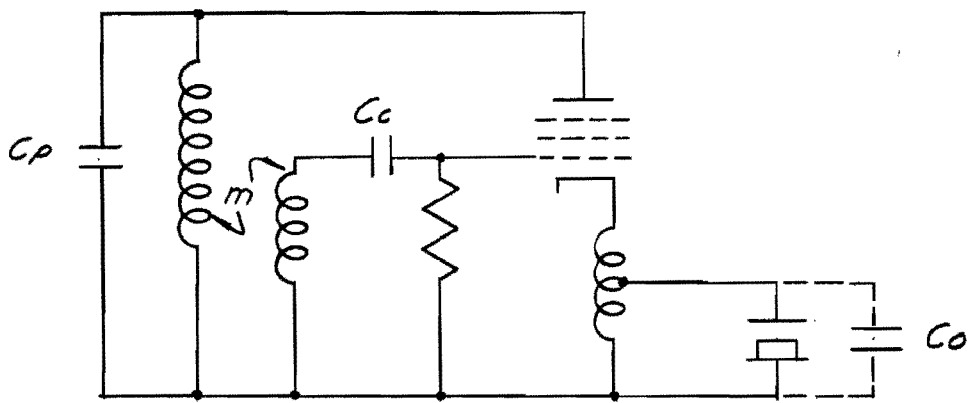


Figure 5.10 - Tuned-Plate Cathode Degenerative Oscillator

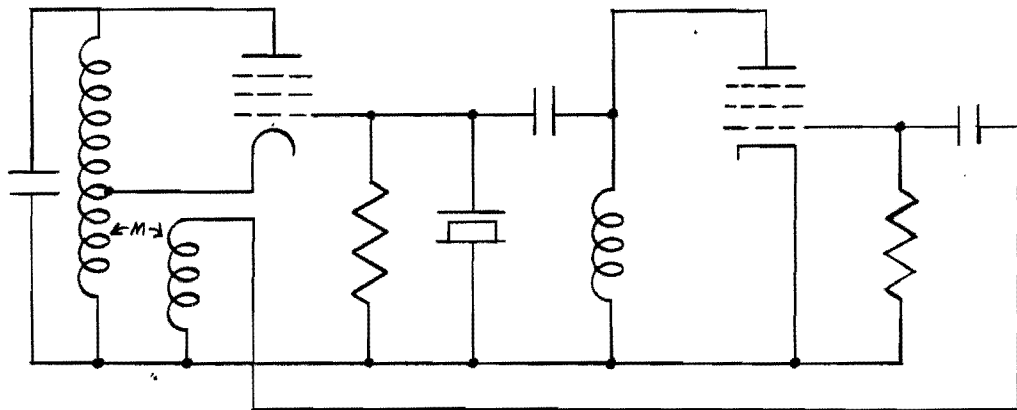


Figure 5.11 - Multitube Multiple Loop Feedback Oscillator

In these circuits, considerable positive feedback is supplied over a broad band of frequencies but control is maintained because adequate negative feedback is maintained in another loop, except at one frequency where the crystal reduces the negative feedback. Oscillation can therefore occur only under control. While these circuits can supply considerable power output, they operate under essentially the same limitations as the single-loop circuits, and are much more difficult to adjust. Since equivalent performance may be obtained from much simpler circuits, little emphasis is placed upon the multiple loop systems.

C. Advantages and Disadvantages of Series-Resonant Operation.

In the Pierce and Miller circuits, the crystal operates as an inductive reactance antiresonated by an external capacitance. The operating frequency is therefore sensitive to changes in this capacitance. In series-resonant operation the crystal appears as a low resistance and this difficulty is largely removed. If the capacitance ratio is not too high, or the Q too low, the series-resonant frequency is not greatly different from the series-arm resonant frequency, and is little affected by external capacity in shunt with the crystal. Therefore, good stability is obtained.

In military equipment, it is desirable to reduce to a minimum the number of adjustments which must be made during operation. In communication equipment where frequency changes must be made, this means that the number of associated adjustments should be held to a minimum. In the oscillator itself, the crystal at least must be replaced, but it is desirable that no other changes in this circuit should be necessary. By this means the operating procedure is simplified and the possibility of obtaining an incorrect operating frequency is minimized. This objective is met at low frequencies by the Pierce oscillator and at high frequencies by Broad-Band Untuned Oscillators.

For a circuit to be capable of operating at various crystal frequencies without retuning, the conditions of oscillation must be satisfied over the desired band when the circuit is considered without the crystal. Thus, the loop gain must be sufficient and the phase shift low over the entire band so that a crystal associated with the circuit becomes the major frequency determining element. In addition, the conditions of oscillation must be satisfied only over the desired frequency band if the circuit is to be free from tendencies to oscillate without crystal control. Circuits designed to meet these requirements have limited power output; however, their frequency stability is excellent. Two of the series-resonant overtone oscillators, the Grounded-Grid and Transformer-Coupled Circuits using special phase compensating networks, have been operated on an untuned basis over a band 20 Mc wide. However, unless special precautions are taken these circuits are limited to a frequency band of about 12 or 15 Mc.

In regard to power output, the series-mode oscillators have essentially the same limitations as the parallel-mode oscillators. In those circuits having the crystal in series with the feedback loop, the driving power for the tube must be transmitted through the crystal. Since from stability considerations the impedances faced by the crystal should be low, the power dissipated in the crystal is comparable to the driving power. The power output of the circuit is therefore determined by the power gain of the tube, the degree to which the Q of the crystal may be degraded by the impedances it faces, and by the allowable power dissipation of the crystal. A similar limitation applies to the impedance-inverting oscillators. In these, the low series-resonant resistance of the crystal is transformed into a fairly high antiresonant resistance by an impedance inverting network, as described in Chapter II. In use, the series-resonant crystal and associated network replaces the parallel-resonant crystal as used in conventional oscillators. Therefore, the driving voltage of the tube appears across the input terminals of the network. Assuming the network to be loss-free, the ratio of the power dissipated in the crystal to the driving power is determined by the ratio of the ac grid resistance to the antiresonant resistance developed by the network. Because this latter resistance is limited by circuit capacitances to values considerably below those obtained from parallel resonant crystals at low frequencies, and since for stability considerations the ac grid resistance should not be much lower than the network resistance, the available driving power is again limited by the allowable crystal dissipation.

At frequencies above 100 Mc, the holder capacity shunts the crystal making crystal control difficult to obtain. Up to 150 Mc, this difficulty has been overcome by antiresonating the holder capacity with a suitable inductance. Above this frequency, the lead and electrode loss of the crystal is usually so great that it is impossible to obtain a sufficiently large antiresonant resistance to remove the shunt effect of the holder capacity, and crystal control is not obtained.

In all high frequency circuits, tube capacities lower the impedance levels that may be obtained and lead to sharply tuned circuits which degrade

Final Report Project No. 131-45

the frequency stability. Best operation is obtained with the lowest possible capacitance levels and with circuit losses reduced to a minimum.

BIBLIOGRAPHY

1. Lister, G. H., "Overtone Crystal Oscillator Design." Electronics, 23, No. 11, 1950.

VI FREQUENCY STABILITY CONSIDERATIONS IN SERIES MODE OSCILLATORS

A. Introduction.

In crystal oscillators of all varieties, the principal requirement is that the frequency remain quite constant in spite of variations of tube parameters, circuit elements, temperature, humidity, and the passage of time. The extent to which this requirement is met is referred to as frequency stability. The causes of frequency instability may be classified into two groups: short-term variations due to changes of temperature, humidity, and potentials; and long-term variations due mainly to aging of the crystal unit. Because an investigation of crystal aging exceeding the scope of the present project, work was confined to short-term effects. For analytic purposes, it is most convenient to express frequency stability in terms of the frequency change which results from a small increment in the loop phase shift or in one of the circuit reactances. Experiments described in Appendix A show that variations in frequency with changes in phase or reactance are closely related to variations in frequency with changes in voltage. The frequency stability of a circuit, in terms of the loop phase shift B , may be defined by the equation

$$S_f = \frac{dB}{d\omega/\omega} . \quad (6.1)$$

For the present purpose, it is convenient to classify oscillators into three groups:

- (1) fixed oscillators - those which operate permanently at one frequency,
- (2) tuned oscillators - those which operate at different frequencies subject to both replacement of the crystal and readjustment of the circuit.
- (3) untuned oscillators - those which operate at different frequencies subject only to replacement of the crystal.

Untuned oscillators which can operate over a considerable range of frequencies are further identified as broadband. Generally, tuned oscillators can yield the greatest power output consistent with good frequency stability. However, the techniques which must be employed in broad-band untuned oscillators may also be used to improve the frequency stability of fixed oscillators.

The general nature of the problem may be understood in terms of Figure 6.1, in which the resonator consists of L , R , and C , and the remaining elements produce conditions conducive to sustained oscillation.

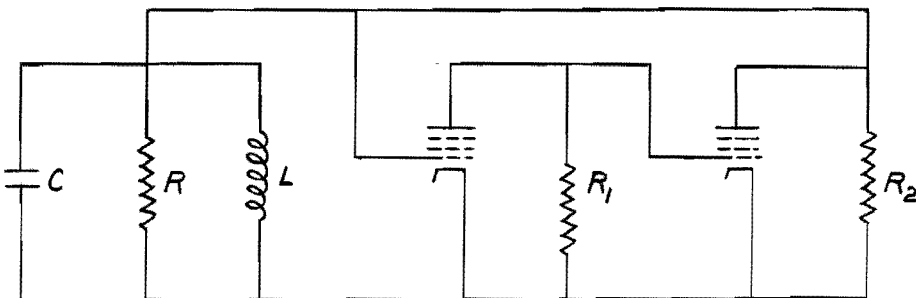


Figure 6.1 - Two-tube Oscillator

If the tubes are assumed to be ideal pentodes with infinite plate resistance, and if the interstage network represented by R_1 produces no phase shift, oscillation occurs at the natural frequency of the tuned circuit

$$\omega_0 = 1/\sqrt{LC} . \quad (6.2)$$

The resonator alone has a selectivity or unloaded Q , given by the expression

$$Q = R/\omega_0 L = \omega_0 RC . \quad (6.3)$$

In the working circuit, however, the resonator experiences an additional loading due to the effect of R_2 . The working or loaded Q is reduced to the value

$$Q_1 = RR_2/\omega_0 L(R + R_2) = \omega_0 CR_2/(R + R_2) . \quad (6.4)$$

The reduction in the resonator Q is conveniently expressed in terms of the Q degradation factor D given by the expression

$$D = Q/Q_1 = (R + R_2)/R_2 = 1 + R/R_2 . \quad (6.5)$$

This parameter has been found very useful and, with a somewhat extended interpretation, is used throughout this report.

If a phase shift dB is introduced in the interstage network R_1 , the frequency must change to restore the total loop phase shift to zero. As shown in the following section, the rate of phase shift with frequency is

directly proportional to Q_1 , the working Q. Therefore, the frequency stability, as given by 6.1, is also directly proportional to Q_1 . The desirability of a large value of Q_1 , and thus a small value of D, is obvious from this equation. (The foregoing statements assume that the interstage network is nonselective compared to the resonator; this situation always prevails in crystal oscillators.)

In the following sections we examine the rate of change of phase with frequency for frequencies near the natural frequency of the crystal. We further consider the extent to which this value is degraded by other elements. Then, evaluation of the rate of change of phase with variations of capacitance or other network properties makes possible the determination of the overall frequency stability of the oscillator.

B. Rate of Phase Change with Frequency for Crystal Series Arm Alone.

In order to compare various methods of exciting or driving the resonator it is desirable to use as a performance reference the rate of change of some phase angle. We select as this reference the phase angle of the self impedance of the series arm of the crystal equivalent circuit. Since the frequency stability is a function of the rate of phase change, $dB/d\omega$, this rate can be used to indicate the relative stability of various circuits.

The series arm of the crystal is shown in its equivalent electrical form in Figure 6.2.



Figure 6.2 - Crystal Series Arm

The impedance of the series arm is

$$Z = R_1 + j\omega L_1 + 1/j\omega C_1 . \quad (6.6)$$

The phase angle B of self impedance may be written

$$B = \tan^{-1} y . \quad (6.7)$$

where the variable y is defined as

$$y = \omega L_1/R_1 - 1/\omega C_1 R_1 . \quad (6.8)$$

Therefore, the derivative of B may be expressed as

$$\frac{dB}{d\omega} = \frac{1}{1 + y^2} \cdot \frac{dy}{d\omega} = \frac{1}{1 + \tan^2 B} \left(\frac{L_1}{R_1} + \frac{1}{\omega^2 C_1 R_1} \right). \quad (6.9)$$

The desired fractional derivative then becomes

$$\frac{dB}{d\omega/\omega} = \frac{1}{1 + \tan^2 B} \left(\frac{\omega L_1}{R_1} + \frac{1}{\omega C_1 R_1} \right) = \frac{Q}{1 + \tan^2 B} \left(\frac{\omega}{\omega_o} + \frac{\omega_o}{\omega} \right), \quad (6.10)$$

where the selectivity Q is introduced from the basic relationship

$$Q = \omega_o L_1 / R_1 = 1 / \omega_o C_1 R_1, \quad (6.11)$$

and the natural frequency is given by

$$\omega_o = 1 / \sqrt{L_1 C_1}. \quad (6.12)$$

Moreover, in the cases of present interest where Q is relatively high, ω and ω_o are nearly equal so that 6.10 may be simplified to the form

$$\frac{dB}{d\omega/\omega} \approx \frac{2Q}{1 + \tan^2 B}. \quad (6.13)$$

This is an important equation because it shows that the maximum possible rate of change of phase shift occurs at the natural frequency for which $\tan B = 0$. At any other frequency a phase shift is produced, and the frequency stability represented by 6.13 is degraded from its maximum value due to a factor which may be written

$$D = 1 + \tan^2 B. \quad (6.14)$$

Therefore, a crystal without shunt capacitance or parasitic resonances could be operated at a phase angle of 45° with only a 2:1 loss in frequency stability. In practice crystals are not free from additional resonances, and it is desirable to limit the phase angle to a somewhat smaller value, such as 20° . The effects of shunting capacitance is treated in a later section.

C. Effect of Shunt Resistance on the Rate of Change of Phase Shift of a Crystal Operated in the Series Mode.

In many applications it is necessary to compensate the shunt capacity of a crystal, especially for operation at high overtones. One method of capacity compensation is to place across the crystal a coil (or network)

which resonates with the shunt capacity and causes the series arm to face a pure resistance R_s . In order that the circuit shall not tend to oscillate at some frequency where the compensation is not fully effective, it is necessary that the compensation be effective over a rather broad frequency band. It is desirable that the compensating network have a frequency bandwidth at least as great as the frequency interval over which the loop gain of the associated oscillator exceeds unity. If a shunt network is used to compensate, it must have a rather low impedance to achieve the frequency bandwidth required in some applications. Thus, the apparent resistance, R_s , shunting the crystal may be of the same order of magnitude as the crystal resistance, R_1 , and a question arises as to the effect of R_s upon frequency stability.

If the compensating network is of fairly wide bandwidth, its impedance variation with frequency in the neighborhood of crystal resonance is small. Thus, in the neighborhood of crystal resonance, the crystal and compensating network can be represented as in Figure 6.3 where the compensating network is shown as the resistance, R_s .

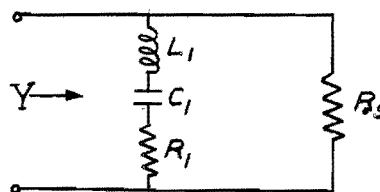


Figure 6.3 - Equivalent Circuit of Crystal and Compensating Network in the Neighborhood of Resonance

The total admittance is given by the equation

$$Y = |Y| \angle B = \frac{1}{R_s} + \frac{1}{R_1 + j(\omega L_1 - 1/\omega C_1)} = \frac{1}{R_s} + \frac{1}{R_1 [1 + jQ(\omega/\omega_0 - \omega_0/\omega)]}. \quad (6.15)$$

Introducing the new variable

$$1 + x = \omega/\omega_0 \quad (6.16)$$

and recalling that if x is small

$$1 + x \approx 1/(1 - x), \quad (6.17)$$

one may rewrite equation 6.15 as

$$Y = \frac{1}{R_s} + \frac{1}{R_1(1 + j2Qx)} . \quad (6.18)$$

Rationalization of this expression yields

$$Y = \frac{R_1(1 + 4Q^2x^2) + R_s - j2QR_s x}{R_1 R_s (1 + 4Q^2x^2)} . \quad (6.19)$$

Thus, the phase angle B of the self-admittance is

$$B = \tan^{-1} y = \tan^{-1} \left[\frac{-2QR_s x}{R_1(1 + 4Q^2x^2) + R_s} \right] . \quad (6.20)$$

Reuse of 6.9 then yields

$$\frac{dB}{d\omega} = \frac{-1}{1 + \tan^2 B} \frac{2QR_s R_1 [(1 + 4Q^2x^2) + R_s] dx/d\omega - 16R_1 R_s Q^3 x^2 dx/d\omega}{[R_1(1 + 4Q^2x^2) + R_s]^2} . \quad (6.21)$$

But, from 6.16,

$$\frac{dx}{d\omega} = \frac{1}{\omega_0} . \quad (6.22)$$

Therefore at the natural frequency where $\omega = \omega_0$, $x = 0$, and one has

$$\frac{dB}{d\omega} = \frac{-2QR_s}{(R_1 + R_s)\omega_0} , \quad (6.23)$$

and the fractional derivative becomes

$$\frac{dB}{d\omega/\omega_0} = - \frac{2QR_s}{R_1 + R_s} . \quad (6.24)$$

Thus the effective Q degradation due to R_s is

$$D = (R_s + R_1)/R_s = 1 + R_1/R_s . \quad (6.25)$$

It is easy to see that values of R_s a few times larger than R_1 will result in only a small loss in frequency stability. If R_s exceeds $5R_1$, the degradation of the effective Q is less than 20 per cent. Values of R_s can be chosen so as to prevent any tendency toward spurious oscillations and to provide capacity compensation without appreciably affecting the frequency

stability.

D. Crystal with Shunt Capacitance.

The complete equivalent circuit of a crystal (with single response) is shown in Figure 6.4.

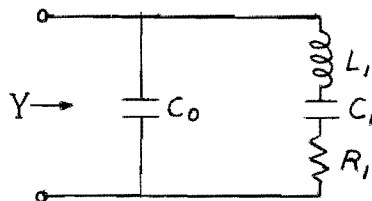


Figure 6.4 - Crystal Equivalent Circuit

By analogy with 6.18, one may write for its self-admittance the expression

$$Y = |Y| \angle B = j\omega C_0 + \frac{1}{R_1(1 + j2Qx)} . \quad (6.26)$$

Rationalization yields

$$Y = j\omega C_0 + \frac{1 - j2Qx}{R_1(1 + 4Q^2x^2)} . \quad (6.27)$$

From this, we may write as the phase angle of self-admittance

$$B = \tan^{-1} y = \tan^{-1} [R_1 \omega C_0 (1 + 4Q^2x^2) - 2Qx] . \quad (6.28)$$

Introduction of the crystal capacitance ratio

$$r = C_0/C_1 \quad (6.29)$$

together with 6.11 and 6.16, reduces 6.28 to the form

$$B = \tan^{-1} [(1 + x)(1 + 4Q^2x^2)r/Q - 2Qx] . \quad (6.30)$$

In the present case, unlike those previously treated, the phase angle is not zero at the natural frequency of the series arm, but the value of x yielding zero phase angle may be found by setting 6.30 equal to zero. Neglecting x in comparison to one yields

$$4Q^2x^2r - 2Q^2x + r = 0 . \quad (6.31)$$

Solution by quadratic formula gives

$$x = \frac{2Q^2 \pm \sqrt{4Q^4 - 16Q^2r^2}}{8Q^2r} = \frac{1 \pm \sqrt{1 - (2r/Q)^2}}{4r}. \quad (6.32)$$

It is readily shown that the positive sign before the radical corresponds to the high impedance of parallel resonance, and that the negative sign corresponds to the desired low impedance at resonance. Moreover, x is real only if the quantity within the radical is positive, which requires

$$Q > 2r, \quad (6.33)$$

a well known result presented by Mason and Fair¹.

Differentiating 6.30 with respect to ω subject to $B = 0$ yields

$$Q \cdot \frac{dB}{d\omega} = \left[\frac{dx}{d\omega} (1 + 4Q^2x^2)r + 8r(1 + x)Q^2x \frac{dx}{d\omega} - 2Q^2 \frac{dx}{d\omega} \right]. \quad (6.34)$$

Reuse of 6.22 yields the fractional derivative

$$\frac{dB}{d\omega/\omega_0} = \left[r/Q + 8rQx + 12rQx^2 - 2Q \right]. \quad (6.35)$$

If, as is desirable and usually the case

$$Q \gg 2r, \quad (6.36)$$

one may expand 6.32 in binomial series and neglect all but the first two terms to obtain

$$x \approx r/2Q^2. \quad (6.37)$$

Substitution of this value in 6.35 yields

$$\frac{dB}{d\omega/\omega_0} = \left[r/Q + 4r^2/Q + 3r^3/Q^2 - 2Q \right]. \quad (6.38)$$

Subject to 6.36, the second term is large compared to the first and third; therefore, the reduction of the phase derivative corresponds to a Q degradation of

$$D = 1/(1 - 2r^2/Q^2). \quad (6.39)$$

Because this result depends upon 6.36, it follows that the Q degradation due to C_o is small in most practical cases. However, C_o does provide a path through which uncontrolled oscillations may take place. Moreover, the maximum inductive phase angle which the crystal may provide is considerably reduced by C_o , even when 6.36 is satisfied. This situation restricts the phase shift

which may be tolerated in the rest of the circuit.

In summary, crystals can usually be operated at overtones up to the fifth without capacity compensation, especially in tuned oscillators. In broadband untuned oscillators, especially those using high overtones, it is usually necessary to employ some form of compensating circuit.

E. Crystal Driven in the Series Mode Between Pure Resistances.

Many overtone oscillator circuits utilize the crystal as a series element in the feedback loop. A typical example of this method of driving the crystal is shown in Figure 6.5.

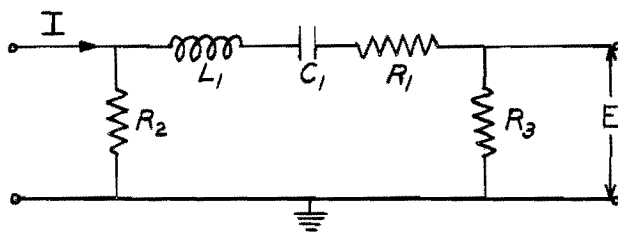


Figure 6.5 - Compensated Crystal Driven Between Fixed Resistances

It is assumed that the crystal capacity has been compensated, or that its effect is negligible and that the crystal works into pure resistance loads. The effect of a compensating network may be included by considering the crystal to have an effective Q somewhat less than its natural Q. We first determine the relation between R_2 and R_3 which leads to a minimum transmission loss and then find the Q degradation caused by R_2 and R_3 . The desired relation between R_2 and R_3 may be conveniently found at the fixed frequency $\omega_0 = 1/\sqrt{L_1 C_1}$, since at this frequency the crystal impedance reduces to the resonant resistance, R_1 . Then

$$\frac{E}{I} = \frac{R_2(R_1 + R_3)}{R_2 + R_1 + R_3} \cdot \frac{R_3}{R_1 + R_3} = \frac{R_2 R_3}{R_1 + R_2 + R_3} . \quad (6.40)$$

We show later that if a fixed Q degradation is to be maintained, the sum of R_2 and R_3 must be held constant. To represent this condition let

$$R_2 + R_3 = R_4, \text{ or } R_3 = R_4 - R_2 . \quad (6.41)$$

To maximize 6.40 with respect to R_2 , we take the derivative

$$\frac{d(E/I)}{dR_2} = 0 = \frac{R_4 - 2R_2}{R_4 + R_1} . \quad (6.42)$$

Therefore, for a minimum transmission loss consistent with a fixed value of Q degradation, one has

$$R_4 = 2R_2, \text{ or } R_2 = R_3 . \quad (6.43)$$

This balanced condition is desirable when the widest possible band must be secured in an untuned oscillator, but it leads to a relatively low value of power output.

Attention is now turned to the Q degradation due to R_2 and R_3 , and to its effect upon the frequency stability of the system. Let $R_2 = R_3 = R$. The transfer impedance, from input to output, is

$$Z_T = \frac{E}{I} = |Z| \underline{B} = \frac{R}{2R + R_1 + j(\omega L_1 - 1/\omega C_1)} , \quad (6.44)$$

where

$$B = -\tan^{-1} \frac{\omega L_1 - 1/\omega C_1}{R_1 + 2R} = -\tan^{-1} \frac{Q(\omega/\omega_0 - \omega_0/\omega)}{1 + 2R/R_1} = -\tan^{-1} \frac{2Qx}{1 + 2R/R_1} . \quad (6.45)$$

Thus at the natural frequency

$$\frac{dB}{d\omega/\omega_0} = \frac{dB}{dx} = \frac{-2Q}{1 + 2R/R_1} . \quad (6.46)$$

Therefore the effective Q degradation is

$$D = 1 + 2R/R_1 . \quad (6.47)$$

It is easily seen that as R is made small, the Q degradation decreases but at the expense of increased transmission loss. For example, if $R = R_1$ (approximately the optimum condition obtainable with present tubes and crystals), the Q is degraded by a factor of three. It should be noted that the addition of R_s , as in the previous section, will decrease the insertion loss but at the expense of a further degradation of the effective Q.

F. Crystal Driven by an Impedance Inverting Network.

Two methods of exciting the crystal are used in the oscillator circuits of this report. In one method the crystal is used as a series element in the

feedback path; in the other method, the crystal is used to terminate an impedance inverting network and thus produces a suitable equivalent antiresonance. The frequency stability of the first case was considered above; it remains to investigate the effect of crystal impedance-inverting networks on frequency stability. An impedance inverting network is shown in Figure 6.6 where C_n includes the tube capacity.

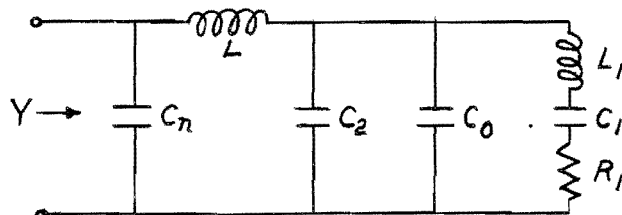


Figure 6.6 - Crystal Impedance Inverting Network

In an earlier chapter we have shown that the phase angle of the impedance presented to the tube has its maximum rate of change when this network is the lumped-circuit equivalent of a quarter-wavelength transmission line, although the impedance presented to the tube is higher for other network element values. In a network of the equivalent line type, the characteristic impedance is given by the expression

$$Z_o = \omega_o L = 1/\omega_o C = \sqrt{L/C} , \quad (6.48)$$

provided

$$C_n = C_2 + C_o = C , \quad (6.49)$$

and using the usual definition $\omega_o^2 = 1/L_1 C_1$. Because the selectivity of the crystal is high, the characteristic impedance of the line is substantially constant over the frequency interval of interest. Therefore, the admittance presented to the tube is given to an excellent approximation by the expression

$$Y = (R_1 + j\omega L_1 + 1/j\omega C_1)/Z_o^2 . \quad (6.50)$$

Because this equation is similar to 6.6, it follows that the line does not degrade the rate of phase change with frequency. Moreover, it is clear that a resistance in shunt with the crystal degrades the effective selectivity in accordance with (6.25). In the event that a conductance due to the tube or

circuit is shunted across C_n , the Q degradation may be expressed by a similar equation. Because the effective Q of a crystal impedance-transforming network can approach the crystal Q, oscillators utilizing impedance inverting networks may have a stability advantage over circuits which use the crystal as an element in the feedback loop, provided the line parameters are relatively stable.

G. Effects of Capacity Variations on the Phase Shift of Impedance Inverting Networks.

One of the major causes of short-term frequency instabilities is the variation of tube capacities. These are particularly important at high frequencies where parasitic elements furnish the entire tuning capacitance. Capacity variations may arise as a result of the introduction of reactances because of circuit nonlinearities², as a result of a space charge redistribution, or because of the change of tube electrode spacing due to heating.

Because capacity variations probably account for much of the frequency instability of high-frequency crystal oscillator circuits, the magnitude of such effects for the two methods of crystal excitation is now investigated. The approach employed is one of determining the rate of change of phase shift with capacity, which can be combined with the rate of change of phase with frequency to give the rate of change of frequency with capacity. This approach could also be used to study the frequency stability with respect to other circuit elements.

With reference to Figure 6.6 under the normal operating conditions corresponding to (6.50), we have a pure input conductance given by

$$Y = R_1/Z_o^2 . \quad (6.51)$$

Now if C_n were increased by an increment dC_n and if the frequency did not change, the input admittance would have a phase angle

$$\text{dB} = \tan^{-1}(Z_o^2 \omega dC_n / R_1) . \quad (6.52)$$

Because a differential increment is assumed, we may use the relation $\tan B \doteq B$ to obtain

$$\frac{\text{dB}}{dC_n} = \frac{\omega Z_o^2}{R_1} . \quad (6.53)$$

Actually, the frequency does change sufficiently to reduce B to zero, and the extent of this change is found by combining (6.53) with (6.13).

Because heating, nonlinearity, space charge, etc. are likely to produce an absolute rather than a proportional change in C_n , we may conclude from (6.53) that the smallest possible value of Z_0 should be used. Reference to (6.13), subject to $B = 0$, shows that fractional frequency stability tends to be better at low than at high frequencies because of the ω factor in (6.53).

In cases where the change in C_n is most accurately expressed on a fractional basis, we may use (6.48) to obtain

$$\frac{dB}{dC_n/C_n} = \frac{Z_0}{R_1} . \quad (6.54)$$

In typical circuits, the capacitance represented by $C_2 + C_0$ is little affected by temperature, voltage, etc. Any deviations which do occur in this capacitance may be treated by an extension of the method just developed. The capacitance $C_2 + C_0$ may be thought of as part of the line, so the capacitance increment is associated with L_1 , C_1 , and R_1 operating at $B = 0$. Therefore, if the frequency did not change, the phase angle of the line terminating impedance would be, by analogy with (6.53),

$$\frac{dB}{dC_0} = \omega R_1 . \quad (6.55)$$

However, Section F showed that the phase angle of the line input impedance equals that of the terminating impedance; therefore, (6.55) may be used directly in calculating frequency stability.

H. Effect of Capacity Variations on the Phase Shift of Transformer Networks.

The incremental phase shift produced by a small change of capacitance in a transformer-coupled oscillator may be determined from Figure 6.7.

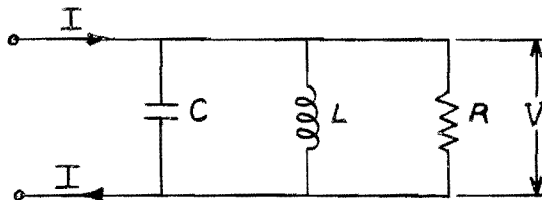


Figure 6.7 - Elementary Output Transformer

For the input admittance, one may write

$$Y = 1/R + j\omega C + 1/j\omega L . \quad (6.56)$$

The phase angle of V with respect to I is

$$B = \tan^{-1} R(1/\omega L - \omega C) = \tan^{-1} \frac{-R\omega}{1 + \tan^2 B} . \quad (6.57)$$

Now if the capacitance is increased by an increment dC , the phase angle of V with respect to I is modified according to the relation

$$\frac{dB}{dC} = \frac{-R\omega}{1 + \tan^2 B} . \quad (6.58)$$

Ordinarily, in the interest of obtaining maximum loop gain, the circuit is adjusted so that $\omega L = 1/\omega C$, and $\tan B = 0$.

The fractional derivative, which is often useful, is obtained by multiplying through by C. The resulting expression is

$$\frac{dB}{dC/C} = \frac{-R\omega C}{1 + \tan^2 B} . \quad (6.59)$$

The foregoing equations were derived for an extremely simple circuit; however, we shall now demonstrate that they apply to a very wide class of networks. First, let the load be separated from L and C by a loss-free, constant-resistance, phase-shifting network. The input phase shift and hence the transfer phase shift of the entire system is still correctly described by (6.58) and (6.59). Next, let an ideal transformer be inserted at any point in the system. Provided the elements to the right of the transformer are readjusted to account for the impedance transformation ratio, the system behavior is unchanged, and (6.58) and (6.59) still apply, provided R is properly interpreted.

Finally, an inductance in series with R (which might correspond to leakage inductance in a physical transformer) may be accounted for by converting from a series to a parallel form of circuit. In general, the equivalent load resistor R is not equal to the actual load resistor, and the input phase angle may not be zero; however, the foregoing equations still govern the transfer phase shift when properly applied.

I. Evaluation of the Frequency Stability of Oscillator Circuits to Capacity Variations.

Separate relations have been developed which govern the rate of change of

phase with frequency and with capacity for transformer and impedance inverting network methods of exciting the crystal. For each method of crystal excitation the corresponding pair of relations can be combined to give the rate of change of frequency with capacity.

For the impedance-inverting network method of crystal excitation, subject to the typical conditions $C_n = C_2 + C_o = C$, and $\omega = \omega_o$, the relations are

$$\frac{dB}{d\omega/\omega_o} \doteq 2Q , \quad (6.60)$$

and

$$\frac{dB}{dC/C} \doteq \frac{Z_o}{R_1} \quad (6.61)$$

Eliminating dB between these equations to obtain the fractional change in frequency which results from a fractional change in the line capacity one has

$$\frac{d\omega/\omega_o}{dC/C} = \frac{Z_o}{2QR_1} = \frac{1/\omega_o C}{2\omega_o L_1} = \frac{C_1}{2C} . \quad (6.62)$$

Therefore, each per cent change in input capacity to the equivalent line results in about $C_1/2C$ per cent change in frequency.

In the event that the capacitance increment is absolute rather than proportional, we may divide 6.62 by C to obtain

$$\frac{d\omega/\omega_o}{dC} = \frac{C_1}{2C^2} . \quad (6.63)$$

The importance of a low-impedance line is further emphasized by the squared term in the denominator. It should be remembered that these results are based on a linear analysis which neglects the effects of any harmonic current. Also, they give only the rate of change of frequency. If the capacity change were large, the corresponding frequency change would be larger than the predicted value because the rate of phase change with frequency is greatest near ω_o .

In high-frequency impedance-inverting oscillator circuits, the crystal shunt capacity C_o usually furnishes one of the line capacities without external padding capacitors. The input capacity to the line section equals the output

capacity of the line, so C is often approximately equal to C_0 in high frequency circuits, where low capacity values are required to achieve the necessary impedance levels. Thus, if $C = C_0$,

$$\left. \frac{d\omega/\omega_0}{dC/C} \right|_{\omega = \omega_0} \stackrel{?}{=} \frac{1}{2r}, \quad (6.64)$$

where r is the crystal capacity ratio.

If the crystal is excited by a transformer network, the rate of change of phase at $\omega = \omega_0$ is

$$\frac{dB}{d(\omega/\omega_0)} = \frac{2Q}{D}, \quad (6.65)$$

where Q is the selectivity of the crystal and $D = 1 + 2R/R_1$ is the effective Q degradation. Likewise, if the output transformer is tuned to ω_0 , 6.58 reduces to

$$\frac{dB}{dC} = -R\omega_0. \quad (6.66)$$

Combination to eliminate dB yields

$$\frac{d\omega/\omega}{dC} = \frac{-DR\omega_0}{2Q}. \quad (6.67)$$

If the change in C is fractional rather than absolute, we should use 6.55 rather than 6.58, in which case, we obtain

$$\frac{d\omega/\omega}{dC/C} = \frac{-DR\omega_0 C}{2Q}. \quad (6.68)$$

It is seen that C should be held to the minimum possible value if the deviations are proportional to C ; and D and R should be minimized in any case. Because the fractional frequency deviation is proportional to ω_0 , it is difficult to maintain a high degree of frequency stability at the higher operating frequencies.

BIBLIOGRAPHY

1. Mason, W. P. and Fair, I. E., "A New Direct Crystal-Controlled Oscillator for Ultra-Short-Wave Frequencies." Proc. I.R.E., 30, October (1942).
2. Groszkowski, J., "The Interdependance of Frequency Variation and Harmonic Content, and the Problem of Constant Frequency Oscillators." Proc. I.R.E. 21, 958-981, (1933).

VII POWER CONSIDERATIONS IN CRYSTAL OSCILLATORS

A. Introduction.

In oscillators where stability and broad-band operation are the primary objectives, essentially class A operation is desirable; with such operation, an analysis which assumes that the tube operates in a linear manner is satisfactory. The efficiency obtained with this type of operation, however, is quite low, and when power output is the primary objective class C operation is necessary. In this type of operation, the circuit conditions that exist when the equilibrium amplitude is reached are quite different from those under which oscillations begin. In particular, the input impedance of the tube is altered due to the flow of grid current, and the effective plate resistance is increased due to the flow of plate current in short pulses. While the difficulty of expressing these changes in analytical form hampers the analysis of this type of operation, a satisfactory design procedure is available. This procedure involves the assumption of class C operating conditions for the tube, and then the synthesis of a circuit consistent with these operating conditions. Additional consideration must be given to the power dissipated in the crystal and to those factors which adversely affect frequency stability.

B. Everitt's Approximate Method of Nonlinear Calculation.

One approximate method for designing power oscillators is to assume class A operating conditions for the tube and to proportion the circuit elements to obtain a loop gain greatly in excess of unity. Oscillations will then build up until class C conditions exist and until the limiting action of the circuit reduces the loop gain to unity. However, in this method, the final amplitude of oscillation is not specified, and the impedances faced by the crystal are not under control. A convenient and more useful approach is to specify a desired set of class C operating conditions and to proportion the circuit elements to give unity loop gain for these desired conditions. To properly proportion the circuit elements, it is necessary to investigate the performance of pertinent amplifier configurations under class C operating conditions. This method of analysis is due to Everitt¹; it assumes that the tube characteristic is a straight line with a sharp cut off and a slope equal to g_m . This

assumption introduces little error, provided the peak plate current is well below saturation.

1. Grounded-Cathode Amplifier.

Herein we derive the desired design equations for the circuit of a grounded-cathode amplifier is shown in Figure 7.1. The plate tank is anti-resonant at the operating frequency and is assumed to have negligible impedance at all harmonic frequencies. Accordingly, if transit time may be neglected, the ac grid and plate voltages are in phase-opposition, and the ac plate voltage equals $I_{p1}R_L$.

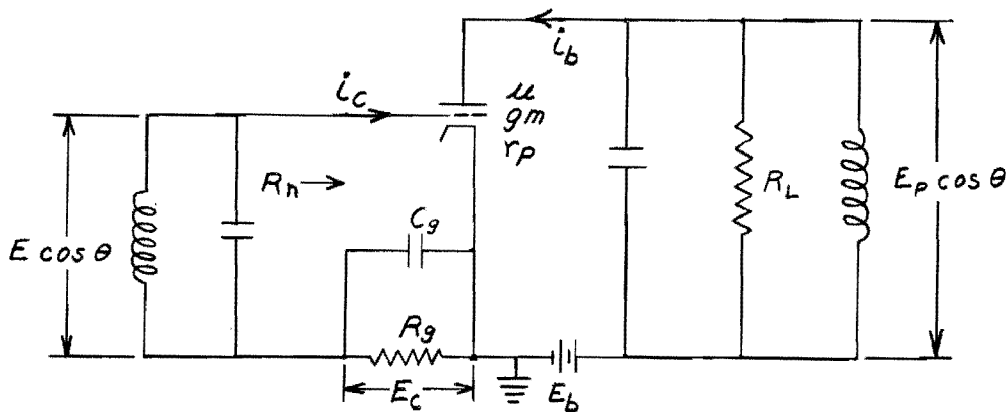


Figure 7.1 - Grounded-Cathode Amplifier

Since a linear characteristic is assumed, we may write for the instantaneous plate current

$$i_b = g_m (e_c + e_b/\mu) . \quad (7.1)$$

The instantaneous grid and plate voltages are

$$e_c = E \cos \theta - E_c , \quad (7.2)$$

and

$$e_b = E_b - E_p \cos \theta . \quad (7.3)$$

From these,

$$i_b = g_m \left[(E - E_p/\mu) \cos \theta + E_c - E_b/\mu \right] . \quad (7.4)$$

or,

$$i_b = g_m (E' \cos \theta + E_a) \quad (7.5)$$

where

$$E' = E - E_p/\mu = E - I_{pl}R_L/\mu , \quad (7.6)$$

and

$$E_a = E_c - E_b/\mu . \quad (7.7)$$

The fundamental component of plate current is given by

$$I_{pl} = \frac{2}{\pi} \int_0^{\pi} i_b \cos \theta d\theta , \quad (7.8)$$

or

$$I_{pl} = \frac{2g_m}{\pi} \int_0^{\theta_p} (E' \cos \theta + E_a) \cos \theta d\theta , \quad (7.9)$$

where θ_p (which is half the plate conduction angle) is given by

$$\theta_p = \cos^{-1}(-E_a/E') . \quad (7.10)$$

Equation 7.9 may be integrated and simplified to yield

$$I_{pl} = \frac{\mu E}{R_L + \beta_p r_p} , \quad (7.11)$$

in which

$$\beta_p = \frac{2\pi}{2\theta_p - \sin 2\theta_p} . \quad (7.12)$$

Comparing equation 7.11 with the expression for the ac component of plate current in a class A amplifier shows that the effective internal impedance of the class C amplifier equals $\beta_p r_p$, and may become quite large if the angle of conduction is small. In cases where $\beta_p r_p$ is very much greater than R_L , the fundamental component of plate current is given to a close approximation by

$$I_{pl} \approx g_m E / \beta_p . \quad (7.13)$$

The direct component (average value) of plate current may be determined from

$$I_b = \frac{1}{\pi} \int_0^{\theta_p} i_b d\theta . \quad (7.14)$$

Substitution from equation 7.5 for i_b , and integration yields

$$I_b = \frac{E g_m}{\pi} (\sin \theta_p - \theta_p \cos \theta_p) . \quad (7.15)$$

Equation 7.6 leads to further simplification, giving

$$I_b = \frac{\mu E}{\pi} \frac{\beta_p}{R_L + \beta_p r_p} (\sin \theta_p - \theta_p \cos \theta_p) . \quad (7.16)$$

Similar relations may be obtained for the grid circuit. It is assumed that the grid characteristic is a straight line having a slope equal to g_1 , the positive grid conductance. Therefore,

$$i_c = e_c g_1 , \quad (7.17)$$

As stated above, the instantaneous grid voltage is given by

$$e_c = E \cos \theta = E_c , \quad (7.18)$$

and

$$\theta_g = \cos^{-1}(E_c/E) , \quad (7.19)$$

where θ_g is equal to half the grid conduction angle. The fundamental component of the grid current is given by

$$I_{g1} = \frac{2}{\pi} \int_0^{\theta_g} i_c \cos \theta d\theta . \quad (7.20)$$

Substitution from equations 7.17 and 7.18 gives

$$I_{g1} = \frac{2g_1}{\pi} \int_0^{\theta_g} (E \cos \theta - E_c) \cos \theta d\theta . \quad (7.21)$$

Integration and the use of equation 7.19 yield

$$I_{g1} = \frac{g_1 E}{2\pi} (2\theta_g - \sin 2\theta_g) , \quad (7.22)$$

or,

$$I_{g1} = g_1 E / \beta_g \quad (7.23)$$

where

$$\beta_g = \frac{2\pi}{2\theta_g - \sin 2\theta_g} . \quad (7.24)$$

In a similar manner the direct component of the grid current, I_c , may be computed

$$I_c = \frac{1}{\pi} \int_0^{\theta_g} i_c d\theta , \quad (7.25)$$

or

$$I_c = \frac{g_1 E}{\pi} \int_0^{\theta_g} (E \cos \theta - E_c) d\theta . \quad (7.26)$$

Integration and the use of equation 7.19 yield

$$I_c = \frac{g_1 E}{\pi} (\sin \theta_g - \theta_g \cos \theta_g) . \quad (7.27)$$

The bias voltage, E_c , is due to the direct component of grid current flowing through R_g , therefore

$$I_c = E_c / R_g = E \cos \theta_g / R_g . \quad (7.28)$$

Eliminating I_c between (7.27) and (7.28), and replacing g_1 by $1/r_g$, yield

$$R_g = \frac{\pi r_g}{(\tan \theta_g - \theta_g)} , \quad (7.29)$$

an expression which may be used to compute the grid leak resistance when the positive grid resistance and θ_g are known.

The effective input resistance of the tube is given by

$$R_n = E / I_{gl} = r_g \beta_g . \quad (7.30)$$

This expression may be used to compute the input resistance, but, since β_g varies rapidly with θ_g , a more satisfactory expression may be obtained by combining equations 7.24, 7.29, and 7.30. From these one has

$$\frac{R_n}{R_g} = \frac{(\tan \theta_g - \theta_g)}{(\theta_g - \sin \theta_g \cos \theta_g)} . \quad (7.31)$$

Since the expressions for β_p and β_g have the same form, a single tabulation of β as a function of θ will suffice for use in both cases. This and the ratio R_n/R_g as given by equation 7.31 are presented in Table 7.1.

TABLE 7.1

β and R_n/R_g Versus θ

θ	β	R_n/R_g	θ	β	R_n/R_g
0°	infinity	0.500	50	8.26	0.839
5	7100	0.504	55	6.41	0.953
10	891.7	0.509	60	5.12	1.113
15	266.3	0.521	65	4.18	1.344
20	113.5	0.538	70	3.49	1.693
25	58.9	0.562	75	2.97	2.290
30	34.68	0.594	80	2.56	3.495
35	22.28	0.633	85	2.25	7.12
40	15.27	0.685	90	2.00	infinity
45	11.01	0.752	180	1.00	-----

It should be noted that the foregoing method of calculating the input resistance of the tube does not consider the input loading due to transit time effects. The high-frequency input resistance is therefore equal to R_n , as given by equation 7.31, in parallel with the input resistance due to transit time loading. This latter resistance, which is approximately equal to 25,000 ohms for a type 6AK5 tube at 50 Mc², has considerable influence on the input resistance that may be obtained at high frequencies. Furthermore, the calculation of R_n is based on Figure 7.1, in which no ac voltage appears across R_g . If the grid leak resistance is connected directly from grid to cathode, an additional loss is incurred and the required driving power is increased. This situation is undesirable because in an oscillator circuit it tends to decrease the ratio of the power in the load to that in the crystal.

2. Grounded-Grid Amplifier.

An analysis similar to that of the grounded-cathode amplifier is applicable to the grounded-grid circuit shown in Figure 7.2.

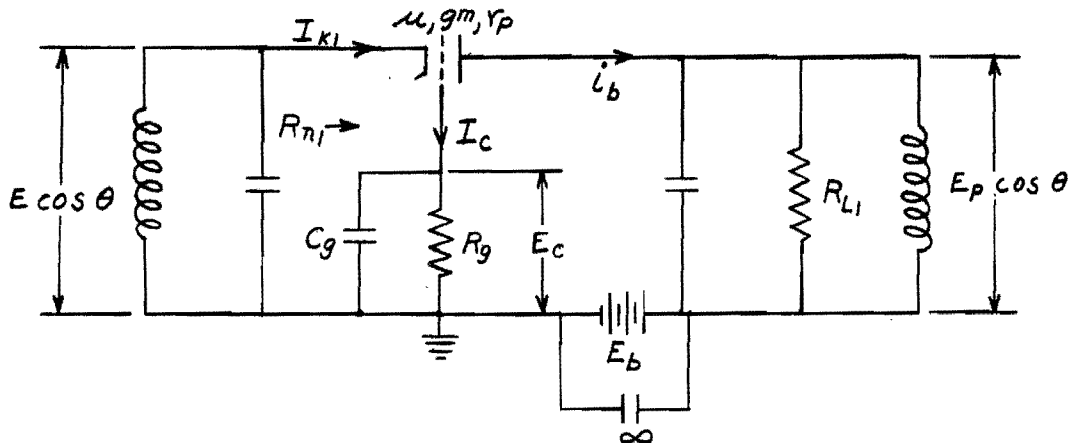


Figure 7.2 - Grounded Grid Amplifier

From the assumption that the tube has a linear characteristic, we write

$$i_b = g_m (e_c + e_b / \mu) . \quad (7.32)$$

If the cathode to plate transit time is negligible, and the cathode and plate circuits are antiresonant at the operating frequency, the input and output voltages will be in phase. Therefore,

$$e_b = E_b - E_p \cos \theta + E \cos \theta . \quad (7.33)$$

The instantaneous grid voltage is

$$e_c = E \cos \theta - E_c . \quad (7.34)$$

Substitution of equations 7.33 and 7.34 in equation 7.32 gives

$$i_b = g_m \left[E_b / \mu - E_c + (E + E / \mu - E_p / \mu) \cos \theta \right] . \quad (7.35)$$

If, for convenience, we set

$$E_1 = E_b / \mu - E_c , \quad (7.36)$$

and

$$E_2 = E(1 + 1/\mu) - E_p / \mu , \quad (7.37)$$

equation 7.35 becomes

$$i_b = g_m (E_1 + E_2 \cos \theta) . \quad (7.38)$$

The fundamental component of the plate current may be written as

$$I_{pl} = \frac{2g_m}{\pi} \int_0^{\theta_p} (E_1 + E_2 \cos \theta) \cos \theta d\theta , \quad (7.39)$$

in which

$$\theta_p = \cos^{-1}(-E_1/E_2) . \quad (7.40)$$

Integration and simplification of equation 7.39 yield

$$I_{pl} = \frac{E(\mu + 1)}{(\beta_p r_p + R_{Ll})} \doteq g_m E / \beta_p . \quad (7.41)$$

The ac component of the cathode current, I_{kl} , is equal to $(I_{pl} + I_{gl})$ where I_{gl} is the ac component of the grid current. Since I_{pl} is much larger than I_{gl} , the input resistance of the tube is given to a close approximation by

$$R_{nl} \doteq E/I_{pl} . \quad (7.42)$$

Eliminating E between 7.41 and 7.42 gives

$$R_{nl} \doteq (\beta_p r_p + R_{Ll}) / (\mu + 1) . \quad (7.43)$$

In cases where $\mu \gg 1$ and $\beta_p r_p \gg R_{Ll}$, this may be reduced to

$$R_{nl} \doteq \beta_p / g_m . \quad (7.44)$$

This expression is recognized as the approximate input resistance of a class A grounded-grid amplifier multiplied by β_p . Since the input resistance in this case is relatively low, transit time loading need not be considered.

The direct component of the plate current is given by

$$I_b = \frac{g_m}{\pi} \int_0^{\theta_p} (E_1 + E_2 \cos \theta) d\theta . \quad (7.45)$$

After integration, this may be simplified, using the approximation that $\mu \gg 1$, to yield

$$I_b \doteq \frac{E(\mu \beta_p)}{\pi(\beta_p r_p + R_{Ll})} (\sin \theta_p - \theta_p \cos \theta_p) . \quad (7.46)$$

While the input resistance of a grounded-grid amplifier is determined largely by the plate circuit conditions and the transconductance g_m , the grid circuit relations developed for the grounded-cathode amplifier may be applied to determine the grid leak resistance in terms of the positive grid

resistance and the grid conduction angle. For the grounded-grid amplifier

$$\theta_g = \cos^{-1} E_c / E , \quad (7.47)$$

and equation 7.29, which is re-stated here for convenience, may be used with the above value of θ_g to compute the value of R_g .

$$R_g = \frac{\pi r_s}{\tan \theta_g - \theta_g} \quad (7.29)$$

3. Grounded-Plate Amplifier.

Figure 7.3 shows the grounded-plate amplifier, or cathode follower.

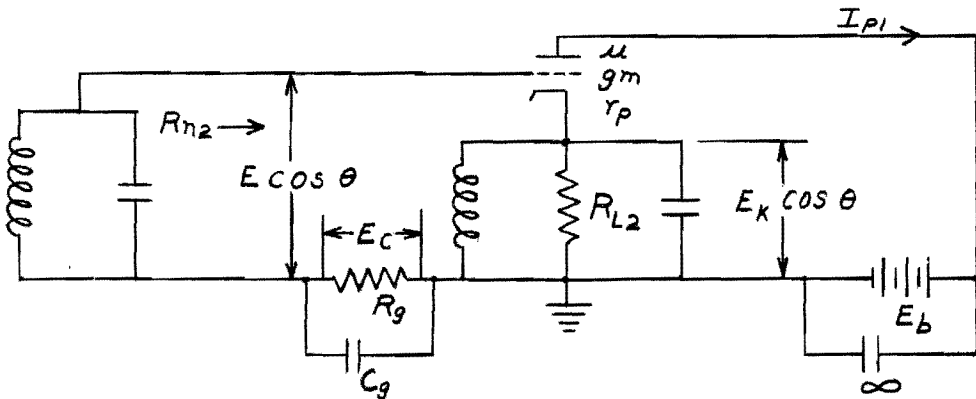


Figure 7.3 - Grounded-Plate Amplifier

If it is again assumed that the input and output circuits are antiresonant and that the tube has a linear characteristic, the following expressions may be written:

$$i_b = g_m (e_c + e_b / \mu) , \quad (7.48)$$

$$e_c = E \cos \theta - E_c - E_k \cos \theta , \quad (7.49)$$

and

$$e_b = E_b - E_k \cos \theta . \quad (7.50)$$

Combination of these gives

$$i_b = g_m (E_3 \cos \theta + E_a) , \quad (7.51)$$

where

$$E_3 = E - E_k - E_k / \mu , \quad (7.52)$$

and

$$E_1 = E_b / \mu = E_c . \quad (7.53)$$

The fundamental component of plate current is given by

$$I_{pl} = \frac{2g_m}{\pi} \int_0^{\theta_p} (E_3 \cos \theta + E_1) \cos \theta d\theta \quad (7.54)$$

where

$$\theta_p = \cos^{-1}(-E_1/E_3) . \quad (7.55)$$

Integration and simplification of 7.54 yield

$$I_{pl} = \frac{g_m E}{\beta_p + g_m R_{L2} (1 + 1/\mu)} , \quad (7.56)$$

and if $\mu \gg 1$, this becomes

$$I_{pl} \doteq \frac{g_m E}{\beta_p + g_m R_{L2}} . \quad (7.57)$$

Comparison of (7.57) with the equivalent expressions for the grounded-grid (7.41) and grounded-cathode (7.13) amplifiers shows that for a given tube and driving voltage the grounded-plate amplifier has the smallest value of I_{pl} . The direct component of plate current is given by

$$I_b = \frac{g_m}{\pi} \int_0^{\theta_p} (E_3 \cos \theta + E_1) d\theta . \quad (7.58)$$

This expression may be integrated and simplified, using equation 7.52 and 7.53, to give

$$I_b = \frac{g_m}{\pi} \left[E - E_k (1 + \mu) \right] (\sin \theta_p - \theta_p \cos \theta_p) . \quad (7.59)$$

The relations $\mu \gg 1$, and $E_k \doteq I_{pl} R_{L2}$, reduce equation 7.59 to

$$I_b = \frac{g_m E \beta_p}{\pi(\beta_p + g_m R_{L2})} (\sin \theta_p - \theta_p \cos \theta_p) . \quad (7.60)$$

In order to determine the grid circuit relations for the grounded-plate amplifier, a linear grid characteristic is again assumed. Therefore

$$i_c = g_m e_c . \quad (7.61)$$

Using equation 7.49, we obtain for the fundamental component of the grid current

$$I_{g1} = \frac{2g_1}{\pi} \int_0^{\theta_g} \left[(E - E_k) \cos \theta - E_c \right] \cos \theta d\theta , \quad (7.62)$$

where

$$\cos \theta_g = E_c / (E - E_k) . \quad (7.63)$$

Integration of (7.62) gives

$$I_{g1} = (E - E_k) / r_g \beta_g . \quad (7.64)$$

Because $E_k \doteq I_{pl}/R_{L2}$, we have

$$I_{g1} = \frac{E}{\beta_g r_g} \left(\frac{\beta_p}{\beta_p + g_m R_{L2}} \right) , \quad (7.65)$$

and

$$R_{n2} = E/I_{g1} = \beta_g r_g (1 + g_m R_{L2} / \beta_p) . \quad (7.66)$$

Similarly the expression for the dc component of the grid current,

$$I_c = \frac{1}{\pi r_g} \int_0^{\theta_g} \left[(E - E_k) \cos \theta - E_c \right] d\theta , \quad (7.67)$$

may be integrated and simplified to yield

$$I_c = \frac{E}{\pi r_g} \left(\frac{\beta_p}{\beta_p + g_m R_{L2}} \right) (\sin \theta_g - \theta_g \cos \theta_g) . \quad (7.68)$$

Because the bias voltage is due to the dc component of grid current flowing through R_g , we may write

$$I_c = \frac{E_c}{R_g} = \frac{(E - E_k) \cos \theta_g}{R_g} . \quad (7.69)$$

Use of the approximation, $E_k \doteq I_{pl}/R_L$, reduces equation 7.69 to

$$I_c \doteq \frac{E}{R_g} \left(\frac{\beta_p}{\beta_p + g_m R_{L2}} \right) \cos \theta_g . \quad (7.70)$$

Eliminating I_c between equations 7.68 and 7.69 gives

$$R_g = \pi r_g / (\tan \theta_g - \theta_g) . \quad (7.71)$$

The ratio R_{n2}/R_g may now be obtained by combining equations 7.66 and 7.71 with the expression for β_g as given by equation 7.24. The result is

$$\frac{R_{n2}}{R_g} = \frac{\tan \theta_g - \theta_g}{\theta_g - \sin \theta_g \cos \theta_g} (1 + g_m R_{L2}/\beta_p) . \quad (7.72)$$

Comparison of this equation with (7.31) which applies to the grounded-cathode amplifier, shows that the ratio R_{n2}/R_g for the grounded-plate amplifier may be obtained by multiplying the values given in Table 7.1 by the factor $(1 + g_m R_{L2}/\beta_p)$.

4. Comparison of Power Gains.

In order to evaluate the relative power-output performance of the various oscillator circuits, it is necessary to determine the relative power gains of the three amplifier configurations. To obtain a significant comparison, we assume that the same tube under the same operating conditions is used in each case.

For the grounded-cathode amplifier

$$P_L = I_{pl}^2 R_L/2 \doteq (g_m E)^2 R_L/2\beta_p^2 , \quad (7.73)$$

and

$$P_n = EI_{gl}/2 = E^2/2r_g \beta_g . \quad (7.74)$$

Defining the power gain as equal to P_L/P_n , we have

$$G_k \doteq g_m^2 R_L r_g \beta_g / \beta_p^2 . \quad (7.75)$$

For the grounded-grid amplifier the appropriate power expressions are

$$P_{Ll} = I_{pl}^2 R_{Ll}/2 \doteq (g_m E)^2 R_{Ll}/2\beta_p^2 , \quad (7.76)$$

and

$$P_{nl} = (I_{pl} + I_{gl})E/2 \doteq \left(\frac{g_m \beta_g r_g + \beta_p}{\beta_p \beta_g r_g} \right) E^2 . \quad (7.77)$$

Again the power gain is equal to P_{Ll}/P_{nl} , and therefore

$$G_g \doteq \frac{g_m^2 R_{Ll} \beta_g r_g}{\beta_p^2 + g_m \beta_p \beta_g r_g} . \quad (7.78)$$

The ratio of the power gain of the grounded-cathode amplifier to that of the grounded-grid amplifier may be obtained from equation 7.75 and 7.77. If R_L is equal to R_{L1} , then

$$\frac{G_k}{G_g} \triangleq 1 + g_m \beta_{g^r g} / \beta_p . \quad (7.79)$$

Since β_p / g_m equals the input resistance of the grounded-grid amplifier, and $\beta_{g^r g}$ equals the input resistance of the grounded-cathode amplifier,

$$\frac{G_k}{G_g} \triangleq 1 + \frac{\text{grounded-cathode input resistance}}{\text{grounded-grid input resistance}} . \quad (7.80)$$

Equation 7.80 gives the relative performance of the grounded-cathode and grounded-grid amplifiers. By determining the relative power gains of the grounded-grid and grounded-plate amplifiers, a comparison of all three circuits may be made.

If we assume that $I_{pl} \gg I_{gl}$, the power output of the grounded plate amplifier is given by

$$P_{L2} \triangleq \frac{I_{pl}^2 R_{L2}}{2} \triangleq \left(\frac{g_m E}{\beta_p + g_m R_{L2}} \right)^2 \frac{R_{L2}}{2} , \quad (7.81)$$

and the power input by

$$P_{n2} = \frac{I_{gl} E}{2} = \frac{E^2}{2 \beta_{g^r g}} \left(\frac{\beta_p}{\beta_p + g_m R_{L2}} \right) . \quad (7.82)$$

Therefore, the power gain in this case is

$$\frac{G_p}{G_g} \triangleq \frac{\frac{g_m^2 R_{L2} \beta_{g^r g}}{\beta_p^2 + g_m \beta_p R_{L2}}} . \quad (7.83)$$

Dividing equation 7.78 by equation 7.83 gives the ratio of the power gain of the grounded-grid amplifier to that of the grounded-plate amplifier. The result is

$$\frac{G_g}{G_p} \triangleq \frac{R_{L1}}{R_{L2}} \left(\frac{\beta_p + g_m R_{L2}}{\beta_p + g_m \beta_{g^r g}} \right) . \quad (7.84)$$

From this equation it is evident that if $R_{L1} = R_{L2} = \beta_{g^r g}$ the grounded-grid and grounded-plate amplifiers have equal power gains. However, if equal

power output is to be obtained from both circuits, the required driving voltage for the grounded-plate amplifier will exceed somewhat even the output voltage for the grounded-grid amplifier; consequently, for equal power outputs, the required driving voltage for the grounded-plate amplifier must exceed greatly the driving voltage for the grounded-grid amplifier. This is not a serious disadvantage at low frequencies, but due to the difficulty of obtaining high impedance circuits at high frequencies, practical considerations require that the load resistance for the grounded-plate amplifier be considerably less than that for the grounded-grid circuit. Therefore, the power gain that may be realized from the grounded-plate amplifier is even less than that which may be obtained from the grounded-grid circuit.

As shown by equation 7.80, the relative power gain of the grounded-cathode and grounded-grid amplifiers depends upon the ratio of their respective input resistances. In typical situations the input resistance of the grounded-grid amplifier is considerably lower than that of the grounded-cathode amplifier. Therefore, the latter circuit will have a considerably higher power gain. It has also been shown that the grounded-grid amplifier has a greater power gain than the grounded-plate amplifier. Hence it follows that this latter circuit is also inferior to the grounded-cathode amplifier with respect to power gain.

C. Relation Between Power Output and Power Dissipation in the Crystal.

Since crystal resonators designed for high frequency overtone operation can dissipate only small amounts of heat, it is usually found that the maximum power that may be obtained from a given crystal-controlled oscillator circuit is limited by allowable crystal dissipation. For this reason, the ratio of the load power to crystal power for a given circuit may be regarded as the "figure of merit" of that circuit as a power oscillator.

1. Circuits with Series Crystal in Feedback Loop.

a. Single Tube Circuits.

From Figures 5.1, 5.2, and 5.4 of Chapter V, it may be seen that the transformer-coupled, grounded-grid, and grounded-plate oscillators may be represented as in Figure 7.4. In this figure the transformers are assumed to be ideal and the amplifier is represented as a device having a power gain of G. For a given tube and circuit configuration, the value of G may be

numerically different for each of the three circuits.

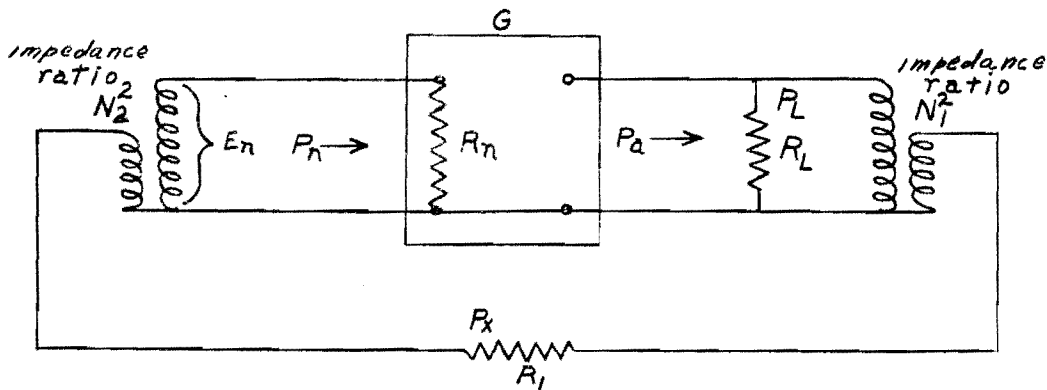


Figure 7.4 - Equivalent Circuit of the Transformer-Coupled, Grounded-Grid and Grounded-Plate Oscillators

In Figure 7.4:

$$P_a = \text{power output of amplifier} = GP_n$$

$$P_L = \text{power into load}$$

$$P_x = \text{power dissipated by the crystal}$$

$$P_n = \text{power into amplifier}$$

$$R_n = \text{input resistance of the amplifier} = E_n^2 / 2P_n$$

$$R_1 = \text{crystal resistance}$$

Conservation of power gives

$$P_a = P_L + P_x + P_n . \quad (7.85)$$

Also,

$$P_a = GP_n . \quad (7.86)$$

Since the input transformer has no losses,

$$P_x/P_n = R_1 N_2^2 / R_n . \quad (7.87)$$

The degradation of the working Q of the crystal is given exactly and approximately by

$$D = \frac{R_1 + R_n/N_2^2 + R_L/N_1^2}{R_1} \approx \frac{R_1 + R_n/N_2^2}{R_1} . \quad (7.88)$$

Eliminating P_a between (7.85) and (7.86) yields

$$P_n (G - 1) = P_L + P_x . \quad (7.89)$$

Eliminating P_a between (7.87) and (7.89) yields

$$(G - 1)P_x R_n / R_1 N_2^2 = P_L + P_x . \quad (7.90)$$

Modifying (7.88) to the form

$$(D - 1) \doteq R_n / R_1 N_2^2 \quad (7.91)$$

permits elimination of R_n and R_1 to yield

$$(G - 1)(D - 1) \doteq P_L / P_x + 1 , \quad (7.92)$$

or,

$$P_L / P_x \doteq GD - G - D . \quad (7.93)$$

Since it is desirable to keep D fairly small in the interest of frequency stability, a large power ratio is possible only if G is relatively large. As a typical example, if D equals 3 and G equals 25,

$$P_L / P_x \doteq 75 - 25 - 3 = 47 . \quad (7.94)$$

Consequently, if the crystal may safely dissipate a power of 25 milliwatts and an adequate tube is available, a power output of 1.2 watts may be obtained.

The foregoing equations indicate that good efficiency and power output may be obtained without excessively degrading the working Q of the crystal, thereby maintaining good frequency stability.

While equation 7.93 applies in general to the transformer-coupled grounded-plate, and grounded-grid oscillators, these circuits have quite different ratios of load-to-crystal power because a higher power gain may be obtained from a given tube in one configuration than in another. From the discussion of relative power gain in section B-4 of this chapter, we conclude that for the circuits considered so far, the transformer-coupled oscillator has the most favorable power ratio, the grounded-grid oscillator the next most favorable, and the grounded-plate the least favorable power ratio.

b. Cathode-Coupled Oscillator.

In the cathode-coupled oscillator, the load may be located

either in the plate circuit of the grounded-grid amplifier, the plate circuit of the cathode follower, or in the cathode circuit of the cathode follower. This latter configuration is shown in Figure 7.5.

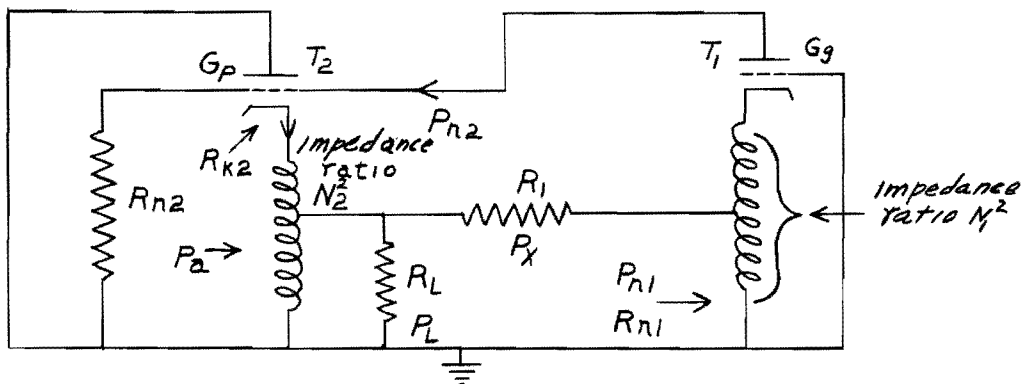


Figure 7.5 - Cathode-Coupled Oscillator with the Load in the Cathode of the Cathode Follower

In Figure 7.5:

$$P_{n2} = \text{power output of grounded-grid amplifier} = G_p P_{n1}$$

$$P_a = \text{power output of cathode follower} = G_p P_{n2}$$

$$P_L = \text{power into load resistance}$$

$$P_{n1} = \text{power input to grounded-grid amplifier}$$

$$R_{k2} = \text{resistance looking into the cathode of the cathode follower}$$

$$R_L = \text{load resistance}$$

In this circuit the input resistance of the cathode follower (grounded-plate amplifier) acts as the plate load for the grounded-grid amplifier. Physically this load consists of the effective input resistance of the tube (as determined by the grid leak resistance and grid rectification) and of the transit time loading. The load resistance (R_L) may be located either on the high or low side of the cathode transformer with identical results at a single frequency. R_{n1} is determined by the cathode impedance of the grounded-grid amplifier and the impedance ratio N_1^2 .

Again, conservation of power in Figure 7.5 gives

$$P_a = P_L + P_x + P_{n1}. \quad (7.95)$$

Also

$$P_a = G_p P_{n2} , \quad (7.96)$$

and

$$P_{n2} = G_g P_{nl} . \quad (7.97)$$

Since the transformers have no losses,

$$P_x/P_{nl} = R_1/R_{nl} . \quad (7.98)$$

The degradation of the working Q of the crystal is given by

$$D \doteq \frac{R_1 + R_{nl} + R_L}{R_1} , \quad (7.99)$$

in which

$$R_L' = \frac{R_L R_{k2}/N_2^2}{R_L + R_{k2}/N_2^2} . \quad (7.100)$$

With reference to Figure 7.5, to obtain a high ratio of output to crystal power, $R_1 + R_{nl}$ must be much larger than R_L' . Therefore the value of R_L' in (7.99) may be neglected, giving

$$D \doteq (R_1 + R_{nl})/R_1 , \quad (7.101)$$

or

$$R_{nl}/R_1 \doteq (D - 1) . \quad (7.102)$$

Eliminating P_{n2} between (7.96) and (7.97) yields

$$P_a = G_g G_p P_{nl} . \quad (7.103)$$

Eliminating P_a between (7.95) and (7.103) yields

$$P_{nl}(G_g G_p - 1) = P_L + P_x . \quad (7.104)$$

Using equation 7.98 to eliminate P_{nl} gives

$$\frac{P_x}{P_L} \doteq (G_g G_p - 1) \frac{R_{nl}}{R_1} - 1 . \quad (7.105)$$

The ratio R_{nl}/R_1 may be eliminated by the use of equation 7.102 to give the important expression

$$\frac{P_x}{P_L} \doteq G_g G_p D - G_g G_p = D . \quad (7.106)$$

If in equipment design the use of the cathode-coupled oscillator is contemplated, space and power supply for two tubes must be provided. Therefore it is of interest to determine whether or not the power ratio given by equation 7.106 is higher than that which may be obtained by using the same two tubes in a circuit consisting of a single tube oscillator followed by a power amplifier. To do this, the power ratio obtained for the single tube circuits should be multiplied by the power gain that can be obtained with tube T_2 (Figure 7.5) operating as a class C amplifier.

Because the gain of T_2 as a simple amplifier can exceed that obtained from the same tube operating as a cathode follower, the power ratio for the cathode coupled oscillator, loaded as in Figure 7.5, is less favorable than that for the transformer-coupled or grounded-grid oscillator followed by a power amplifier. As an example if G_g equals 10, G_p equals 5, and D equals 4, the power ratio of the cathode coupled oscillator is given by

$$\frac{P_L}{P_x} \doteq 200 - 50 - 4 = 146 . \quad (7.107)$$

If the two tubes are used in a grounded-grid oscillator, and grounded-cathode power amplifier combination, G_g remains the same. By using T_2 as a grounded-cathode power amplifier, its power gain may be increased some 500 per cent. Therefore, the power ratio for the oscillator-amplifier combination is

$$\frac{P_L}{P_x} \doteq 5G_p(G_g - G_g - D) = 650 , \quad (7.108)$$

which is much more favorable than that given by (7.107).

A cathode-coupled oscillator with the load in the plate circuit of the grounded-grid amplifier is shown in Figure 7.6.

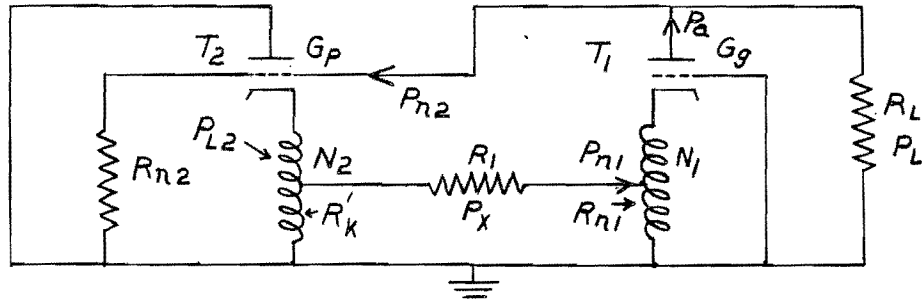


Figure 7.6 - Cathode-Coupled Oscillator with the Load in the Plate of the Grounded-Grid Amplifier

From this figure we may write

$$P_a = P_L + P_{n2} , \quad (7.109)$$

$$P_a = G_g P_{nl} , \quad (7.110)$$

$$P_{L2} = G_p P_{n2} , \quad (7.111)$$

$$P_{L2} = P_x + P_{nl} , \quad (7.112)$$

and

$$P_x/P_{nl} = R_1/R_{nl} . \quad (7.113)$$

Eliminating P_a between (7.109) and (7.110) gives

$$P_L = G_g P_{nl} - P_{n2} . \quad (7.114)$$

Eliminating P_{nl} between (7.112) and (7.113) yields

$$P_{L2} = P_x (1 + R_{nl}/R_1) . \quad (7.115)$$

From (7.114) and (7.111) we have

$$P_L = G_g P_{nl} - P_{L2}/G_p . \quad (7.116)$$

Substitution from (7.113) and (7.115) into (7.116) gives

$$\frac{P_L}{P_x} = G_g \frac{R_{nl}}{R_1} - \frac{1}{G_p} \left(\frac{R_1 + R_{nl}}{R_1} \right) . \quad (7.117)$$

As in the previous circuit, the value of R_k should be small compared to $R_1 + R_{nl}$ if a large power ratio is to be obtained. Therefore, the approximate expression for D , equation 7.101, may be used to simplify (7.32) to the following form:

$$\frac{P_L}{P_x} \approx G_g D - G_g - D/G_p . \quad (7.118)$$

In this case, the cathode follower serves largely as an impedance transforming device, and its power gain contributes little to the improvement of the power ratio. As shown by (7.118) this ratio is only slightly higher than that for the single tube circuits considered earlier. We therefore conclude that this configuration is not advantageous for use as a power oscillator.

The remaining configuration of the cathode coupled oscillator to be considered is shown in Figure 7.7. In this case the power output is taken from the plate circuit of the cathode follower, and essentially the same

current flows through R_L and R_{L2} making the ratio of load power to feedback power very nearly equal to the ratio of these two resistors. Since R_L may be very much greater than R_{L2} the power gain approximates that of a grounded-cathode amplifier. If T_2 is a pentode, sufficient isolation of the load may be obtained to give good stability in spite of variations in the load.

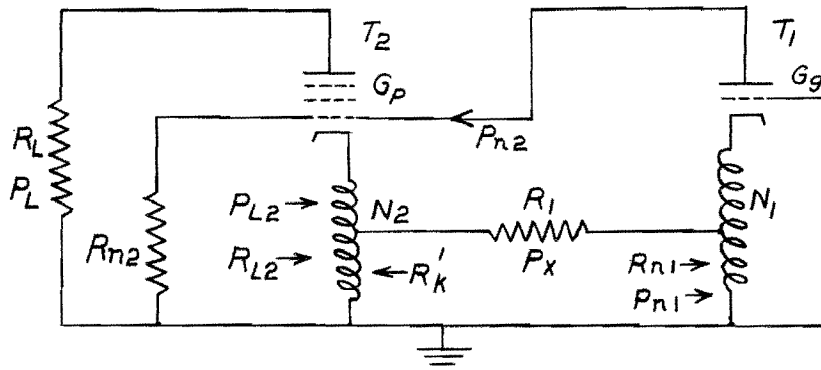


Figure 7.7 - Cathode-Coupled Oscillator with the Load in the Plate Circuit of the Cathode Follower

From Figure 7.7 the following relations are obtained:

$$\frac{G_p}{P_n 2} = P_L + P_{L2} , \quad (7.119)$$

$$P_{L2} = P_x + P_{nl} , \quad (7.120)$$

$$P_{n2} = \frac{G_p}{G_g} P_{nl} , \quad (7.121)$$

$$\frac{P_x}{P_{nl}} = R_1 / R_{nl} . \quad (7.122)$$

Combining (7.119), (7.120), and (7.121) gives

$$P_L = \left(\frac{G_g}{G_p} - 1 \right) P_{nl} = P_x . \quad (7.123)$$

Eliminating P_{nl} between 7.122 and 7.123 gives

$$\frac{P_L}{P_x} = \left(\frac{G_g}{G_p} - 1 \right) R_{nl} / R_1 = 1 . \quad (7.124)$$

Use of the approximation for D (equation 7.101) reduces 7.124 to

$$\frac{P_L}{P_x} \approx \frac{G_g}{G_p} / D = \frac{G_g}{G_p} = D . \quad (7.125)$$

The above expression is the same as that obtained for the cathode-loaded cathode follower in Figure 7.5. However, with the load in the plate circuit of the cathode follower, it is possible to obtain a power gain nearly

equal to that of a grounded-cathode amplifier if the cathode-to-ground impedance of T_2 is made small. This may be done by shunting the high side of the cathode transformer with a low resistance and compensating for the resulting loss in loop gain by an appropriate adjustment of impedance levels elsewhere in the circuit. Under these conditions the power ratio of this configuration compares favorably with that of the grounded-grid oscillator followed by a power amplifier.

2. Circuits with Crystal in Shunt with the Feedback Loop.

a. Miller Oscillator.

The power relations in the Miller oscillator are illustrated in Figure 7.8, in which R_x represents either the direct antiresonant resistance (P.I.) of the crystal, or the input resistance of an impedance inverting network associated with a series mode crystal.

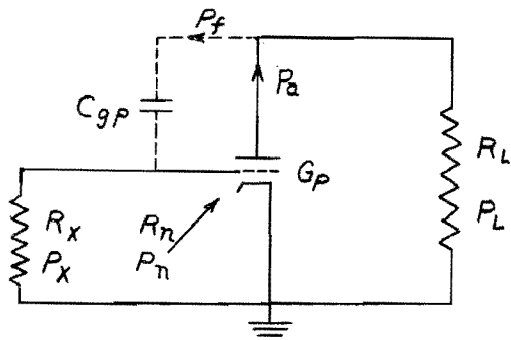


Figure 7.8 - Power Relations in the Miller Oscillator

The feedback power, P_f , is supplied through C_{gp} . Since this capacitor is usually small, the effect of R_L may be neglected in computing the degradation of the working Q of the crystal. Therefore,

$$D \doteq (R_x + R_n)/R_n . \quad (7.126)$$

Conservation of power gives

$$P_a = P_L + P_x + P_n . \quad (7.127)$$

Since the voltage applied to R_x equals that across R_n ,

$$P_x/P_n = R_n/R_x . \quad (7.128)$$

Also

$$P_a \doteq G_k P_n . \quad (7.129)$$

Using equations 8.127, 7.128, and 7.129 to eliminate P_a and P_n , we find

$$P_L/P_x \doteq G_k R_x/R_n - R_x/R_n = 1. \quad (7.130)$$

Eliminating R_x/R_n between (7.130) and (7.126) gives

$$P_L/P_x \doteq G_k D \doteq G_k = D. \quad (7.131)$$

This expression is the same as that obtained for the transformer-coupled oscillator, and indicates that the Miller oscillator can supply considerable power output. However, because the plate circuit exhibits an inductive reactance during operation, the power gain for a given tube will be lower than that obtained in the transformer coupled oscillator. In addition, the use of an input transformer in the latter circuit permits more freedom in the choice of D and in establishing the desired driving conditions for the tube.

b. Pierce Oscillator.

The parallel-mode Pierce has found wide application at frequencies up to 20 Mc, and some of its advantages are retained in the impedance-inverting series-mode overtone oscillators at higher frequencies. However, we shall show that this circuit is not well suited for use as a power oscillator.

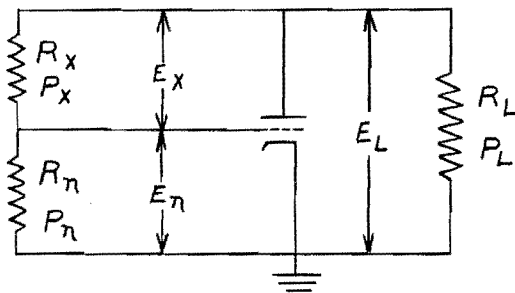


Figure 7.9 - Power and Voltage Relations in the Pierce Oscillator

Because the plate and grid voltages in Figure 7.9 are in phase opposition we have

$$E_x = E_n + E_L. \quad (7.132)$$

Also

$$P_x = E_x^2/R_x, \quad (7.133)$$

and

$$P_L = E_L^2/R_L. \quad (7.134)$$

From these, one obtains

$$\frac{P_L}{P_x} = \left(\frac{E_L}{E_L + E_n} \right)^2 \frac{R_x}{R_L}. \quad (7.135)$$

The excitation ratio for this circuit is defined as

$$h = -E_L/E_n. \quad (7.136)$$

From (7.135) and (7.136)

$$\frac{P_L}{P_x} = \left(\frac{h}{h+1} \right)^2 \frac{R_x}{R_L}. \quad (7.137)$$

The excitation ratio may vary from zero to minus infinity, and for this range of variation, the quantity $\left(\frac{h}{h+1} \right)^2$ varies from zero to plus one. Therefore, the power ratio for the Pierce oscillator is determined largely by the ratio of the antiresonant resistance of the crystal or impedance inverting network to the load resistance. From stability and power gain considerations the load resistance may not be made low, so a high value of R_x is required if a large power ratio is to be obtained.

At this stage of the analysis two of the circuits studied may be eliminated from further consideration as power oscillators, on the grounds that inefficient use is made of the available tube. These are the Pierce oscillator and the cathode-coupled oscillator with the load in the plate circuit of the grounded-grid amplifier. The other circuits show promise but have power ratios that differ considerably, principally because a higher power gain may be obtained with a given tube in the grounded cathode connection than in any other.

Of the circuits considered, the transformer-coupled is best suited for use as a power oscillator at high frequencies. For use at low frequencies where a high antiresonant resistance may be obtained directly from the crystal, the Miller circuit is the most convenient and satisfactory arrangement. The design and adjustment of the Miller oscillator is greatly facilitated by use of electron coupling. The electron-coupled form of the Miller oscillator, often referred to as the tri-tet, is capable of relatively high power output and good stability. Electron coupling also gives a considerable improvement in the performance of the Pierce oscillator; it is much less advantageous in

Final Report Project No. 131-45

those circuits which use the crystal in the series mode.

BIBLIOGRAPHY

1. Everitt, W. L., Communication Engineering. Second Edition., McGraw-Hill Book Co., Inc., New York, 1937.
2. Spangenberg, K. R., Vacuum Tubes. McGraw Hill Book Co., Inc., New York, 1948.

VIII NETWORKS FOR USE IN OSCILLATORS

A. Introduction.

A crystal oscillator ordinarily comprises a vacuum tube, a crystal resonator, and such other electrical elements as are required to produce conditions favorable to oscillation. These elements comprise one or more networks. In this chapter we describe the behavior of such networks and develop certain relations which limit the performance which may be obtained.

In conventional crystal oscillators, where the number of elements is small and the resulting networks are simple, it is practical to discuss the behavior of such oscillators without employing the network viewpoint. However, in oscillators which operate the crystal at series resonance, the networks are more complicated. The analysis and design of such oscillators is greatly simplified by grouping certain elements as a network, which performs certain functions and has a limited variety of possible characteristics.

For amplifiers it is well known that the amplification and pass band of amplifiers is limited by parasitic capacitance, and the resulting restrictions on available characteristics are generally known. The following sections will show that network performance for oscillators is limited in much the same way. However, one important additional restriction exists. In a bandpass (tuned) amplifier for the transmission of signals, it is desirable that the phase characteristic be linear with frequency, whereas in the amplifier for a broad-band untuned oscillator, it is desirable that the phase shift be zero or a multiple of 360° throughout the band of interest. This requirement seriously limits the band width of such oscillators.

An entire class of oscillators uses some form of impedance inverting network to transform the series resonance of a crystal into an equivalent parallel resonance. The network used most commonly on this project for impedance inversion was the equivalent lumped-element quarter-wavelength line. The properties of the equivalent-line network, and its comparison with other impedance inverting networks is extensively treated in Chapter II of this report.

As a basis for later analytical work, we first consider the design of a broad-band grounded-grid oscillator. The circuit of this oscillator, which is

treated in detail in Chapter XI is shown in Figure 8.1.

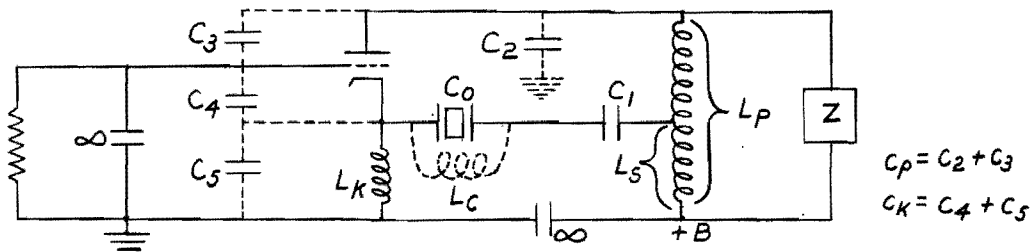


Figure 8.1 - Grounded Grid Oscillator

The band of frequencies over which satisfactory operation can be obtained by substitution of crystals is limited by the parasitic capacitances C_p and C_k , and by the coupling coefficient k of the transformer.

At any specified frequency, the parasitic capacitances C_p and C_k may be antiresonated by means of the inductances L_p and L_k ; similarly, the leakage inductance of the transformer may be resonated by C_1 . Then, if the resistance of the primary coil is negligible, and if the load impedance Z is a pure resistance, oscillation occurs at a frequency for which the crystal acts as a small pure resistance. If the crystal holder capacitance C_o is excessive, or if operation at the resonant frequency of the series arm is desired, the compensating coil L_c may be added as indicated. If we substitute a crystal having a different frequency (but the same value of C_o), the phase conditions are upset, the loop gain is reduced, and operation does not occur at the exact frequency intended.

In the present example, it is appropriate to group the elements into three networks. The cathode network consists of the irreducible capacitance C_k in parallel with the dynamic cathode conductance. Subject to the restrictions imposed by these elements, the effective impedance from cathode to ground should approximate a pure constant resistance over the broadest possible frequency band. The crystal network is limited by C_o ; in conjunction with C_o , any network which may be substituted for L_c should present a high and essentially resistive impedance over the band of interest. The plate network has as its controlling element the plate capacitance C_p . Subject to such control, the impedance to ground presented by the load Z and the high side of the transformer should also approximate a pure constant resistance over the

broadest possible frequency band. The leakage inductance to be resonated by C_1 should be made as small as possible. We shall show later that the unavoidable residual phase shift produced by this element may be partially compensated by modifying the plate network.

The cathode and crystal networks are essentially two-terminal impedances and may therefore be treated by the methods which have been developed for two-terminal amplifier interstage networks, the principal difference being that zero phase rather than a constant impedance magnitude is desired. Taken together, the plate and transformer constitute a four-terminal network in which the transmission phase shift should be zero. However, as previously indicated, the problem may often be simplified by first minimizing the effect of the series element (leakage inductance) and then obtaining the best possible compensation by consideration of the self-impedance of the high side as a two terminal network. For Figure 8.1 it has been found that excellent results are obtained if the load impedance Z is replaced by a series-tuned tertiary winding having an appropriate magnetic coupling to the plate winding L_p .

B. Wide-Band Low-Phase Two-Terminal Networks.

The analysis and design of two-terminal networks is greatly facilitated by means of the low-pass to band-pass network transformation described in detail in Appendix B. Because a great deal of information on the impedance and phase characteristics of capacitance-limited two-terminal low-pass networks is available from video amplifier applications, it is possible to obtain practical designs with a minimum of calculation by means of this band-pass transformation method.

Two essentially different approaches to the design problem may be made. The first and simplest is to inspect available curves of impedance and phase angle for various two terminal networks. Because the band-pass transformation doubles the number of reactive elements, the practical designer is interested in only a few relatively simple networks. Having selected a network configuration and relative element values, one first adjusts the impedance level and bandwidth to the parasitic capacitance value in question. Then the low-pass to band-pass transformation can be applied to obtain a design which is final except for the substitution of an equivalent network which is superior in

convenience or physical realizability. The normalized curves given by Bode¹ on pages 445 to 450 furnish an excellent starting point for this procedure. The alternative process, which is a formal network synthesis, is described in the following section.

Several low pass networks together with their band pass equivalents are shown in Figure 8.2.

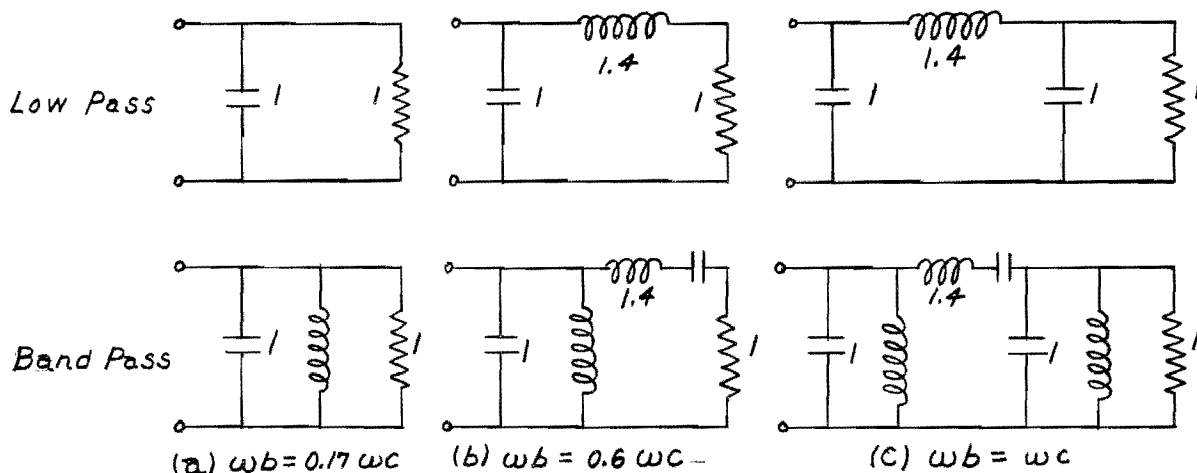


Figure 8.2 - Two-Terminal Networks

Network (a) includes no attempt at phase compensation, and may be regarded as the fundamental reference form. Network (b) is the "shunt-peaking" arrangement widely used in video amplifiers. It will be shown that one form of the band-pass equivalent of this network is a pair of magnetically coupled tuned circuits. Network (c) may be thought of as a full section of low-pass filter. The bandpass equivalent, which may include a transformer, is so complicated that it is rarely used.

The networks are represented in a normalized form such that ω_c , the angular frequency at which the susceptance of the limiting capacitance equals the load conductance, is unity. The useful bandwidth, ω_b , which is usually less than ω_c , is here based on an assumed phase tolerance of $\pm 10^\circ$; the element values given represent approximately optimum designs for this requirement. By use of smaller compensating elements, a somewhat greater bandwidth may be obtained at the expense of a wider phase of tolerance.

To illustrate the use of these relationships, let us assume that a 100 Mc

crystal having a holder capacitance of $C_0 = 10 \text{ mmf}$ and a resistance $R_1 = 1000 \text{ ohms}$ is to be compensated over a relatively wide frequency band. The normalized low pass network of Figure 8.2 (b) is chosen as representing a practical limit of network complexity. Proceeding on the low-pass basis, we have as the critical frequency in the actual network

$$\omega_c = 1/R_1 C_0 = 10^8 \text{ radians/sec.} \quad (8.1)$$

For the network configuration assumed, the useful bandwidth is

$$\omega_b = 0.6 \omega_c = 6 \times 10^7 \text{ radians/sec.} \quad (8.2)$$

which corresponds to a frequency band of 9.5 Mc. In the actual network, the impedance level is 1000 times higher, and the critical frequency is 10^8 times higher, than in the normalized network; therefore, the series inductance in the actual network must have a value of

$$L = 1.4 \times 10^3 / 10^8 \text{ h} = 14 \mu\text{h} . \quad (8.3)$$

The correctness of this value may be checked by noting that it yields a reactance 1.4 times the load impedance at the critical frequency.

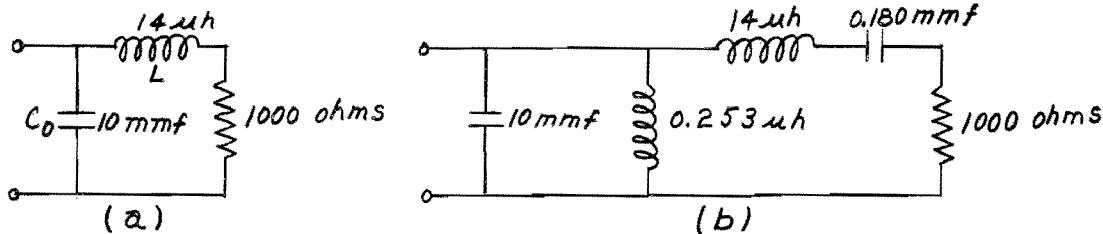


Figure 8.3 - Illustrated Two-Terminal Design

The low-pass network just developed is shown in Figure 8.3 (a). It is transformed into the band-pass network of Figure 8.3 (b) by adding an inductance and a capacitance which, with the original elements, resonate at the specified frequency of 100 Mc. The resulting configuration is unsatisfactory, however, because it is impractical to construct elements having the indicated values. To avoid this difficulty, the adjacent pair of inductances is represented as a two-winding transformer having elements, as indicated in Figure 8.4 (a) which lead to equivalent inductances on open and short circuit. The impedances of the secondary circuit can then be readjusted to any convenient

values which keep the coupling coefficient, and hence the primary response characteristic, constant.

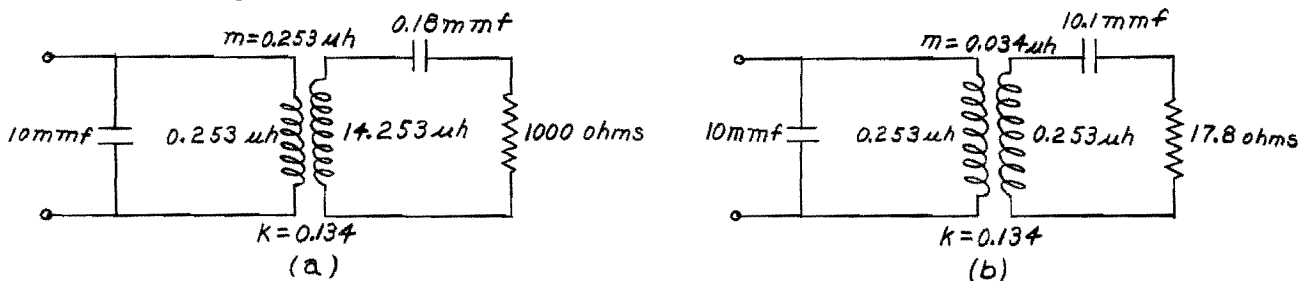


Figure 8.4 - Use of Transformer in Illustrative Design

In the example shown in Figure 8.4 (b), the primary and secondary inductances are made equal, in which case the capacitances differ very slightly.

C. Synthesis of a Specified Phase Characteristic.

As an alternative to the experimental design method described in the preceding section, we may employ formal network synthesis methods. The procedure starts with an assumed phase characteristic, which from physical considerations must be zero at zero frequency and 90° at very high frequencies because of the action of the shunting capacitor. An example of such a phase characteristic is shown in Figure 8.5.

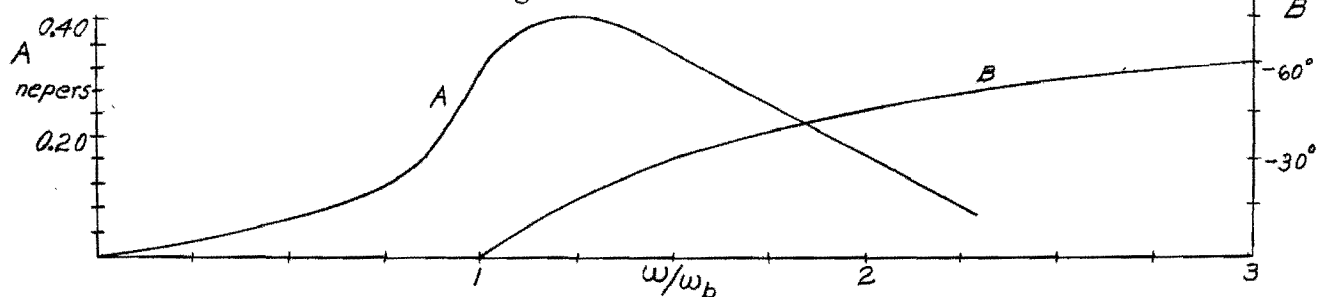


Figure 8.5 - Assumed Low-Pass Phase Characteristic

Bode¹ shows in Chapter 14 that the real and imaginary components of network functions are uniquely related. In terms of a self-impedance, the variation of the absolute magnitude of the impedance is determined as soon as the phase angle is specified as a function of frequency. Therefore, the assumption of a phase characteristic automatically determines an impedance characteristic, which may be calculated by means of formulas given by Bode.

The phase characteristic shown in Figure 8.5 may be represented by the equation

$$(\omega > \omega_b) B = \pi(\omega - \omega_b)/2\omega . \quad (8.4)$$

The associated impedance is obtained by use of equation III (c) from P. 335 of Bode, and is

$$A_a = \frac{\omega_a}{\pi} \int_0^{\infty} \frac{d(B/\omega)}{d(l/\omega)} \ln \left(\frac{\omega_a + \omega}{\omega_a - \omega} \right) d(l/\omega) \text{ nepers} \quad (8.5)$$

where the subscript (a) represents the frequency at which the magnitude is being determined. In turn, A represents the logarithm of the ratio of the zero-frequency impedance of the impedance at ω_a . Integration of 8.5 yields

$$A_a = 2 + (\omega_a/\omega_b - 1) \ln \left| \frac{\omega_b/\omega_a - 1}{\omega_b/\omega_a + 1} \right| - (\omega_a/\omega_b + 1) \ln (\omega_b/\omega_a + 1) \text{ nepers.} \quad (8.6)$$

This function is sketched in Figure 8.5. It is emphasized that the characteristics shown are not necessarily optimum or even desirable.

From a pair of magnitude and phase angle curves such as those presented, one may readily calculate the corresponding curves of resistance and reactance. One may then approximate these by empirical equations, which in turn may be used to synthesize a physical network by the methods of Brune or Darlington, as given by Bode¹ in Chapter 9. In practice, this method is unattractive because of the amount of work required and because the assumed curve can be approximated only roughly unless an intolerably large number of elements is assumed.

The proof that the results obtained by the simplified method of the preceding section are not capable of any major improvement depends upon the impedance integral described by Bode in Chapter 17. The essential fact is that the parasitic capacitance sets a definite limit to the frequency band over which the phase shift and magnitude may remain respectively small and nearly constant.

D. Four Terminal Networks Having Low Transfer Phase Shift.

The synthesis method described in the preceding section can be readily extended, at least in principle, to the design of four terminal networks such as transformers. Because a physical transformer with appreciable leakage inductance must usually be included in the final design, the limiting phase shift is at least π rather than $\pi/2$ radians. Therefore, the magnitude variation which corresponds to attenuation or insertion loss in nepers is

approximately twice as great as that which must be tolerated in a self impedance.

An additional difficulty of considerable importance arises at this point. In a self-impedance, the absolute magnitude is uniquely fixed by the bandwidth and the shunting capacitance; however, this is not true of a transfer impedance. This point is discussed in some detail by Gewertz² and in Chapter 16 by Bode¹. The difficulty may be avoided if the network includes only one resistance, in which case conservation of energy may be used to relate the input impedance to the output current. One may then calculate the input impedance characteristic which corresponds to the desired transmission response and synthesize a network having the desired impedance. A unique impedance level, which determines the effective transformer ratio, is determined by the resistance integral of Bode, p. 362.

One remaining pitfall must be avoided. We have assumed that the network includes only one resistance and have determined the input or self impedance characteristic which is consistent with this assumption and the desired transmission. We must now choose a network which has only one resistor. This may be accomplished by using Darlington's method³ for synthesizing a self impedance, because his network consists of a group of reactances terminated in a single resistor. However, there is no assurance that the resulting configuration will include either a single capacitor which may be identified with the limiting parasitic capacitance, or on a self inductance which may be identified with the leakage of a physical transformer. The alternative synthesis method of Brune¹ is even less satisfactory because it ordinarily leads to more than one resistance.

The remaining objection to the foregoing methods is that two separate resistors or dissipative impedances are usually desirable. In a typical oscillator, one wishes to deliver a large fraction of the power produced to a useful load impedance and to deliver only a small fraction through the feedback path to the grid circuit. Also, the phase angle of the load current is of no importance, so the desired operating condition has little relation to those cases considered above. Accordingly, the direct design methods described below are preferred in practice.

E. Four Terminal Networks.

Oscillators employing conventional vacuum tubes require a phase reversal between the plate and grid voltages. This phase reversal may be obtained in many ways of which the simple transformer of Figure 8.6 is the most generally useful. Ordinarily, the coupling coefficient k is made as large as possible and the elements are adjusted so that at the nominal operating frequency resonance occurs between C_p and L_s , as well as between C_p and L_p .

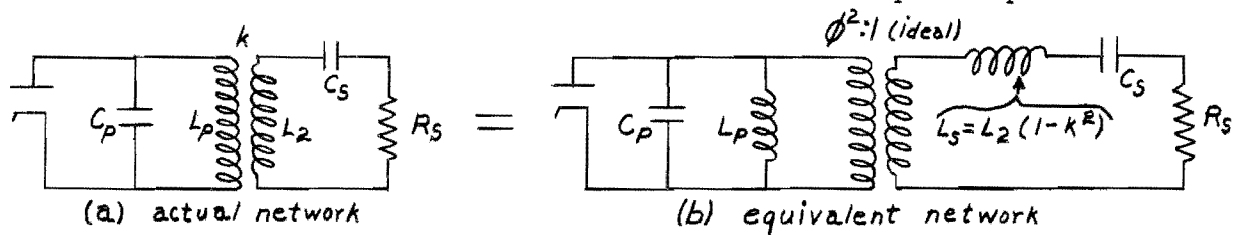


Figure 8.6 - Simple Transformer

The resistance R_s represents the series combination of the crystal and some input network. It is a pure resistance at the desired operating frequency of each particular crystal. It is appropriate to examine the response of such transformers at this time because an understanding of the limitations imposed by stray capacitances and inductances is fundamental to the following work, which is directed toward a partial compensation of these effects.

The primary impedance and the insertion phase shift are unaffected if the ideal transformer is assigned a ratio of one and removed from the circuit, as shown in Figure 8.7a. Moreover, this network has the configuration (but not the element values) of a half section of bandpass filter; therefore, its response may be obtained from that of the low-pass structure of Figure 8.7b by frequency transformation. Because this network has already been studied, and because its transfer characteristics are readily derived from Bode's curves, a considerable simplification of the problem results.

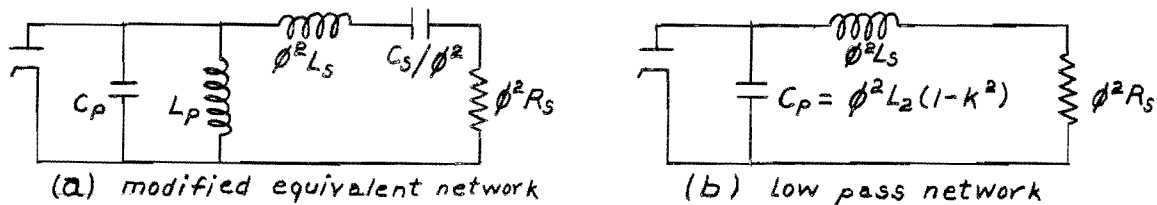


Figure 8.7 - Network Transformations

Suitable element values may be found by using the definitions

$$1/\omega_o^2 = L_p C_p = L_s C_s , \quad (8.7)$$

$$1/\omega_c^2 = \phi^2 R_s C_p , \quad (8.8)$$

and

$$m^2 = \omega_c L_s / R_s . \quad (8.9)$$

Our parameter m corresponds to the k used by Bode in the chart on page 445. by imagining the secondary shorted in Figure 8.6, we may write

$$L_p (1 - k^2) = L_p \phi^2 L_s / (L_p + \phi^2 L_s) . \quad (8.10)$$

Solving this for the square of the coupling coefficient yields

$$1/k^2 = 1 + \phi^2 L_s / L_p . \quad (8.11)$$

Using 8.7, 8.8 and 8.9 to eliminate ϕ^2 , L_s , and L_p , we get

$$1/k^2 = 1 + m^2 \omega_o^2 / \omega_c^2 . \quad (8.12)$$

Analysis or careful physical considerations of Figure 8.7b shows that, although the addition of inductance in L_s improves the phase angle and constancy of magnitude of the self impedance, the transfer phase angle steadily increases with increase of inductance. Therefore, the smallest possible value of m and the largest possible value of k is desirable. Solving 8.12 explicitly for m yields

$$m^2 = \frac{1 - k^2}{k^2} - \frac{\omega_c^2}{\omega_o^2} . \quad (8.13)$$

If we substitute the value $k^2 = 1/2$ (the tightest coupling readily achieved in practice), we find $m^2 = \omega_c^2 / \omega_o^2$. For a typical broad-band untuned oscillator the ratio ω_c / ω_o is in the neighborhood of 1/5. Consequently, a value of $m = 1/5$ is typical. Consistent with these parameters, at the critical frequency ω_c the insertion phase shift is about 55° , of which only about 12° is contributed by the leakage inductance.

In actual oscillators, the plate impedance of the vacuum tube is high compared to the impedance presented to it by the transformer. Therefore, it is necessary to add some essentially resistive shunt element to lower the

impedance faced by the crystal. If this is not done, the effective Q of the crystal is excessively degraded, and the frequency stability is poor.

The most obvious method of controlling the degradation of the crystal Q is to add a resistor in shunt at the crystal terminals; that is, across the low impedance side of the transformer. However, the following sections show that the bandwidth over which untuned operation may be secured is appreciably increased by applying this added load to the high impedance side and adjusting its reactance so as to minimize the loop phase shift.

F. Four-Terminal Transformer Networks Using Two-Terminal Phase Correctors.

As previously stated, a network representing an output transformer must include an input condenser to represent the tube capacitance, a series inductance to represent the leakage inductance, and at least one resistance. A configuration meeting these conditions and showing three possible positions for a phase correcting network is presented in Figure 8.8.

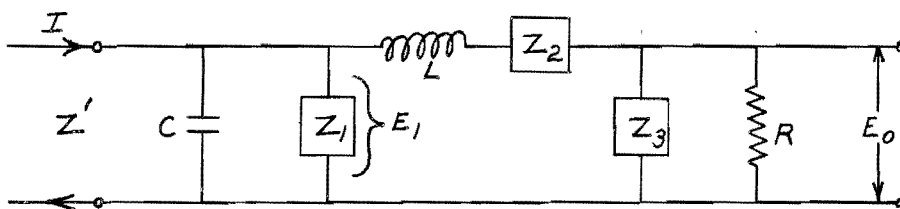


Figure 8.8 - Low-Pass Form of Transformer Network

However, it is assumed that only one phase corrector will be used at any one time. The following discussion indicates the variety of responses which may be obtained from various combination of elements in the three positions indicated.

We first show that the addition of a single reactive element in any of the three positions is not helpful. It is clear that adding an inductor as Z_1 or Z_3 , or a capacitor as Z_2 , destroys the zero-frequency transmission and is therefore prohibited. Addition of an inductor as Z_2 or a capacitor as Z_1 directly degrades the response by increasing the parasitic elements; addition of capacitance as Z_3 may also be shown to increase rather than decrease the phase shift at all frequencies. Therefore, no single reactor is helpful.

By an extension of the foregoing argument, we may show that a combination

of purely reactive elements in any of the three positions degrades the insertion phase shift. The argument is closely related to one presented by Bode on page 181, where he shows that a complex reactive network always has a greater ratio of reactance slope to reactance, than does a simple one. In view of this conclusion, it is not surprising that the direct network synthesis method discussed in the preceding section leads to no practical results.

We next show that the phase characteristic can be improved by adding simple dissipative networks as Z_1 or Z_3 . Fortunately, any single added resistance may be regarded as the useful load; therefore, it is actually desirable to dissipate a large fraction of the available power in the phase corrector. The design is relatively straight-forward, because the unique relation between insertion phase shift and loss is quite independent of the method by which either is obtained. All low-phase networks exhibit a common characteristic: the attenuation decreases below its zero-frequency value and then increases at the edge of the useful band. This fact may be used as a guide to the design of two-terminal phase correcting networks. Thus, we see that a resistance in series with an inductance is appropriate as Z_1 or Z_3 . One might also suppose that a resistance shunted with a capacitance as Z_2 would serve as a phase corrector; however, under the assumption of a constant input current, no possible series element can cause the load voltage to increase with frequency. Therefore, no series network can, without additional shunt elements, give a phase correcting action.

G. Low-Side Two-Terminal Phase Corrector.

Because the load, R , of Figure 8.8 is normally a low impedance, it is appropriate to refer to a phase compensator in the Z_3 position as a low side compensator. Referring to Figure 8.8 and assuming Z_3 finite, $Z_2 = 0$, and $Z_1 = \infty$, one may write the nodal equations

$$\begin{aligned} E_1 Y_{11} - E_0 Y_{12} &= I \\ -E_1 Y_{12} + E_0 Y_{22} &= 0 \end{aligned} \tag{8.14}$$

where

$$Y_{11} = j\omega C + 1/j\omega L, \quad Y_{12} = 1/j\omega L$$

and

$$Y_{22} = 1/R + 1/Z_3 + 1/j\omega L . \quad (8.15)$$

Combining to obtain the transfer impedance, we have

$$Z_t = E_o/I = Y_{12}/(Y_{11}Y_{22} - Y_{12}^2) . \quad (8.16)$$

Substituting values yields

$$Z_t = \frac{I}{j\omega L} \cdot \frac{-\omega^2 L^2}{(1 - \omega^2 LC)(1 + j\omega L/R + j\omega L/Z_3) - 1} . \quad (8.17)$$

This shows that at the particular frequency for which $\omega^2 LC = 1$, the transfer impedance has the pure imaginary value $j\omega L$ and is entirely independent of Z_3 . Evidently, phase correction can be effected only at frequencies substantially lower than this value.

By inspection, or by appropriate reduction of 8.17, we see that at zero frequency the transfer impedance is simply

$$Z_t = R_o (\omega = 0) \quad (8.18)$$

where R_o represents the zero-frequency resistance of R and Z_3 in parallel. Referring to the attenuation curve of Figure 8.5 and remembering to double both ordinates, we see that $\beta = \pi/2$ when $\omega = 2\omega_b$, and the corresponding transfer impedance is

$$|Z_t| = 1.42R_o (\omega = 2\omega_b) . \quad (8.19)$$

Combined with the fact that at this same frequency

$$|Z_t| = \omega L , \quad (8.20)$$

we have

$$L = 1.42R_o/2\omega_b = 0.71R_o/\omega_b . \quad (8.21)$$

The additional relationship

$$(2\omega_b)^2 LC = 1$$

yields

$$C = 1/(2.84\omega_b R_o) = 0.35/\omega_b R_o . \quad (8.22)$$

The critical frequency ω_c may be defined by the usual equation

$$\omega_c = 1/CR_o . \quad (8.23)$$

The limiting bandwidth obtainable with low side compensation then becomes

$$\omega_b = 0.35 \omega_c . \quad (8.24)$$

Subject to the characteristics assumed in Figure 8.5, it is impossible to exceed the limit set by 8.23 regardless of the configuration or number of elements in Z_3 . It might appear that R rather than R_o should be used in 8.23. However, R_o represents the mid-band impedance of the final band-pass network and therefore is of basic significance.

H. High-Side Two-Terminal Phase Corrector.

The phase corrector in the Z_1 position of Figure 8.8 is referred to as a high-side corrector. In the following treatment it is shown that the bandwidth of low phase shift which may be produced in this way is considerably greater than that produced by the low side compensator. This is plausible, because in the present case only a small fraction of the total power is transmitted through the series inductance L .

Before proceeding with the detailed analysis of this system, it may be well to point out that in the oscillators with which this project has been concerned, the shunt capacitance is far more important than the series (leakage) inductance in limiting the bandwidth of low phase shift. When this is true, the analysis and design of low-phase networks is greatly simplified. The effect of the series inductance may be first neglected, and the high side phase corrector designed in terms of the specified capacitance and conductance. Because the conductance of the phase corrector (useful load) is usually large compared to the original conductance (associated with the feedback loop), the problem corresponds closely to the simple two-terminal phase corrector discussed in Section B. When this process is completed, it is then appropriate to examine the phase shift produced by the series (leakage) inductance at the edge of the useful band. If necessary, the two-terminal phase compensator may be readjusted to obtain an improved overall correction. As in other transformer designs, it is convenient to use the low-pass to band-pass transformation and to adjust the secondary impedance level of the resulting two-winding transformer to suit the particular application.

The problem of evaluating the relative merit of the several possible

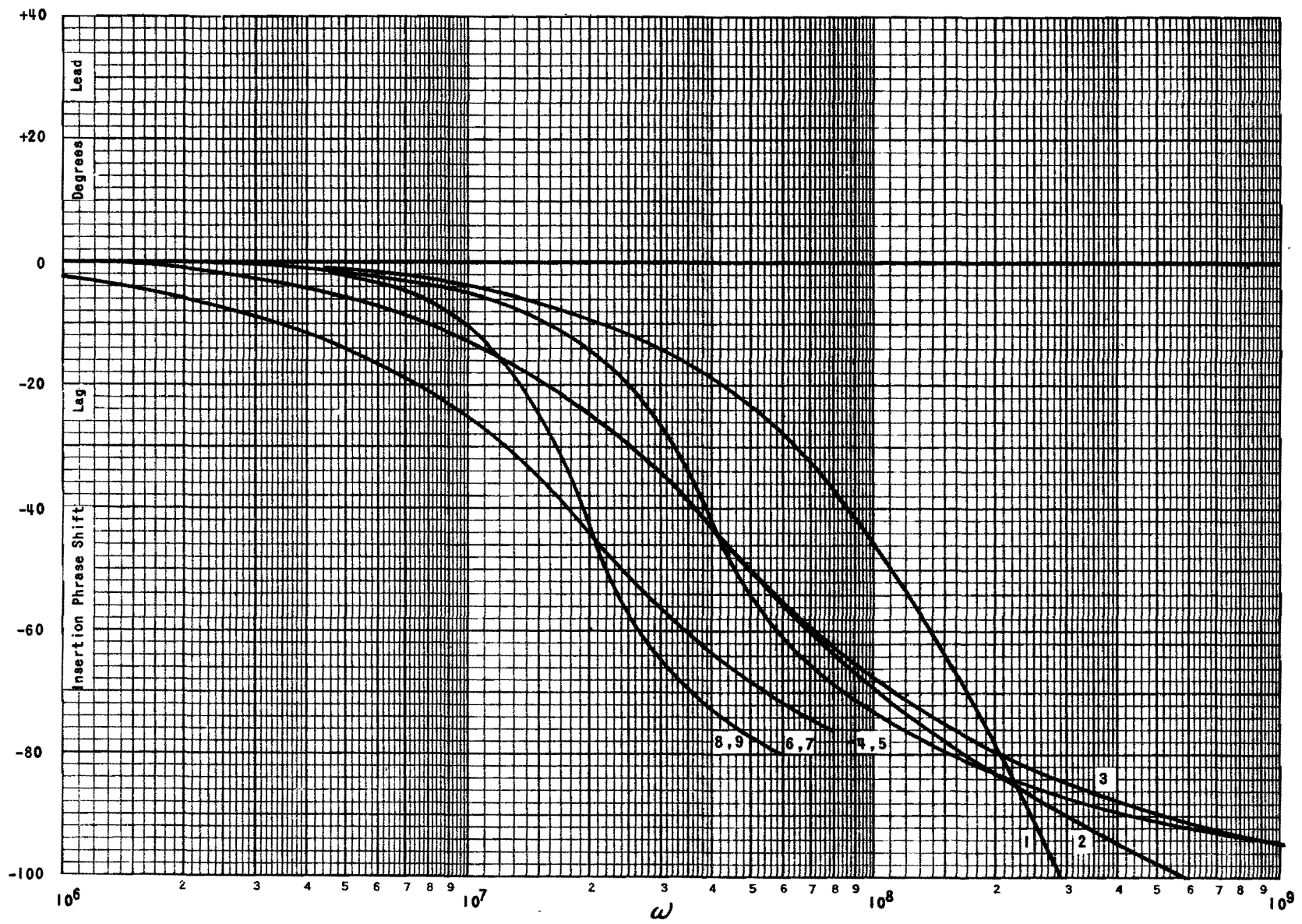
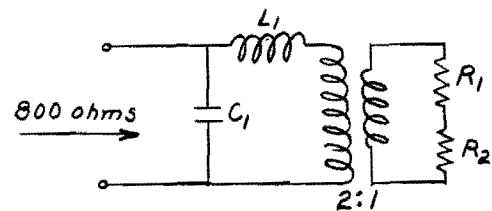
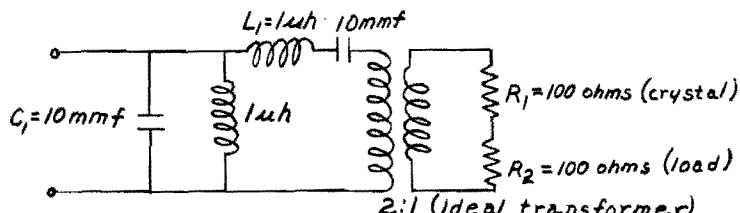


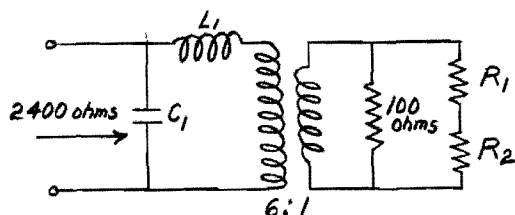
Figure 8.9a Comparison of Network Responses, On Low Pass Basis.



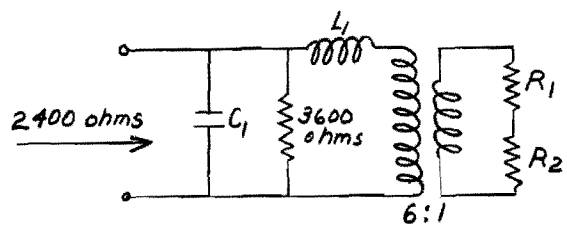
$$K = 0.707 \quad Z_t = 400 \text{ ohms} \quad w_0 = 3.16 \times 10^8 \text{ (50 mc)}$$

Basic Band Pass Network ($D = \infty$)

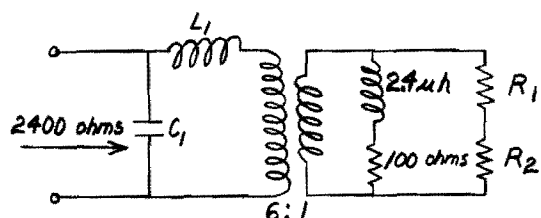
1. Basic Low Pass Network ($D = \infty$)



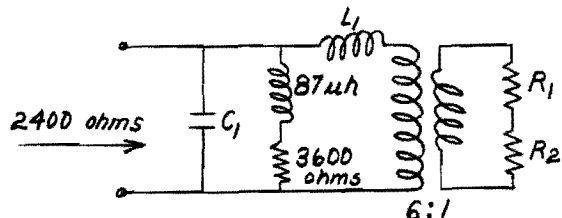
2. Low Side Terminated ($D = 3$)



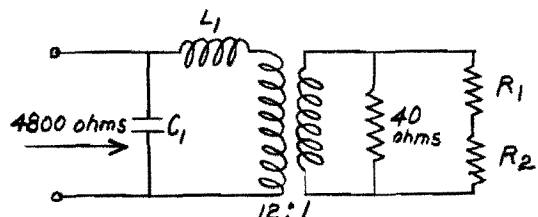
3. High Side Terminated ($D = 3$)



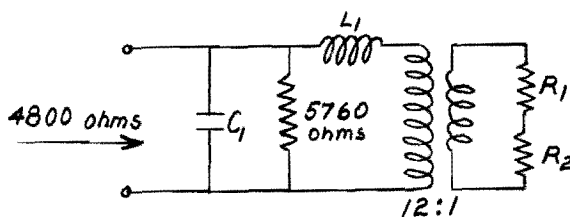
4. Low Side Compensated ($D = 3$)



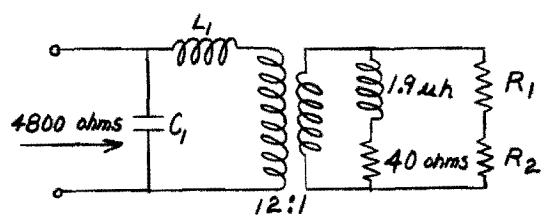
5. High Side Compensated ($D = 3$)



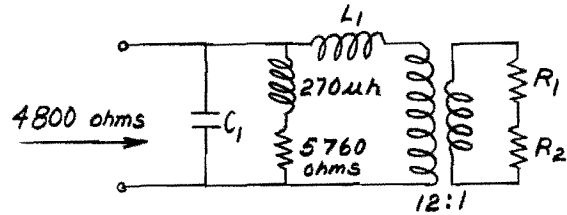
6. Low Side Terminated ($D = 2.4$)



7. High Side Terminated ($D = 2.4$)



8. Low Side Compensated ($D = 2.4$)



9. High Side Compensated ($D = 2.4$)

Note: In all cases $R_1 = 100 \text{ ohms}$, $R_2 = 100 \text{ ohms}$, $C_1 = 10mmf$, $L_1 = 1\mu h$

Figure 8.9b - Element Values Corresponding to Figure 8.9a

forms of phase correcting networks is complicated by the considerable number of parameters which must be considered. Thus, the impedance presented to the plate of the tube is a function of the factor D by which the effective Q of the crystal is degraded. Moreover, in practice, the coupling coefficient which may be obtained depends somewhat upon the effective turns ratio. In view of these difficulties, it is felt that the numerical examples of Figure 8.9 may be more informative than formal analytic work. The networks compared have equal values of shunt capacity, coupling coefficient, and transfer impedance; therefore, they correspond to systems having equal values of loop gain. The added phase compensating network was chosen for its simplicity; and the element values were adjusted so that in each case the original and compensated phase curves cross at the 45° point. It is found from experiment that a greater degree of phase correction is rarely desirable.

It is seen that the high-side impedance must increase as the impedance facing the crystal is reduced in order to reduce the Q degradation, D. Unfortunately, the critical frequency ω_c , (given by equation 8.1), decreases so rapidly as a result of this change that the frequency band over which a low phase angle may be maintained is seriously restricted. The most important conclusion from these calculations is that the lowest possible impedance levels should be maintained when broad-band untuned operation is required, even at the expense of considerable Q degradation. Further, it is concluded that low and high side compensation of phase shift are substantially equivalent under the conditions assumed; however, if the capacitance were smaller or the coupling looser, the high-side compensation would be superior.

The band-pass transformation of a high-side phase-compensated network is shown in Figure 8.10. The elimination of the ideal transformer is then accomplished by the further step indicated in Figure 8.11a. Both the preceding transformations represent exact equivalents. The final modification indicated in Figure 8.11b is an approximation, but contributes only a negligible error under the conditions of present interest. The use of a tertiary winding for phase compensation is desirable because it permits use of convenient values of element values, whereas the directly-connected compensator does not.

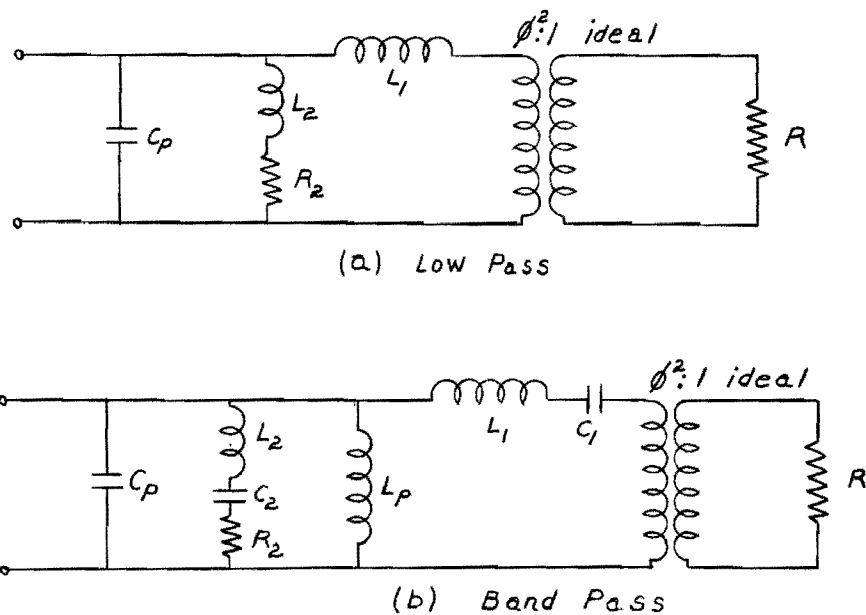


Figure 8.10 - Low-Pass to Band-Pass Transformation

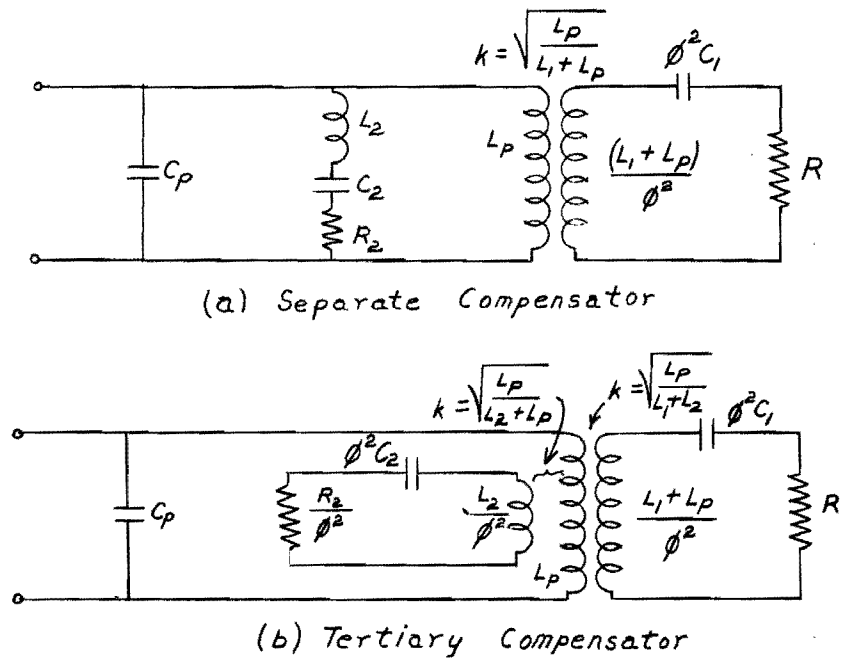


Figure 8.11 - Use of Tertiary Winding for Phase Compensation

Moreover, stray capacitance is minimized by use of mutual inductance coupling.

To summarize the foregoing work on transformers, we may state that parasitic capacitance causes the principal limitation on the frequency interval over which a low phase shift may be maintained, and that the most effective means for extending this frequency band is a reduction of the general impedance level. Because very low impedance levels are associated with excessive degradation of the effective crystal selectivity, a compromise is necessary. Consistent with prescribed values of impedance level and Q degradation, the frequency interval over which the phase angle may be quite small, (for example $\pm 10^\circ$) may be extended by the addition of reactive elements as described in the preceding sections. However, these compensating networks always produce a degradation of the phase angle at more remote frequencies and are therefore of little help if the phase tolerance is as great as $\pm 45^\circ$.

I. Phase Shift Due to Electron Transit Time.

Although electrons are very mobile, they require a finite interval of time to traverse the space between the electrodes of a vacuum tube. For the present application, the principal consequence of this transit time is the introduction of an additional phase shift between the voltage at the grid and the voltage at the plate. The associated increase in magnitude of the input conductance is of little importance because a low impedance level is desirable. In the 6AK5 pentode, for example, the additional phase shift due to transit time is about 0.2° per. megacycle or 20° at 100 Mc. Unless compensated for, this is sufficiently large to upset the loop phase conditions of oscillation. However, the rate of change of transit-time phase is rather small; therefore, one may regard the angle as constant over the operating band of frequencies. In broad-band untuned oscillators the effect is almost completely compensated by inserting some simple, relatively non-selective, network which produces a suitable phase lead at the center of the operating band. In tuned oscillators, the effect is most conveniently compensated by slightly detuning one or more of the circuits in such a way as to obtain the proper loop phase relationship without appreciable loss of gain.

A very simple network which may be used to compensate transit time phase shift is shown in Figure 8.12.

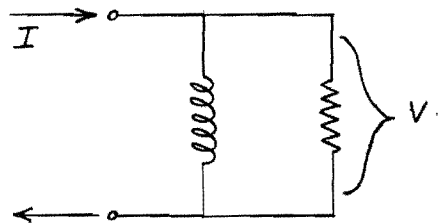


Figure 8.12 - Transit-Time Phase Corrector

It is readily seen that the output voltage leads the driving current by an angle given by the simple formula

$$\theta = \tan^{-1} R/\omega L . \quad (8.25)$$

In typical situations, the angle is about half a radian and the associated power loss is very small.

IX CATHODE COUPLED OSCILLATOR

A. Introduction.

The cathode-coupled crystal-controlled oscillator¹ has been widely used at low and moderate frequencies for evaluating quartz crystal performance and for other purposes. In high-frequency applications, the basic circuit configuration remains the same, but the circuit elements must be more carefully proportioned to retain the proper loop-phase conditions. In particular, phase shift due to the grid-to-cathode capacity of the cathode follower and due to the cathode-to-ground capacity of the grounded grid amplifier must be compensated for, if good high-frequency operation is to be obtained.

The method of analysis used for this circuit is based on the Nyquist criterion of stability, as described in Chapter III of this report. This criterion is applied by separately considering the gain and phase requirements of the circuit.

B. Gain Requirements.

The basic circuit of the cathode-coupled crystal-controlled oscillator is shown in Figure 9.1.

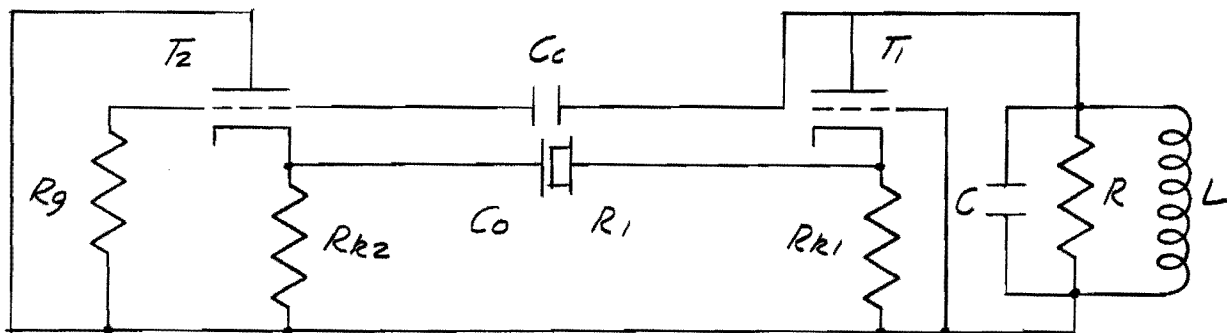


Figure 9.1 - Cathode-Coupled Oscillator

In most applications, the two tubes are identical, and the cathode resistors R_{k1} and R_{k2} are equal. Unless otherwise indicated the following discussion assumes that these conditions exist.

At the desired frequency of operation, the crystal should appear as approximately its series resistance, R_1 , and the tank circuit should appear as its antiresonant resistance, R . If for the moment the effects of the parasitic tube capacities are neglected, and the circuit is broken for

analysis at the grid of the cathode follower, the circuit takes the form shown in Figure 9.2. Ordinarily, $R_g \gg R$, therefore $R_L \doteq R$.

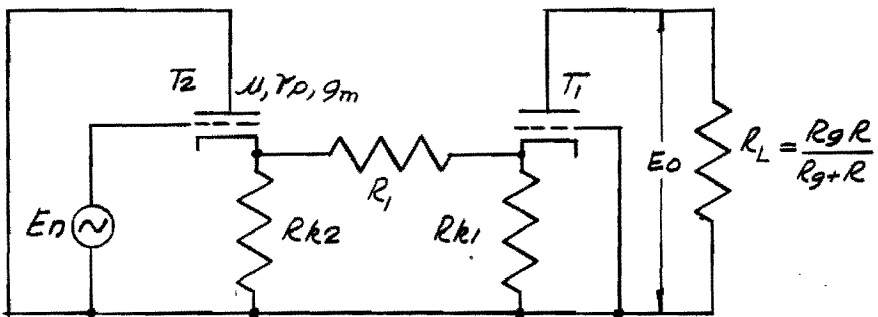


Figure 9.2 - Analysis of Cathode-Coupled Oscillator

In the analysis, it is assumed that the tubes operate as class A amplifiers and that the blocking capacitor, C_c , has negligible reactance. The input resistance of the grounded-grid amplifier T_1 is²

$$R_k = \frac{(r_p + R_L)R_{kl}}{R_{kl}(\mu + 1) + R_L + r_p} \quad (9.1)$$

The ratio of the return voltage E to the assumed signal E_n may be shown to be

$$\frac{E_o}{E_n} = \frac{R_L R_{kl} (\mu + 1) \mu}{[r_p/R_k + \mu + 1][R_{kl}(R_1 + \mu R_1 + r_p + R_L) + R_1(r_p + R_L)]} \quad (9.2)$$

If the circuit is to be capable of oscillating, the ratio, E_o/E_n , must be at least equal to one. Ordinarily, the values of the circuit elements are chosen to give a ratio somewhat greater than unity and the amplitude of oscillation increases until limiting occurs. However, if the loop gain is not greatly in excess of unity, the departure from class A conditions is small, and a linear analysis is satisfactory.

For cases in which the resistors R_{kl} and R_{k2} are not equal, or where the two tubes are not identical, it is convenient to express the loop gain in the following manner:

$$\frac{E_o}{E_n} = A_1 A_2 A_3 \quad (9.3)$$

Here A_1 , the gain of the grounded-grid amplifier, is given by

$$A_1 = \frac{(\mu + 1)R_L}{r_p + R_L}, \quad (9.4)$$

and A_2 , the gain of the cathode follower, is given by

$$A_2 = \frac{\mu R'}{r_p + (\mu + 1)R'}, \quad (9.5)$$

in which

$$R' = \frac{R_{k2}(R_1 + R_k')}{R_{k2} + R_1 + R_k'}. \quad (9.6)$$

The term, A_3 , represents the voltage drop due to transmission through the crystal and is given by

$$A_3 = \frac{R_k'}{R_1 + R_k'}. \quad (9.7)$$

C. Phase Requirements.

In the foregoing we have not considered the important phase requirement of Nyquist.

In the cathode-coupled circuit, phase shift is most easily studied by considering the phase shift contributed by each reactive element. The loop phase characteristic may be found by successively examining, (1) the tuning in the plate circuit of the grounded-grid amplifier, (2) the cathode-to-ground capacity of the same tube, and (3) the grid-to-cathode capacity of the cathode follower.

1. Phase Shift in the Grounded-Grid Amplifier Plate Circuit.

The output capacity of the grounded-grid amplifier, and the input capacity of the cathode follower, cause a phase shift in the plate network. These capacities are of course part of the plate load network, which in its simplest form, is a tuned circuit. Therefore, the capacity to ground should be kept low, as should the plate impedance level, in order that the circuit may have the maximum possible bandwidth. Broad-band circuits are desirable in that the rate of phase change with frequency can be kept low; thus, the crystal may operate more nearly independently of its driving circuit.

2. Phase Shift in the Grounded-Grid Amplifier Cathode Circuit.

The cathode-to-ground capacity in T_1 causes the cathode impedance to become complex, thus introducing a phase shift in the loop transmission. However, if the cathode capacity is antiresonated by a coil across the cathode resistance R_{k1} , the phase shift is small over a considerable band of frequencies because of the low Q of the resulting circuit.

3. Phase Shift Due to Grid-to-Cathode Capacity in Cathode Follower.

It should be noted that no attempt is made to antiresonate the cathode-to-ground capacity of the cathode follower, shown in Figure 9.3. The grid-to-cathode (C_{gk}) and cathode-to-ground (C_k) capacities of the cathode follower may be made to compensate each other so that the output will be in phase with the input at all frequencies of interest. The operation is similar to that of the well-known resistance-capacitance voltage divider. If the voltage transferred to the effective resistive load R' by tube conduction can be made equal to the voltage appearing across C_k due to the voltage-divider action of C_k and C_{gk} , the net output will be independent of frequency, and hence there will be zero phase shift.

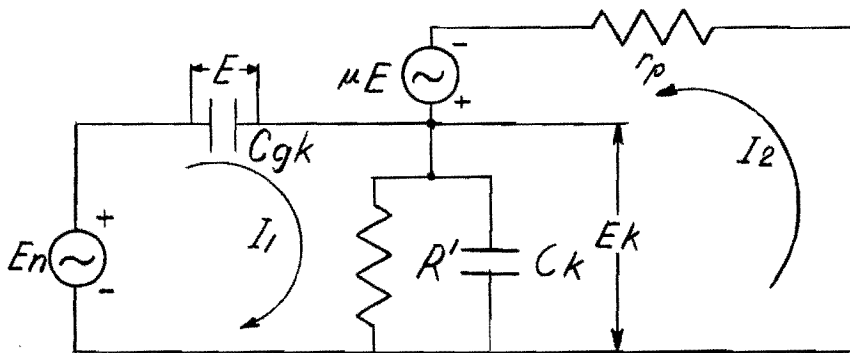


Figure 9.3 - Equivalent Circuit of Cathode Follower

The equations which describe the behavior of this circuit are

$$E = I_1 / j\omega C_{gk} , \quad (9.8)$$

$$E_n = I_1 (1/j\omega C_{gk} + Z_k) + I_2 Z_k , \quad (9.9)$$

$$\mu E = I_1 Z_k + I_2 (r_p + Z_k) , \quad (9.10)$$

$$E_k = Z_k (I_1 + I_2) , \quad (9.11)$$

where

$$Z_k = \frac{R'}{1 + j\omega C_k R'} . \quad (9.12)$$

The phase shift through the circuit is the angle associated with the phasor ratio, E_k/E_n , as given by

$$\frac{E_k}{E_n} = \frac{Z_k(r_p + \mu/j\omega C_{gk})}{Z_k[r_p + (\mu + 1)/j\omega C_{gk}] + r_p/j\omega C_{gk}} , \quad (9.13)$$

or, if $\mu \gg 1$

$$\frac{E_k}{E_n} = \frac{\frac{g_m R'}{1 + j\omega C_k R'}}{\frac{g_m R'}{1 + j\omega C_{gk}/g_m}} . \quad (9.14)$$

The voltage division will be constant, independent of ω and free from phase shift, if $C_k R' = C_{gk}/g_m$. It departs somewhat from this condition if either g_m or R' is modified. However, a ± 50 per cent departure from the normal value of R' leads to a calculated phase departure of only ± 13 degrees at 138 Mc.

D. Crystal Operation and Compensation.

The primary requirement on the crystal to be used in the cathode-coupled circuit is that it shall appear as a low resistance. This, of course, means that the crystal must operate at or near series resonance, and that its impedance should be approximately equal to the series resistance R_1 .

It is well known that AT cut quartz resonators operating at their mechanical overtones up to about the seventh overtone exhibit high reactances at frequencies removed from their series resonant points³. Therefore, crystals operating up to the seventh overtone can themselves yield a high impedance at other than the desired frequency, and thereby insure that a circuit properly designed for series operation of the crystal is a true crystal oscillator. On the higher overtones, the admittance of the shunt capacitance (C_o) is so large that the series resonant branch cannot exercise positive control of the oscillation. It then becomes necessary to provide some means of reducing the effect of the holder capacity.

Two general methods of accomplishing this are known, and both have many modifications. The simplest method is to shunt the crystal with an inductance which antiresonates the capacitance in the region of the operating frequency. This method has definite limitations of performance, but operates well if the frequency and order of overtone are not too high. Since large values of reactance are not required of the crystal, it is permissible to place a relatively low-impedance network across the crystal with little effect on its series resonant operation. The compensating network, including C_o , then becomes an antiresonant circuit shunted by a resistor equal to about five times the value of R_1 , and has a bandwidth considerably wider than that of the plate circuit of the grounded-grid amplifier. The crystal network impedance then remains relatively high over a frequency band wide enough to allow the plate circuit impedance to become low, thus reducing the loop gain and insuring that the crystal will control any oscillations generated. That is, the crystal network and the entire cathode network must be designed for greater band-width than the plate network, which itself should be a wide band network for best frequency stability.

In cases where R_1 is considerably greater than the reactance of the holder capacitance, or when it is necessary to realize a greater low-phase bandwidth than may be obtained with the foregoing circuit, a two-terminal low-phase-shift network as described in Chapter VIII may be used.

The second method of crystal compensation involves the use of a bridge circuit which is balanced if the crystal is replaced by its static capacitance. A substantial unbalance is produced at the frequency of series resonance. Variants of this method have long been used in crystal filters. While this method is ideal in concept, it leads to relatively complicated networks and substantial problems of adjustment. As described by Mason and Fair³, the capacity bridge compensation method can only be used with circuits which utilize transformers. Other bridge compensation methods can be devised for particular applications, but their balance is rarely independent of frequency.

In the study of capacity compensation for the cathode follower, a principle was evolved that may be particularly useful for adjusting low-frequency crystal oscillators to operate at the true series resonance of the crystal.

It is conveniently stated in terms of the cathode-coupled and similar circuits where the phase shift through the circuit (except for the crystal and cathode of the grounded-grid amplifier) is made zero. The loop phase shift is zero, or $2\pi n$ radians at the resonant frequency of the series arm of the crystal if

$$C_o R_1 = C_k R'_k \quad (9.15)$$

Unfortunately this method of compensation is of limited usefulness at high frequencies, because it does not maintain a high impedance across the crystal at undesired frequencies.

E. Degradation of the Crystal Q.

If the frequency stability of a crystal oscillator is to approach that of the quartz resonator alone, the Q of the resonator must not be seriously degraded by the associated circuit. This means that a crystal operated in the series mode should ideally work into a short circuit. Conversely, a parallel mode crystal should operate into an open circuit.

In practical circuits, these ideals are only roughly approximated. The crystal Q is usually degraded by the driving circuit to between 20 and 50 per cent of its intrinsic value. The ratio of the intrinsic Q to the working Q of the crystal (Q_1) is given by

$$Q/Q_1 = D = \frac{R_1 + R'_k + R''_k}{R_1}, \quad (9.16)$$

where R'_k is the input resistance of the grounded-grid amplifier as given by equation 9.1, and where R''_k , the output impedance of the cathode follower, is given by

$$R''_k = r_p R_{k2} / (r_p + R_{k2} + \mu R_{k2}). \quad (9.17)$$

It is now evident that R'_k and R''_k should be in the same order of magnitude as R_1 , if the crystal Q is not to be seriously degraded. In addition, we have shown in Chapter VI that for a fixed value of D , a minimum transmission loss from the cathode follower to the input of the grounded-grid amplifier is obtained if R'_k and R''_k are equal. For given tubes, there is a definite lower limit on these resistances because the gain required of the grounded-grid amplifier increases as the cathode-circuit impedances decrease.

This required increase of gain tends to increase the impedance of the tuned plate load circuit.

A basic conflict exists, because frequency stability is also promoted by the use of networks which have a low rate of phase change with frequency. Low rates of phase shift call for low, rather than high, impedances. A suitable engineering compromise is therefore necessary.

F. Range of Element Values.

The values of the resistances which establish the impedance levels in the various parts of the system should be selected so as to make the ratio E_o/E_n equal to two or three for average tubes. This circuit will then continue to oscillate even if poor tubes are used. An obvious alternative to this method is to assume a value of r_p , for use in equations 9.1 and 9.2, that represents the minimum acceptable tube quality and to design for a E_o/E_n ratio of one.

A good sequence to follow in the circuit design is first to select values for R_{k1} and R_{k2} (normally $R_{k1} = R_{k2}$) so that the Q degradation is reasonable; then a value is chosen for the load resistance, R_L , so as to obtain adequate loop gain. If the tank circuit has a reasonable Q and if R_g is large, the effective load is equal to R . In this way the tuned circuit will always be degraded, which leads to a moderately wide band in the plate circuit.

If the tube used as the grounded-grid amplifier has a high transconductance the approximate value of R_k is given by

$$R_k \doteq \frac{R_{k1}}{1 + g_m R_{k1}}. \quad (9.18)$$

Use of this approximation considerably simplifies computation of the loop gain.

G. Load and Power Considerations.

When a cathode-coupled oscillator is designed (as in the preceding section) to have a loop gain not much greater than one, then the operating conditions will be essentially class A. The amplitude of oscillation will build up until the grid current drawn in the cathode follower develops a sufficiently negative bias across R_{gL} . Since the voltage gain of the cathode-

follower is a function of its transconductance, and this in turn is a function of the bias voltage, the loop gain is reduced to unity and an equilibrium is reached. Also, the use of this design procedure results in low impedance levels throughout the circuit, and in relatively wide bandwidths in the crystal, cathode, and plate networks. This condition is desirable from the standpoint of frequency stability. However, the efficiency and power output of such an oscillator are low.

When output power is taken from the plate circuit of the grounded-grid amplifier, the value of the grid leak resistance is increased so that the parallel combination of it and the load resistance satisfies the loop gain requirements. Generally, the useful load will be the effective input impedance of a buffer amplifier and will include a shunt capacity which tends to reduce the obtainable bandwidth of the plate circuit. Furthermore, variation of the load impedance will affect the frequency of oscillation. If the load impedance is low, it may replace the resistor (R_{k2}) in the cathode circuit of the cathode follower. Typically, the input impedance of a grounded grid amplifier is comparable to the resistance of the crystal unit. Since the load is located in a low impedance circuit, the effect of load variation on the frequency of operation is reduced. However, the power gain that may be obtained from a grounded-grid amplifier is small.

A more satisfactory arrangement for loading the cathode-coupled oscillator is shown in Figure 9.4.

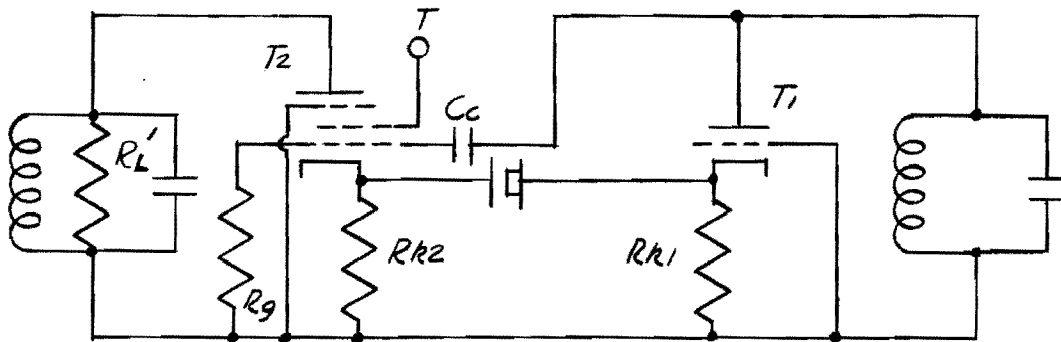


Figure 9.4 - Cathode Coupled Oscillator with Load in Plate of Cathode Follower
For moderate power output, the design procedure based on class A operation may be used. Since a pentode is used, the load R_L' has little effect on the

gain of the cathode follower, and may be ignored in determining values of R_{k1} , R_{k2} , and R_L which give the required loop gain. By the same token, variation of the load impedance has little effect on the operating frequency.

In order to obtain greater power output and higher efficiency, class C operation is desirable. While no detailed design procedure for this type of operation has been developed for the cathode-coupled oscillator, procedures such as those developed for the grounded-grid and transformer-coupled oscillators in Chapters X and XI may be applied. As shown in Chapter VII, considerable power output may be obtained with reasonably good stability. Experience with other circuits and the relations developed in Chapter VII for class C operating conditions indicate the general design objectives for high power output. The value of R_{k2} should be reduced to about 25 per cent of the value required for class A operation, and the resulting loss in gain compensated for by increasing the value of R_{k1} and R_L . The power rating of the tube used as the cathode follower should be greater than that of the tube used as the grounded-grid amplifier, and R_L should be appropriate to load the plate circuit of the cathode follower.

H. Experimental Data.

The cathode-coupled oscillator shown in Figure 9.5 has been constructed and operates as a crystal controlled oscillator at 126 Mc on the ninth overtone of a 14 Mc crystal. The holder capacity of the crystal is 12 mmf, and its series resistance is approximately 300 ohms. Both tubes are 6J4 triodes, and the total capacitance shunting the plate coil is 11 mmf.

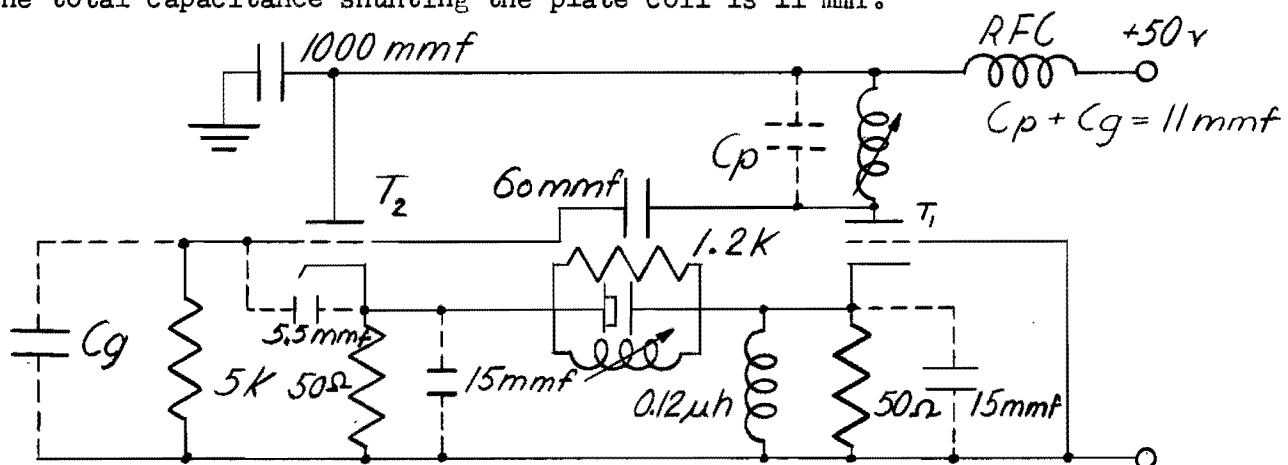


Figure 9.5 - 126 Mc Cathode-Coupled Oscillator

In this circuit, the plate, crystal, and cathode networks are in their simplest form; i.e. tuned circuits with their Q's degraded so as to yield the proper impedances. The Q of the crystal compensating network is degraded more than that of the plate network, but the 1,200 ohms impedance is large enough to prevent oscillation at undesired frequencies. The circuit inductances may be adjusted to antiresonate their respective shunt capacities by methods described in Chapter XIX.

This circuit has a relatively narrow bandwidth with low phase angle; however, the frequency stability is reasonably good. The frequency stability was determined with respect to several types of variations. A change in plate supply voltage from 50 to 85 volts resulted in a frequency increase of 18 parts per million. The circuit ceased to oscillate at voltages below 50 volts and exhibited excessive frequency shift at voltages above 85 volts. The frequency stability of the circuit is 0.22 parts per million per volt (ppm/v)^{*} over the normal operating range of plate supply voltage. The frequency variation caused by changing from hot to cold tubes was found to be very slight. It was also found that a change of a few per cent in the crystal coil produced only a very small change in frequency, but that the frequency varied more rapidly with changes in the plate coil. The latter observation is in agreement with the fact that the crystal network has a greater bandwidth than the plate network.

Additional experimental work has been done on the cathode-coupled oscillator with results similar to those reported here, and the circuit has been used to measure values of series resonant resistance as high as 500 ohms at 150 Mc.

I. Advantage and Disadvantages.

In the cathode-coupled oscillator, the necessary impedance transformation from the plate circuit of the amplifier to the low impedance crystal loop is obtained by using a cathode follower. The use of a vacuum tube to obtain this transformation is advantageous at very low frequencies and at the very high frequencies where it is difficult to construct impedance transforming

- - - - -

* See Appendix A of this report.

networks, because the required elements are either too large or too small. Furthermore, by proper choice of circuit elements, this impedance transformation may be made independent of frequency. This advantage is obtained, however, at the expense of increased plate and filament power.

In comparison with the grounded-grid and transformer-coupled oscillators, the cathode coupled oscillator will, with similar tubes, require higher plate and cathode impedance levels. This, and the additional capacity at the input of the cathode follower, reduces the bandwidth over which untuned operation may be obtained. The cathode-coupled oscillator suffers an additional disadvantage which is common to most multi-tube oscillator circuits, in that each contributes to the transit-time phase shift. While this has not proven to be a serious limitation on the circuit performance, it does increase tuning difficulties at the higher frequencies.

BIBLIOGRAPHY

1. Goldberg, H., and Crosby, E. L., "Series Mode Crystal Circuits," Tele-Tech 1, No. 5, (1948).
2. Arguimbau, L. B., Vacuum Tube Circuits John Wiley and Sons, Inc., New York, (1948).
3. Mason, W. P., and Fair, I. E., "A New Direct Crystal-Controlled Oscillator for Ultra-Short-Wave Frequencies." Proc. I.R.E. 30, 464-472, (1942).

X THE TRANSFORMER-COUPLED OSCILLATOR

A. Introduction.

The transformer-coupled oscillator is obtained by adding a crystal controlled feedback path to a grounded-cathode amplifier. This circuit differs from the cathode-coupled oscillator in that impedance transforming networks are used to obtain suitable impedance levels for series resonant operation of crystals. Correct phase relations are obtained by antiresonating the input and output capacities at the operating frequency, and providing a phase reversal in one of the transformer networks.

Since the grid and plate circuits are antiresonant at the same frequency, the transformer-coupled oscillator, with the crystal removed, has the configuration of a tuned-plate tuned-grid oscillator. Oscillations in this condition are prevented by the use of pentodes having low grid-to-plate capacities in conjunction with low grid and plate impedances. Furthermore, the effects of the grid-plate and crystal-holder capacitances balance, provided the ratios of the plate and grid transformers are suitable; therefore, it is usually unnecessary to compensate the crystal holder capacitance.

B. Impedance Levels and Loop Gain Considerations.

The basic circuit of the transformer coupled oscillator (Figure 10.1) may be used to determine the gain requirements for oscillation.

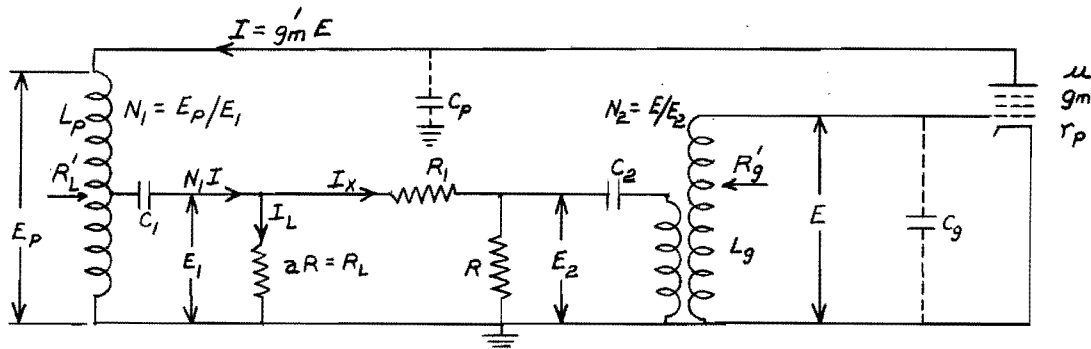


Figure 10.1 - Basic Transformer-Coupled Oscillator

In practice the unity coupled transformers of Figure 10.1 are replaced by more complex networks which produce the indicated impedance ratios, N_1 and N_2 ; and the effective plate to ground resistance, R'_L , is small compared to the plate resistance of the tube. Therefore, the secondary current of the plate

transformer is $N_1 g_m' E$, so that

$$E_1 = N_1 g_m' E \frac{aR(R_1 + R)}{aR + R_1 + R} , \quad (10.1)$$

the resistor R includes the input resistance of the tube, a equals R_L/R , and g_m' is the normal transconductance of the tube divided by β_p . The factor β_p is a function of the angle of plate current flow as tabulated in Chapter VII. From Figure 10.1 we also have

$$E_2 = E_1 R / (R_1 + R) \quad (10.2)$$

and

$$E = N_2 E_2 . \quad (10.3)$$

Elimination of the voltages from the foregoing equations yields, as the condition for sustained oscillation, the loop gain equation

$$g_m' = \frac{R_1 + R(a + 1)}{N_1 N_2 a R^2} . \quad (10.4)$$

Because the frequency stability is dependent on the Q degradation, D, it is desirable to express the loop gain in terms of this variable which is given by

$$D = (R_1 + R + aR)/R_1 , \quad (10.5)$$

or

$$R = R_1(D - 1)/(a + 1) . \quad (10.6)$$

Substitution of (10.6) in (10.4) yields

$$g_m' = \frac{D(a + 1)^2}{aN_1 N_2 R_1 (D - 1)^2} , \quad (10.7)$$

which gives the minimum value of g_m' for oscillation in terms of the parameters R_1 , D , a , and the product $N_1 N_2$. In order to make an intelligent choice of these parameters, it is necessary to investigate their relation to frequency stability, ratio of load to crystal power, and the value of the effective plate-and grid-to-ground resistances.

In the transformer-coupled oscillator the load should be located at

either the high or low side of the plate transformer in order to avoid transmitting the load current through the crystal, the exact location depending on whether a high or low resistance load is to be driven. If aR is the load resistor, then I_L becomes the load current and I_x the crystal current. From Figure 10.1 we have

$$I_L/I_x = (R_1 + R)/aR, \quad (10.8)$$

and

$$P_L/P_x = I_L^2 aR/I_x^2 R_1. \quad (10.9)$$

The currents I_L and I_x may be eliminated between (10.8) and (10.9) to yield

$$P_L/P_x = (R_1 + R)^2/aRR_1, \quad (10.10)$$

and substitution of equation 10.6 for R yields

$$\frac{P_L}{P_x} = \frac{(D + a)^2}{a(a + 1)(D - 1)}. \quad (10.11)$$

Because the power ratio is independent of N_1 and N_2 , we may choose D and a from power considerations and the product $N_1 N_2$ to satisfy the gain requirements of equation 10.7. However, additional investigation is necessary to determine how the values of D and a affect the plate and grid impedances (R'_L and R'_g) and the frequency stability.

For broad-band untuned operation the plate and grid capacities should both be as small as possible, and low values of R'_L and R'_g are desirable. From Figure 10.1 we may obtain the equivalent plate and grid impedances as

$$R'_L = N_1^2 \frac{aR(R_1 + R)}{aR + R_1 + R}. \quad (10.12)$$

and

$$R'_g = N_2^2 \frac{R(R_1 + aR)}{aR + R_1 + R}. \quad (10.13)$$

Substitution of equation 10.6 for R in both the above equations results in the following expressions:

$$R'_L = \frac{N_1^2 R_1 a(D - 1)(D + a)}{D(a + 1)^2}, \quad (10.14)$$

and

$$R_g' = \frac{N_2^2 R_1 (D - 1)(aD + 1)}{D(a + 1)^2} . \quad (10.15)$$

Equation 10.7 may be used to eliminate R_1 from equations 10.14 and 10.15 to give

$$R_L' = \frac{N_1(D + a)}{N_2 g_m'(D - 1)} , \quad (10.16)$$

and

$$R_g' = \frac{N_2(D + 1/a)}{N_1 g_m'(D - 1)} . \quad (10.17)$$

In many cases C_p and C_g are very nearly equal; and if the design objective is maximum bandwidth of untuned operation, R_L' and R_g' should be made equal and as low as possible. Inspection of equations 10.16 and 10.17 shows that for specified values of D and g_m' , the plate and grid impedances become a minimum when $N_1 = N_2$ and $a = 1$, as given by the equation

$$R_L' = R_g' = \frac{D + 1}{g_m'(D - 1)} . \quad (10.18)$$

This expression reaches a minimum value of $1/g_m'$ for $D = \infty$; however, the frequency stability is very poor if D is allowed to become large. Fortunately, as shown in the following section, the impedances are only moderately increased from their minimum values when D is assigned a value consistent with good frequency stability.

C. Frequency Stability Considerations.

The following development of optimum conditions for frequency stability is based on the results of Section I, Chapter VI, of this report where it is shown that the fractional frequency deviation of a crystal excited by a transformer network is given by

$$\frac{d\omega}{\omega} = \frac{-RD\omega_0}{2Q} dC . \quad (10.19)$$

As applied to the present circuit, D is the Q degradation given by equation 10.5, R represents either R_L' or R_g' and dC is the differential change in

either the plate or grid capacity. In equation 10.19 the product RD represents the factor which is most subject to design control; minimizing this product leads to conditions for optimum frequency stability.

From equations 10.16 and 10.17

$$R_L'D = \frac{N_1 D(D + a)}{N_2 g_m'(D - 1)} \quad (10.20)$$

and

$$R_g'D = \frac{N_2 D(D + 1/a)}{N_1 g_m'(D - 1)} . \quad (10.21)$$

Upon differentiating equations 10.20 and 10.21 to establish a minimum subject to prescribed values of N_1 , N_2 , and g_m' , it is found that $R_L'D$ is a minimum when $D = 1 + \sqrt{1 + a}$ and that $R_g'D$ is a minimum for $D = 1 + \sqrt{1 + 1/a}$. Therefore a must be equal to one if both $R_L'D$ and $R_g'D$ are to be minimum for the same value of D, and this optimum value of D is equal to $1 + \sqrt{2}$ or 2.414. It should be noted that the choice of D and a fixes the ratio of load to crystal power as given by equation 10.11, and that for optimum frequency stability the power ratio is relatively low, as is shown by the computation

$$\frac{P_L}{P_X} = \frac{(2.414 + 1)^2}{2(1.414)} = 4.12 . \quad (10.22)$$

Because overtone crystals can dissipate only small amounts of power, say 0.05 watt, the power output is limited to approximately 0.2 watt under conditions for optimum stability. If a higher power output is required, we must depart somewhat from these optimum conditions. Fortunately, $R_L'D$ and $R_g'D$ depart quite slowly from the minimum values as a and D are varied, so that a relatively large power output may be obtained without seriously degrading the stability of the oscillator.

Examination of equation 10.11 shows that high power ratios may be obtained for values of D near unity. However, equations 10.20 and 10.21 show that for this condition $R_L'D$ and $R_g'D$ become quite large; therefore, we must confine our attention to large values of D and small values of a.

Since the plate capacity of the tube is likely to be substantially more

stable than the grid capacity, it is desirable to favor the grid circuit with a relatively low impedance. This may be done by increasing the ratio N_1/N_2 and at the same time holding the product N_1N_2 constant so as not to alter the loop gain. The choice of values of a , N_1 , N_2 , and D to give the desired ratio R'_L/R'_g is facilitated by combining equations 10.20 and 10.21 to give

$$\frac{R'_L}{R'_g} = \frac{N_1^2(D + a)}{N_2^2(D + 1/a)}. \quad (10.23)$$

This equation shows that when a is small the plate impedance will be lower than the grid impedance, unless the ratio N_1/N_2 is suitably increased. Fortunately, this ratio may be chosen without affecting either a or D , provided that the loop gain (equation 10.7) is adequate. It should be noted that increasing R'_L and decreasing R'_g are both conducive to increased power output; the former provides a more favorable load impedance to the tube, the latter leads to larger currents for a given grid-limiting voltage.

D. Phase Considerations and Crystal Compensation.

Correct phase relations at the operating frequency may be obtained by antiresonating C_p and C_g with L_p and L_g , which are respectively the high side inductances of the plate and grid transformers, and by resonating the leakage inductance of the transformers with C_1 and C_2 in Figure 10.1. This leakage inductance is equal to the transformer high-side inductance multiplied by $(1 - k^2)$ and may be measured at the low-side terminals with the high side shorted. Because of the inherent phase reversal associated with the amplifier, one of the transformers must produce a compensating phase reversal to satisfy the loop phase requirements. With these conditions satisfied, the crystal will operate as a pure resistance at a frequency slightly above ω_o , the resonant frequency of the crystal arm.

If the reactance of the holder capacity (C_o) is not large compared to the series resistance (R_1) of the crystal, or if operation at the series resonant frequency is desired, the crystal must be compensated. Networks used for this purpose should maintain a high impedance across the crystal terminals over a frequency band greater than that of the grid and plate networks, and should not seriously degrade the crystal Q. Because the crystal

resistance is normally much lower than the values of R_L' and R_g' , these requirements may be met. In most cases a simple network consisting of an inductor shunted by a resistor will suffice; however, for large values of R_L and C_o or for extreme broad-band operation, more complex networks may be required.

E. Balance Between Tube and Crystal Capacitance.

In the transformer-coupled circuit it is practical to compensate the holder capacitance by means of the grid-to-plate capacitance of the tube. The general arrangement is shown in Figure 10.2.

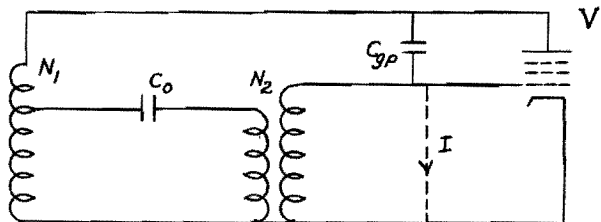


Figure 10.2 - Balance of Tube and Crystal Capacitance

The analysis is facilitated by assuming that a voltage V exists at the plate of the tube and that the grid is shorted to ground. The desired balance then exists if no current flows through the short circuit. This condition is represented by the equation

$$Vj\omega C_{gp} - (V/N_1)j\omega C_o/N_2 = 0 . \quad (10.24)$$

Simplification yields as the condition for compensation

$$C_o = N_1 N_2 C_{gp} . \quad (10.25)$$

Fortunately, it is practical to achieve this desired relationship. If, for example, $C_o = 10$ mmf and $N_1 = N_2 = 10$, the required value is $C_{gp} = 0.1$ mmf which is representative of a pentode in which no special attention has been given to shielding. These numerical values, however, also show that high efficiency operation is not practical with triodes in this circuit because of the large crystal holder capacitance which would be required to balance the grid-to-plate capacitance.

This arrangement, which is merely one form of the familiar bridge circuit, is convenient in practice and serves as a useful supplement to other methods of crystal compensation. It is also possible to achieve crystal compensation

by means of mutual inductance between the plate and grid transformers. An analysis of this method is presented in the following chapter on the grounded-grid oscillator.

F. Design Procedure.

Because of the flexibility of the transformer-coupled circuit, several design procedures are available. These procedures vary in detail according to the design objectives and are best compared by means of typical examples. In order to facilitate computation and to obtain results that may be applied to a number of cases, the design equations are modified to the following dimensionless forms:

$$g_m^R L = \frac{N_1(D + a)}{N_2(D - 1)} \quad (10.26)$$

$$g_m^R g = \frac{N_2(D + 1/a)}{N_1(D - 1)} \quad (10.27)$$

$$N_1^2 g_m^R L = \frac{N_1 D(a + 1)^2}{N_2 a(D - 1)^2} \quad (10.28)$$

$$N_2^2 g_m^R L = \frac{N_2 D(a + 1)^2}{N_1 a(D - 1)^2} \quad (10.29)$$

$$\frac{R}{R_1} = \frac{D - 1}{a + 1} \quad (10.30)$$

Equation 10.11, for the power ratio, can be used without modification. An expression which relates the power output to the driving voltage can be derived from Figure 10.1:

$$\frac{P_L}{g_m^R E^2} = \frac{N_1(D + a)^2}{N_2 D(D - 1)(a + 1)} \quad (10.31)$$

This expression is important because a given tube with a particular screen voltage and grid leak will limit at a fixed value of grid voltage E ; therefore, the power outputs of alternative designs may be compared in this way.

Table 10.1 presents, in normalized form, parameters for five different

designs chosen to illustrate significantly different performance characteristics as described in the following paragraphs:

1. Symmetrical Circuit Design.

In this case, which represents the simplest design procedure, N_1 is made equal to N_2 and a is equal to one. Therefore, a value of D equal to 2.414 yields minimum values of both $R_L'D$ and $R_g'D$. If the grid and plate capacities are equally stable, this yields optimum conditions for frequency stability. However, the power output is low, and greater bandwidth may be obtained, at the expense of stability, by increasing D . The resulting design represents Case No. 1 of Table 10.1.

2. Design Conditions for Optimum Stability with Dissymmetrical Plate and Grid Impedances.

If the grid capacity is less stable than the plate capacity, it is desirable to favor the grid circuit with a low value of $R_g'D$, and at the same time keep the product $R_L'D$ as small as possible. This may be accomplished by making a equal to one, D equal to 2.414, and by adjusting the ratio N_1/N_2 to give the desired ratio of plate to grid impedance.

On the assumption that the plate capacity is ten times as stable as the grid capacity, R_L' is made equal to 10 R_g' . Equation 10.23 may then be used to compute the required ratio of N_1/N_2 . The results of this design are presented as Case No. 2 in Table 10.1.

3. Design Conditions Favoring Power Output and Stability.

Starting with Case No. 2 we may adjust the circuit parameters to obtain a more favorable power ratio and observe the resulting decrease in frequency stability. We again assume that the plate capacitance is ten times as stable as the grid capacitance so R_L' is made equal to 10 R_g' . The products $R_L'D$ and $R_g'D$ are kept low in the interest of stability by leaving $D = 2.414$. A value of a equal to 0.0985 is selected so as to obtain a power ratio ten times larger than in Case No. 2. Consistent with the foregoing parameters, the ratio $N_1/N_2 = 7.07$ may be obtained from equation 10.23. The results of the remaining computations are presented as Case No. 3 in Table 10.1.

4. Design Conditions for Broad-Band Untuned Operation.

The circuit requirements for broad-band untuned operation differ

Final Report Project No. 131-45

TABLE 10.1
TRANSFORMER-COUPLED OSCILLATOR DESIGNS

	(Case No. 1) $R_L' = R_g'$ $a = 1$ $D = 2.414$ $N_1 = N_2$	(Case No. 2) $R_L' = 10R_g'$ $a = 1$ $D = 2.414$ $N_1 = N_2 \sqrt{10}$	(Case No. 3) $R_L' = 10R_g'$ $a = 0.0985$ $D = 2.414$ $N_1 = 7.07N_2$	(Case No. 4) $R_L' = R_g'$ $a = 1$ $D = 10.65$ $N_1 = N_2$	(Case No. 5) $R_L' = R_g'$ $a = 0.24$ $D = 10.65$ $N_1 = 1.165N_2$
$\frac{g_m}{N_1} R_L'$	2.414	7.63	12.55	1.207	1.315
$\frac{g_m}{N_2} R_g'$	2.414	0.763	1.255	1.207	1.315
$\frac{g_m}{N_1} R_L'^D$	5.83	18.4	30.3	12.85	14.0
$\frac{g_m}{N_2} R_g'^D$	5.83	1.84	3.03	12.85	14.0
$N_1^2 \frac{g_m}{N_1} R_L'$	4.828	15.25	104.0	0.457	0.854
$N_2^2 \frac{g_m}{N_2} R_g'$	4.828	1.525	2.10	0.457	0.63
P_L/P_x	4.12	4.12	41.2	7.05	41.2
R/R_1	0.707	0.707	1.285	4.825	7.78
$P_L/g_m E^2$	1.705	5.40	11.9	0.662	1.08

from those for stability in that the products $R_L' C_p$ and $R_g' C_g$ rather than $R_L' D$ and $R_g' D$ should be minimized. Tubes having large transconductances and small input and output capacities are desirable for this purpose. It is found that D must be relatively large and the impedance ratios small. Moreover, the values of $R_L' C_p$ and $R_g' C_g$ must be equal if maximum bandwidth is to be obtained.

In the present example we assume that C_p is equal to C_g . A value of unity is selected for both a and N_1/N_2 so as to obtain equal values of R_L' and R_g' . To reduce R_L' and R_g' to one half the values obtained in Case No. 1, it is necessary to make D equal to 10.65. The complete set of parameters is presented as Case No. 4 in Table 10.1.

5. Design Conditions Favoring Power Output and Broad-Band Operation.

The design of Case No. 4 may be modified to yield a more favorable power ratio by reducing a to 0.24, holding D constant at 10.65, and altering N_1/N_2 so as to keep the required equality of R_L' and R_g' . The results of this design, which yields a power ratio ten times that in Case No. 1, are presented as Case No. 5 in Table 10.1.

G. Conclusions.

As indicated by equation 10.19, the relative frequency stability of the five cases in Table 10.1 may be obtained directly from their respective RD products, provided the same crystal and tube is used in each case. Also, the relative instability of the grid and plate capacities is readily compensated for. If we assume the grid capacity to be an order less stable than the plate capacity the fractional frequency stability of Case No. 1 becomes

$$\left(\frac{d\omega}{\omega}\right)_1 = K(R_L'D)_1 + 10K(R_g'D)_1 = 64.13K \quad (10.32)$$

where

$$K = \omega_0 dC_p / 2Qg_m , \quad (10.33)$$

$$(R_L'D)_1 = R_L'D \text{ for Case No. 1} , \quad (10.34)$$

and

$$(R_g'D)_1 = R_g'D \text{ for Case No. 1} . \quad (10.35)$$

This same computation, with appropriate redefinition of terms, may be made for each of the other designs.

Comparisons of the results of these computations show that:

- a. the fractional frequency deviation in Case No. 2 is reduced to 57 per cent of that in Case No. 1,
- b. the modifications made to obtain high power output in Case No. 3 result in a frequency stability approximately equal to that obtained in Case No. 1,
- c. and the designs for broad-band operation are the least stable with respect to capacity variations. The fractional frequency stabilities of cases No. 4 and No. 5 are poorer than that in Case No. 1 by a factor slightly greater than two.

The quantities P_L/P_X and $P_L/g_m E^2$ indicate respectively the limitations imposed on power output by the crystal and the tube. Comparison of the values of these two quantities obtained in Cases No. 3 and 4 shows that while equally high power ratios are obtained, the broad-band design, because of its relatively low plate impedance, requires a value of $g_m E^2$ about ten times that of the power design. In practice this may result in the limitation of power output by the tube rather than the crystal.

Relative bandwidths may be obtained by comparing the values of R_L' and R_g' , it being understood that in the cases where R_L' is equal to $10R_g'$, the former controls the bandwidth. The results for Case No. 2 show that favoring the grid circuit with a low impedance reduces the obtainable bandwidth of untuned operation to about one third of that in Case No. 1. From the results of Case No. 4 it may be seen that a two to one increase in bandwidth results in approximately a two to one reduction in frequency stability. The results of Case No. 5 show that a slight reduction in bandwidth from that of Case No. 4 yields a considerable improvement with respect to power output.

H. Typical Designs and Experimental Results.

The following designs were executed and tested prior to the development of the methods presented in the preceding section; consequently, they are not representative of the particular cases in Table 10.1. However, the results obtained are good, and emphasize the fact that departure from optimum conditions must be great before serious degradation of performance occurs.

1. Basic Transformer-Coupled Oscillator.

The schematic diagram of a basic transformer-coupled oscillator

is shown in Figure 10.3. This particular circuit is designed to operate at a center frequency of 55 Mc with crystals having series resistances of 82 ohms or less.

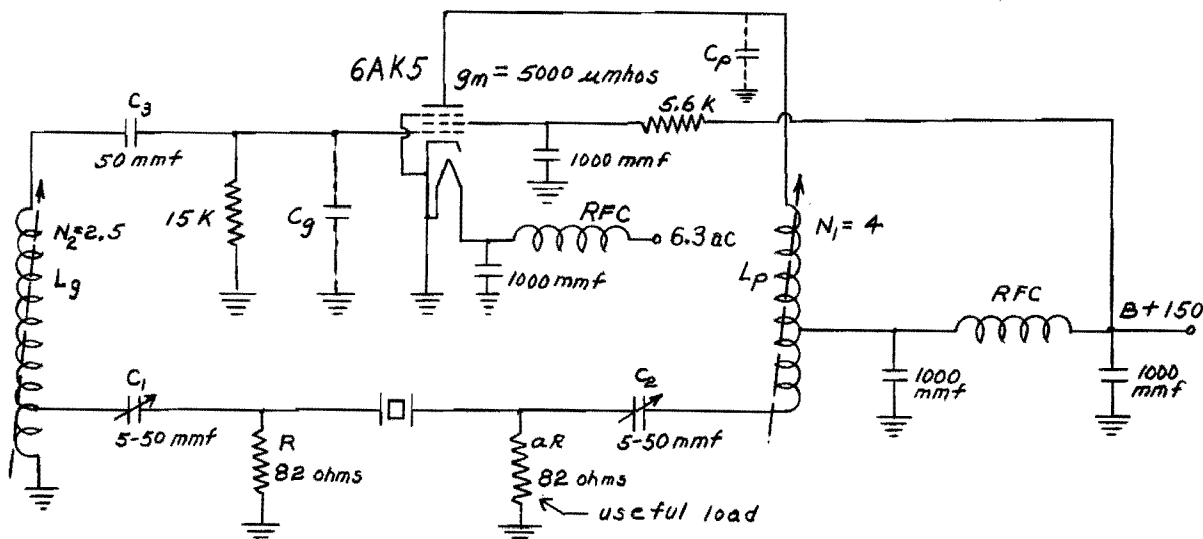


Figure 10.3 - Basic Transformer-Coupled Oscillator

The low sides of the plate and grid transformers are loaded with 82 ohm resistors making \underline{a} equal to one and D equal to three. Using these values and the values of N_1 and N_2 shown in Figure 10.2, we find the required value of g_m from equation 10.7 to be

$$g_m' = \frac{3(4)}{2.5(4)(82)(4)} = 0.0037 \text{ mho} . \quad (10.36)$$

Since the 6AK5 tube has a nominal transconductance of 0.005 mho, a suitable gain margin is provided.

Computed values of the impedance levels, stability criteria and power criteria are presented in Table 10.2.

TABLE 10.2
PARAMETERS FOR BASIC TRANSFORMER-COUPLED OSCILLATOR

R_L' = 865 ohms	$R_L'D$ = 2595	P_L/P_X = 4.0
R_g' = 338 ohms	$R_g'D$ = 1014	$P_L/g_m'E^2$ = 3.2

Final Report Project No. 131-45

The transformers in Figure 10.3 were constructed according to the principles set forth in Chapter XVIII, and their high side inductances were adjusted to antiresonate C_p and C_g at the center frequency of 55 Mc. The capacitors C_1 and C_2 were adjusted to resonate the equivalent leakage inductance referred to the low side of the transformers at the same frequency. Because the reactance of the holder capacitance of all the crystals used in this oscillator was high compared to the series resistance, R_L , it was not necessary to provide crystal compensation.

Operating data for the circuit are presented in Table 10.3.

TABLE 10.3
OPERATING DATA FOR BASIC TRANSFORMER-COUPLED OSCILLATOR

f (Mc)	Overtone	C_o (mmf)	R_L (ohms)	Stability ppm/v	Δf (Kc)	Power (mw)
50	5	5	48	0.6	1.5	100
54	9	5	60	0.18	0.5	80
54.8	7	6	80	0.11	0.0	50
58.3	7	8	82	0.625	1.4	40
60	3	13	25	0.66	1.7	40

The power output in Table 10.3 was obtained by measuring the voltage across the useful load (Figure 10.3), and Δf is the difference between the frequency produced by the oscillator and that produced by the same crystal operating at unity power factor in high frequency crystal impedance meter TS-683()/TSM. This circuit will tolerate a considerable variation in series resistance and shunt capacity of the crystal used as well as in tube transconductance. It has moderate power output over a ten Mc band with good frequency stability. It was found experimentally that compensation of the crystal holder capacity resulted in a slight improvement in frequency stability and in a reduction of Δf near the edge of the band.

This oscillator will operate even if considerable error in tuning exists; but to obtain symmetrical operation about a specified center frequency,

the adjustments to antiresonate C_p and C_g and those to resonate the leakage inductances must be carefully performed. As a check on these adjustments a resistor equal to 82 ohms may be substituted for the crystal. The tuning is unsatisfactory if the operating frequency differs from the design frequency by more than two per cent.

2. Broad-Band Transformer-Coupled Oscillator.

Because the transformer-coupled oscillator will operate with very low values of effective grid and plate impedance, it is well suited for broad-band untuned operation; as shown in the preceding section, bandwidths up to ten Mc may be obtained with simple circuits. By using phase compensating networks as described in Chapter VIII, the low phase bandwidth of the impedance transforming network may be considerably extended.

The circuit in Figure 10.4 was constructed before the analysis in Chapter VIII was available, and some of the principles of this chapter are violated. In spite of this, satisfactory operation over a 20 Mc band was obtained.

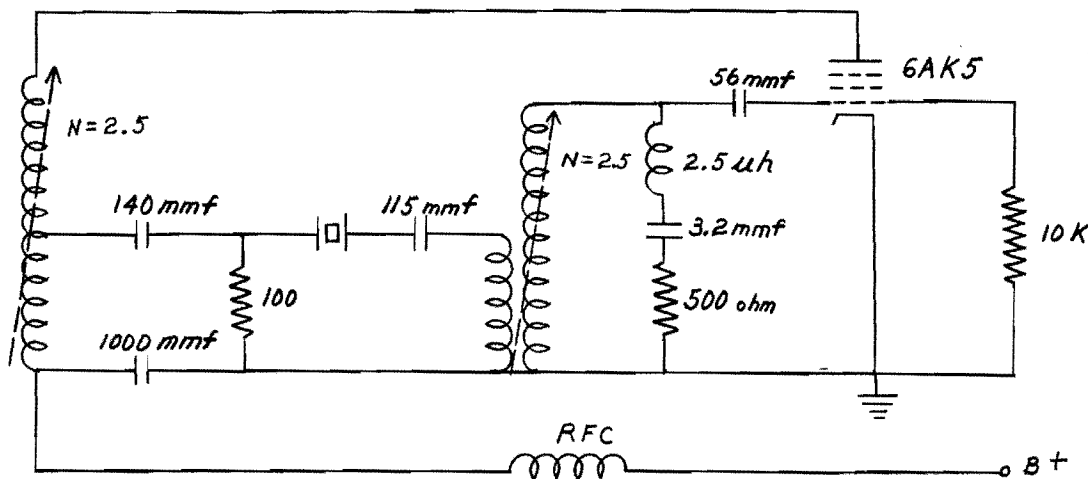


Figure 10.4 - Broad-Band Transformer-Coupled Oscillator

The elements R, L, and C of Figure 10.4 were selected with the help of Chart I, Bode¹, p. 445, to compensate the phase shift produced by the other elements over a considerable frequency band centered on 65 Mc. The grid circuit was found to be more critical with respect to tuning and for this reason the compensating network was located at the high side of the grid

transformer. It is now realized that this was an unfortunate choice of location. It is believed that better results would have been obtained had the compensating network been located in the plate circuit. Nevertheless, with crystals having low to moderate series resistance and shunt capacity, the circuit operated on a crystal plug-in basis from 53 to 73 Mc.

3. Transformer Coupled Oscillator Design for Power Output.

The following is an illustrative design of a class C transformer-coupled oscillator operating at 50 Mc with a 50 ohm crystal and designed for a power output of one watt. The circuit of this oscillator is shown in Figure 10.5, and the initial and final circuit parameters are presented in Table 10.4.

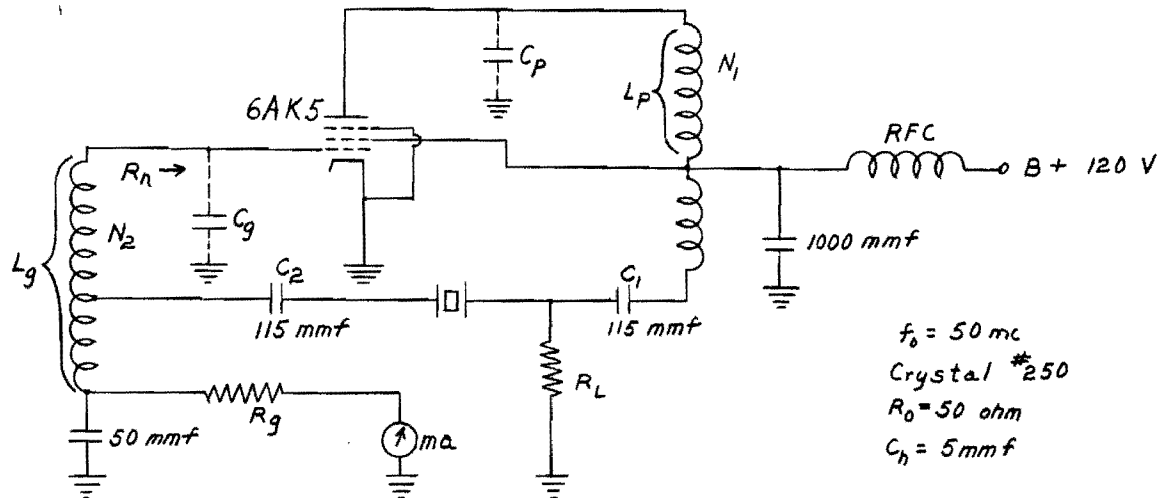


Figure 10.5 - High Power Transformer-Coupled Oscillator

TABLE 10.4
CIRCUIT CONSTANTS FOR FIGURE 10.5

	Initial	Final
N_1	13	10
N_2	13	11
R	10 ohms	15 ohms
R_g	52,000 ohms	47,000 ohms

The type 6AK5 tube used has as nominal parameters a transconductance of 0.005 mho, an input resistance due to transit time loading of approximately 23,000 ohms, and a positive grid resistance, R_g , of about 500 ohms.

Selection of 25° as a suitable value of θ_g (half the grid conduction angle) permits the computation of the grid leak resistance. From equation 7.29, Chapter VII, we find

$$R_g = \frac{\pi r_g}{\tan \theta_g - \theta_g} \doteq 52,000 . \quad (10.37)$$

It should be noted that in Figure 10.5, R_g is located so that it dissipates no ac power, and that equation 10.37 gives the correct value of resistance for this location only.

The effective resistance due to grid conduction is given by $\beta_g r_g$. Since θ_g is known, β_g may be obtained from Table 7.1 and is equal to 58.9, therefore the loading due to grid conduction is equivalent to 29,500 ohms. Since the loading due to transit time is comparable, the total input resistance is determined by combining this resistance in parallel with the resistance due to grid conduction. This results in a value of R_n equal to 12,900 ohms.

The values of N_2 and a were selected on the basis of stability and power considerations. It is known that low values of a are conducive to high ratios of load to crystal power and that N_2 must be large to avoid excessive Q degradation. For N_2 equal to 13, the resistance faced by the crystal (R_n/N_2^2) is equal to 76.5. The selection of a ten ohm load resistance results in a value of 0.13 for a , and a value of D which is given by

$$D = \frac{R_1 + R_n/N_2^2 + R_L}{R_1} = 2.73 . \quad (10.38)$$

The selection of the condition $N_1 = N_2$ permits the calculation of the effective transconductance required for oscillation. From equation 10.7

$$g_m' = \frac{2.73(1.13)^2}{169(0.13)50(1.73)^2} = 0.001 . \quad (10.39)$$

Since the tube has a nominal transconductance of 0.005 mho, this value of g_m' corresponds to a β_p given by

$$\beta_p = \frac{g_m'}{g_m} = 5.0 . \quad (10.40)$$

From Table 7.1 it is seen that this value of β_p corresponds to a plate conduction angle of approximately 120° , which is consistent with good class C operation.

Computed values of the impedance levels, stability criteria, and power criteria for this circuit are presented in Table 10.5.

TABLE 10.5
PARAMETERS FOR FIGURE 10.5
(Initial Design)

R_L'	= 1570 ohms	R_{gD}'	= 15,500 ohms
R_g'	= 5690 ohms	P_L/P_x	= 32
$R_L'D$	= 4300 ohms	$P_L/g_m'E^2$	= 1.54

The adjustment procedure used for this circuit is the same as that for the basic-transformer-coupled oscillator, and data on its operating characteristics are presented in Table 10.6.

TABLE 10.6
OPERATING DATA

	Initial	Final
Supply Voltage	120 volts	150 volts
DC power input	1.4 watts	1.8 watts
RF power output	0.42 watts	0.6 watts
Crystal Power	0.045 watt	0.02 watt
Efficiency	30 per cent	33 per cent
Power Ratio	9.3/1	30/1
Grid Bias	-13 volts	-19 volts
Frequency Stability	0.4 ppm/v	0.3 ppm/v

The final circuit values were obtained by experimental adjustment, using the RF voltages in the circuit as a guide. In particular, it was found initially that the voltage at the low side of the grid transformer was too low, indicating that the estimated value of R_n was low.

Comparison of the values of the parameters in Table 10.5 with those in Table 10.1 shows that the present circuit conditions depart considerably from the optimum. However, reasonably good results were still obtained.

I. Advantages and Disadvantages.

The transformer-coupled oscillator is the most flexible circuit considered in this report. This circuit may be designed to operate as a highly stable single-frequency oscillator, as a broad-band untuned oscillator, and as an efficient power source having good stability. The design procedures are, however, somewhat more complex than those for other circuits.

The design of this circuit for class C operation is further complicated by the difficulties encountered in determining the input resistance of the tube. Due largely to this fact, the experimental results for this circuit do not agree as closely with the predicted results as do those for the grounded-grid oscillator.

BIBLIOGRAPHY

- (1) Bode, H. W., "Network Analysis and Feedback Amplifier Design," First Edition, D. Van Nostrand Co., Inc., New York (1945).

XI THE GROUNDED-GRID OSCILLATOR

A. Introduction.

A grounded-grid oscillator can be obtained by adding a crystal-controlled feedback path to a grounded-grid amplifier. The arrangement is quite simple because it requires only one transformer in conjunction with a simple triode. Moreover, the transformer has a moderate turns ratio and does not produce a phase reversal; therefore, a simple autotransformer is appropriate. This type of transformer inherently has a high coefficient of coupling, which is desirable from stability and bandwidth considerations.

Because the input (cathode) impedance of a typical tube operating as a grounded-grid amplifier is low, the crystal faces low impedances in both directions without the use of a second transformer. The excellent shielding between input and output circuits, which is characteristic of the grounded-grid arrangement, substantially eliminates any tendency toward oscillations which are not under crystal control.

If the grounded-grid oscillator is designed to give a large power output then the tube is operated in class C, and (as shown in Chapter VII) the input impedance becomes large. In this case an autotransformer having a moderate turns ratio is used in the cathode circuit to avoid seriously degrading the crystal Q. While it is true that, aside from grid losses, the energy used in driving the tube is recovered in the output, the grounded-grid amplifier has a considerably lower power gain than the grounded-cathode amplifier. For this reason the ratio of the power output to the power dissipated in the crystal is lower than in the transformer coupled oscillator.

B. Impedance Levels and Loop Gain Considerations.

The design of the grounded-grid oscillator is conveniently studied in terms of the schematic diagram of Figure 11.1. In this circuit, the plate-to-grid and cathode-to-grid capacitances are antiresonated at the series resonant frequency of the crystal by their associated inductances, and the useful load is represented by R_L .

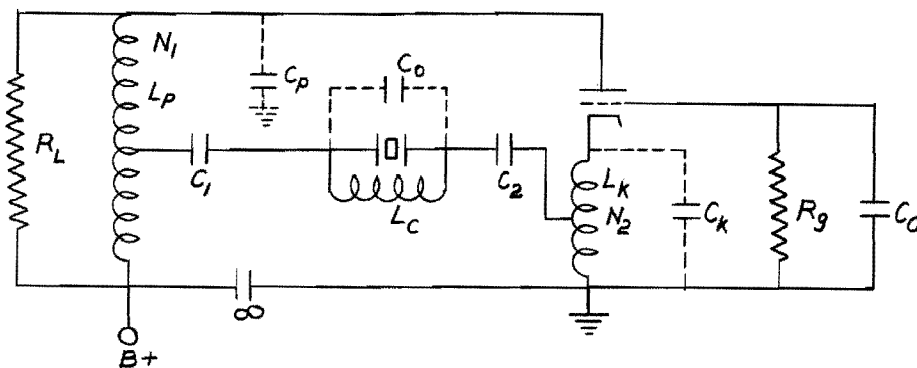


Figure 11.1 - Grounded-Grid Oscillator

Figure 11.2 illustrates the equivalent circuit which results from assuming that, (a) the plate and cathode transformers have unity coupling, (b) the losses in L_k and L_p are negligible, and (c) the crystal holder capacity is negligibly small, or is antiresonated by a suitable shunt inductance. Since the input and output networks of the amplifier may be designed* to give a specified voltage ratio N_1 , the assumption of unity coupling need introduce no error in the gain equations. The conditions of the latter two assumptions are readily met in practice.

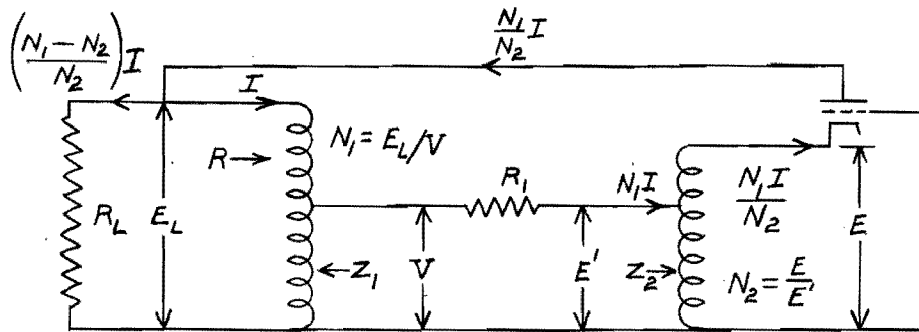


Figure 11.2 - Idealized Equivalent of Figure 11.1

From Figure 11.2 one may write the following equations:

$$E_L = (N_1/N_2 - 1)IR_L \quad (11.1)$$

$$E_L = N_1 V, \quad (11.2)$$

and

$$V = N_1 IR_1 + E/N_2. \quad (11.3)$$

* Chapter XVIII of this report.

In Chapter VII it was shown that the fundamental component of plate current of a class C grounded-grid amplifier is given by

$$I_{pl} = \frac{E(\mu + 1)}{\beta_p r_p + R_L}, \quad (11.4)$$

where the effective plate load impedance R_L' represents the parallel combination of R and R_{Lj} , as given by

$$R_L' = (1 - N_2/N_1)R_L; \quad (11.5)$$

r_p represents the normal plate resistance of the tube, and β_p is a function of the angle of flow of plate current. Values of β_p are tabulated in Chapter VII. Replacing I_{pl} by its equivalent in Figure 11.2 and eliminating R_L' in terms of E_L , one has

$$\frac{N_1}{N_2} I = \frac{E(\mu + 1) - E_L}{\beta_p r_p}. \quad (11.6)$$

Combination of equations 11.1 and 11.2 yields

$$N_1 V = (N_1/N_2 - 1)IR_L. \quad (11.7)$$

Elimination of E_L between 11.2 and 11.6 yields

$$\frac{N_1 I \beta_p r_p}{N_2} = E(\mu + 1) - N_1 V. \quad (11.8)$$

Use of 11.3 to eliminate V from these equations results in the expressions

$$EN_1/N_2 + N_1^2 IR_L = (N_1/N_2 - 1)IR_L, \quad (11.9)$$

and

$$\frac{N_1}{N_2} I \beta_p R_p = E(\mu + 1) - (N_1/N_2 - 1)IR_L. \quad (11.10)$$

Finally, E and I may be eliminated between these expressions to give as the condition for sustained oscillation

$$R_L = \frac{N_1^2 [(\mu + 1)R_L + \beta_p r_p / N_2]}{(N_1/N_2 - 1)(\mu + 1 - N_1/N_2)}. \quad (11.11)$$

The impedances Z_1 and Z_2 in conjunction with R_L determine the Q degradation and are of considerable importance. From Figure 11.2 one may write

$$Z_2 = E' / N_1 I . \quad (11.12)$$

Since E' is equal to E/N_2 ,

$$Z_2 = E/N_1 N_2 I . \quad (11.13)$$

By eliminating E between equations 11.9 and 11.2, the following expression for Z_2 is

$$Z_2 = \frac{\beta_p r_p}{N_2^2(\mu + 1)} + \frac{(N_1/N_2 - 1)R_L}{N_1 N_2 (\mu + 1)} . \quad (11.14)$$

The first term is approximately equal to $\beta_p / N_2^2 g_m$; the second term, which is small in class A operation, shows the effect of the load resistance on Z_2 .

The impedance Z_1 may be found from the parallel combination of the load resistance and the effective plate resistance of the tube including the impedance ratio of the transformer. The effective plate resistance r_p' of the tube is affected by the impedance in the cathode circuit, which itself involves Z_1 , the equation being:

$$r_p' = \beta_p r_p + (\mu + 1)(R_L + Z_1)N_2^2 \quad (11.15)$$

and

$$Z_1 = R_L r_p' / N_1^2 (R_L + r_p') . \quad (11.16)$$

Simultaneous solution of these equations is not justified because r_p' must be between the limits $\beta_p r_p$ and ∞ , and the corresponding limits on Z_1 are quite near each other. In any event, an approximate value of Z_1 , say $Z_1 \approx R_L / N_1^2$, may be substituted in (11.15), and the resulting value of r_p' used in equation 11.16 to compute Z_1 to a very close approximation.

In order to estimate the effect of cathode capacity variation of frequency, the effective cathode-to-ground resistance, R_k' , must be known. This may be found from R_L , N_2 , and previously determined values of Z_1 and Z_2 . Therefore,

$$R_k' = \frac{N_2^2 Z_2 (R_L + Z_1)}{R_L + Z_1 + Z_2} . \quad (11.17)$$

The ratio of load power to power dissipated in the crystal is an important factor in oscillator design; it is readily expressed in terms of the power

gain of the amplifier and the degradation of the crystal Q. For the present purposes, however, it is preferable to express this ratio in terms of the circuit parameters. From Figure 11.2 it may be seen that the power dissipated in the crystal is $(N_1 I)^2 R_1$ and the load power is equal to $(N_1 - N_2)^2 I^2 R_L / N_2^2$. From these, the ratio of load to crystal power is

$$\frac{P_L}{P_x} = \left(\frac{N_1 - N_2}{N_1 N_2} \right)^2 \frac{R_L}{R_1}. \quad (11.18)$$

The degradation of the crystal selectivity may be found by using

$$D = \frac{Z_1 + Z_2 + R_1}{R_1}. \quad (11.19)$$

The foregoing derivations are based on the assumption that the plate and cathode currents of the tube are equal. If a pentode tube is used this will not be true; however, computation of a typical example with the cathode current equal to 1.25 times the plate current shows that the values of R_L and D differ by only 5 per cent from the values obtained with the cathode and plate currents equal. Thus, this assumption appears to be justified.

Experimental work has borne out the correctness of this analysis; however, for convenience the load resistance, R_L , has been replaced by a correspondingly smaller resistance R_L / N_1^2 , across the low winding of the plate transformer. If the plate transformer has a high coefficient of coupling, this connection has little effect on the frequency stability and provides a low impedance load across which voltage measurements can be made without seriously disturbing the operation of the circuit.

C. Frequency Stability Considerations.

In the grounded-grid oscillator, the plate-to-ground and grid-to-ground capacities are the two parameters which are least subject to design control. Since these capacities are subject to variations with time, temperature, and electrode potentials, it is desirable to consider means of reducing their effect on the frequency stability of the oscillator.

In Chapter VI of this report it is shown that for a given crystal excited by a transformer network, the fractional frequency deviation caused by a small variation in shunt capacity is directly proportional to the product

of the Q degradation and the effective resistance R shunting the capacity. Therefore, it is appropriate to attempt to minimize the pertinent RD products. Let us first direct our attention toward reducing frequency variations due to C_p . That is, let us seek to minimize the product of D and the effective plate impedance R_L' as given by equation 11.5.

The normal procedure would be to combine equations 11.5 and 11.19 and differentiate to establish a minimum. However, the resulting expression is so complicated and involves so many parameters that the situation is confused rather than clarified by this process. This also applies to the expression resulting from an attempt to minimize the product of D and the effective cathode resistance R_k' . Therefore, the operating characteristics corresponding to a variety of reasonable parameter values are calculated. The ratio N_1/N_2 and the tube parameters μ and g_m' are used in this procedure where

$$g_m' = g_m/\beta_p . \quad (11.20)$$

The process begins by rewriting equation 11.11 in the form

$$g_m'^R_L = \frac{(N_1/N_2)^2 [(\mu + 1)N_2^2 g_m'^R_L + \mu]}{(N_1/N_2 - 1)(\mu + 1 - N_1/N_2)} . \quad (11.21)$$

Equation 11.14 yields

$$\frac{N_2^2}{N_2} g_m'^Z_2 = \frac{\mu}{\mu + 1} + \frac{(1 - N_2/N_1)g_m'^R_L}{(\mu + 1)} . \quad (11.22)$$

Equations 11.16 and 11.15 respectively yield the expressions

$$\frac{N_2^2}{N_2} g_m'^Z_1 = \frac{(g_m'^R_L)(g_m'^r_p N_2^2)}{(g_m'^R_L + g_m'^r_p N_1^2)} , \quad (11.23)$$

where the particular grouping is chosen in anticipation of later usefulness, and

$$g_m'^r_p = \mu + (\mu + 1)(N_2^2 g_m'^R_L + N_2^2 g_m'^Z_1) . \quad (11.24)$$

Using the same parameters, equations 11.18 and 11.19 become respectively:

$$\frac{P_L}{P_X} = (1 - N_2/N_1)^2 \frac{g_m'^R_L}{\frac{N_2^2}{N_2} g_m'^R_L} , \quad (11.25)$$

and

$$D = \frac{N_2^2 g_m^2 Z_1 + N_2^2 g_m^2 Z_2 + N_2^2 g_m^2 R_1}{N_2^2 g_m^2 R_1} . \quad (11.26)$$

The expressions for the effective plate and cathode impedances (11.5 and 11.7) yield

$$g_m^2 R_L' = (1 - N_2/N_1) g_m^2 R_L , \quad (11.27)$$

and

$$g_m^2 R_k' = \frac{N_2^2 g_m^2 Z_2 (N_2^2 g_m^2 R_1 + N_2^2 g_m^2 Z_1)}{N_2^2 g_m^2 R_1 + N_2^2 g_m^2 Z_1 + N_2^2 g_m^2 Z_2} . \quad (11.27a)$$

In these expressions g_m^2 may be regarded as the effective transconductance so as to obtain a suitable gain margin.

Using the foregoing relationship, we may now compute values of $g_m^2 R_L' D$, $g_m^2 R_k' D$, $g_m^2 R_L$ and P_L/P_X as a function of N_1/N_2 with μ and $N_2 g_m^2 R_1$ as parameters. Plots of these quantities are shown in Figures 11.3, 11.4, 11.5, and 11.6. While these curves were computed for $\mu = 55$, they apply with little error to cases involving larger values of μ . For low values of N_1/N_2 and for any values of μ between 30 and ∞ , the curves give values of R_L' and power ratios and values of $g_m^2 R_L' D$ within 20 per cent. If, however, N_1/N_2 is as high as 10, the error in R_L' and the power ratio increases to about 20 per cent, while $g_m^2 R_L' D$ may be in error by much as 30 per cent. For each of the three parameters, the curves give values that are low for low μ tubes and high for high μ tubes. These errors represent extremes; therefore, the utility of the design curves is not seriously limited, because most tubes suitable for use in grounded-grid oscillators have a value of μ above 30.

Due to the relative instability of the cathode capacity, it is desirable to favor the cathode circuit with a relatively low effective shunt resistance. Comparison of Figures 11.4 and 11.6 shows this objective is normally met. For values of N_1/N_2 greater than four, $g_m^2 R_L' D$ is at least ten times greater than $g_m^2 R_k' D$, and a variation of cathode capacity at least ten times that of the plate capacity is required to produce equal frequency shifts.

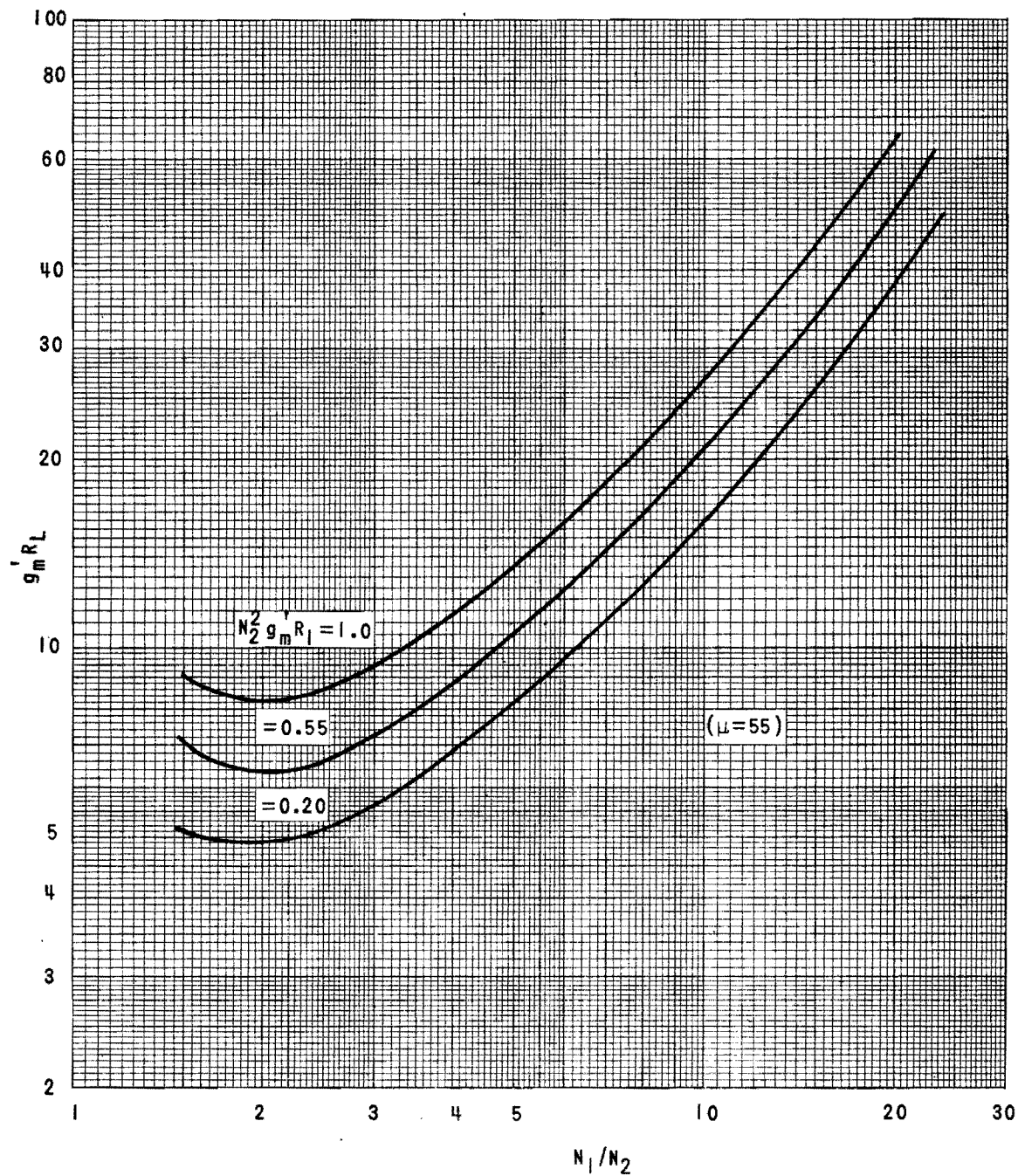


Figure 11.3 $g_m R_L$ Versus N_1/N_2

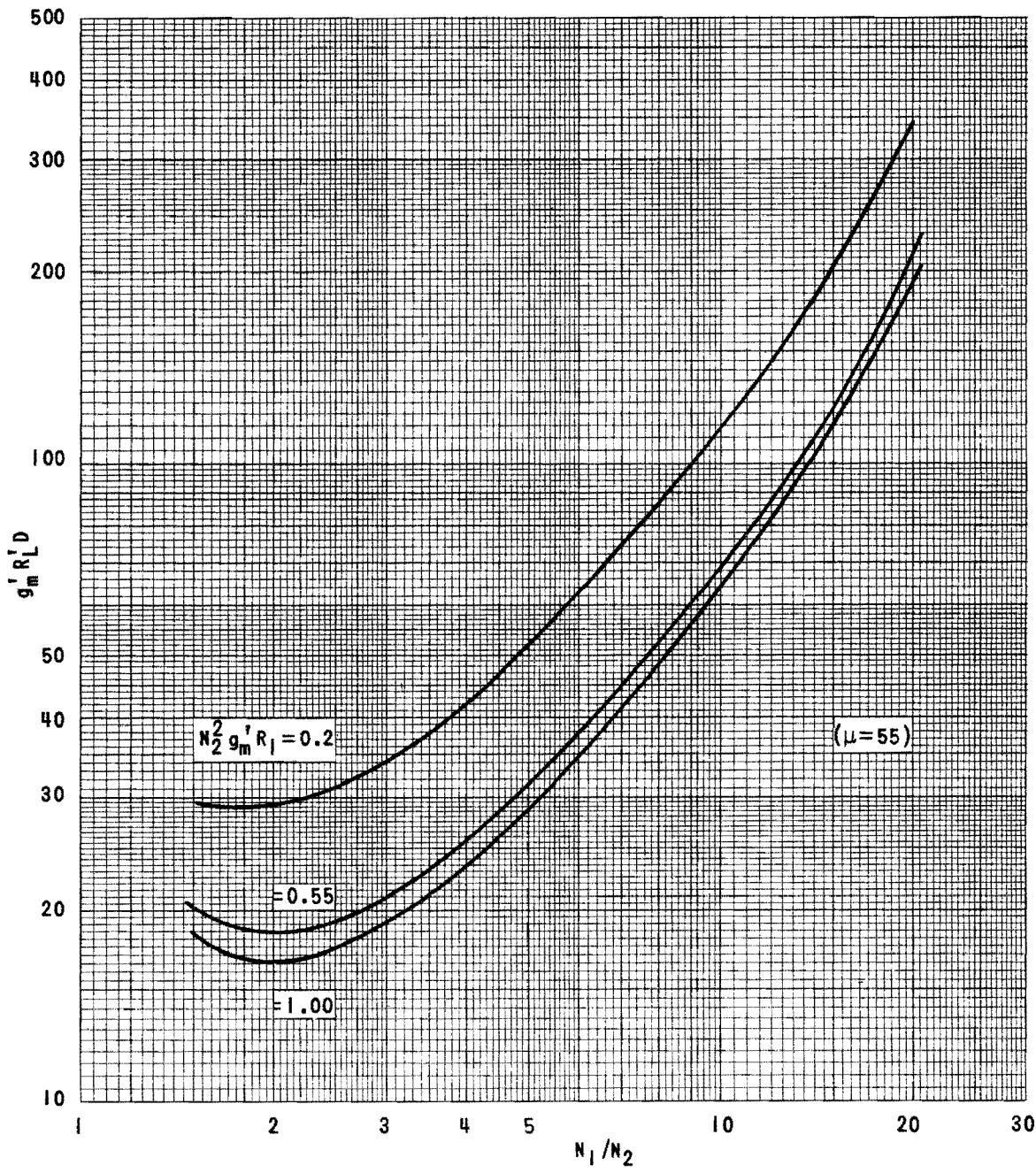


Figure 11.4 $g_m' R_L' D$ Versus N_1/N_2

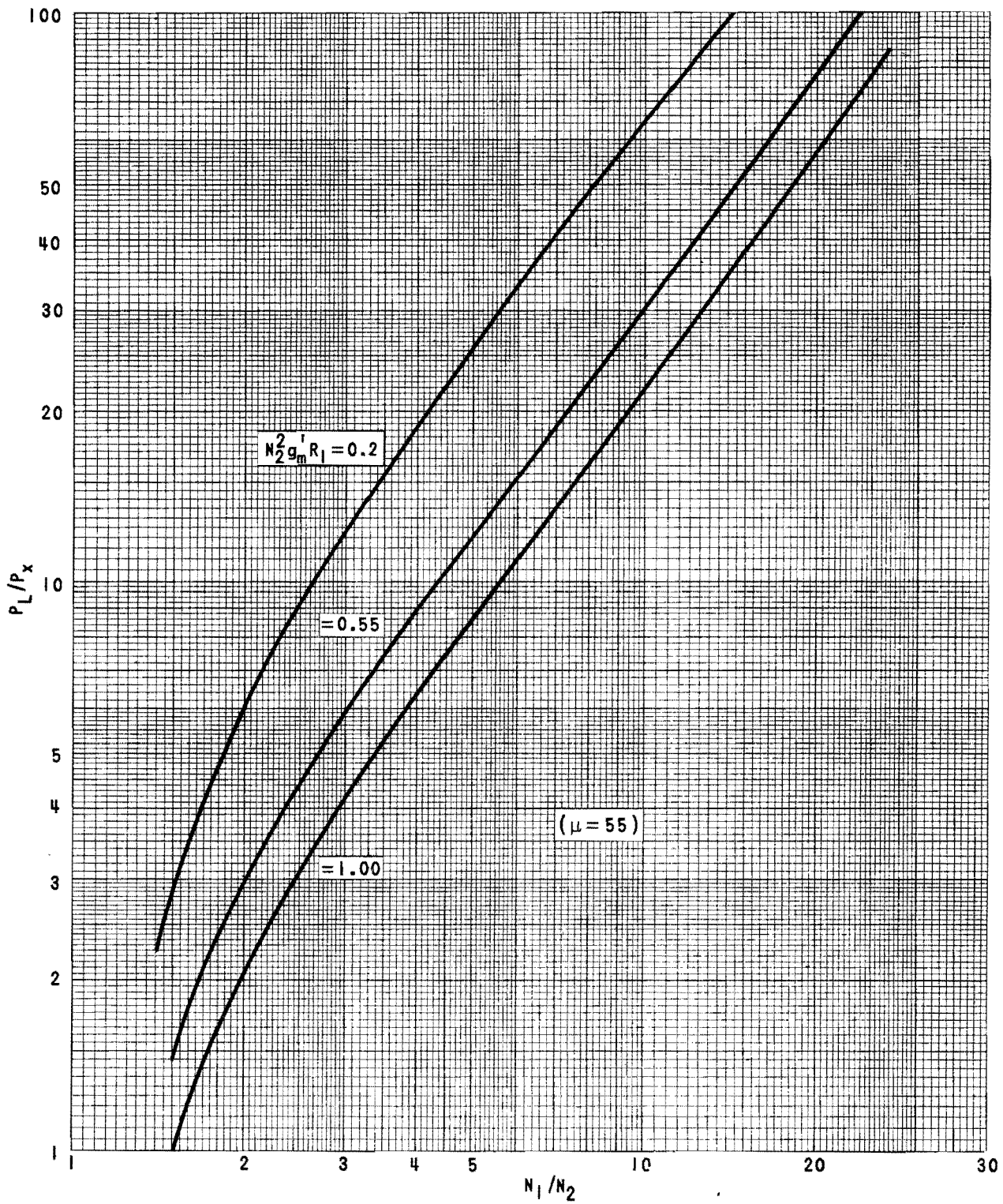


Figure 11.5 Ratio of Load To Crystal Power Versus N_1/N_2 .

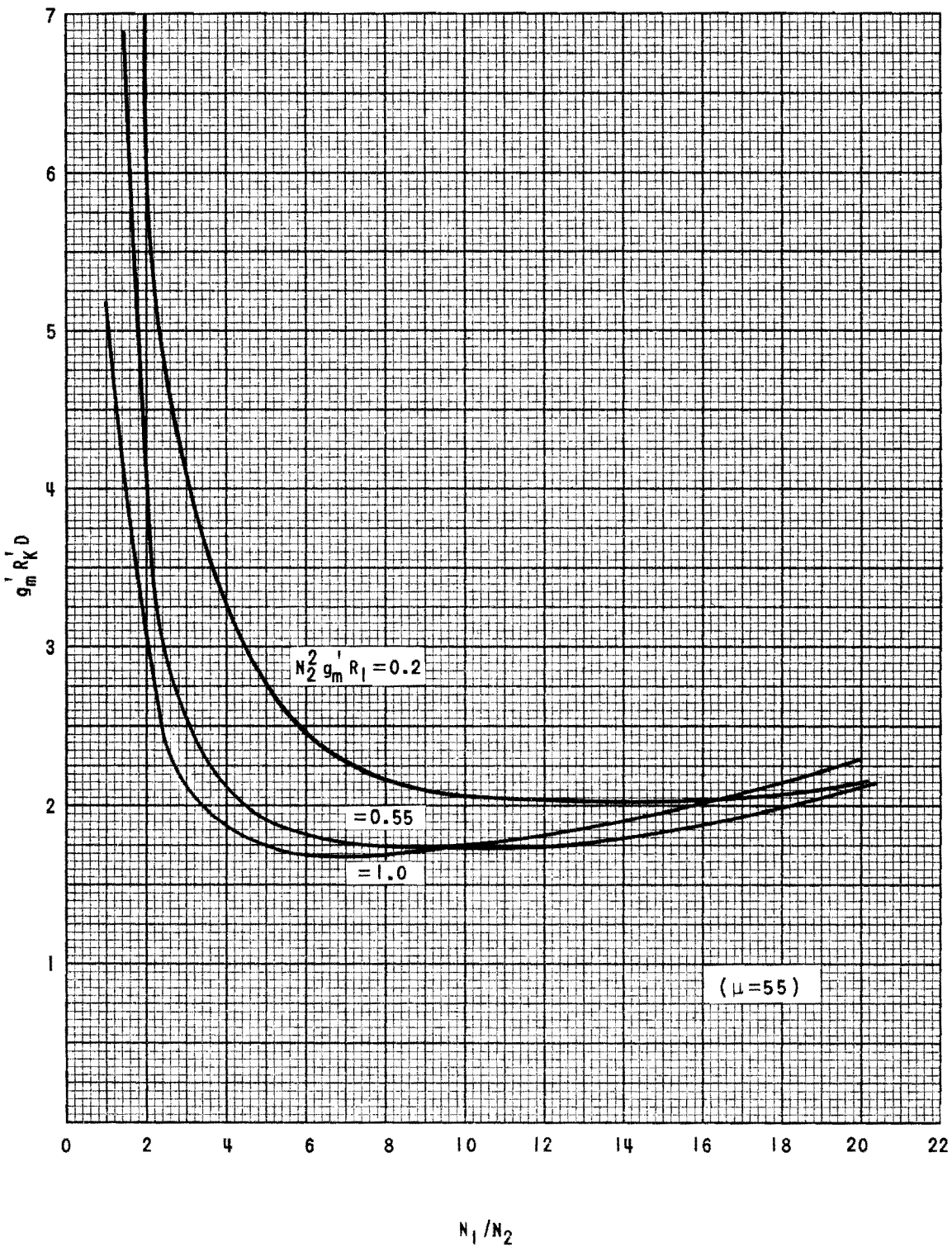


Figure 11.6 $g_m' R_K D$ Versus N_1/N_2

The use of the design curves is illustrated in the following sections on typical designs.

D. Phase Considerations and Crystal Compensation.

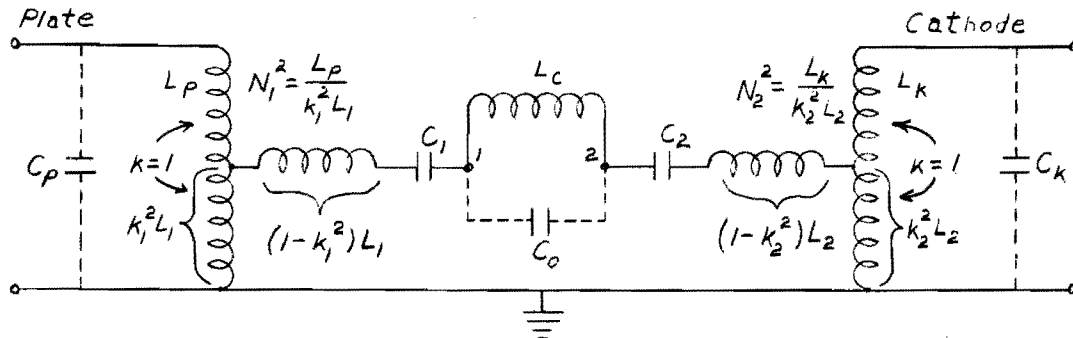
Because the input impedance of the grounded-grid amplifier is very much smaller than the required plate-to-ground impedance in either class A or class C operation, the bandwidth of the input circuit (L_k and C_k) will normally be much greater than that of the plate network. Also the low impedance considerably reduces the effect of the input capacity on frequency stability; therefore, even though a higher load resistance is required, the grounded-grid oscillator may be made as stable with respect to capacity variations as the transformer coupled circuit.

Correct phase relations at the operating frequency may be obtained by antiresonating C_k and C_p with L_k and L_p which are respectively the high side inductances of the input and output transformers, and by resonating the leakage inductance of the transformers with C_1 and C_2 . This leakage inductance is that seen looking into the low side of the transformer with the high side shorted. Under these conditions the crystal will operate as a pure resistance at a frequency (f_r , Chapter II) which is above the resonant frequency of the series arm.

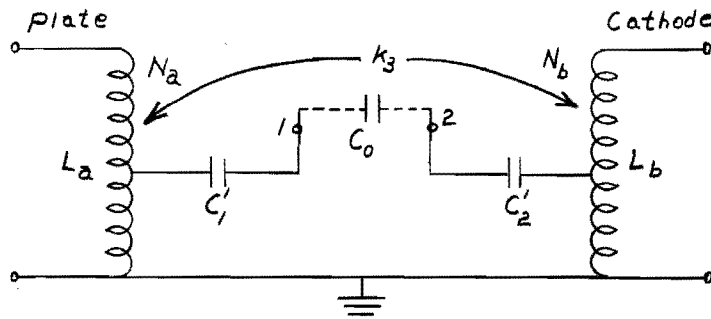
If operation at the resonant frequency of the series arm (f_o , Chapter II) is desired or if the reactance of the holder capacity is not large compared to R_1 , the crystal must be compensated. For single frequency or moderately broad-band operation with low resistance crystals, a simple network consisting of an inductor and resistor in shunt with the crystal may be used for compensation. If the resistance of the crystal is high or if broad-band operation is desired, a more complex two terminal network may be necessary. The main requirements of the compensating network are that the network, in conjunction with the crystal holder capacity, should present a high impedance across the crystal terminals over a frequency band greater than that of the plate network, and that the network should not seriously degrade the crystal Q. Since the holder capacity is seldom more than twice the plate capacity of the tube, and the crystal resistance is typically less than one tenth the load resistance, these requirements may be met successfully.

An equivalent method of compensation is illustrated in Figure 11.7. Here

the reactance required to antiresonate C_o is obtained by virtue of mutual coupling between the input and output transformers. Circuits using this type of compensation require fewer components and are less susceptible to troubles due to stray magnetic coupling, because the couplings are kept under control.



(a) With physical coil



(b) With mutual inductance

Figure 11.7 - Crystal Compensation Using Two Transformers

In Figure 11.7a, the plate and cathode transformers are shown in the well-known equivalent form¹ in which the total leakage inductance is referred to the low side of the transformer. The symbols used are:

k = coefficient of coupling,

L_1 = low side inductance of the plate transformer,

L_2 = low side inductance of the cathode transformer,

and

$$1/\omega_o^2 = L_p C_p + L_k C_k + L_c C_o + (1 - k_1^2)L_1 C_1 + (1 - k_2^2)L_2 C_2 ,$$

where ω_o is the operating frequency of the crystal.

The values of L_a , L_b and k_3^2 required to make Figure 11.7b the equivalent of Figure 11.7a, may be found by equating corresponding open-and short-circuit inductances in the following manner. With the cathode terminal shorted to ground and terminals 1 and 2 open, the inductance between the plate terminal and ground in Figure 11.7b is found to be $L_a(1 - k_3^2)$. For Figure 11.7a, the same inductance under the same conditions is $N_1^2 L_p L_c / (L_p + N_1^2 L_c)$. Equating these expressions to solve for L_a yields

$$L_a = \frac{L_p N_1^2 L_c}{(1 - k_3^2)(L_p + N_1^2 L_c)} . \quad (11.28)$$

Similarly the measurement of the inductance between the plate and ground terminals for both circuits with all other terminals open gives another expression for L_a :

$$L_a = \frac{L_p N_1^2 (L_c + L_k/N_2^2)}{L_p + N_1^2 (L_c + L_k/N_2^2)} . \quad (11.29)$$

From equations 11.28 and 11.29,

$$k_3^2 = \frac{L_p L_k/N_2^2}{(L_p + N_1^2 L_c)(L_c + L_k/N_2^2)} . \quad (11.30)$$

By measuring between the cathode terminal and ground with the plate terminal shorted to ground and terminals 1 and 2 open, the value of L_b is found to be

$$L_b = \frac{L_k N_2^2 L_c}{(L_4 + N_2^2 L_c)(1 - k_3^2)} . \quad (11.31)$$

The relation between the impedance transforming ratios in Figure 11.6a and b may be examined in the following manner. In Figure 11.7a, a voltage E_1 applied between plate and ground produces a voltage E_1/N_1 at terminal 1, and a voltage E_2 applied between cathode and ground produces a voltage E_2/N_2 at terminal 2. (It is to be understood that E_1 and E_2 are applied separately and that all terminals other than those driven are left open.) In Figure 11.6b, the application of E_1 and E_2 as above, results in voltages at terminals

1 and 2 of E_1/N_a and E_2/N_b respectively. Therefore, if 11.7a is to be equivalent to 11.7b, it is necessary that N_a equal to N_1 and N_b equal N_2 . The sign of the mutual inductance between L_a and L_b may be found by observing that the plate and cathode voltages must be in phase.

The values of C_1 and C_2 are chosen to resonate the leakage inductance of L_a and L_b respectively. In principle, these values can be determined from calculations of open and short-circuit inductance. In practice they are best determined experimentally since the leakage inductances can not be found without knowledge of the dimensions of the windings.

E. Design Procedures and Experimental Results.

1. Basic Grounded-Grid Oscillator.

By properly choosing load resistance and transformer turns ratio and by carefully tuning the transformer leakage inductance, the basic grounded-grid oscillator may be made to operate on a plug-in basis over a ten Mc band. The frequency stability throughout the band is good. By increasing the plate load impedance and turns ratio, a considerable increase of power output may be secured, but at the expense of frequency stability and bandwidth of untuned operation.

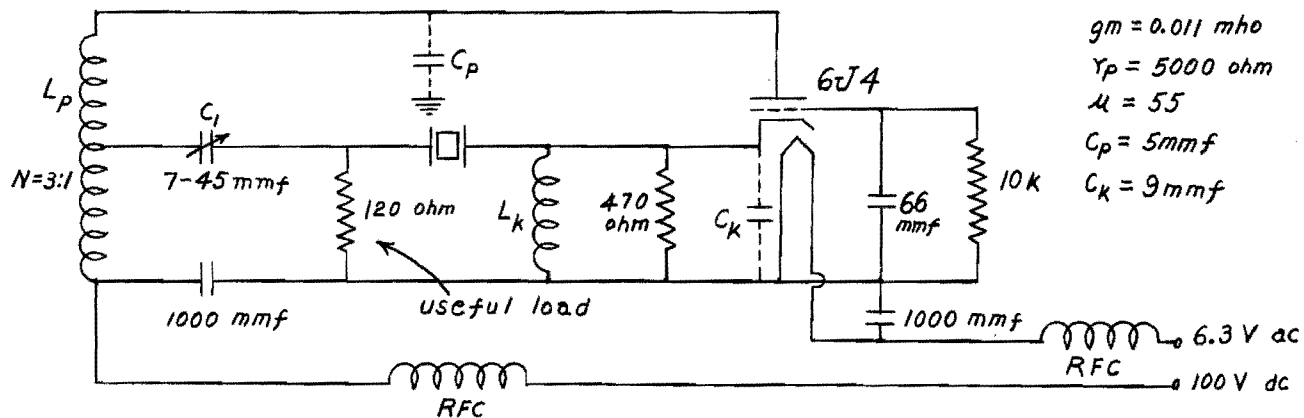


Figure 11.8 - Basic Grounded-Grid Oscillator

The circuit shown in Figure 11.8 was designed to give a relatively wide band of untuned operation. To this end, the effective plate-to-ground resistance, R_L , was made as small as possible consistent with a useable power output, and crystals having values of series resistance, R_1 , not over 50 ohms were chosen. The 6J4 tube was selected because its high transconductance

yields an input impedance so low that no cathode transformer is required. To provide a suitable gain margin, the parameter β_p was assigned the value two. This corresponds to a plate conduction angle of 180° , i.e. class B operation. With these values and the tube constants of Figure 11.8

$$N_2^2 g_m R_1 = (1)^2 (0.011/2) 50 = 0.275 . \quad (11.32)$$

Using the above value of $N_2^2 g_m R_1$ and Figures 11.3 and 11.5, one finds that for N_1/N_2 equal to 3, $g_m R_L$ and P_L/P_x are equal respectively to 6 and 10. Therefore, the required load resistance across the high side of the transformer is

$$R_L \doteq (6/g_m) \doteq 1090 \text{ ohms.} \quad (11.33)$$

In the final circuit the load resistor R_L is replaced by a resistor equal to $1090/(3)^2$, or 120 ohms across the low side of the transformer.

The use of Figure 11.4 yields

$$R_L'D = (35/g_m) = 6400 . \quad (11.34)$$

The value of $g_m R_K D$ from Figure 11.6 is 3.5, making $R_K D$ equal to 640 or one tenth $R_L D$. Therefore the circuit should be capable of stable oscillation even if the cathode capacity is subject to variations ten times as great as those of the plate capacity. Since the Q's of the crystals used in this circuit are not known, it is not possible to determine the frequency deviation resulting from an increment in C_p . However, the value of $R_L D$ and the frequency stability of this circuit may be compared with the values of the corresponding quantities obtained from other circuits to test the validity of the factor $R_L D$ as a criterion of frequency stability.

The plate and cathode inductances were selected to antiresonate C_p and C_k at the design frequency of 55 Mc. The plate transformer was wound on a Millen type 69048 slug-tuned coil form, and consisted of 12 turns of number 26 PE wire tapped at 4 turns. Since R_1 was low, satisfactory operation was obtained without the use of a compensating network.

The only adjustments made prior to obtaining the data of Table 11.1 were the adjustment of L_p and L_k to antiresonate C_p and C_k , and C_1 to resonate the transformer leakage inductance. The methods used in making these adjustments are described in Chapter XIX.

TABLE 11.1
OPERATING DATA FOR NARROW-BAND GROUNDED-GRID OSCILLATOR

f.Mc	Overtone	C_o ,mmf	R_L Ohms	Stability ** ppm/v	f *** kc	Power output * mw
48	3	14.0	45	0.42	3.0	55
50	3	12.5	35	0.20	1.5	103
54	3	13.5	45	0.11	9.0	78
58	7	9.0	32	0.14	0.6	28
60	3	13.0	25	0.24	1.6	40

* The power output was determined by measuring the voltage across R_L .

** Frequency stability was measured in parts per million per volt using a 50 volt change in plate supply voltage.

*** f is the deviation in kilocycles between the frequency of oscillation in this circuit and the frequency produced by the same crystal operating at unity power factor in the high frequency crystal impedance meter TS-683 ()/TSM. There is evidence that some of the crystals used have several modes of vibration separated by a few kilocycles, and that the present circuit selected a different mode than the C.I. meter.

The operating data indicate that plug-in operation over a moderate band width is possible and that good stability may be attained.

2. Broad-Band Grounded-Grid Oscillator.

The circuit in Figure 11.9 was designed to give the greatest practical bandwidth of untuned operation. In this grounded-grid oscillator the value of R_L is relatively large and the high-side phase compensating network is most easily realized in the form of a coupled tertiary winding. Since the same tube and crystals having approximately the same value of R_L were used in this circuit as in the preceding one, the same values of R_L and N_1 were used. A center frequency of 57.5 Mc was selected, and the values of L_p , L_k and L_c required to antiresonate C_p , C_k , and C_o were calculated. Since the holder capacities of the crystals used were not uniform, a different compensating coil was used with each crystal. However, a single fixed inductor shunted by a resistor would have sufficed if a set of crystals with uniform capacitance

had been available. The tertiary winding L_t was made equal to L_p , and both were wound on a special form to permit variation of their mutual inductance. The details of this transformer are shown in Figure 11.10.

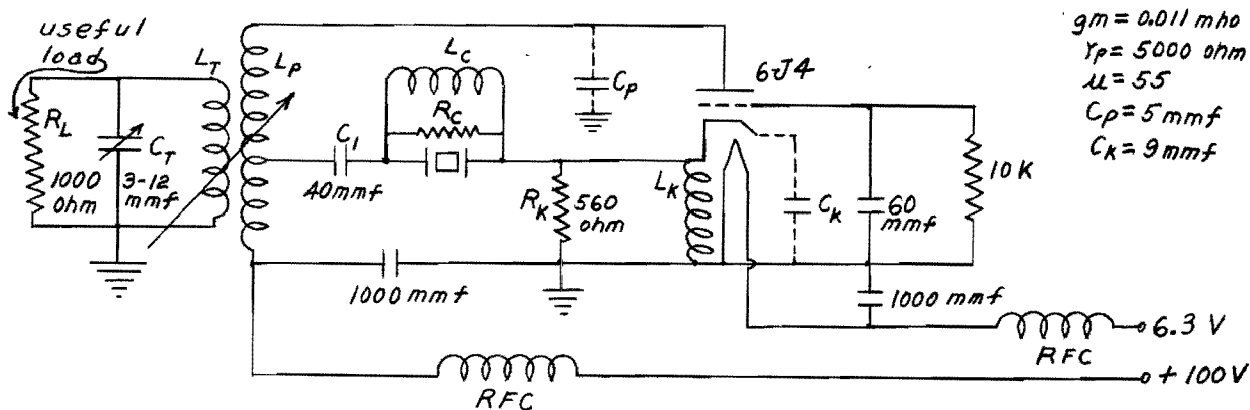
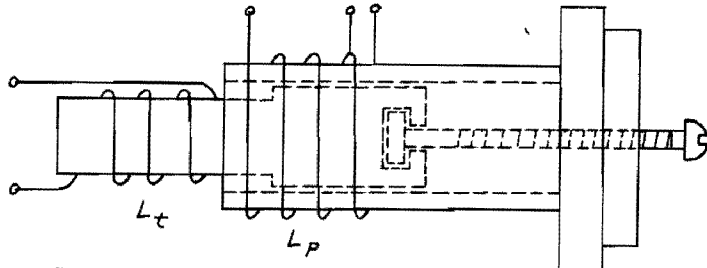


Figure 11.9 - Broad-Band Grounded-Grid Oscillator



$$L_p = 10 \text{ T}, \text{No. } 30 \text{ PE wire on } 0.4 \text{ inch form with tap at } 3.3 \text{ turns}$$

$$L_t = 17 \text{ T}, \text{No. } 30 \text{ PE wire on } 0.24 \text{ inch form}$$

Figure 11.10 - Transformer for Broad-Band Grounded-Grid Oscillator

In the adjustment of this circuit C_t was antiresonated with L_t , and C_1 was selected to resonate the leakage inductance of L_p (with the tertiary open) at 57.5 Mc. Then with a compensated crystal operating near 57.5 Mc, a 1000 ohm load across L_p , and the tertiary open, the grid current was recorded. The 1000 ohm load was then transferred to the tertiary, the tertiary circuit closed, and the coupling adjusted to give a grid current equal to the previously recorded value. The circuit was then tested, and without further adjustment, the results presented in Table 11.2 were obtained.

TABLE 11.2
PERFORMANCE OF BROAD-BAND GROUNDED-GRID OSCILLATOR

Frequency (Mc)	Overtone	C_o (mmf)	R_1 (ohms)	Grid Current (μ A)	Power * (mw)	Frequency Stability ** (ppm/v)	f (kc) ***
48	3	14.5	25	58	41	0.21	5.0
50	3	11	28	85	45	0.25	-0.5
58.31	7	8	80	60	52	0.01	0.0
65.31	7	10	80	65	46	0.15	0.2
66.65	5	4	65	90	50	0.21	2.0
67.2	7	14	80	62	47	0.07	4.0

*, **, ***, See Table 11.1.

The advantages of this circuit over the basic circuit are its wider band of untuned operation, slightly better frequency stability, and more uniform power output throughout the band.

3. Grounded-Grid Oscillator with Mutual Inductance Crystal Compensation.

The circuit of Figure 11.11 illustrates the design of a grounded-grid oscillator using mutual-inductance crystal compensation.

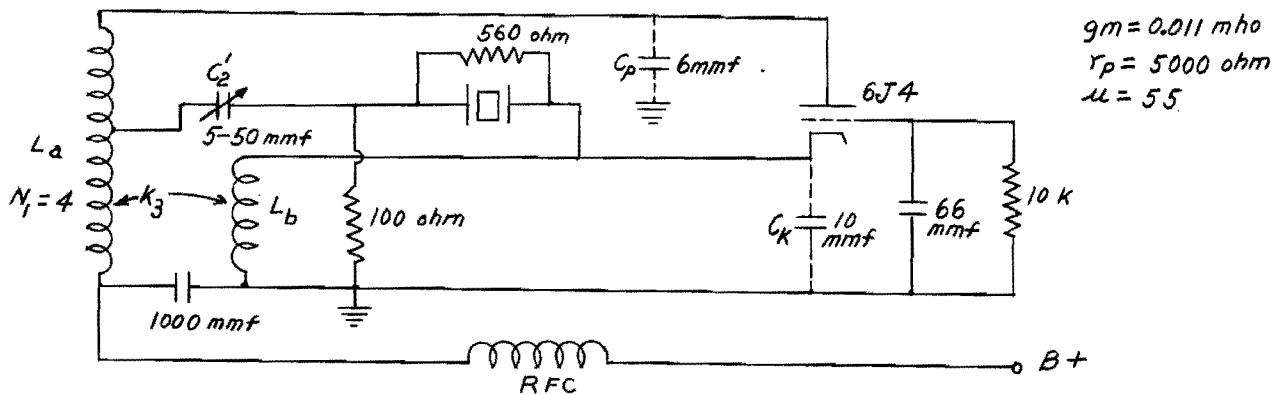


Figure 11.11 - Grounded-Grid Oscillator
with Mutual Inductance Crystal Compensation

The values of C_p and C_k shown in this Figure consist of tube capacities, wiring strays, and the shunt capacity of L_a and L_b . Since the shunt capacity

of a single layer solenoid of a given diameter is almost independent of the number of turns, these values can be determined from measurements made on coils approximating the expected dimensions of L_a and L_b .

The crystal used in this circuit has a series-resonant frequency, f_o , of 58.31 Mc, a holder capacity equal to 8.0 mmf, and a series resistance of 80 ohms. Again no cathode transformer is necessary, and a value of two is selected for β_p . Therefore

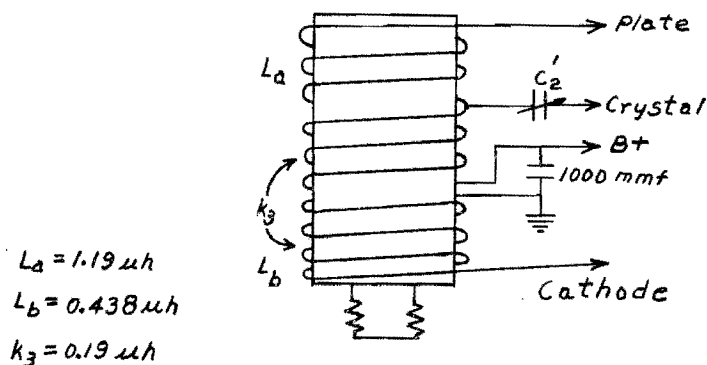
$$N_2^2 g_m R_L = \frac{(1)^2 (0.011) 80}{2} = 0.44 . \quad (11.36)$$

Using N_1/N_2 equal to 4 and the design curves, we find a value of 1530 ohms for the high side load resistance and a power ratio of 14. A 100 ohm resistor is used across the low side of the transformer in the final design.

Since

$$1/\omega_o^2 = L_p C_p = L_c C_o = L_k C_k , \quad (11.37)$$

the magnitude of L_a , L_c , and k_3 may be computed from equations 11.28, 11.29, and 11.30. The position of the tap on L_a is determined after the over-all winding dimensions are known. Construction details of the complete transformer are shown in Figure 11.11. Adjustment of k_3 was facilitated by winding L_c on a thin spacer that slides on the coil form.



Winding diameter = 0.40 (in.)

$L_a = 9$ turns No. 30 PE wire close-wound, top at 2.5 turns
 $L_b = 4.5$ turns No. 30 PE wire close-wound, on thin spacer

Figure 11.12 - Details of Transformer Used in Figure 11.10

The relative winding directions were chosen to give the proper polarity relations and to minimize capacity coupling between L_a and L_b . Final

adjustment of L_a and L_b to the design values was accomplished by spreading the end turns of the coil. It should be noted that L_a and L_b alone do not anti-resonate C_p and C_k at ω_0 . The adjustment of these inductances is facilitated by calculating the frequencies.

$$\omega_a^2 = 1/L_a C_p \quad (11.38)$$

and

$$\omega_b^2 = 1/L_b C_k \quad (11.39)$$

Then L_a is adjusted at ω_a with L_b open, and L_b is adjusted at ω_b with L_a open, a grid dip meter being used in both cases. Placing a capacitor equal to C_o in the crystal socket, shorting L_a and L_b , and sliding L_b results in final adjustment of k_3 so that resonance is obtained at the crystal frequency ω_0 .

The operating characteristics of this circuit are presented in Table 11.3.

TABLE 11.3
OPERATING DATA FOR GROUNDED-GRID OSCILLATOR

f_0	= 58.31 Mc
frequency stability	= 0.28 ppm/v
f	= -100 cycles
power output	= 90 mw

As a further check on the characteristics of this oscillator, the frequency shifts caused by changes in C_p , C_k , and C_o were determined. The results are presented in Table 11.4.

TABLE 11.4
EFFECTS OF CAPACITY VARIATION

C_k increased from 10 to 13 mmf	$f = -60$ Cycles
C_o increased from 8 to 11 mmf	$f = -45$ Cycles
C_p increased from 6 to 6.5 mmf	$f = -90$ Cycles

This circuit, while requiring a slightly more complex design procedure, contains the same number of closely controlled elements as does the circuit from which it was derived. The substitution of a mutual inductance for a self inductance results in the elimination of one winding and two coil forms from the system and permits a very compact arrangement of components. In addition, the combination of all windings on a single form removes the possibility of trouble from stray magnetic coupling. As the operating data indicate, these advantages can be obtained in practice with no sacrifice in performance.

4. Design of a High-Efficiency Grounded-Grid Oscillator.

The design procedure for class C oscillators is more complex than that for class A or B operation. Moreover, because large values of N_1/N_2 are encountered, the design curves in Figures 11.3, 11.4 and 11.5 can yield values which are as much as 20 per cent below the correct values for very high μ tubes. However, the curves may be used to indicate desirable operating conditions, and then simplified forms of the design equations may be used to compute more accurate values of the circuit parameters.

A high efficiency grounded-grid oscillator is shown in schematic form in Figure 11.13.

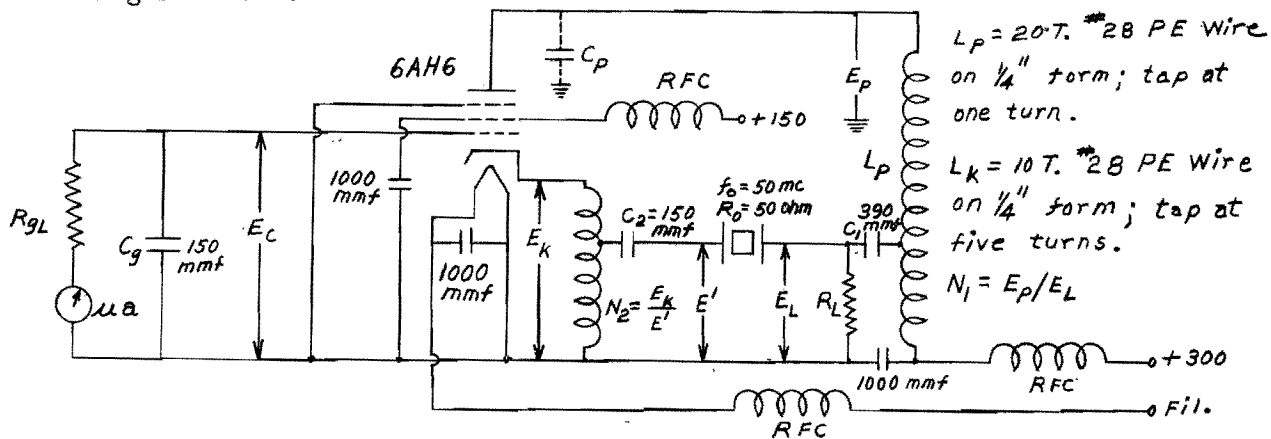


Figure 11.13 - High Efficiency Grounded-Grid Oscillator

The tube used in this circuit has a transconductance equal to 0.009 mho, and an allowable plate dissipation of 3.2 watts. The crystal used has a series resonant frequency of 50 Mc, a series resistance of 50 ohms, and can dissipate 0.05 watt.

In designing the circuit, a value of β_p equal to 5.12, which corresponds to θ_p equal to 60° , was selected. If we also use N_2 equal to two, we obtain

$$N_2^2 g_m' R_1 = (2)^2 (0.009/5.12) 50 \approx 0.35 . \quad (11.40)$$

Using this value of $N_2^2 g_m' R_1$ and the design curves, we see that for N_1/N_2 equal to 10, a larger power ratio is obtained. Further, by comparing values of the R_L^D product we see that the frequency stability with respect to capacity variations will be approximately one seventh that obtained at the center frequency of the circuit in Figure 11.8. Because the circuit in Figure 11.8 has a frequency stability of 0.11 ppm/v at its center frequency and because comparable crystals are used in both circuits, there is reason to believe that satisfactory stability will be had if the foregoing values of N_1/N_2 , N_2 and β_p are used.

Since a pentode having a high μ and r_p is used, the design equations may be simplified for a more accurate computation of the circuit parameters. From equation 11.21,

$$g_m' R_L \approx \frac{(N_1/N_2)^2 (N_2^2 g_m' R_1 + 1)}{(N_1/N_2 - 1)} . \quad (11.41)$$

From equation 11.22

$$N_2^2 g_m' Z_2 \approx 1 . \quad (11.42)$$

Since r_p is much larger than R_L

$$N_2^2 g_m' Z_1 \approx N_2^2 g_m' R_L / N_1^2 . \quad (11.43)$$

Equations 11.25, 11.26 and 11.27 may be used without modification.

From equation 11.41

$$g_m' R_L = \frac{100(0.35 + 1)}{9} = 15 , \quad (11.44)$$

so that

$$R_L = \frac{15 \times 5.12}{0.009} \approx 7700 \text{ ohms} . \quad (11.45)$$

In the circuit R_L is replaced by a resistor approximately equal to R_L/N_1^2

(20 ohms) across the low side of the transformer. From equation 11.25

$$\frac{P_L}{P_X} = (1 - 0.1)^2 \frac{15}{0.35} = 35. \quad (11.46)$$

Since the crystal can safely dissipate about 0.05 watt, a power output near 2 watts may be obtained. The value of D may be computed using equation 11.26.

$$D = \frac{1 + 0.15 + 0.35}{0.35} = 4.0. \quad (11.47)$$

Then from equation 11.27,

$$g_m^{\prime} R_L^{\prime} D = (1 - 0.1)(15)4 = 54, \quad (11.48)$$

or

$$R_L^{\prime} D = 30,800. \quad (11.49)$$

Comparison of this value of $R_L^{\prime} D$ with that obtained for the narrow-band grounded-grid oscillator shows that the present circuit should have a frequency stability near 0.55 ppm/v.

Having determined the values of P_L , N_1 , N_2 and the impedance levels throughout the circuit, it is advisable to calculate the cathode voltage, E_k , and to determine whether it is consistent with the desired operating conditions. The following expressions may be used for this purpose:

$$E_L^2 = 2R_L P_L / N_1 \quad (11.50)$$

$$E_k = E_L \frac{N_2 \beta_p}{N_2 g_m^{\prime} R_1 + \beta_p} \quad (11.51)$$

It should be kept in mind that E_k must be large enough to give the desired β_p without requiring an excessively large value of R_g . If this condition is not obtained, the assumed values of N_2 or β_p should be modified.

The cutoff bias (E_{co}) may be found from the known dc operating conditions, and the bias voltage required to give the assumed plate conduction angle may be found from the expression

$$E_c = E_{co} - E_k \cos \theta_p. \quad (11.52)$$

The corresponding half angle of grid conduction (θ_g) is given by

$$\theta_g = \cos^{-1}(E_c/E_k) . \quad (11.53)$$

The value of the grid leak resistance may be computed from an expression developed in Chapter VII,

$$R_g = \frac{\pi r_g}{\tan \theta_g - \theta_g} \quad (11.54)$$

where r_g is the positive grid resistance of the tube. It is realized that the grid characteristic is definitely nonlinear for class C operation and that the value of R_g will probably be modified in the final design.

The results of this design are given in Figure 11.13 and Table 11.5. The operating conditions are presented in Table 11.6.

TABLE 11.5
CIRCUIT PARAMETERS

Element	Calculated Value	Final Value
R_L (low side)	20 ohms	22 ohms
R_g	100,000 ohms	86,000 ohms
N_1	2:1	2:1
N_2	20:1	20:1

TABLE 11.6
OPERATING CONDITIONS

Quantity	Calculated	Observed
E_L	8.94 volts	9.0 volts
E_c	11.5 volts	10.0 volts
P_L	2.0 watts	1.9 watts
P_x	0.05 watt	0.08 watt
Frequency Stability	0.55 ppm/v	0.6 ppm/v
P_b	3.2 watts	3.0 watt
Efficiency	- - - - -	63 per cent
f_o	- - - - -	50 Mc

As shown by the above table, the observed conditions are remarkably close to those calculated. With further adjustment of N_1 and N_2 , the power dissipated in the crystal might be reduced more nearly to the design value.

F. Advantages and Disadvantages.

The use of the grounded-grid circuit with high transconductance triodes results in a compact and economical circuit arrangement, and the excellent shielding between the input and output circuits eliminates substantially all tendencies toward oscillations which are not under crystal control. Moreover, the low input impedance of the grounded-grid amplifier reduces the effect of cathode capacity variations on frequency, and good stability may be obtained.

Due to the inherently low power gain of the grounded-grid amplifier, this circuit does not produce as high load-to-crystal power ratios as does the transformer coupled circuit.

XII IMPEDANCE-INVERTING OSCILLATORS

A. General Theory.

The Pierce, Miller and Transitron impedance-inverting oscillators as used at high frequencies have the same basic circuit configurations as their low frequency counterparts. They differ from the prototypes in that the crystal is operated at or near its series resonant frequency, and in that a network is used which inverts the low resonant impedance to the required antiresonant impedance. Thus, the series resonant crystal and impedance inverting network replace the parallel resonant crystal as used at low frequencies.

Impedance-inverting networks have been discussed in detail in Chapter II. Because the antiresonant impedance that may be obtained from such networks is limited by the crystal and circuit capacities, as well as by the series resistance of the crystal, the use of impedance-inverting oscillators is restricted to frequencies below about 100 Mc.

The basic network used in the following circuits is shown in Figure 12.1.

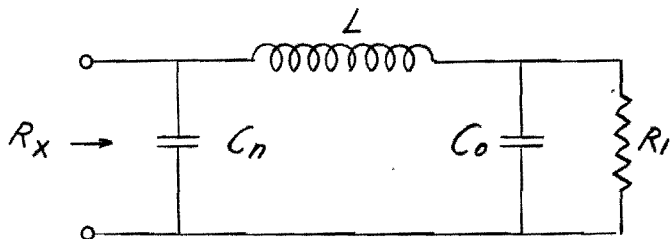


Figure 12.1 - Impedance-Inverting Network

In its simplest form this network is the lumped-constant equivalent of the quarter-wave line, and the element values are related by the following expressions:

$$\omega_0^2 = 1/LC_0 = 1/LC_n , \quad (12.1)$$

$$R_x = Z_0^2/R_1 , \quad (12.2)$$

and

$$Z_0 = \omega_0 L = 1/\omega_0 C_n , \quad (12.3)$$

where ω_0 is the series-resonant angular-frequency of the crystal. This network can meet the impedance requirements of the Pierce, Miller, and transitron

oscillators provided the capacities are not too large. At frequencies remote from ω_0 , the crystal impedance becomes simply $1/j\omega C_0$, and the network has an additional antiresonance at a frequency given by

$$\omega_n^2 = \frac{C_n + C_0}{C_n C_0 L} . \quad (12.4)$$

This undesired response may be damped by shunting the crystal with a resistance approximately equal to Z_0 .

It may be shown analytically that for a given input capacity, the quarter-wave line configuration has the best frequency stability with respect to variation of C_n . However, if C_n is less than C_0 , higher values of input resistance may be obtained at the expense of frequency stability. The design procedure for this condition has been described in Chapter II. In typical tubes, C_n is seldom less than C_0 , and values of input resistance higher than that given by the quarter wave line may be obtained only by adding a shunt inductance at the input of the network.

If shunt inductors are added at both the input and termination of the network, as in Figure 12.2, the effective capacities may be reduced. This modification results in a higher input resistance and permits higher operating frequencies, however, the tendency toward oscillation which is not under crystal control is increased, and the frequency stability of the circuit is degraded.

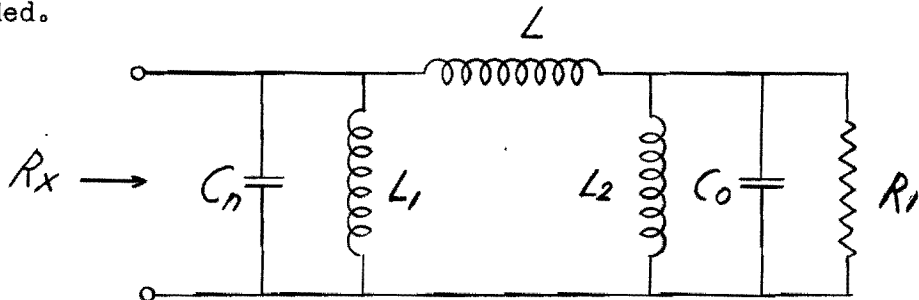


Figure 12.2 - High Frequency Impedance-Inverting Network

The design equations are:

$$L = R_x R_1 / \omega_0 , \quad (12.5)$$

$$R_x R_1 = \left(\frac{L_1 / C_n}{\omega_0 L_1 - 1 / \omega_0 C_n} \right)^2 , \quad (12.6)$$

and

$$R_x R_1 = \left(\frac{L_2 / C_o}{\omega_o L_2 - 1 / \omega_o C_o} \right)^2. \quad (12.7)$$

The choice of L_1 and L_2 is not unrestricted; if these elements are chosen so that they are respectively antiresonant with C_n and C_o near f_o , a pronounced tendency toward uncontrolled oscillation may be expected. In practice both L_1 and L_2 should be substantially larger than the values corresponding to antiresonance.

The pi of inductances in Figure 12.2 may be converted to a two winding transformer by means of the well known Wye-Delta relations. The configuration resulting from such a conversion of the transformer network is shown in Figure 12.3.

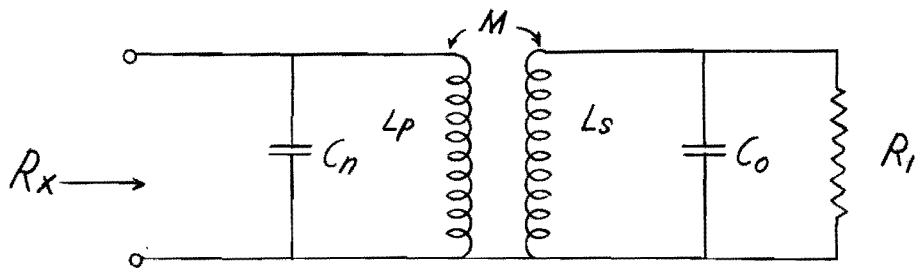


Figure 12.3 - Transformer Equivalent of Impedance-Inverting Network

Satisfactory oscillators may be constructed by using either three isolated inductors or two inductors with magnetic coupling. The choice between the two methods is primarily one of convenience in realizing the proper network values and applying tube potentials.

Since the input resistance of the impedance-inverting network (R_x) is easily calculated, a negative resistance analysis is convenient. The following analytical work is applicable to the parallel mode oscillators which are specified in terms of the crystal performance index (P.I.).

B. Impedance-Inverting Pierce Oscillator.

1. Analysis.

Due to its simplicity, economy of parts, and wide band operation, the Pierce oscillator is perhaps the most useful of all fundamental mode crystal oscillators. As modified for high frequency operation it retains the

advantages of simplicity and economy, but is not suitable for wide band untuned operation.

The impedance-inverting Pierce oscillator is shown in Figure 12.4, in which C_1 and C_2 include respectively the grid-to-cathode and plate-to-cathode capacities of the tube.

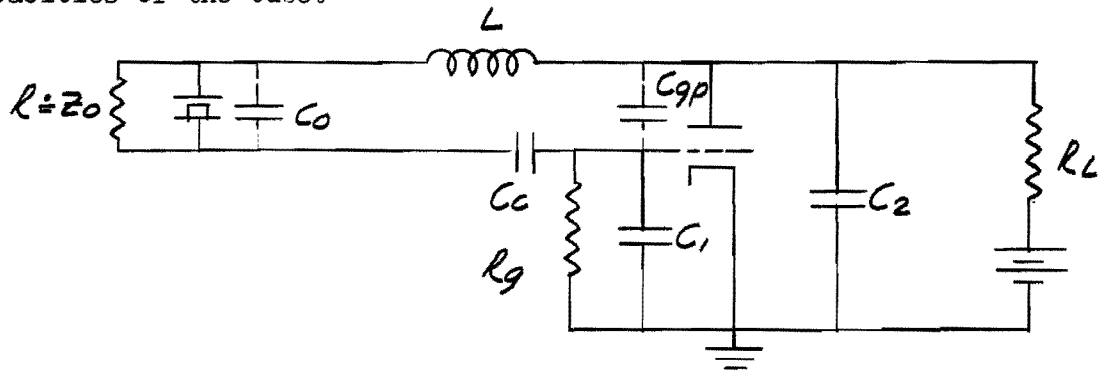


Figure 12.4 - Impedance-Inverting Pierce Oscillator

This circuit will oscillate if the resistance presented to the tube by the network is equal to or greater than the magnitude of the negative resistance developed between grid and plate of the tube. The relations which express the magnitude of this negative resistance may be obtained by investigating the admittance between grid and plate in Figure 12.4 with the impedance inverting network removed. If $R_g \gg 1/\omega C_1$ and $R_L \gg 1/\omega C_2$, the equivalent of Figure 12.4 may be drawn as in Figure 12.5, which is in turn equivalent to Figure 12.5.

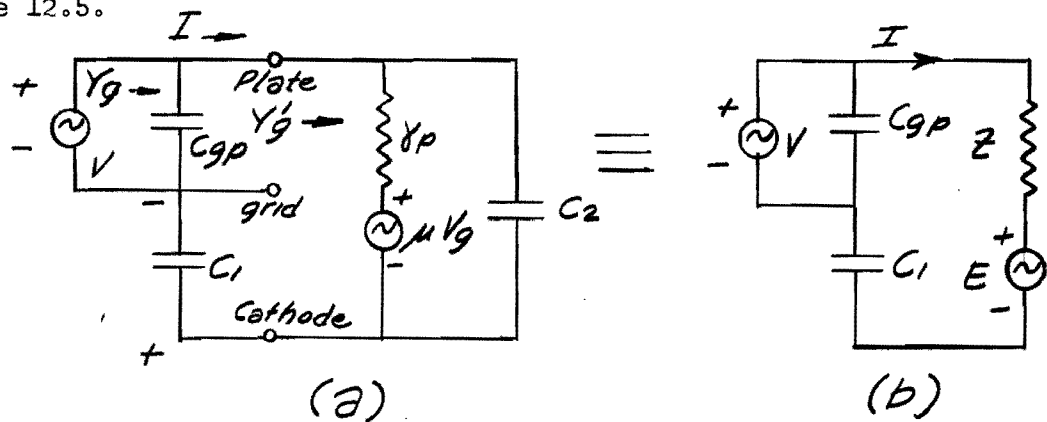


Figure 12.5 - Approximate Equivalent Circuits of Pierce Oscillator

In Figure 12.5

$$* \quad Z = \frac{r_p/j\omega C_2}{r_p + 1/j\omega C_2}, \quad (12.8)$$

$$E = \frac{\mu V}{1 + j\omega C_2 r_p} \quad (12.9)$$

where

$$V_g = I/j\omega C_1 . \quad (12.10)$$

Since r_p is very much greater than $1/\omega C_2$,

$$Z \doteq 1/j\omega C_2 , \quad (12.11)$$

and

$$E \doteq g_m V_g / j\omega C_2 . \quad (12.12)$$

The current, I , is given by

$$I \doteq \frac{V - E}{1/j\omega C_1 + 1/j\omega C_2} . \quad (12.13)$$

Substitution of equations 12.10 and 12.12 into equation 12.13 and simplifying, gives as the dynamic input admittance

$$Y'_g = I/V = (1/j\omega C_1 + 1/j\omega C_2 - g_m/\omega^2 C_1 C_2)^{-1} . \quad (12.14)$$

Since

$$Y'_g = G'_g + jB'_g , \quad (12.15)$$

equation 12.14 may be separated into its real and imaginary components to determine the equivalent parallel grid-to-plate resistance and capacitance. Therefore,

$$r'_g = 1/G'_g \doteq - (C_1 + C_2)^2 / g_m C_1 C_2 - g_m / \omega^2 C_1 C_2 , \quad (12.16)$$

and

$$C_g = B'_g / \omega = \frac{\omega^2 C_1 C_2 (C_1 + C_2)}{\omega^2 (C_1 + C_2)^2 + g_m^2} . \quad (12.17)$$

The total capacity, C_n , which the tube presents to the impedance-inverting network is

$$C_n = C_{gp} + C_g . \quad (12.18)$$

If C_1 equals C_2 , a condition which is conducive to good frequency stability, the expression for C_n becomes

$$C_n = C_{gp} + \frac{C'}{2 + g_m^2/2(\omega C')^2}, \quad (12.19)$$

where

$$C' = C_1 = C_2. \quad (12.20)$$

For this same condition r'_g is given by

$$r'_g = -4/g_m - g_m/(2\omega C')^2. \quad (12.21)$$

Since in the frequency bands of interest, $\omega C'$ is very much greater than g_m . C_n and r'_g are given to a close approximation by

$$C_k \approx C_{gp} + C'/2, \quad (12.22)$$

and

$$r'_g \approx -4/g_m. \quad (12.23)$$

The equivalent circuit of the impedance-inverting Pierce oscillator is shown in Figure 12.6. The criterion of oscillation is that R_x be equal to or greater than $|r'_g|$.

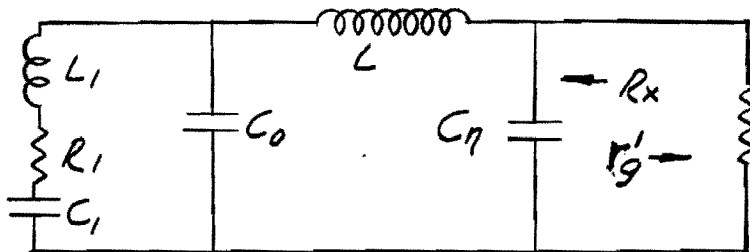


Figure 12.6 - Equivalent Circuit of Impedance-Inverting Oscillator

The tube that is available and best suited for use in this circuit is the 6J4 triode, having as typical values $C_{gk} = 5.5$ mmf, $C_{gp} = 4$ mmf, and $g_m = 11,000$ micromhos. The Pierce oscillator using this tube, a quarterwave impedance-inverting network, and a crystal having low resistance and shunt capacity, is capable of operating up to about 100 Mc. If, for example, C_1 and C_2 are both made equal to 6 mmf, C_n , as given by equation 12.22 is 7 mmf. The value of r'_g obtained with the 6J4 is, from equation 12.23 equal to -364 ohms. To provide a two-to-one transconductance margin, R_x must be twice as large as r'_g . Therefore, for the quarterwave line,

$$R_x = Z_o^2/R_1 \geq 728 \text{ ohms.} \quad (12.24)$$

From equations 12.3 and 12.24,

$$f_o = 1/2\pi C_n \sqrt{R_1 R_x} . \quad (12.25)$$

If the crystal used has C_o equal to 7 mmf and R_1 equal to 71 ohms

$$f_o = 10^{12}/6.28 \times \sqrt{728 \times 71} = 100 \text{ Mc.} \quad (12.26)$$

Since crystals having a shunt capacity as low as 7 mmf are likely to have resistances in excess of 71 ohms, the upper frequency limit of this particular configuration is about 100 Mc.

2. Experimental Results.

The experimental oscillator uses a type 6J4 tube, a 50 Mc crystal with C_o equal to 11 mmf and R_1 equal to 30 ohms, and a quarter-wave impedance-inverting network. The circuit capacities are as follows:

$$C_{gp} = 4 \text{ mmf ,}$$

$$C_{gk} = 5.5 \text{ (tube)} + 3.5 \text{ (stray)} = 9 \text{ mmf ,}$$

$$C_{pk} = 1.9 \text{ mmf .}$$

By the proper choice of C_1 and C_2 , it is possible to obtain the desired value of network capacity, C_n , without padding C_{gp} . Setting $C_1 = C_2$ for an excitation ratio of unity, equation 12.22 may be used to obtain the values

$$C_1 = C_2 = C' = 2(C - C_{gp}) . \quad (12.27)$$

Since a quarterwave line is used, C_n equals C_o and

$$C' = 2(11 - 4) = 14 \text{ mmf .} \quad (12.28)$$

Therefore, a capacitor equal to C' minus C_{pk} or 12.1 mmf must be placed in shunt with C_{pk} , and a capacitor equal to C' minus C_{gk} or 5 mmf must be connected from grid-to-ground.

With the foregoing values of the circuit elements,

$$Z_o = 1/\omega_o C_o \doteq 290 \text{ ohms .} \quad (12.29)$$

Therefore,

$$R_x = (290)^2/30 \doteq 2800 \text{ ohms ,} \quad (12.30)$$

which is sufficiently large to insure operation with tubes having a considerably lowered g_m .

The final circuit is shown in Figure 12.7.

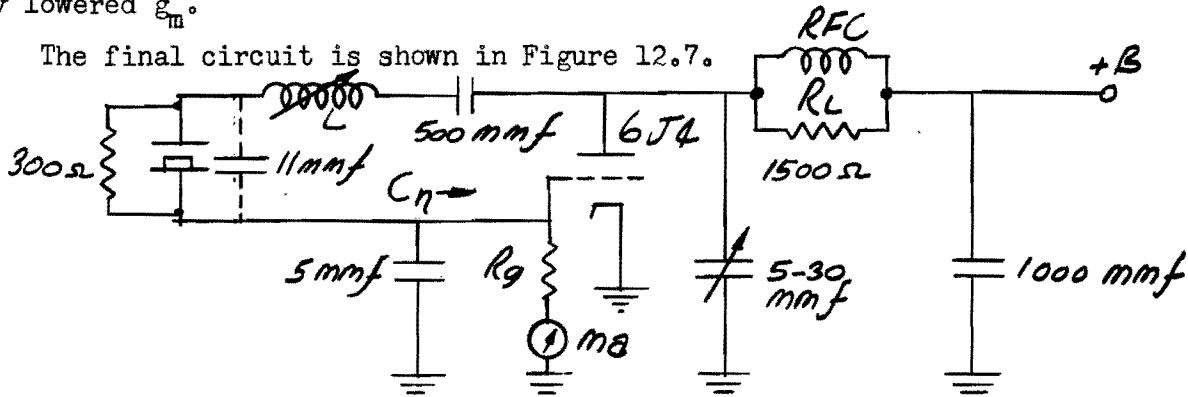


Figure 12.7 - Impedance-Inverting Pierce Oscillator

The network inductance and the plate-to-ground padding capacitor are made variable for tuning purposes. The following tuning procedure has been found adequate to insure proper operation at the desired frequency:

- a. short plate to grid of tube,
- b. replace the crystal with a capacitor equal to the holder capacitor and remove the 300 ohm line terminating resistor,
- c. adjust L (using a grid dip meter) to obtain resonance at the crystal frequency,
- d. remove the short from the tube, replace the line terminating resistor, and short the crystal socket terminals,
- e. adjust the plate-to-ground padding capacitor to resonate L at the crystal frequency thus making C equal to C_0 .

When tuned by the above procedure, this circuit operated with a frequency stability of 0.6 ppm per volt change in supply voltage, and supplied 70 milliwatts into the 1500 ohm load. The measured crystal dissipation was very low and it is felt that a somewhat greater power output could be obtained by increasing the excitation ratio.

C. The Miller Impedance Inverting Oscillator.

1. Analysis.

An impedance inverting network can be used in conjunction with the Miller circuit to operate high-frequency overtone crystals at series resonance in a manner similar to that used in the Pierce. An appropriate arrangement, which has the familiar advantage that the crystal and line have one terminal at ground potential, is shown in Figure 12.8.

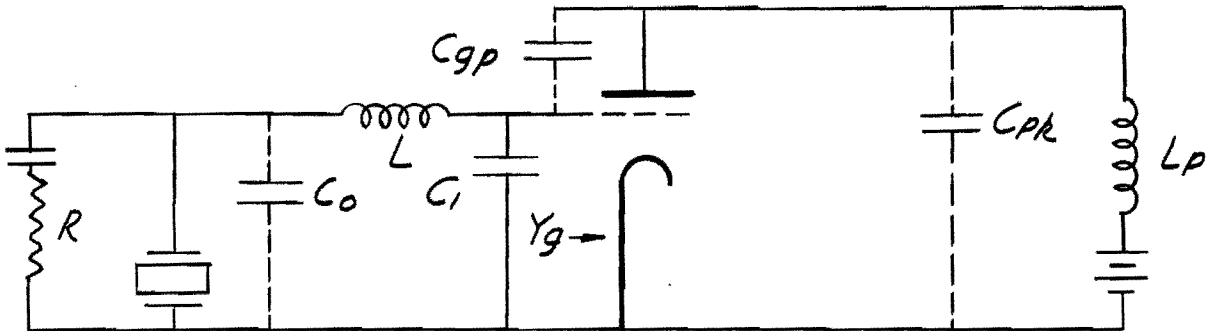


Figure 12.8 - Impedance Inverting Miller Oscillator

This circuit may be analyzed by methods similar to those used in connection with the Pierce oscillator. Assuming the static grid-to-cathode capacitance to be part of C_1 , the input admittance of the tube, $Y_g = G_g + jB_g$, may be shown to be

$$Y_g = \left(1 + \frac{\mu Z}{r_p + Z_L} \right) \left(\frac{1}{1/j\omega C_{gp} + r_p Z_L / (r_p + Z_L)} \right), \quad (12.31)$$

where

$$Z_L = \frac{L_p/C_{pk}}{j\omega L_p + 1/j\omega C_{pk}}. \quad (12.32)$$

If r_p is very much greater than Z_L the admittance expression simplifies to the form

$$Y_g = \frac{g_m \omega L_p}{\omega L_p - (1 - \omega^2 L_p C_{pk})/\omega C_{gp}} - j \frac{1}{\omega L_p / (1 - \omega^2 L_p C_{pk}) - 1/C_{gp}}. \quad (12.33)$$

From this expression the equivalent grid resistance is

$$r'_g = 1/G_g \doteq \frac{1}{g_m} \left(\frac{C_{gp} + C_{pk}}{C_{gp}} - \frac{1}{\omega^2 L_p C_{gp}} \right), \quad (12.34)$$

and the equivalent grid capacitance is

$$C_g = \frac{B_g}{\omega} \doteq \frac{C_{gp} (1 - \omega^2 L_p C_{pk})}{1 - \omega^2 L_p (C_{pk} + C_{gp})}. \quad (12.35)$$

The input capacity of the network is given by

$$C_n = C_1 + C_g . \quad (12.36)$$

As shown by equation 12.34, the input resistance of the tube may be made negative by properly proportioning the circuit constants, and the magnitude of this negative resistance may be controlled by varying the plate inductance L_p . The equivalent circuit of the impedance inverting Miller oscillator is the same as that in Figure 12.6, and the condition for oscillation is that r'_g be negative and smaller in magnitude than R_x .

If a 6J4 triode is used, r'_g may be about 150 ohms and C_g about 15 mmf; therefore, a circuit employing this tube, a quarter-wave impedance inverting network, and a 50 ohm crystal has an upper frequency limit of about 125 Mc. Because crystals operating above 100 Mc are likely to have values of series resistance in excess of 50 ohms, practical upper frequency limit is near 100 Mc.

2. Typical Design and Experimental Results.

A crystal having a shunt capacity, C_o , of 15 mmf, and a series resistance, R_1 , of 50 ohms at 50 Mc was chosen. The tube used in this circuit is the type 6J4 triode which has a nominal transconductance of 0.01 mho. The measured values of the tube capacities with the tube in its socket are given in Figure 12.9.

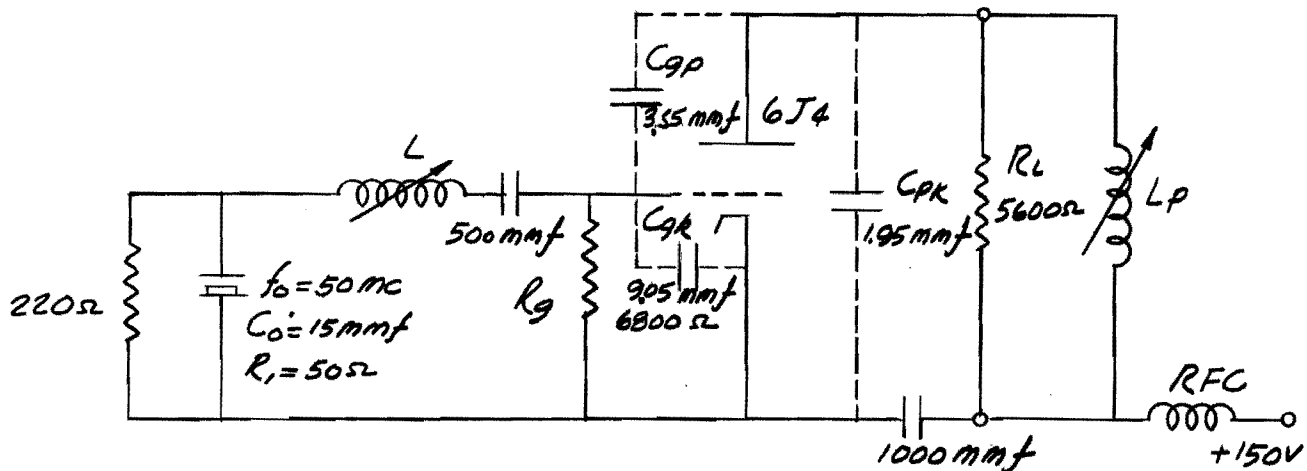


Figure 12.9 - Experimental Impedance-Inverting Miller Oscillator

A quarter wave impedance inverting network was used and no capacity was added at the input of the tube. To achieve these conditions, $C_g + C_1$ was made equal to C_o ; the required value of L_p was computed from the modified

form of equation 12.35 as shown below

$$L_p = \left(\frac{C_g - C_{gp}}{C_g(C_{gp} + C_{gk}) - C_{gp}C_{gk}} \right) \frac{1}{\omega^2}, \quad (12.37)$$

or

$$L_p = 0.744 \mu h. \quad (12.38)$$

With this value of L_p the value of r'_g was found by equation 12.34 to be -158 ohms. Since the input resistance of the line is equal to 900 ohms, this value of r'_g provides a suitable gain margin. In fact, the effective g_m of the tube must be reduced to 0.0017 mho for equality of R_x and r'_g . This is equivalent to class C operation with β_p (Chapter VII) equal to 5.9 or a total plate conduction angle of approximately 115 degrees.

The circuit was adjusted by the following procedure:

- a. with the crystal and line terminating resistor removed, a capacitor equal to C_o was placed in the crystal socket, and the grid side of L shorted to ground. L was then adjusted, using a grid dip meter, to obtain antiresonance at 50 Mc.
- b. with the crystal and line terminating resistor replaced and the short removed from the grid circuit, L_p was adjusted to obtain operation at the series resonant frequency of the crystal. The frequency was checked by comparing the oscillator frequency with the frequency produced with the same crystal operating at unity power factor in the high frequency crystal impedance meter TS-683 ()/TSM.

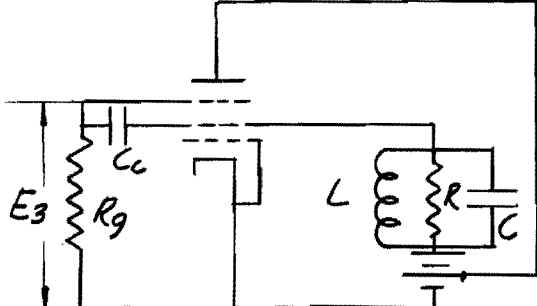
Upon completion of the adjustment procedure it was found that a power of 0.5 watt was developed in R_L , and the frequency stability was 0.6 ppm/v. The power dissipated in the crystal was found to be 0.07 watt: no further attempt was made to increase the power output of the circuit.

D. Impedance-Inverting Transitron Oscillator.

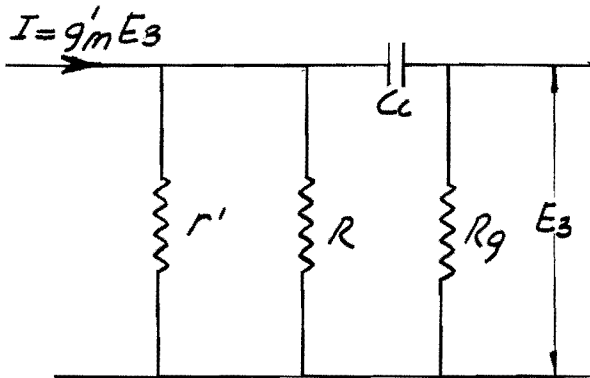
1. Analysis and Circuit Description.

Because the total space current of a pentode tends to remain constant, the suppressor grid, when made negative with respect to the cathode, will cause the screen current to increase and the plate current to decrease. Use is made of this behavior in the transitron oscillator, where the negative transconductance developed between the suppressor and screen grids is employed to drive an oscillatory circuit in the screen circuit. The basic transitron

circuit and its equivalent are shown in Figure 12.10.



(a) Actual



(b) Equivalent

Figure 12.10 - Transitron Oscillator

In normal use, C_c is a coupling capacitor having low reactance at the operating frequency, and R_g is very much greater than R . Therefore, for the circuit to be capable of oscillating

$$g_m'E_3r'R/(r' + R) \geq E_3 , \quad (12.39)$$

or

$$1/g_m' \leq \frac{r'R}{r' + R} , \quad (12.40)$$

where g_m' is the suppressor to screen grid transconductance and r' is the dynamic screen grid resistance. Since a positive increment of suppressor voltage results in a negative increment of screen grid current, g_m' is inherently negative. Therefore, equation 12.40 is simply a statement of the familiar criterion of oscillation as applied to negative resistance systems.

In contrast to the Pierce and Miller circuits, the transitron is a true two-terminal negative resistance oscillator. That is, the magnitude of the negative resistance developed depends largely on the tube characteristic and operating potentials rather than on the circuit configuration. Therefore the choice of a suitable tube and operating potentials is an important step in the design procedure.

2. Design and Experimental Results.

Because of its high screen-to-suppressor transconductance, the 6AS6 tube is ideally suited for use in this oscillator. The transconductance g_m'

of the tube actually used was measured and found to be 1500 micromhos. Therefore oscillations can occur only if the external load has a resistance in excess of $10^6/1500$ or 667 ohms. Since the dynamic screen resistance r' is very much larger than 667 ohms, it may be neglected.

The crystal selected for this oscillator has a series resistance of 20 ohms, a shunt capacity of 11 mmf, and a series resonant frequency of 50 Mc. Therefore, the use of a quarter wave line for the impedance inverting network gives

$$Z_0 = 1/\omega_0 C_1 \doteq 290 \text{ ohms}, \quad (12.41)$$

and

$$R_x = Z_0^2/R_1 = 4,200 \text{ ohms}. \quad (12.42)$$

This value of R_x is considerably greater than the value required for oscillation. However, the useful load is connected effectively from screen to ground and the resistance presented to the screen is given by

$$R = R_x R_L / (R_x + R_L). \quad (12.43)$$

Using a load resistance of 2000 ohms, R becomes 1350 ohms, which gives about a two-to-one margin in gain.

Since the total screen-to-ground capacity is only 7 mmf, a padding capacitor was added to increase this to the 11 mmf required for the network.

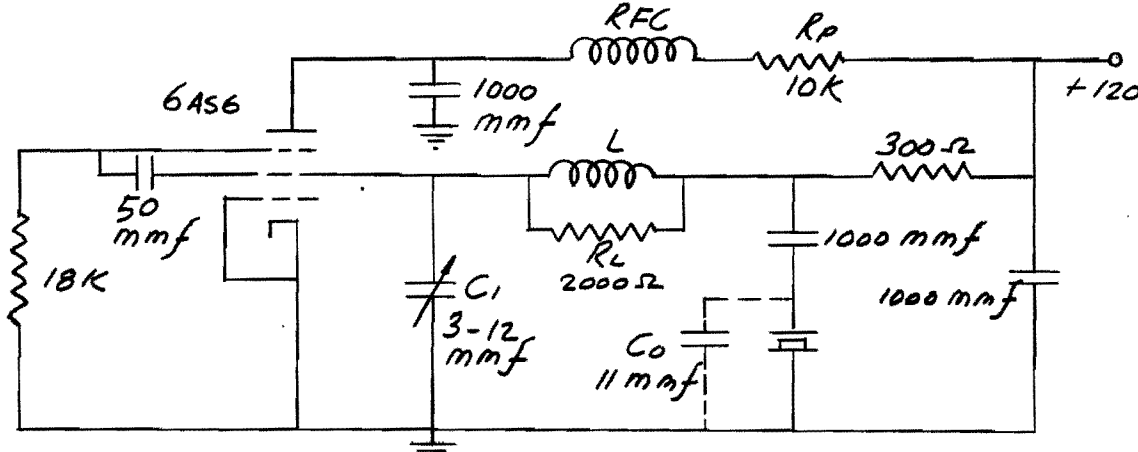


Figure 12.11 - Schematic Diagram of Impedance Inverting Transitron
The adjustment procedure for this circuit is given in Chapter XIX.
The frequency stability of this circuit was determined by varying the supply voltage from 70 to 120 volts. This resulted in a frequency change of

250 cycles, or a variation of 0.1 ppm per volt. The power output obtained with a supply voltage of 120 volts was 15 milliwatts.

An interesting feature of this circuit is that the plate dropping resistor, R_p , has a decided influence on the frequency stability with respect to supply voltage variations. Increasing R_p to 40,000 ohms resulted in a variation of 10 cycles-per-second for a 50 volt change in supply voltage, or a stability of 0.004 ppm per volt.

E. Conclusions.

Impedance-inverting oscillators are capable of excellent frequency stability, and are relatively simple to design and adjust. Because the impedance inverting property is limited to a relatively narrow band of frequencies, they are not suitable for broad-band untuned operation. However, this natural selectivity is useful in avoiding trouble due to oscillation at undesired crystal frequencies. The power output capability is good, but not superior to that of the transformer-coupled oscillator.

XIII. THE GROUNDED-PLATE OSCILLATOR

A. Circuit Description

The grounded-plate oscillator employing a series-resonant crystal is shown in Figure 13.1. This circuit differs from the grounded-grid oscillator principally in the point chosen for grounding and in the resulting redistribution of parasitic capacitances. It is of interest mainly because a useful electron coupled oscillator results when a pentode is substituted for the triode shown.

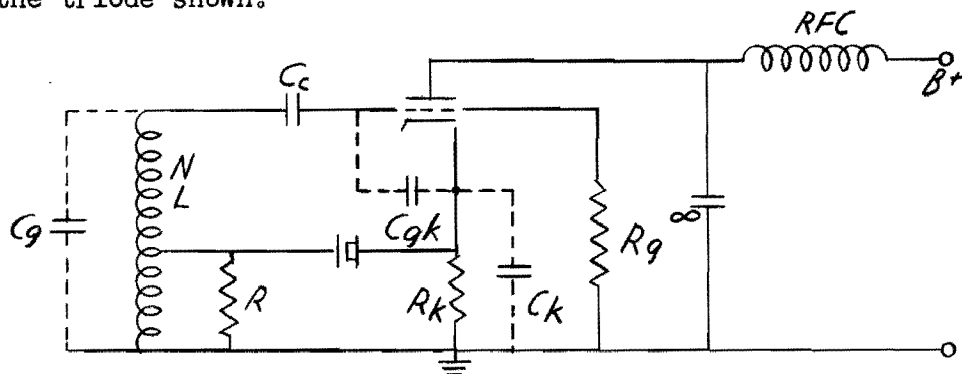


Figure 13.1 Grounded-Plate Oscillator

The basic feature of this circuit is that the tube functions as a cathode follower, thus providing a low impedance from which the crystal is driven. Because cathode followers furnish no voltage gain, oscillation can occur only if a step-up transformer is inserted between cathode and grid. The high side inductance of this transformer serves to tune the parasitic grid capacity, C_g , which is the equivalent of C_{gk} and C_k in series. Because exact phase compensation may be secured by the combined action of C_{gk} and C_k , as shown in Chapter IX, no inductance is used to tune the cathode circuit.

B. Linear Analysis

The equivalent linear circuit of the grounded-plate oscillator is shown in Figure 13.2, in which N is the voltage step-up ratio of the transformer, R_k and R are small physical resistors; it is assumed that $R \gg R_g/N^2$.

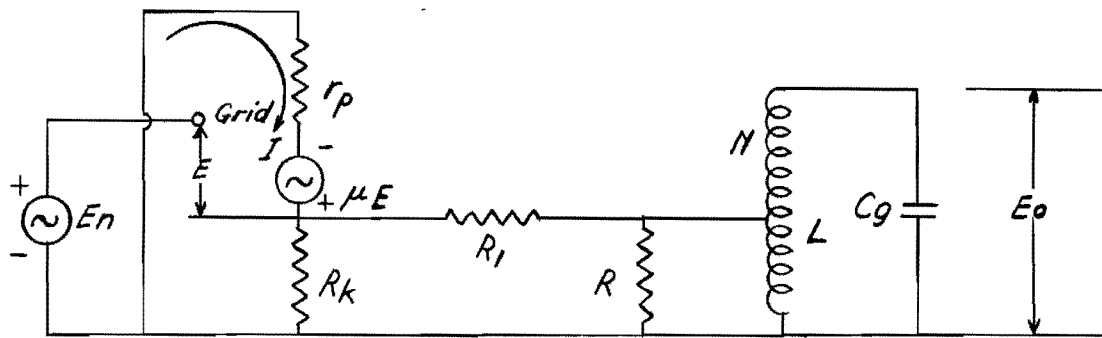


Figure 13.2 Linear Equivalent of Grounded-Plate Oscillator Circuit
The circuit equations at the series resonant frequency of the crystal are:

$$I = \mu E / (r_p + R'_k) , \quad (13.1)$$

$$E = E_n - IR'_k , \quad (13.2)$$

$$E_o = N I R'_k R / (R_1 + R) , \quad (13.3)$$

and

$$R'_k = R_k (R_1 + R) / (R_k + R_1 + R) . \quad (13.4)$$

Solving these equations simultaneously for E_o gives:

$$E_o = \frac{\mu N R'_k R E_n}{(R_1 + R) (r_p + R'_k + \mu R'_k)} . \quad (13.5)$$

The loop gain, given by

$$A = E_o / E_n , \quad (13.6)$$

must have a value equal to or greater than unity to sustain oscillations.

Substituting this condition in 13.5 yields

$$A = 1 = \frac{\mu N R'_k R}{(R_1 + R) (r_p + R'_k + \mu R'_k)} . \quad (13.7)$$

As shown in Chapter IX, the condition for phase compensation in the cathode circuit, subject to the restriction $\mu \gg 1$, may be written

$$R'_k \doteq C_{gk} / C_{km} . \quad (13.8)$$

This relationship may be satisfied either by adjusting R'_k or by increasing one of the capacitances. Ordinarily, it is preferable to increase the

appropriate capacitance; and in any event the compensation should be based on the effective value of transconductance corresponding to actual operating conditions. The degradation of the crystal Q is given by

$$D \doteq (R_1 + R + R_k'')/R_1 \quad (13.9)$$

where for high μ tubes

$$R_k'' \doteq R_k/(1 + g_m R_k) . \quad (13.10)$$

The design parameter most easily controlled is the transformer turns ratio, N , since R_1 is a property of the crystal itself, and R is determined by the allowable Q degradation.

The grounded-plate circuit is best suited for use with high transconductance tubes such as the 6J4 triode. Suitable values for use with this tube and crystals having a resistance, R_1 , of 50 ohms or less are:

$$R_k \doteq 68 \text{ and } R \doteq 100 \text{ ohms.}$$

The value of R may be made somewhat higher if desired, but the degradation of the crystal Q increases more rapidly than the loop gain. To provide margin against crystal and tube variations, equation 13.7 indicates that the transformer should have a turns ratio of about nine. This presents an impedance of about 4000 ohms to the tube grid, and corresponds to a loop gain of two.

C. Analysis and Design of a Triode Grounded-Plate Oscillator.

If the grounded-plate circuit is to perform satisfactorily as a power oscillator the tube must operate in class C, and all unnecessary dissipative elements must be eliminated. The cathode transformer is added to obtain a considerable power output and a suitable value of loop gain.

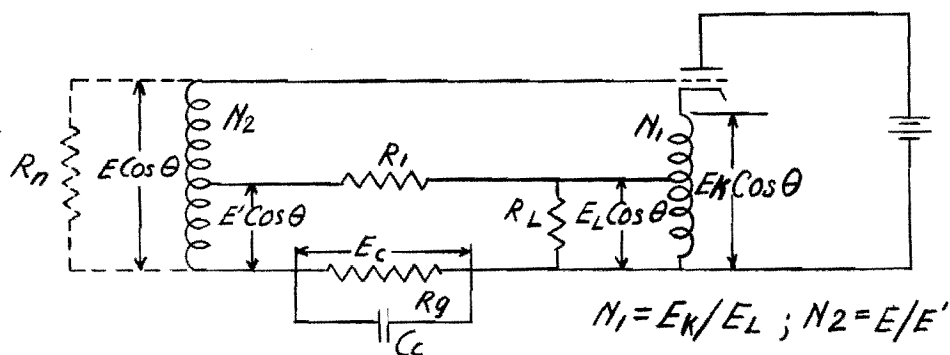


Figure 13.3 - Grounded-Plate Power Oscillator

As shown in Figure 13.3, the resistor, R , of Figure 13.1 is replaced by R_n/N_2^2 , where R_n is the input resistance of the tube, and the grid leak resistor is so located that it dissipates no ac power. The load resistance R_L is made much lower than $R_1 + R_n/N_2^2$ to obtain high load to crystal power ratio, therefore,

$$D = \frac{R_1 + R_n/N_2^2}{R_1} \quad (13.11)$$

If we assume that the fundamental component of the grid current is negligible compared to the fundamental component of plate current, I_{pl} , the useful power output is given by

$$P_L = E_k^2/2N_1^2 R_L, \quad (13.12)$$

where the factor two is required to account for the fact that peak voltage is used. Under the same conditions the power dissipated by the crystal is

$$P_x = \left(\frac{E_k}{N_1} \right)^2 \left(\frac{1}{R_1 + R_n/N_2^2} \right)^2 \frac{R_1}{2}. \quad (13.13)$$

Division of equation 13.12 by equation 13.13, gives the load to crystal power ratio:

$$P_L/P_x = D^2 R_1/R_L, \quad (13.14)$$

or,

$$R_L = R_1 P_x D^2 / P_L. \quad (13.15)$$

In a specific design, the desired power output is specified, the allowable crystal dissipation is known, and the Q degradation may be selected. The load resistance may then be determined from equation 13.15. Suitable grid and plate current conduction angles are then selected, and the input resistance, R_n , is calculated as in Chapter VII. Equation 13.11 then specifies the turns ratio of the grid transformer as

$$N_2^2 = R_n/R_1(D - 1). \quad (13.16)$$

The remaining parameter N_1 may be determined from loop gain considerations. Since the load resistance and power are known, the load voltage may be computed from

$$E_L^2 = 2P_L R_L \quad (13.17)$$

and the grid driving voltage, E , from

$$E = N_2 E_L R_n / (R_n + N_2^2 R_L) . \quad (13.18)$$

An expression for the cathode voltage may be obtained from equation 7.63 which is restated here for convenience.

$$\cos \theta_g = E_c / (E - E_k) , \quad (7.63)$$

or,

$$E_k = (E \cos \theta_g - E_c) / \cos \theta_g . \quad (13.19)$$

The values of E_L and E_k , as given by equations 13.17 and 13.19, specify the voltage ratio of the cathode transformer. Therefore, N_1 may be determined from

$$N_1 = E_k / E_L . \quad (13.20)$$

It is possible to write an expression for N_1 in terms of β_p , g_m , D and R_L , but, its solution requires taking the difference of two quantities that are often nearly equal. Because a considerable error may result, the foregoing method is preferred.

D. Analysis and Design of Class C Electron-Coupled Grounded-Plate Oscillator.

The electron-coupled grounded-plate oscillator is shown in Figure 13.4

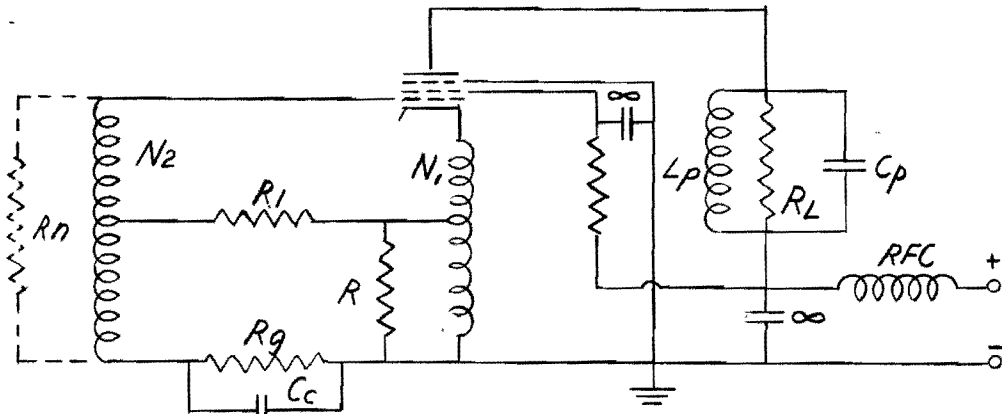


Figure 13.4 Electron-Coupled Grounded-Plate Oscillator.

In this circuit, the full transconductance of the tube is effective in sustaining oscillations, so that the values of R , N_1 , and N_2 may be determined as for the triode grounded-plate oscillator. In this case, however, emphasis should be placed on obtaining the desired operating conditions rather than on obtaining high power into R . The inclusion of this resistor, while somewhat detrimental to efficiency of the circuit, improves the frequency stability and reduces the tendency toward uncontrolled oscillation.

If we assume that R is much less than $R_1 + R_n/N_2^2$, the Q degradation is given by equation 13.11, and the crystal power may be written as

$$P_x = \frac{R_1}{2} \left(\frac{I_{kl} N_1 R}{R_1 + R_n/N_2^2} \right)^2, \quad (13.21)$$

where I_{kl} is the fundamental component of the total cathode current. The load power is given by

$$P_L = \frac{I_{pl}^2 R_L}{2}. \quad (13.22)$$

Therefore,

$$\frac{P_L}{P_x} = K^2 D^2 R_1 R_L / N_1^2 R^2 \quad (13.23)$$

where

$$K = I_{pl}/I_{kl}. \quad (13.24)$$

Because R_L may be very much larger than R^2 , a favorable power ratio may be obtained.

E. Conclusions.

While no experimental work has been done with the grounded plate oscillator as a source of power at the fundamental frequency of the crystal, experience with this oscillator in frequency multiplying circuits indicates that in the electron-coupled form it can supply moderate power with good stability. However, the circuit has a pronounced tendency to free-run, particularly when the operating conditions are extreme class C. This is believed to be due to incorrect compensation of grid to cathode phase shift, which necessarily changes as the effective transconductance varies with overload. Work on frequency multiplying circuits is described in Chapter 17.

XIV. MULTIPLE FEEDBACK OSCILLATORS

A. Introduction.

Multiple Feedback oscillators were briefly discussed in Chapter V of this report. The circuit arrangement of these oscillators is characterized by the presence of two feedback loops; one provides considerable positive feedback over a broad band of frequencies, the other provides sufficient negative feedback to prevent oscillation except at one frequency where the crystal reduces the negative feedback.

The use of multiple feedback circuits for obtaining large power output was conceived prior to the development of suitable procedures for designing the transformer-coupled and grounded-grid oscillators; it was then felt that the multiple feedback circuits offered a solution to the problem of obtaining considerable output power from series-resonant crystal controlled oscillators. However, subsequent analysis has indicated that these circuits are subject to the same limitations on power output as the more conventional oscillators.

B. Cathode-Degenerative Oscillator.

A simple form of the single-tube multiple-feedback circuit is one in which a negative feedback voltage is developed across an impedance in the cathode circuit. If there is sufficient cathode degeneration, the circuit will not oscillate when positive feedback is applied. The cathode impedance is made to vary directly with the impedance of a crystal, so that the negative feedback is very low at the crystal resonant frequency. Therefore, the circuit will oscillate as a crystal-controlled oscillator, if sufficient positive feedback is provided.

Any of the common oscillator circuits, such as the tuned-plate, Colpitts, etc., could be made a cathode-degenerative oscillator by introducing into its cathode circuit a tightly coupled transformer with a crystal across its secondary. Moreover, there is reason to believe that all such circuits have basically similar properties.

C. Analysis.

A tuned-plate cathode-degenerative oscillator is shown in Figure 14.1. If we open the positive feedback loop at the grid of the tube and apply an input voltage, we can apply the Nyquist test to the circuit.

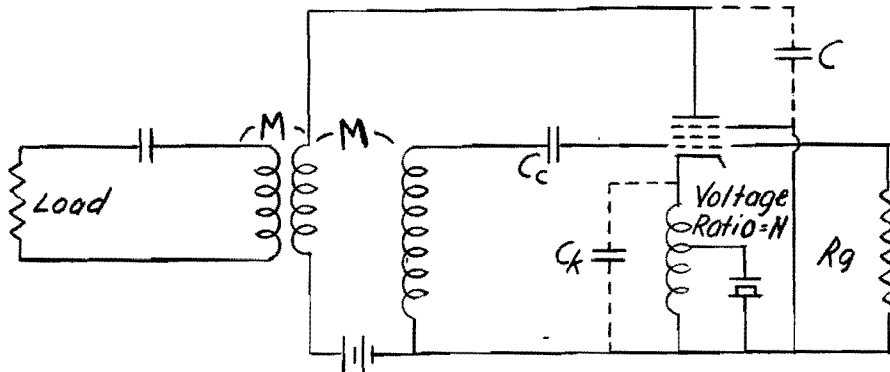


Figure 14.1 Tuned-Plate Cathode-Degenerative Oscillator.

If the grid leak is high, the equivalent linear circuit becomes, near resonance, approximately that shown in Figure 14.2. In this figure, R_L represents the coil loss plus the reflected resistance of the tuned-load circuit, and Z_1 is the crystal impedance.

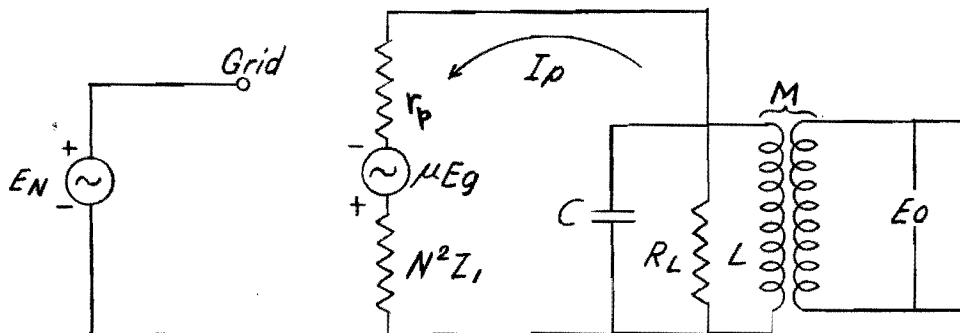


Figure 14.2 Approximate Equivalent Linear Circuit

Near the operating frequency, the crystal impedance varies much more rapidly than the other circuit impedances. Thus, in this range, the tank impedance is approximately constant and equal to its parallel resonant resistance, R_L . The plate current is given by

$$I_p = \mu E_g / (r_p + N^2 Z_1 + R_L) , \quad (14.1)$$

and the output voltage is given by

$$E_o = I_p R_L M / L . \quad (14.2)$$

Moreover,

$$E_g = E_n - I_p N^2 Z_1 . \quad (14.3)$$

Therefore, we may substitute 14.1 and 14.3 in 14.2 to obtain

$$E_o = \mu E_g R_L M / L (r_p + N^2 Z_1 + R_L) \quad (14.4)$$

Also we may obtain

$$E_n - E_g = N^2 Z_1 E_o L / M R_L . \quad (14.5)$$

Elimination of E_g leads to the loop gain expression

$$\frac{E_o}{E_n} = \frac{\mu M R_L}{L(r_p + R_L) + L N^2 Z_1 (\mu + 1)} . \quad (14.6)$$

If the tube has a high plate resistance so that $r_p \gg R_L$ and if $\mu \gg 1$, the loop gain expression simplifies to

$$\frac{E_o}{E_n} = \frac{M R_L g_m}{L(1 + N^2 Z_1 g_m)} . \quad (14.7)$$

If the cathode transformer has a high coefficient of coupling, and its primary inductance antiresonates the cathode-to-ground capacity plus the crystal shunt capacity reflected from the transformer secondary, the crystal impedance, Z_1 , becomes the crystal series arm impedance. Then

$$Z_1 = R_1 + j\omega L_1 + 1/j\omega C_1 . \quad (14.8)$$

For this condition, the loop gain equation shows that crystal control is possible if the plate tank circuit and cathode transformer are properly designed. At frequencies appreciably off crystal resonance, Z_1 is a high impedance, and the loop gain is less than unity. But at the crystal resonant frequency, Z_1 becomes the crystal series resistance alone; so, with a proper value of M , the Nyquist conditions of gain and phase are satisfied.

The frequency stability of this circuit may be determined, as in Chapter VI, by comparing the rate of phase change of the circuit to that of the crystal alone.

From equations 14.7 and 14.8,

$$\frac{E_o}{E_n} = \frac{M R_L g_m}{L(1 + N^2 R_1 g_m) + j N^2 L g_m (\omega L_1 - 1/\omega C_1)} . \quad (14.9)$$

By writing equation 14.9 in the polar form, the loop transmission E_o/E_n may be expressed as $E_o/E_n = |E_o/E_n| \angle B$,

where

$$B = \tan^{-1} \frac{(\omega L_1 - 1/\omega C_1) N^2 g_m}{1 + N^2 R_1 g_m}. \quad (14.10)$$

The derivative of θ , with respect to ω at ω_o , is

$$\left. \frac{dB}{d\omega} \right|_{\omega=\omega_o} = \frac{g_m N^2 (L_1 + 1/\omega_o^2 C_1)}{1 + g_m N^2 R_1}. \quad (14.11)$$

Since $\omega_o^2 = 1/L_1 C_1$,

$$\left. \frac{dB}{d\omega} \right|_{\omega=\omega_o} = \frac{2L_1 g_m N^2}{1 + g_m N^2 R_1}, \quad (14.12)$$

or

$$\left. \frac{dB}{d(\omega/\omega_o)} \right|_{\omega=\omega_o} = \frac{2\omega_o L_1 g_m N^2}{1 + g_m N^2 R_1}. \quad (14.13)$$

Reference to equation 6.13 shows that the expression can be interpreted to be twice the effective Q of the circuit.

The crystal alone is known to have

$$\left. \frac{dB}{d(\omega/\omega_o)} \right|_{\omega=\omega_o} = 2Q = 2\omega_o L_1 / R_1. \quad (14.14)$$

Therefore, the circuit is seen to degrade the crystal Q by the ratio:

$$\frac{Q_{\text{crystal}}}{Q_{\text{effective}}} = D = 1 + \frac{1}{g_m N^2 R_1}. \quad (14.15)$$

Since it is possible to make the factor $g_m N^2 R_1$ approximately unity, the frequency stability of this circuit should be comparable with the stability of other existing oscillator circuits.

If the plate tank loss is small, and if the tube used has considerable power gain, the output power is given approximately by

$$P_L \approx I_{pl}^2 R_L. \quad (14.16)$$

The power dissipated in the crystal is

$$P_x = (I_{kl} N)^2 R_L \quad (14.17)$$

where I_{kl} is the fundamental component of the total cathode current. The ratio of the load to crystal power is

$$P_L/P_x = K^2 R_L / N^2 R_L , \quad (14.18)$$

where

$$K = I_{pl}/I_{kl} . \quad (14.19)$$

Because K is nearly one for typical tubes, and because N may be made small, it is possible to obtain a large load-to-crystal power ratio. However, equation 14.18 is of the same form as the similar expression developed for the electron-coupled grounded-plate oscillator in Chapter XIII, hence the cathode-degenerative oscillator has no fundamental advantage with regard to power output.

D. Experimental Results.

The tuned-plate oscillator, which is known to produce high power output, was selected for the experimental work. Because this work was done prior to the development of class C design procedures, the design was based on the class A analysis, and the circuit proportioned to give considerable excess loop gain, thus assuring class C operation. The circuit shown in Figure 14.3 was used with the constants adjusted for operation at 36 Mc.

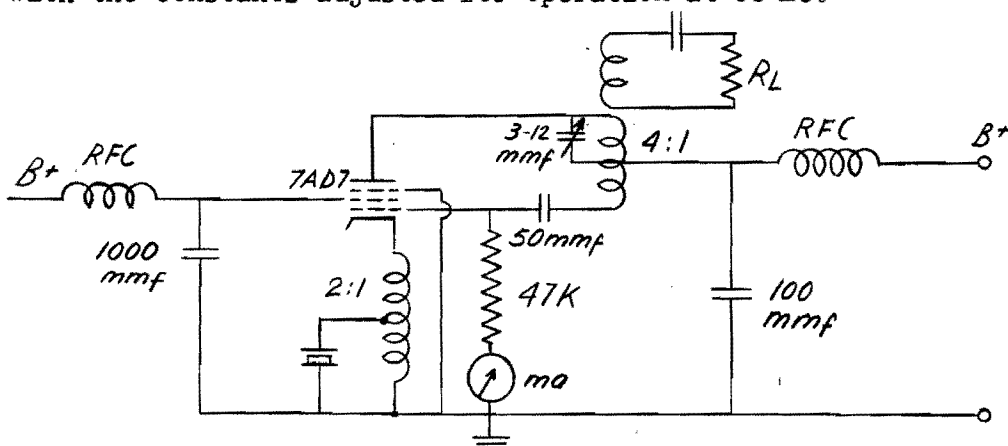


Figure 14.3 - Cathode-Degenerative Tuned-Plate Oscillator

The 7AD7 tube was chosen because of its high transconductance and power

rating, and the fact that the lead to the suppressor grid is available for direct grounding, thus reducing the plate-to-cathode capacity. This circuit has a tendency to free-run with the crystal in place and the plate circuit detuned; but the tendency is not strong, and tuning the plate circuit to the crystal frequency causes a pronounced increase in grid current. With proper tuning, oscillations cease when the crystal is removed from its socket. The measured power output of this circuit is 2.5 watts, and the frequency stability under full load conditions is 0.3 ppm/volt.

A similar oscillator was constructed to operate at 60 Mc with a 6AQ5 tube. This oscillator would operate crystal-controlled and free-run simultaneously; the difference between the two frequencies being about 250 kc. Connection of a neutralizing capacitor between grid and cathode eliminated the tendency to free-run, but it also reduced the power output at the crystal frequency. Tubes having a different ratio of plate-to-cathode and grid-to-cathode capacities may operate in this circuit without neutralization. The maximum power obtained from this circuit was 1.5 watts.

E. Conclusions.

While the cathode-degenerative oscillator can supply considerable power output, it has no fundamental advantage over the more conventional oscillator circuits. Furthermore, its performance is sensitive to parasitic feedback capacities, and it is difficult to adjust for optimum performance. Because equivalent performance is available in simpler circuits, it is believed that the cathode-degenerative oscillators are of limited importance.

XV STABILIZATION OF A FREE-RUNNING OSCILLATOR

A. Introduction.

Among the problems specified for study by the governing contract is the use of automatic-frequency-control to stabilize the frequency of a free-running oscillator. Accordingly, attention was turned to circuits which use a crystal resonator as a frequency reference or discriminator to develop error voltages for the control of a free-running oscillator. The frequency range of present interest is from about fifty to two hundred megacycles.

The principles of automatic frequency control were first published by Travis¹ who used the method to stabilize the frequency of the local oscillator of a superheterodyne receiver with respect to a transmitter frequency by means of a low frequency discriminator. The discriminator in such a system need not possess great stability because it operates at a frequency low compared to that of the oscillator, so this method is successful whether the transmitter frequency be stable or somewhat variable.

Automatic frequency control (afc) has been applied to a number of other situations, notably microwave oscillators. In the region of 10 kmc, available oscillators have poor frequency stability. Although good cavity resonators are available, it is difficult to integrate them into oscillator designs. Pound², Tuller³, and others have found that it is practical to use afc to stabilize microwave reflex oscillators with respect to a tunable external cavity. For somewhat higher frequencies the molecular resonance of ammonia provides a frequency reference which is believed to be absolute. Papers by Hershberger⁴ and by Smith⁵ describe systems in which afc is used to control the frequency of a (K band) microwave oscillator with respect to the resonance frequency of ammonia. However, these systems are relatively complex and are not directly applicable to the present problem. Hedeman⁶ has used afc in the range of present interest for frequency synthesis. In his system, which employs several modulators, frequency multipliers, and filters, a frequency differing from the desired one by a specified amount is built up by adding harmonics of several crystal oscillators. A free-running oscillator is then controlled at the desired frequency by a stable low frequency discriminator and afc. This system can deliver a large number of useful output frequencies

from rather few crystals and discriminators; moreover, the output is free from unwanted modulation products.

B. Principles of Automatic Frequency Control.

The fundamental features of an afc system are shown in Figure 15.1.

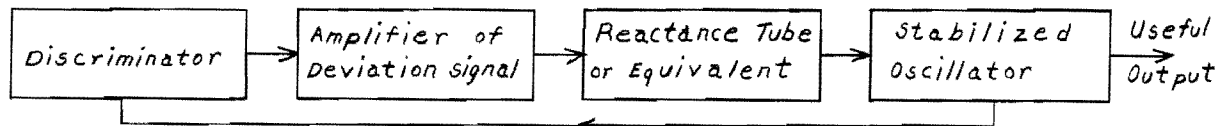


Figure 15.1 - Basic Automatic Frequency Control System

If the output frequency deviates from the desired value, the discriminator develops a voltage which is amplified and applied to the reactance tube to reduce the frequency deviation. Assuming that the amplifier has a gain A, that the reactance tube produces a susceptance change of B ohms per volt, that the control factor of the stabilized oscillator is C cycles per ohm, and that the discriminator response is D volts per cycle, deviations of the oscillator are reduced by the factor $(1-ABCD)^{-1}$. That is, the frequency stability of the oscillator is improved by the factor $(1-ABCD)$, which is readily made large. In situations such that an amplification in excess of a few hundred is required, it is usually necessary to convert the error voltage to an alternating voltage. This results in an improvement in stability and inherent noise, which more than justifies the additional modulator and demodulator required.

The basic discriminator circuit and its response are shown in Figure 15.2. It consists of identical rectifier circuits fed from two antiresonant circuits tuned to different frequencies. Arguimbau⁷ has shown that in properly proportioned circuits, the net output voltage is accurately linear with frequency. Moreover, he has shown that a number of different circuits, used as discriminators, have exactly the same response. Fortunately, exact linearity is unnecessary in afc systems, and any device producing a response having the general form of Figure 15.2b may be employed.

The control device may be mechanical or electrical; or both may be used together. However, an electrical control is preferable in the present situations and will be assumed in the following discussion. Of electronic control devices the reactance tube is probably oldest and most familiar. The common arrangement employs a pentode in which the control grid is excited in

quadrature with the plate. The plate current is thus in quadrature with the plate voltage, so the tube acts as a reactance, the magnitude of which may be controlled by variation of some bias voltage.

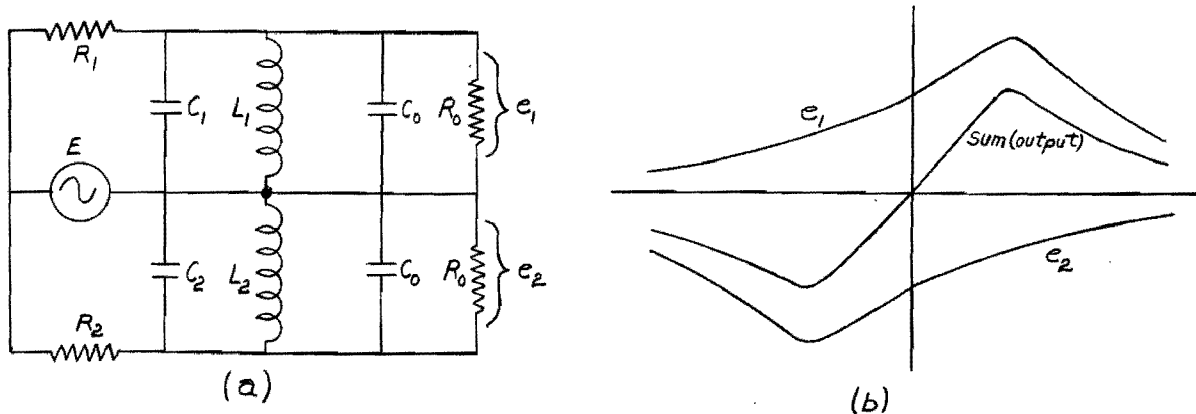


Figure 15.2 - Discriminator Circuit and Response

In microwave reflex oscillators the reactance tube is unnecessary because the operating frequency is sensitive to the voltage applied to the repeller electrode. Moreover, the function of the reactance tube is readily performed by the oscillator tube at frequencies of present interest. In the conventional oscillator-reactance tube combination the first tube contributes real volt-amperes or power as a negative resistance to annul the losses of the system, while the second tube contributes quadrature volt-amperes to vary the frequency at which oscillation occurs. Evidently, it should be possible to provide both these functions in a single tube. Chang⁸, Bradley⁹, Johnson¹⁰, and Bruch¹¹ have described single-tube oscillators in which the amplitude is substantially constant and the frequency may be varied over a considerable range by means of a single bias voltage.

The arrangement of Bradley is particularly adaptable to the present situation, although designed for an entirely different purpose. The basic arrangement is shown in Figure 15.3. The circuit constants are such that the tube operates in class C with a relatively small conduction angle. Circuit B has a relatively high Q and serves as the principal frequency determining element. Circuit A has a low Q and is rather loosely coupled to B. The essential fact is that the circuits are tuned so that pulses of plate current and of cathode current produce voltages which are in quadrature in

Circuit B. Therefore, variation of the control voltage V does not affect the amplitude but does affect the frequency of oscillation by varying the magnitude of the plate current. Although designed for frequencies in the order of 10 Mc, this circuit should be capable of operation at much higher frequencies.

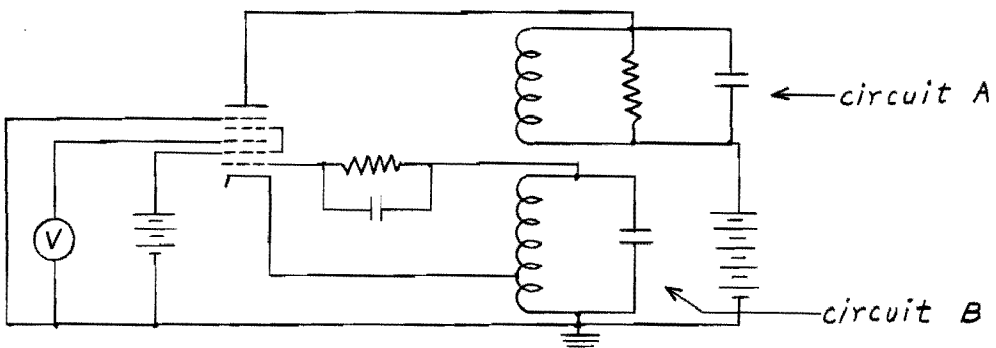


Figure 15.3 - Single-Tube Frequency Modulated Oscillator

C. Quartz Crystal Discriminators.

A search of the literature disclosed only one form of discriminator based on quartz crystals. This circuit, due to Hollis¹², is reproduced in Figure 15.4. It is seen to resemble that of Figure 15.1, and it has a similar response curve. However, the behavior is relatively complicated because the addition of the physical inductor L_1 (or L_2) in shunt with the crystal causes each branch to have two antiresonant frequencies.

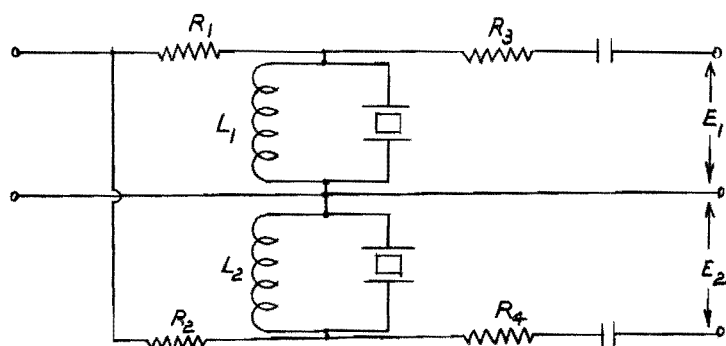


Figure 15.4 - Crystal Discriminator of Hollis

The resistors R_1 and R_2 are so large that the crystals may be thought of as driven by a constant current; consequently, the magnitude of the output voltages is proportional to the impedances of the crystal arms. Therefore,

the outputs may be given the form shown in Figure 15.5, and the net output, which represents the difference of these curves, approximates the typical discriminator response. The principal drawback of this arrangement is that it requires two crystals which are very similar except for a controlled difference of frequency.

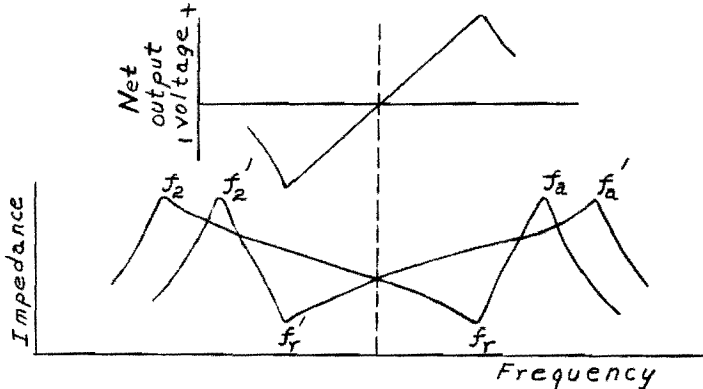


Figure 15.5 - Response of Crystal Discriminator Circuit

In his paper on afc in microwave oscillators, Rideout¹³ points out that the circuit of Figure 15.6 serves as a convenient discriminator.

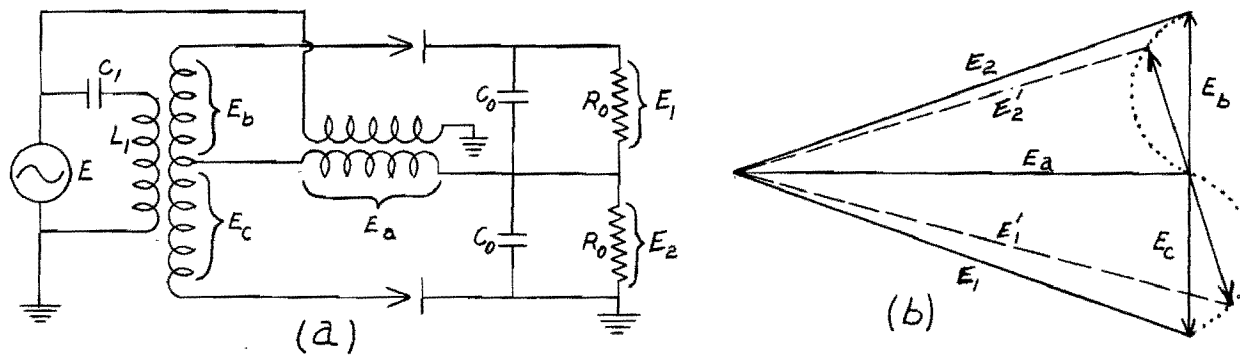


Figure 15.6 - Discriminator Using Single Tuned Circuit

At the frequency of resonance between L_1 and C_1 the primary current is in phase with E . Therefore, E_b and E_c are in quadrature with E_a , and no output results because E_1 and E_2 are equal and opposite. At a slightly different frequency, however, the quadrature relationship is upset and an output exists. The source and magnitude of this output is conveniently studied by means of the phasor diagram of Figure 15.6b.

Rideout demonstrated that the properties of this circuit may be accurately realized at a frequency near 10 kmc by substituting a cavity

resonator for $L_1 C_1$ and making other appropriate changes. It appears probable that satisfactory results could also be obtained at frequencies of present interest by means of a single quartz crystal; however, the idea was conceived too late to permit experimental verification.

D. Control Circuits.

At least two basic types of response may be demonstrated by the control system. In one the frequency deviation produced by an arbitrary change in the tuning of the oscillator is reduced by a fixed factor; in the other the deviation is reduced to zero. The former has already been illustrated in Figure 15.2 and discussed in the associated section. If, for example, a small capacitance were added to the resonator the frequency would tend to decrease by some amount δf and would actually decrease by the amount $\delta f/(1-ABCD)$.

The second type of behavior is displayed by systems in which frequency correction is produced by a motor-driven variable condenser. The motor will continue to turn as long as a frequency deviation exists; that is, until the frequency deviation is reduced to zero. Therefore, in such a system the addition of a capacitance would produce no permanent frequency change. Moreover, in such systems the correction system will remain at rest or "wait" in the event of failure of the afc. This is desirable because the frequency will then drift away from its initial value only at a very slow rate.

The system of Hollis is of the second type, i.e. it provides complete frequency correction. It is entirely electronic and is therefore capable of very rapid response. The essential features of his arrangement are shown in Figure 15.7.

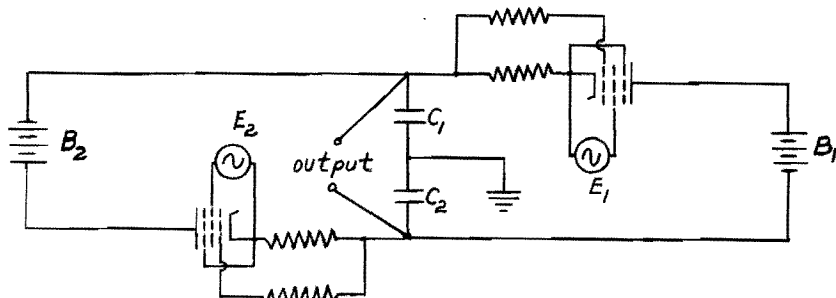


Figure 15.7 - Simplified Schematic of Differential Bridge

Two identical pentodes having substantially infinite plate resistance are connected in a closed ring with two separate sources of B voltage, and initially biased so that no current flows. In normal operation, equal alternating voltages, E_1 and E_2 , are applied, the tubes conduct equal rectified currents, and no charge accumulates in C_1 and C_2 . However, if E_1 exceeds E_2 the currents are unbalanced, and an increasing output voltage appears. The output voltage becomes constant, but does not disappear, if E_1 and E_2 are again made equal; it may be reduced to zero only by creating an opposite unbalance for a suitable interval. In the event of failure in the discriminator, E_1 and E_2 disappear, but the output voltage persists at the value which existed at the instant of failure. Thus the frequency will not change suddenly even if the discriminator fails, just as with the motor driven variable condenser.

E. Experimental Work.

Two crystal discriminators, as shown in Figure 15.4, have been constructed, one using crystals at their fundamental frequencies of 5.445 and 5.475 Mc, the other using crystals at third overtone frequencies of 52.695 and 53.695 Mc. The low frequency unit was tested by applying signals from a crystal-controlled Miller oscillator for which a large number of crystals, having closely spaced frequencies in the range of interest, were available. No particular experimental difficulties were met, and the output, as observed by means of a vacuum tube voltmeter, agreed very closely with that predicted by theory.

The performance of the high-frequency crystal discriminator was tested with a signal generator and vacuum tube voltmeter. No satisfactory performance was obtained, although a considerable number of adjustments were attempted. The failure of this attempt is attributed, at least in part, to spurious responses of the crystal unit.

A vacuum-tube differential bridge, using two 6AK5 pentodes in the circuit of Figure 15.7, was constructed to utilize the output of the low-frequency discriminator. This circuit was found to be very difficult to balance. It was necessary to use matched tubes to produce balanced DC outputs with no applied signal, and DC leakage paths were quite troublesome. The addition of a cathode-follower output stage did not appreciably improve the results

obtained.

F. Conclusions.

It appears, from both theoretical and experimental work, that a crystal which is to serve as a frequency reference or a discriminator element in an afc system must have characteristics which are substantially the same as those required of a crystal that is to operate in an ordinary oscillator circuit. Because afc systems are inherently more complicated than direct oscillators, they would be used only if the performance were substantially superior to that of an oscillator employing a comparable crystal. It appears unlikely that sufficient improvement may be secured in this way to justify the added complexity.

BIBLIOGRAPHY

- (1) Travis, C., "Automatic Frequency Control", Proc. I.R.E. 23, 1125-1141, (1935).
- (2) Pound, R. V., "Frequency Stabilization of Microwave Oscillators", Proc. I.R.E. 35, 1405-1415, (1947).
- (3) Tuller, W. G., Galloway, W. C., and Zaffarano, F. P., "Recent Developments in Frequency Stabilization of Microwave Oscillators", Proc. I.R.E. 36, 794-800, (1948).
- (4) Hershberger, L. E. and Norton, L. E., "Frequency Stabilization with Microwave Spectral Lines", RCA Review 9, 38-49, (1948).
- (5) Smith, W. V., de Guevedo, J. L. G., Carter, R. L., and Bennett, W. S., "Frequency Stabilization of Microwave Oscillators by Spectrum Lines", Jour. Appl. Physics, pp 1112, Dec. 1947 and p 811, Sept. 1948.
- (6) Hedeman, W. R., "Few Crystals Control Many Channels", Electronics 21, 118-121, (1948).
- (7) Arguimbau, L. B., "Discriminator Linearity", Electronics 18, 142-144, (1945).
- (8) Chang, H. and Rideout, V. C., "The Reactance Tube Oscillator", Proc. I.R.E. 37, 1330-31 1096 (1950).
- (9) Bradley, W. E., "Single Stage F-M Detector", Electronics 19, 88-91, (1946).
- (10) Johnson, K. C., "Single-Valve Frequency Modulated Oscillator", Wireless World 55, 122-123, 168-170, (1949).
- (11) Bruck, G. S., "Simplified Frequency Modulation", Proc. I.R.E. 34, 458 (1946).
- (12) Hollis, J. L., "Simplified Automatic Stabilization of a Frequency-Modulated Oscillator", Proc. I.R.E. 36, 1164-71, (1948).

- (13) Rideout, V. C., "Automatic Frequency Control of Microwave Oscillators",
Proc. I.R.E. 35, 767-77, (1947).

XVI MISCELLANEOUS OSCILLATOR CIRCUITS

A number of circuits not described in the preceding chapters were investigated during the term of this project. Some of these have advantages which are worthy of presentation even though the circuit may be shown to be the equivalent of more familiar forms.

A. Line-Coupled Oscillator.

The circuit shown in Figure 16.1 is a modification of the transformer-coupled oscillator in which artificial quarter wave-line sections are used as impedance transforming networks. The required polarity reversal is obtained by virtue of the 90° phase shift of each of the line sections.

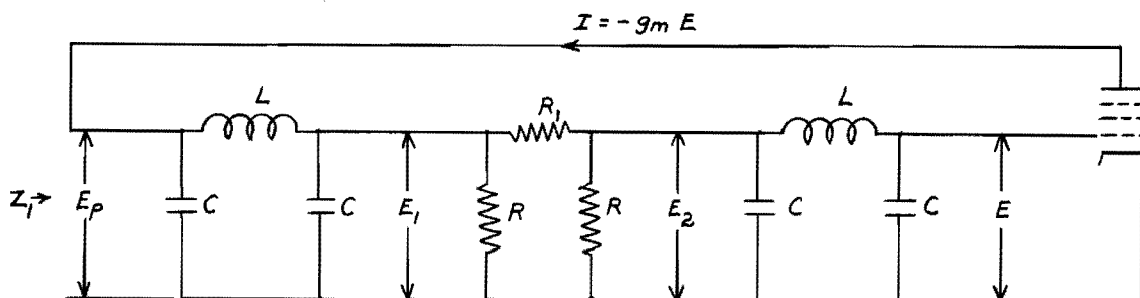


Figure 16.1 - Symmetrical Line-Coupled Oscillator

Application of nodal equations to the network of Figure 16.1 gives the system of simultaneous equations

$$I = (j\omega C + 1/j\omega L)E_p - E_1/j\omega L , \quad (16.1)$$

$$0 = -E_p/j\omega L + E_1(j\omega C + 1/j\omega L + 1/R + 1/R_1) - E_2/R_1 , \quad (16.2)$$

$$0 = -E_1/R_1 + E_2(1/R_1 + 1/R + j\omega C + 1/j\omega L) - E/j\omega L , \quad (16.3)$$

$$0 = -E_2/j\omega L + E(j\omega C + 1/j\omega L) . \quad (16.4)$$

This system of equations, when solved simultaneously, yields

$$E = (-I/\omega^2 L^2 R_1)(1/\Delta) , \quad (16.5)$$

$$\Delta \equiv \begin{vmatrix} (j\omega C + 1/j\omega L) & -1/j\omega L & 0 & 0 \\ -1/j\omega L & (j\omega C + 1/R + 1/R_1 + 1/j\omega L) & -1/R_1 & 0 \\ 0 & -1/R_1 & (1/R_1 + 1/R + j\omega C + 1/j\omega L) & -1/j\omega L \\ 0 & 0 & -1/j\omega L & (j\omega C + 1/j\omega L) \end{vmatrix}$$

At the design frequency $\omega_o L = \frac{1}{\omega_o C}$, and the determinant reduces to Δ_o , where

$$\Delta_o = C/\omega_o^2 L^3. \quad (16.7)$$

Thus,

$$E = -IL/CR_1. \quad (16.8)$$

Since

$$I = -g_m E, \quad (16.9)$$

the loop gain A is given by

$$A = g_m L/CR_1. \quad (16.10)$$

It is somewhat surprising that R does not appear in 16.10; however, it is characteristic of a 90° network that the output voltage is proportional to the input current but independent of the load resistor. Because ω_o^2 equals $1/LC$ and Z_o is given by $\omega_o L$, the gain equation becomes

$$A = g_m Z_o^2/R_1. \quad (16.11)$$

The required characteristic impedance of the line may be determined from equation 16.11, but the values of R remain to be specified. Since the network is symmetrical, equal impedances will be presented to the plate and grid of the tube. The plate and grid circuit impedances, which are equal and may be designated Z_1 , are given by the equation

$$Z_1 = Z_o^2 \frac{R + R_1 + R}{R(R_1 + R)}. \quad (16.12)$$

Because of the impedance inverting properties of the lines, the crystal faces a short circuit in each direction if the tube input and output impedances are infinite. In practice, the tube impedances are high compared to the line impedance, so this condition is approximated, therefore D is almost equal to one. Thus, maximum frequency stability is anticipated when Z_1 is a minimum. To explore this situation let $R = KR_1$, in which case

$$Z_1 = \frac{Z_o^2}{R_1} \left(\frac{2K + 1}{K^2 + K} \right). \quad (16.13)$$

Using g_m to represent the transconductance which gives unit loop gain in 16.11 we have

$$Z_1 = \frac{1}{g_m} \left(\frac{2K + 1}{K^2 + K} \right) . \quad (16.14)$$

It is seen that arbitrarily low values of Z_1 may be obtained by making K large; however, values of K in excess of two or three are undesirable in practice. If, for example, we set $g_m = 0.0025$ mho and $K = 2$, we have $Z_1 = 333$ ohms a very low value.

A typical design is presented in Figure 16.2 and experimental results obtained with this circuit are given in Table 16.1

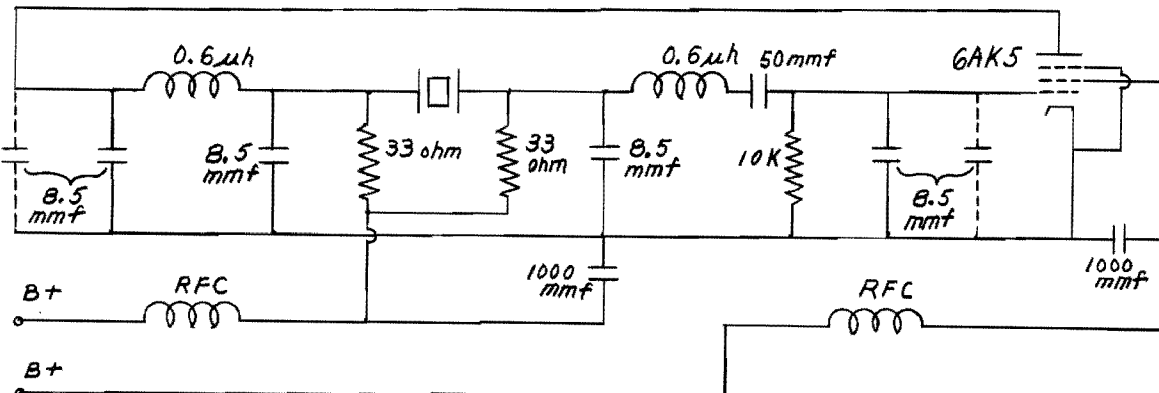


Figure 16.2 - Quarter-Wave Artificial Transmission Line Oscillator

TABLE 16.2
FREQUENCY STABILITY OF THE CIRCUIT IN FIGURE 16.2

Frequency (Mc)	Screen Potential (volts)	Plate Potential (volts)	Voltage Varied	Stability ppm/v
70	65	100	Screen	0.9
100	65	60-70	Screen	0.5
100	65	70-80	Screen	0.4
100	65	100-150	Plate	0.1

This oscillator may be expected to perform satisfactorily over most of

the 50 to 150 Mc frequency range. It is, however, sharply tuned to one frequency and does not lend itself to rapid adjustment for operation at a different frequency.

It should be noted that the design procedures in Chapter II are applicable to the network of this circuit, and are particularly useful when the input and output capacities of the line sections are unequal. Moreover, by using unequal resistors in conjunction with the crystal it is possible to obtain unequal impedances in the grid and plate circuits. This may be desirable in the interest of frequency stability, power output or both.

B. Parallel Mode Overtone Oscillator.

The most widely used parallel-mode oscillators are the Miller and the Pierce. In the Miller the crystal is connected between grid and cathode, and in the Pierce between the grid and plate. In the present oscillator the crystal is connected between plate and cathode. The operation of this circuit may be explained in terms of that of the well known Colpitts circuits shown in Figure 16.3.

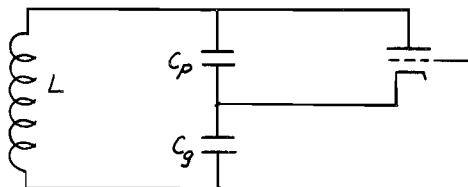


Figure 16.3 - Grounded Grid Colpitts Oscillator

Provided the resistance losses in the coil (L) and the associated capacitors (C_p and C_g) are not excessive, oscillations will occur at a frequency such that the reactance of L is equal to the sum of the reactance of C_g and C_p . Moreover, it is readily shown that if the sum of the reactances of C_p and C_g is fixed, oscillations with a given tube may be sustained in conjunction with an inductance having the largest possible resistance if C_p is equal to C_g . This fact is of importance because it explains, in part, the operation of the present oscillator. In Figure 16.4, R_g is the grid leak resistance and C_1 and C_2 are blocking capacitors. The crystal is connected from plate to cathode; therefore, its reactance corresponds to that of C_p in Figure 16.3.

The plate inductor (L_1) corresponds to L in Figure 16.3, and the inductor, L_2 , partially resonates the intrinsic cathode-to-ground capacity, so as to control the effective value of C_g in Figure 16.3.

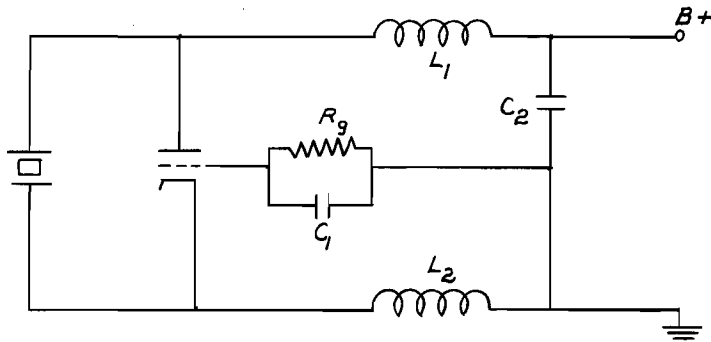


Figure 16.4 - Plate-Cathode Oscillator

Let it be supposed that the crystal in parallel with the plate-to-cathode capacity of the vacuum tube has such properties that at one frequency its total impedance is a pure resistance as shown in Figure 16.5.

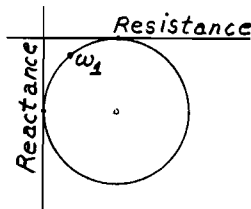


Figure 16.5 - Variation of Crystal Impedance With Frequency

Then, at some frequency (ω_1) the reactance of the crystal unit is equal to the effective grid-to-cathode reactance in Figure 16.4.

If the losses in the inductors (L_1 and L_2) are small and the tube has a suitable transconductance, the circuit oscillates at a frequency extremely close to ω_1 and under control of the crystal. Moreover, the circuit does not oscillate if the crystal is removed.

This circuit will operate either at the fundamental frequency of the crystal or at a mechanical overtone; it has been made to operate as high as the 11th overtone of a 9.5 Mc crystal. Further, it exhibits some of the broad-band properties of the Pierce oscillator, especially at the fundamental frequency of the crystal. With L_1 and L_2 adjusted to antiresonate the stray capacitances at 10 Mc, operation from 4 to 18 Mc was obtained without

retuning. The frequency stability at fundamental frequencies is comparable to that of other parallel-mode oscillators, but is inferior to that of the series-mode oscillators at high overtones and frequencies. Because the circuit has little intrinsic selectivity, it does not operate stably with crystals which have several responses only slightly separated in frequency. Under these circumstances the operating frequency is subject to small discontinuous jumps when the circuit is slightly disturbed. Other circuits are subject to the same basic difficulty, but usually to a smaller degree. The power output is somewhat lower than that of other oscillators using the same tube. For example, a 6J4 triode operating at 70 Mc provides a power output of about 50 milliwatts.

C. The Negative Transconductance Oscillator.

The negative transconductance oscillator is obtained by placing a crystal-controlled transmission network between the screen and suppressor grids of a pentode. Because the cathode current of a pentode tends to remain constant, variations of the suppressor potential cause plate and screen current variations which are opposite to each other, the screen current variations being such that the voltage produced across a resistive impedance in the screen circuit is in phase with the suppressor voltage variations. For this reason the network between screen and suppressor need not produce a phase reversal. The circuit of this oscillator is presented in Figure 16.6.

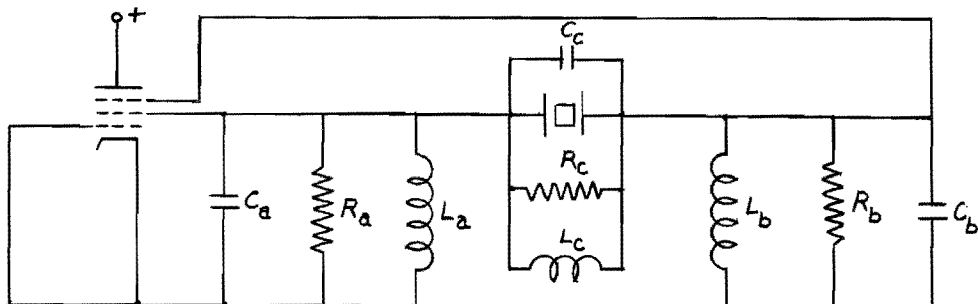


Figure 16.6 - Negative Transconductance Oscillator

The capacitors C_a and C_b include the tube capacities, C_c includes the tube and crystal holder capacity, and all are antiresonated by their respective shunt inductors. The resistors include physical loads and coil losses.

One advantage of this circuit is its ability to oscillate with crystals having high series resistance, but to realize this advantage and avoid tendencies to oscillate out of crystal control the holder capacity must be carefully compensated. This may be done by properly proportioning the RC products of the network.

If we remove the inductors and ignore the series arm of the crystal in Figure 16.6, we obtain the following circuit:

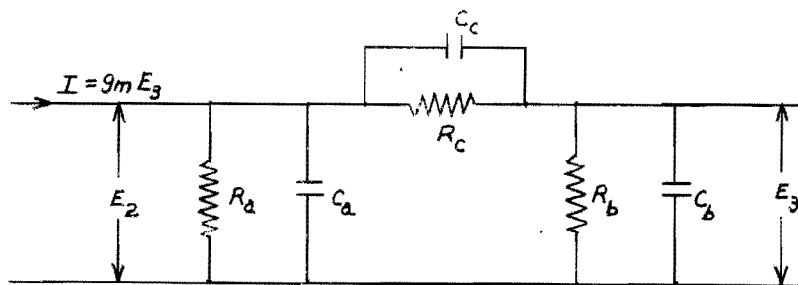


Figure 16.7 - Reduced Equivalent of Figure 16.6

From Figure 16.7 it may be seen that if $R_c C_c$ is equal to $R_b C_b$, the output voltage E_3 is given by

$$E_3 = E_2 R_b / (R_b + R_c) . \quad (16.15)$$

Therefore E_3 is a constant fraction of E_2 at all frequencies; under no circumstance is the ratio of E_3/I greater than that found at zero frequency. The Nyquist diagram of Figure 16.7, with the resistances adjusted according to (16.15) is shown in Figure 16.8a.

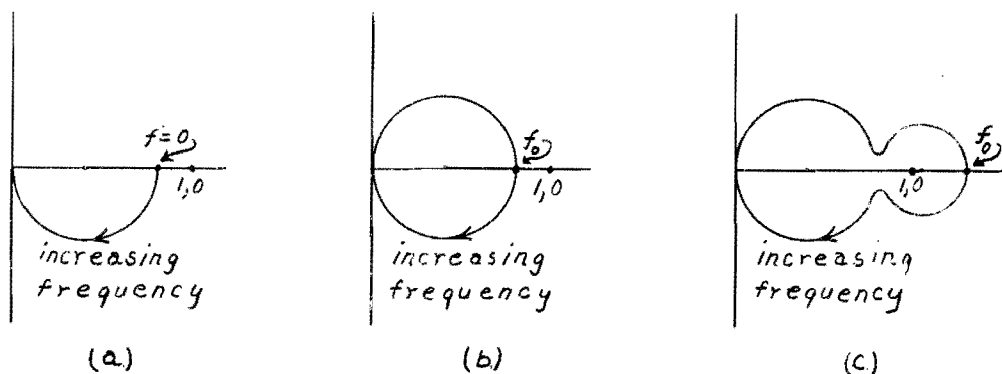


Figure 16.8 - Nyquist Diagrams

If we now assume the inductors to be replaced in Figure 16.6 the Nyquist diagram takes the form of Figure 16.8b. With the products $R_c C_c$ and $R_b C_b$ equal, the zero frequency response of Figure 16.8a becomes the antiresonant response; and the total phase shift becomes 0° . Replacing the series arm of the crystal returns the circuit to its original condition for which the diagram of Figure 16.8c is applicable. Since the crystal series arm is a high impedance at frequencies slightly different from ω_0 , the response of the complete system at these frequencies is the same as that in Figure 16.8b. Near ω_0 , however, the low impedance of the series arm causes the loop gain to increase, and at ω_0 , where the series arm is a pure resistance, the loop phase is zero and the loop gain may be made greater than one. Thus, by making the RC products i.e. the Q's of the compensating and suppressor circuits equal, oscillations due to transmission through the crystal holder capacity may be avoided. Unfortunately, if the required value of L_c is small the circuit may oscillate upon removing the crystal. A similar analysis may be applied to the transformer-coupled, cathode-coupled and grounded-grid oscillators. Moreover, by an appropriate redefinition of symbols, the design equations for the transformer-coupled oscillator may be applied to the present circuit. Because the equivalent grid-plate capacitance of this arrangement is high and the effective transconductance relatively low, the ordinary transformer-coupled oscillator is superior in performance.

XVII ELECTRON COUPLING AND FREQUENCY MULTIPLICATION

A. Introduction.

The objectives sought in this study were the extension of the upper frequency limit of crystal control using simple circuits, and isolation of the useful load from the frequency-determining portion of the circuits. The use of electron coupling in single-tube oscillators to achieve these ends at low frequencies is highly successful; and this technique may be extended to high frequencies with fair success. The cathode-coupled oscillator may also be used for frequency multiplication by extracting power output at the harmonic frequency from the plate circuit of the cathode follower. By using a pentode tube good isolation of the load can be obtained, and due to the low impedance of the tank circuit at the fundamental frequency, satisfactory load isolation is obtained even when triodes are used. Although this circuit is capable of supplying considerable power output (0.4 watt at 256 Mc), its efficiency is poor.

The single-tube electron coupled circuits, here reported, while requiring smaller plate and filament power, have not proved to be more efficient; and the available power output at harmonic frequencies is small. However, these arrangements give excellent isolation of the load circuit and good power output at fundamental frequencies.

B. Cathode-Coupled Oscillator for Frequency Multiplication.

The cathode-coupled oscillator is described in Chapter IX of this report; and it is shown in Chapter VII that locating the load in the plate circuit of the cathode follower produces a favorable ratio of load to crystal power. Because the circuit is capable of good class C operation, the angle of plate current flow may be made low, thereby favoring the production of harmonic frequencies.

The basic cathode-coupled oscillator has been used with success at frequencies up to 150 Mc, and by using a tuned load in the plate circuit of the cathode follower considerable power may be obtained at harmonic frequencies. This resonant circuit has relatively low impedance at the fundamental frequency and, therefore, does not seriously disturb the function of the cathode-follower in the oscillating loop.

The circuit of Figure 17.1 utilized a crystal operating on its ninth overtone at a frequency of 126 Mc. The holder capacity of this crystal was 12 mmf and its series resistance, R_1 , was estimated to be greater than 200 ohms.

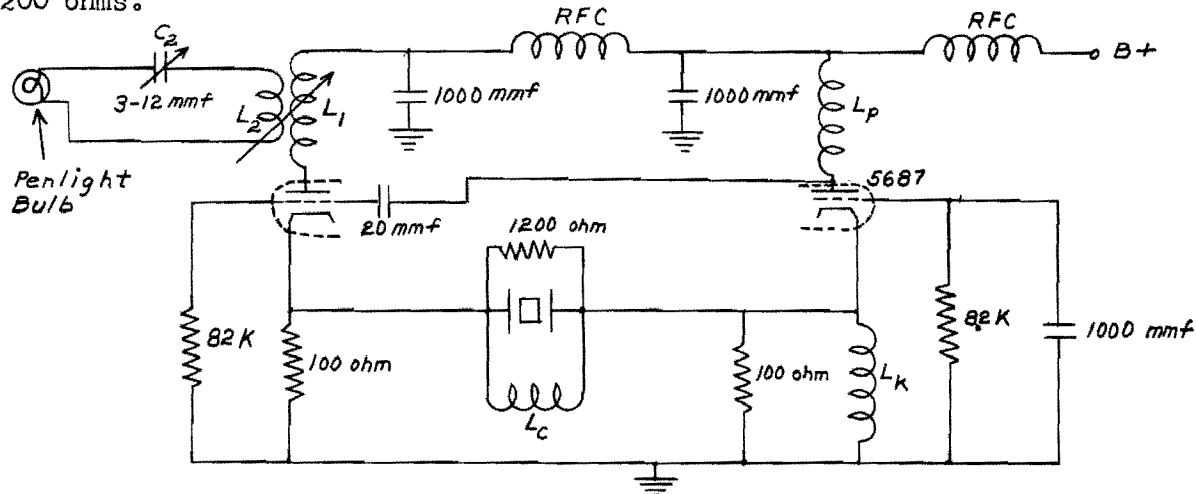


Figure 17.1 - Cathode-Coupled Oscillator for Frequency Multiplication
 Because of the low reactance of the holder capacity and the relatively high value of R_1 , it was necessary to compensate the crystal; a simple network consisting of L_c and a 1200 ohm shunt resistor was found to be satisfactory for this purpose.

The inductances L_p , L_c , and L_k antiresonate the corresponding shunt capacities at 126 Mc, while L_1 is antiresonant with the output capacity of the cathode follower at 252 Mc. The secondary of the output transformer was resonated with C_2 at 252 Mc, and a penlight bulb was used to give a visual indication of power output. Because its resistance varies with voltage, a bulb is not an ideal load; however, its use permits the measurement of power output by comparing its brilliance with that of a similar bulb heated with direct current.

This current supplied an output power of 0.4 watt at 252 Mc. The frequency stability was found to be 0.8 ppm/volt which is comparable to that of other overtone oscillators designed for considerable power output. There was some interaction between the tuning of the doubler and that of the crystal oscillator. Presumably this would be considerably reduced by the use of a pentode with its screen and suppressor at RF ground potential.

C. Electron-Coupled Impedance-Inverting Pierce Oscillator.

Figure 17.2 presents the impedance-inverting Pierce oscillator as modified for frequency multiplication. The screen of a 6AH6 tube is used as the equivalent oscillator plate, and power at harmonic frequencies is taken from the plate circuit of the tube.

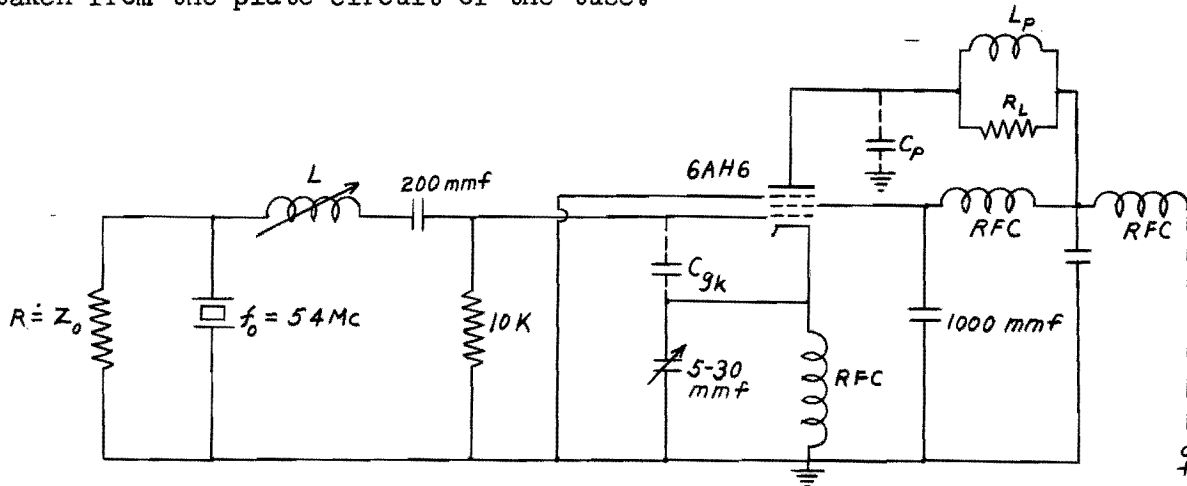


Figure 17.2 - Electron-Coupled Impedance Inverting Pierce Oscillator

The upper frequency limit of this circuit with available crystals was found to be near 70 Mc, and the experimental circuit was designed for operation at 54 Mc. The crystal used has a shunt capacity of 5 mmf and a series resistance of 20 ohms.

In order to minimize the effect of load variations on the frequency of oscillation, the circuit was constructed in the grounded-plate form. The screen of the tube (serving as oscillator plate) was at RF ground potential, and the cathode was isolated from ground by a choke coil. This arrangement has the advantage that one side of the impedance inverting network is grounded. Also, because of the shielding effect of the screen and suppressor, the effect of load tuning on the frequency of oscillation became negligible.

The capacity at the tube-end of the line is largely determined by the grid-to-cathode and cathode-to-ground capacities, and was found to be approximately equal to the crystal holder capacity. Adjustment to exact equality was obtained by means of a variable capacitor placed across the cathode choke. The characteristic impedance of the line (Z_0) is 590 ohms, and with the 20 ohm crystal a value of input resistance (R_x) equal to

approximately 17,000 ohms was obtained. This was found to be sufficiently large to give good class C operation.

The tuning procedure used corresponds to that used for the conventional Pierce oscillator. After the oscillator section was tuned, the plate coil (L_p) was changed to determine the output at several different orders of multiplication. As shown by Table 17.1, the available power fell off quite rapidly as the order of multiplication was increased.

The frequency stability was equal to that of the conventional impedance-inverting Pierce Oscillators and practically independent of tuning and load conditions in the multiplier circuit.

TABLE 17.1
POWER OUTPUT VERSUS ORDER OF MULTIPLICATION

Order	Frequency (Mc)	Power Output (mw)
f_o	54	400
$2f_o$	108	225
$3f_o$	162	50
$4f_o$	218	10

D. Electron-Coupled Grounded-Screen Oscillator.

Chapter XIII of this report presents a theoretical study and design procedure for the electron-coupled grounded-plate oscillator. These results may be made applicable to the circuit in Figure 17.3 by considering the screen of the tube to be the equivalent plate of the oscillator. The significant feature of this circuit is the effective isolation of the output circuit by virtue of the shielding action of the grounded screen and suppressor grids. Moreover, as in all grounded-screen arrangements, the total space current of the tube flows through the cathode circuit so that the full transconductance of the tube is available for the maintenance of oscillations.

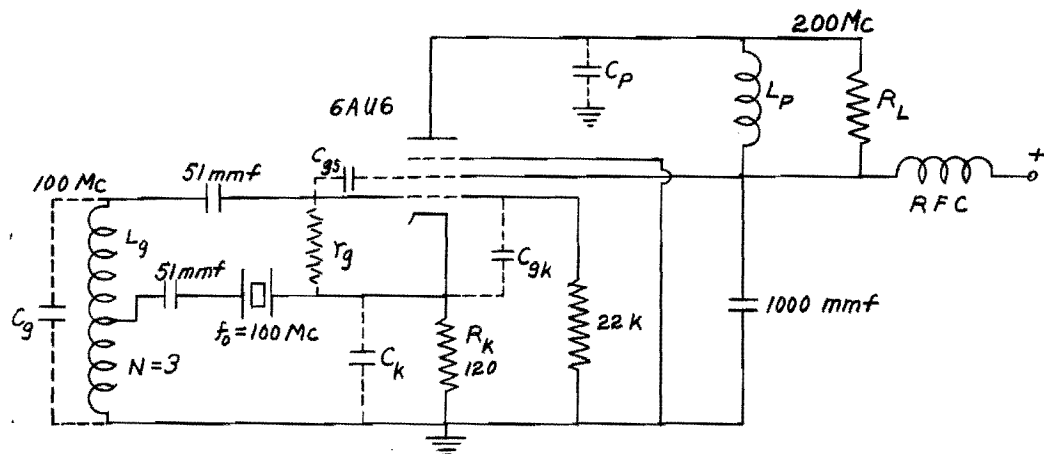


Figure 17.3 - Electron-Coupled Grounded-Screen Oscillator

An experimental circuit was constructed for operation at 100 Mc with crystals having a series resonant resistance of 100 ohms. The output circuit was tuned to the second harmonic (or 200 Mc), and L_g was antiresonated with the input capacity of the tube. This capacity (C_g) is given by

$$C_g = C_{gs} + \frac{C_{gk} C_k}{C_{gk} + C_k} \quad (17.1)$$

Where C_{gs} is the control grid-to-screen capacitance, C_{gk} is the control grid-to-cathode capacitance and C_k is the total cathode-to-ground capacitance.

Phase shift due to C_{gk} and C_k is eliminated when

$$C_{gk} r_g = C_k R_k \quad (17.2)$$

Where r_g is the dynamic grid-cathode resistance, and R_k is the effective cathode to ground resistance.

With the element values shown in Figure 17.3, the circuit operated with a frequency stability of 1.0 ppm/volt supply voltage variation, and gave about 20 milliwatts output power at 200 Mc. However, the circuit was difficult to adjust. In the belief that the low power output was due to the feedback being insufficient to produce good class C operating conditions, the circuit was redesigned.

A type 6AH6 pentode, and a 90.6 Mc crystal were used in the second experimental oscillator. The voltage ratio (N) of the grid transformer was increased to 8:1, and a cathode transformer having voltage ratio of two was

included. While these modifications resulted in good class C operation, and a power output of about 50 milliwatts at 181.2 Mc; the frequency stability was very poor, and the circuit would oscillate with the crystal removed from its socket. It is believed that this unsatisfactory operation was due to failure to realize proper compensation of grid-to-cathode phase shift. Unfortunately, both grid and cathode impedances vary with the amplitude of oscillation, so the problem of phase compensation is very difficult.

E. Conclusions.

The cathode-coupled oscillator as used for frequency multiplication is capable of supplying a moderate power output with good frequency stability. Moreover, the circuit is quite simple to design and adjust, and is particularly useful where requirements are modest and must be met with a minimum expenditure of effort.

The single tube electron-coupled circuits give excellent load isolation and good power output at fundamental frequencies, but the output at harmonic frequencies is low.

There are two factors which are largely responsible for the reduction of output with an increase in harmonic order. First, the grid driving power must be increased above the minimum value which yields good fundamental-frequency operation in order to reduce the angle of current flow. Second, I^2R losses in the tube increase rapidly with increasing frequency. The first factor is a fundamental limitation which is aggravated by transit-time loading as the fundamental frequency is increased. Since the fundamental frequencies of most of the circuits investigated were below 100 Mc, fairly good driving voltages were obtained. However, large values of grid leak resistances were needed to give the required conduction angles, and it was apparent that the grid was never greatly positive. This reduced the available peak plate current and considerably reduced the power output.

If a tube is to operate efficiently in a frequency-multiplying circuit, its plate load impedance must be somewhat greater than would be used with an ordinary class C amplifier. For third harmonic operation in a typical case the plate tank impedance should be about 2.5 times that for class C operation.¹ This impedance, to a first approximation, may be represented as in Figure

17.4, where C_p represents the output capacity of the tube and is antiresonant with L_p at the harmonic frequency.

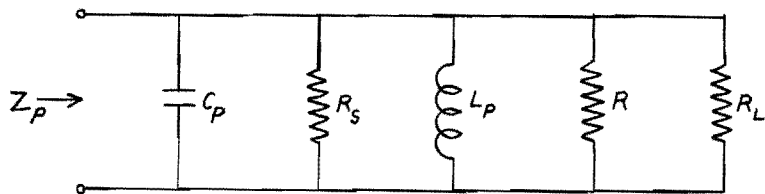


Figure 17.4 - Plate Impedance with Tube and Coil Losses

The resistances, R_s and R , represent respectively the equivalent losses of the tube and coil, while R_L is the useful load. If the tube is to perform efficiently, the parallel combination of all three of these must be a suitably high resistance; and for efficient transfer of power from the tank to load, the parallel combination of R_s and R must be much greater than R_L . In practice, neither of these requirements is readily met at frequencies above 150 Mc. The difficulty is due to the low reactance of the plate tank as well as the high coil and tube losses. Typical values of R_s are presented in Table 17.2. These were obtained from measurements made at 180 Mc on a high-frequency Q meter with the tube in its socket and shield.

TABLE 17.2
HIGH FREQUENCY RESISTANCE LOSS (180 Mc)

Tube	C_p (mmf)	R_s (ohms)
6AN5	4.5	50,000
6AH6	4.9	60,000
6AK5	5.0	100,000
5687	7.0	16,000
5763	--	Too low to measure

Of the tubes listed the 6AK5 has the lowest loss; however, its peak plate current is relatively low, and more power may be obtained from the 6AN5 or the 6AH6. When the 6AH6 is used with a coil having a Q of 250 at 180 Mc, the parallel combination of R_L and R is approximately equal to 26,000 ohms

which is about the correct value of plate impedance for good efficiency as a frequency tripler. Thus, it is clear that the addition of a shunt load having a value suitable for efficient transfer of power from the tank to the load will result in a plate impedance which is too low for efficient operation of the tube. Furthermore, reduction of the coil loss to zero and the use of a load resistance of 60,000 ohms results in a tank circuit efficiency of only 50 per cent. Although transmission line reactances having values of Q near 1000 are available in this frequency range, significant improvement in performance can be achieved only by the reduction of tube loss.

It is believed that most of this loss is due to the material used in the glass-to-metal seals in current miniature tubes. If this is true, the performance of these and other V.H.F. circuits could be greatly improved by redesign of miniature tubes, particularly if this redesign made provision for more efficient connection to coaxial structures.

XVIII COMPONENTS AND ADJUSTMENT PROCEDURES

A. Components.

1. Vacuum Tubes.

Except for the high resistance losses (Chapter XVII) encountered at frequencies in excess of 150 Mc, currently available miniature vacuum tubes adequately met the needs of this project. Ordinary miniature tubes are small enough for most applications; and in typical cases the thermal radiation from the tube is small enough to permit a compact arrangement without overheating the crystal or other components. However, a notable exception is the type 5687 dual-triode. When operated at rated input, the envelope temperature of this tube is near 200° centigrade, and the crystal must be isolated to avoid overheating.

While high transconductance tubes are preferred in the interest of frequency stability and broad-band operation, experiments with filamentary type tubes (3A5) and with high transconductance tubes in class C operation indicate that satisfactory operation may be obtained with transconductances as low as 1000 micromhos.

The tubes most frequently used on this project are the type 6AK5 pentode and the type 6J4 triode. The former has given excellent results in the transformer-coupled oscillator while the latter performs well in the grounded-grid and impedance-inverting circuits. For higher output power the type 6AH6 pentode may be used in any of these circuits.

2. Resistors.

Measurement of the high-frequency impedance characteristics of commercially available composition resistors has shown that, for low values of resistance, the conductance tends to remain constant with frequency. The total impedance, however, is reduced by the decreasing reactance of the shunt capacity. The value of this capacity was found to be between 0.4 and 0.5 mmf for the Allen Bradley type EB-0.5 and I.R.C. type BTS resistors, and is equivalent to a shunt reactance of approximately 3200 ohms at 100 Mc. Most of the circuits considered in this report may be loaded at a low impedance point with resistance of about 100 ohms, thereby making the effect of

this shunt reactance negligible.

In cases where higher values of resistance were required, as for terminating impedance-inverting lines, use was made of Globar type 997A resistors. These components have a shunt capacity of approximately 0.2 mmf, or an equivalent shunt reactance of approximately 8000 ohms at 100 Mc. While their power rating is low (0.2 watt), these resistors have good recovery-from-overload characteristics and require a minimum amount of space.

3. Capacitors.

In most of the circuits described in this report the tube and stray capacities alone constitute the total capacity tuned by the high side inductance of the impedance-transforming networks. While one has little control over the characteristics of these capacitances, good frequency stability may be obtained by the use of suitably low impedance levels. However, other tuned circuits are present which affect the stability even though the crystal is the major source of control; and maximum stability with respect to temperature and time will be obtained only if suitable components are used.

For fixed capacitance, particularly in high impedance circuits, silvered-mica capacitors are desirable because of their low temperature coefficient and good secular stability. These units are constructed by vacuum evaporating silver on high grade sheets of ruby mica. The leads are attached to exposed plated areas, and the assembly packaged in a high-grade thermosetting plastic. Since the electrodes are attached directly to the mica, the secular stability is determined by the mica alone.

Silvered-mica capacitors are available in the value range of 5 to 5000 mmf, and have a temperature coefficient of approximately +20 ppm per degree centigrade in the range of -60° to +80° C. These units, particularly in the higher capacity range, are physically large, and a more compact layout may be obtained by using ceramic capacitors.

In general ceramic bodies have good secular stability and are not greatly affected by temperature, humidity, etc. However, the dielectric behavior of these materials is complicated and discrimination must be used in choosing a ceramic capacitor.

Ceramic materials which include compounds of titanium have two outstanding

properties namely, high dielectric constants and negative temperature coefficients. The first leads to small physical size with low residual inductance, and the second is useful in partially compensating for the positive temperature coefficient of the usual inductor. Capacitors made of these materials may be obtained in a range of values from 1 to 10,000 mmf, and are well suited for use in high-frequency oscillators. The electrodes for these units are produced by painting with a metallic suspension and firing to a temperature which fuses the metal. Leads are attached by soldering to the metallic electrodes. Insulation is provided by a low-loss phenolic coating, and impregnation with a high-melting-point wax gives further protection against humidity. These components are also available in a non-insulated form, having a protective coating of baked enamel.

Ceramic body materials are classified, by trade designation, in three groups. Group A, which is based on titanium dioxide, has temperature coefficients ranging from +100 ppm/ C° through zero to -750 ppm/ C° , power factors between 0.02 and 0.05 per cent, and dielectric constants from 12 to 85. Group B, which is also based on titanium dioxide, provides larger dielectric constants and temperature coefficients, but inferior values of stability and power factor. Materials in this group are useful where a large temperature coefficient is required in small capacity values. The materials in Group C are based on barium titanate and have dielectric constants in excess of 1000. The dielectric constant is, however, nonlinear with respect to voltage. Capacitors made from these materials behave in a complicated manner with respect to voltage and frequency and are suitable only for bypass applications. However, the large capacitance which may be secured in a compact low-inductance structure makes these materials attractive for this application.

4. Chokes.

The use of low-impedance circuits and series-feed arrangements considerably reduces the requirements on radio frequency chokes, and the needs of this project were adequately met by simple single-layer solenoids wound on insulated forms. Because of the relatively high operating frequencies, suitably large values of reactance were obtained in physically small configurations without the use of magnetic core materials. Typical chokes

were constructed by winding plain enamel wire on insulated composition resistor bodies, using the resistor leads as terminals. In this arrangement the resistor shunts the choke, but by choosing a relatively large value of resistance, the terminal impedance becomes simply the reactance of the choke. However, the shunt capacity of the resistor is in parallel with that of the choke, and the dielectric losses of some resistor bodies become appreciable at frequencies near 100 Mc. While satisfactory results were obtained with chokes constructed in this manner, better and more uniform results were obtained by using commercially available components such as the IRC type CLA and CL-1 insulated chokes. These are available in values ranging from 0.47 to 10.0 microhenrys, and have self resonant frequencies ranging from 300 Mc for the lowest value to 65 Mc for the highest. These components are physically small, and have adequate current ratings for the present application.

5. Crystals.

The crystals used on this project were the type CR-23/U and CR-19/U units supplied by the Signal Corps, and similar units supplied by various manufacturers. These are metal-plated, wire-mounted units designed for series-resonant operation. The type CR-23/U units are designed for operation on the third or fifth mechanical overtone in the frequency range from 10 to 75 Mc, and the type CR-19/U units operate at fundamental frequencies in the 1.0 to 20 Mc range. It was found expedient to operate these crystals at overtones higher than the design values, but this practice is not recommended for other than experimental purposes.

The mechanical characteristics of these units are good, and the space requirements are small. It is of interest to note that of approximately one hundred crystals used on this project, only one suffered mechanical failure.

Allowable values of crystal dissipation for use in circuit design were obtained from studies of the operating characteristics of a relatively small number of crystal units. It was concluded that if the power dissipated by the crystal is near 0.1 watt the frequency stability is seriously degraded, and that values of 0.05 watt can be used only if a reduction in frequency stability may be tolerated in the interest of power output. In oscillators designed for high stability or broad band operation, the crystal dissipation

was commonly near 0.01 watt. Information recently published by the Bliley Electric Company (Bulletin 42) indicates that, for maximum stability and freedom from the effects of spurious responses, the dissipation of high frequency overtone crystals should be limited to approximately 1.5 milliwatts. Since the design procedures described in this report utilize the ratio of load to crystal dissipation, limitation of the allowable crystal dissipation merely increases the emphasis on circuits capable of providing a high power ratio.

B. Transformers.

1. Physical Configuration.

In oscillators which employ conventional vacuum tubes it is necessary to provide appropriate impedance transformations between the input, output, and crystal circuits. Moreover, it is necessary to provide a phase reversal between the input and output circuits when a grounded-cathode amplifier is used. While there are a number of ways of meeting these requirements, the simple transformer of Figure 18.1 is most generally useful.

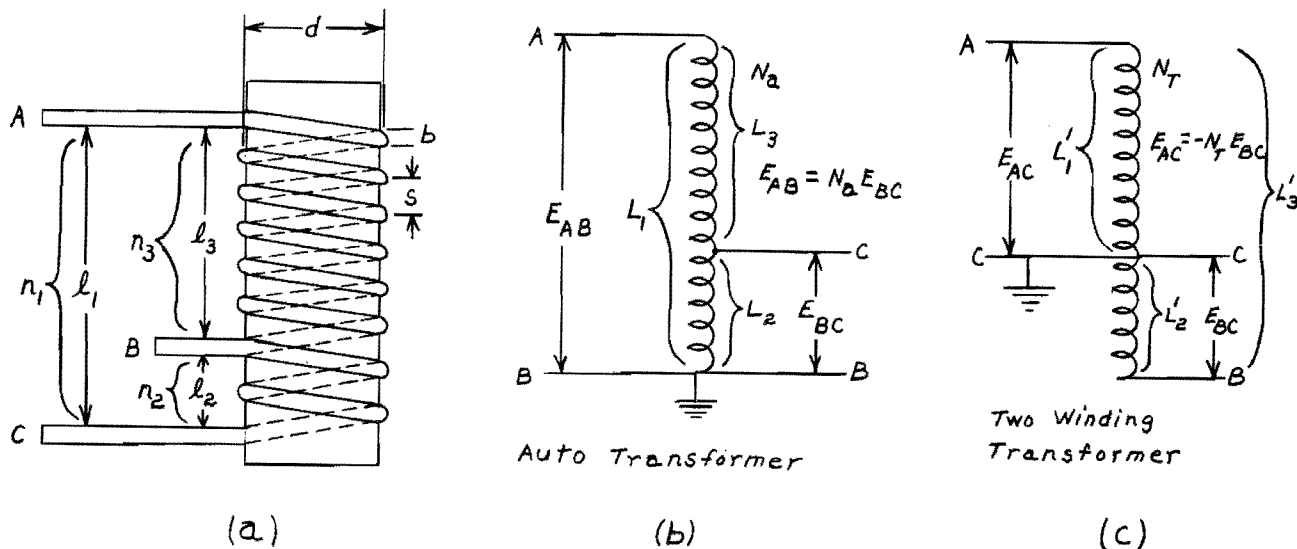


Figure 18.1 - Transformer Configurations

This transformer has the configuration of a tapped continuous single-layer solenoid, closely-wound and connected, as shown in Figures 18.1b and 18.1c, to provide either a zero or 180° phase relation between the input and output

voltages. While the same basic equations apply for either connection, a higher coefficient of coupling may be obtained with the autotransformer arrangement.

In addition to the impedance and phase requirements, the high side inductance of the transformer must be antiresonant at the operating frequency with the capacity comprising tube and wiring strays. The adjustment of this inductance is facilitated by the use of slug tuned coil forms.

The response of transformers and the limitations imposed by parasitic capacitance and leakage inductance has been discussed in Chapter VIII. It is the purpose of the following paragraphs to describe methods of designing transformers to give a specified impedance ratio and to discuss attendant parasitic effects.

2. Distributed Capacitance.

The distributed capacitance in mmf of a single layer solenoid is given by^{1,2}

$$C_d = \frac{\pi d}{3.6 \cosh^{-1}(s/b)}, \text{ (mmf)} \quad (18.1)$$

where

d = winding diameter,

b = wire diameter,

and

s = center to center spacing of turns, all in cm .

The value of this capacitance is of interest because it appears across the high-side terminals of the transformers in Figure 18.1, thereby contributing to the magnitude of the input and output capacitances of the amplifier and reducing the available bandwidth of untuned operation. Moreover, the presence of this capacitance often leads to an error in measuring the inductance of the coil. In typical cases the measured equivalent inductance differs from the actual inductance in the following manner¹:

$$\frac{L(\text{equivalent})}{L(\text{actual})} = \frac{1}{1 + (\omega/\omega_0)^2}, \quad (18.2)$$

where ω_0 is the self-resonant frequency of the solenoid.

Q meter measurements of inductance are often used as a guide in "cut and try" design procedures. It should be noted that this instrument measures the equivalent inductance as given by equation 18.2. Therefore, the Q meter may be used without correction to adjust inductances to antiresonate the tube and wiring capacities. However, if the winding dimensions are computed from any of the standard inductance formulas³, the design value of inductance is the actual value, and it must antiresonate a capacity equal to the sum of the distributed capacity and the tube and wiring strays.

Reasonably good correlation between measured⁴ and computed values of distributed capacity has been obtained, and values ranging from 0.8 to 1.5 mmf were found to be typical of transformers used on this project. Since the tube and wiring strays are typically near 5 mmf, the distributed capacity of the transformer becomes a significant factor in determining the bandwidth of untuned operation. As shown by equation 18.1, the distributed capacity may be reduced only by decreasing d or by increasing the ratio s/b . These steps, however, lead to a reduction in the coefficient of coupling with an attendant reduction in bandwidth. Therefore, it appears that an optimum configuration exists, but because of the limited advantage to be gained the question has not been pursued.

3. Coefficient of Coupling.

The coefficient of coupling of a two-winding transformer is most conveniently determined from the effect of short-circuiting one of the windings. That this method is valid may be shown by means of Figure 18.1c. As shown, the high side inductance with the low side open is simply L_1' . When L_2' is short-circuited, the inductance seen at the high side becomes $L_1' - M^2/L_2'$ as is readily shown by coupled circuit theory. The ratio of these inductances is

$$1 - M^2/L_1'L_2' = 1 - k^2 , \quad (18.3)$$

or

$$k^2 = 1 - L_{ls}'/L_1' , \quad (18.4)$$

where

k = coefficient of coupling between the transformer windings,

L_1' = high side inductance,

L_{1s}' = high side inductance with the low side shorted.

In a similar manner the coefficient of coupling of the autotransformer in Figure 18.1b may be shown to be

$$k^2 = 1 - L_{1s}/L_1 \quad (18.5)$$

where

L_{1s} = high side inductance with low side shorted,

L_1 = high side inductance with low side open.

That this equation should have the same form as equation 18.4 is evident from the fact that the two-winding transformer and the autotransformer have the same equivalent circuit provided the mutual inductance of the autotransformer is recognized as being

$$M_a = L_2 + M_{23} \quad (18.6)$$

where M_{23} is the mutual inductance between L_2 and L_3 in Figure 18.1b.

The inductances in the foregoing expressions may be accurately measured on a Q meter, provided the measurement frequency is well below the self-resonant frequency of the windings.

The coefficient of coupling of an autotransformer consisting of a tapped, uniform, single-layer winding may be calculated with reference to Figure 18.1b in the following manner:

$$L_1 = L_2 + L_3 + 2M_{23} \quad (18.7)$$

or

$$M_{23} = \frac{L_1 - (L_2 + L_3)}{2} \quad (18.8)$$

For a given transformer the values of L_1 , L_2 , L_3 and M_{23} may be calculated from the dimensions. Then:

$$k^2 = \frac{M_a^2}{L_1 L_2} = \frac{(L_2 + M_{23})^2}{L_1 L_2} \quad (18.9)$$

TABLE 18.1
CALCULATED AND MEASURED COEFFICIENTS OF COUPLING

Type Transformer	P.E. Wire Size	d (inch)	n_1	n_2	ℓ_1 (inch)	ℓ_2 (inch)	ℓ_3 (inch)	Calculated κ	Measured κ	Frequency of Measurement Mc
Autotransformer	22	1.525	12	4	0.346	0.115	0.231	0.74	0.73	9.0
Autotransformer	16	3.057	15	5	0.844	0.281	0.562	0.85	0.84	4.0
Autotransformer	24	0.375	9	3	0.188	0.0625	0.125	0.77	0.79	43.0
Autotransformer	30	0.387	15	3	0.156	0.052	0.104	0.67	0.70	45.0
Autotransformer	30	0.214	9 (n_3)	3 (n_2)	0.094	0.0312	0.0625	0.78	0.77	36.0
Two-Winding	22	1.525	12	4	0.462	0.115	0.346	0.51	0.58	9.0

The coefficient of coupling for a two-winding transformer may be calculated in a similar manner.

The above formulas have been used to calculate the coupling coefficients of several transformers. The results, together with measured coefficients of coupling are presented in Table 18.1. The symbols used in this table are defined by Figure 18.1.

4. Design for Specified Impedance Ratio.

In the design of oscillators using series-resonant crystals, four-terminal networks are necessary to provide suitable impedance levels at the crystal terminals. In addition, these networks should produce no phase angle at the operating frequency other than a polarity reversal where required. One method of designing this type of network⁵ starts with a half-section prototype filter and results in a network of the type shown in Figure 18.2.

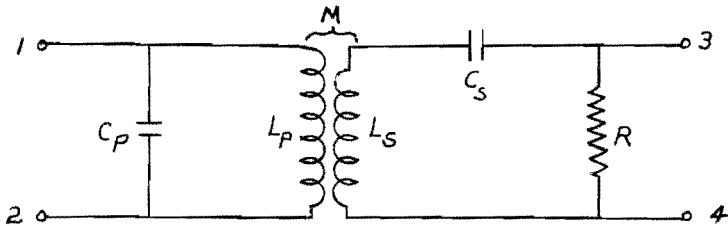


Figure 18.2 - Impedance Transforming Network
Using a Physical Transformer

In this network

$$\omega_0^2 = 1/L_p C_p = 1/(1 - k^2)L_s C_s , \quad (18.10)$$

where $(1 - k^2)L_s$ is the inductance seen between the secondary terminals with the primary terminals shorted. The impedance seen at terminals 1 and 2 is, at ω_0 , equal to $N^2 R$ where

$$N^2 = k^2 L_p / L_s , \quad (18.11)$$

and

$$k^2 = M^2 / L_p L_s . \quad (18.12)$$

To complete the design of the network it is necessary to determine the dimensions of the transformer used in Figure 18.2.

Another and somewhat simpler method of obtaining the final design of a network of this type is outlined in the following paragraphs. This method depends upon the use of a particular type of winding for the transformer and upon the determination of the relation between the impedance transforming ratio and numerical turns ratio for transformers of this type. Because of its high coefficient of coupling and relatively low distributed capacity the configuration shown in Figure 18.1a was chosen.

The equivalent circuit of Figure 18.1c is shown in Figure 18.3. With the winding directions and connections as shown in Figure 18.1a and c, there is a polarity reversal between the input and output terminals; this transformer is therefore suited for use in the transformer-coupled oscillator where such a polarity reversal is required.

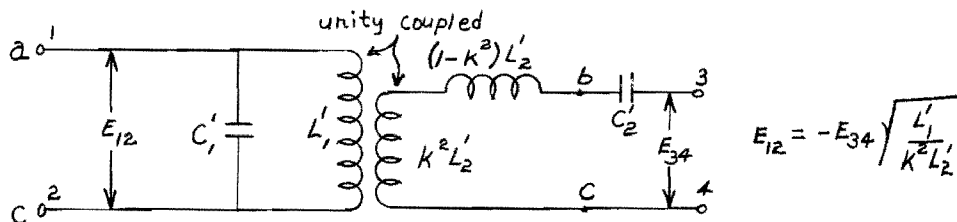


Figure 18.3 - Equivalent Circuit of Figure 18.1c

The capacitor C_2' is selected to resonate $(1 - k^2)L_2'$ at ω_0 ; therefore, the impedance transformation between the high side and low side terminals at this frequency is given by

$$N_t^2 = L_1'/k^2 L_2' . \quad (18.13)$$

The values of L_1' , L_2' and L_3' are given by the following expressions based on the well known Nagaoka formula:

$$L_1' = F_3 N_3^2 d , \quad (18.14)$$

$$L_2' = F_2 N_2^2 d , \quad (18.15)$$

$$L_3' = F_1 N_1^2 d . \quad (18.16)$$

F_1 , F_2 and F_3 are functions of the respective diameter-to-length ratios and are tabulated in reference (4). The number of turns in the high and low

side windings are, respectively, n_3 and n_2 while $n_t = n_3 + n_2$. The numerical turns ratio is defined as $n_t = n_3/n_2$.

Substituting the values of L_1' and L_2' as given by equations 18.14 and 18.15 in equation 18.13 yields the following result:

$$N_t^2 = (n_t/k)^2 F_3^2 / F_2^2 , \quad (18.17)$$

in which the coefficient of coupling k is defined by

$$k^2 = M_{12}^2 / L_1' L_2' . \quad (18.18)$$

Also

$$L_3' = L_1' + L_2' + 2M_{12} \quad (18.19)$$

or

$$M_{12} = \frac{L_3' - (L_1' + L_2')}{2} , \quad (18.20)$$

which by substitution in (18.18) gives

$$k = \frac{L_3' - (L_1' + L_2')}{2\sqrt{L_1' L_2'}} . \quad (18.21)$$

Substitution from (18.14), (18.15) and (18.16) yields

$$k = \frac{F_1 n_1^2 - (F_3 n_3^2 + F_2 n_2^2)}{2n_2 n_3 \sqrt{F_2 F_3}} . \quad (18.22)$$

From equations 18.17 and 18.22

$$N_t = n_t \frac{2n_2 n_3 F_3}{F_1 n_1^2 - (F_3 n_3^2 + F_2 n_2^2)} . \quad (18.23)$$

Since $n_3 = n_t n_2$ and $n_1 = n_2(n_t + 1)$

$$N_t = \frac{2F_2}{F_1(n_t + 1)^2 - F_3 n_t^2 - F_2} . \quad (18.24)$$

The ratio of the diameter to length for L_2' and L_3' may be determined from the value of n_t and the diameter-to-length ratio of L_1' . Therefore, the above

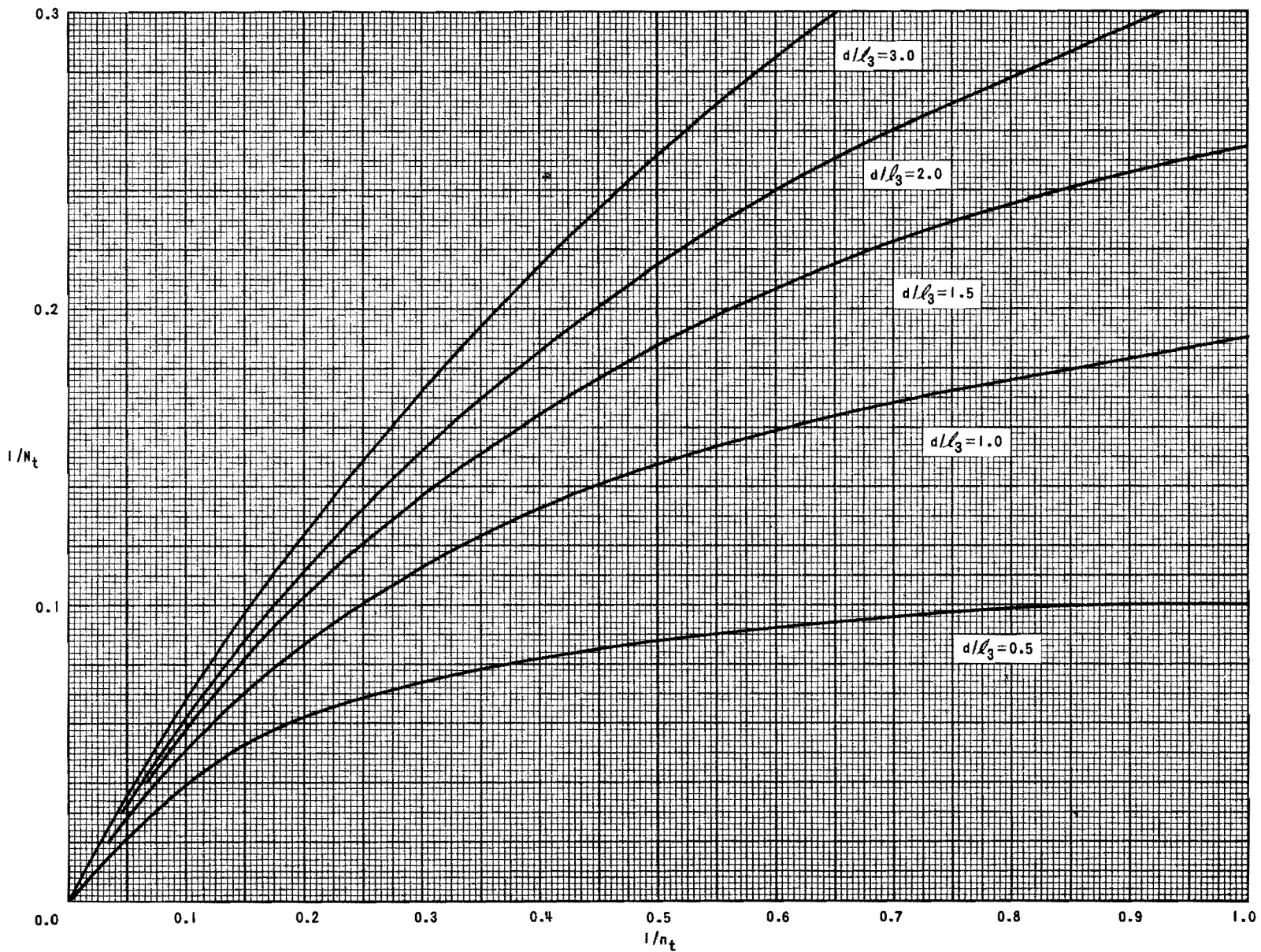


Figure 18.4 Characteristics of a Single Layer Solenoid as a Two-Winding Transformer.

expression may be used to plot the relation between N_t and n_t for several values of d/λ_3 . This plot is given in Figure 18.4 and permits the construction of the desired transformer from a knowledge of the shape of the high side inductance (L_1').

The design procedure may be summarized as follows: The value of L_1' is determined from the requirement that it antiresonate C_1' at the operating frequency and a coil is designed to give this value of inductance; moderate to large values of d/λ_1 are desirable in the interest of obtaining a large coefficient of coupling. Next, from the required value of N_t , Figure 18.4, the value of n_t is obtained, thus determining the number of turns to be added as L_2' . Now that the dimensions of the transformer are known, the values of k and L_2' may be found, thus permitting the computation of C_2' . Alternatively, the required value of C_2' may be obtained experimentally by shorting the high side of the transformer and adjusting a capacitor placed across the low side to give resonance as indicated by a grid-dip meter.

An analysis similar to the foregoing may be applied to the autotransformer (Figure 18.1b) to obtain the relation between its impedance and turns ratio. The result is

$$N_a = \frac{2n_a^2 F_{a1}^2}{n_a^2 F_{a1}^2 + F_2^2 - F_3(n_a - 1)^2}, \quad (18.25)$$

where n_a is equal to n_1/n_2 . The other quantities are as previously defined. This relation is plotted in Figure 18.5. It should be noted that N_a and n_a are never greatly different, and that they approach equality for both small and large values of d/λ_1 .

In designing an autotransformer the value of L_1 is obtained from the requirement that it antiresonate C_1 at the operating frequency. A coil is then designed to give the required inductance, and the location of the tap is determined from Figure 18.5. The value of capacitor (C_2) required to resonate the leakage inductance may be determined as for the two winding transformer.

5. Parasitic Losses and Difficulties.

In the design of inductors or transformers for use at high frequencies

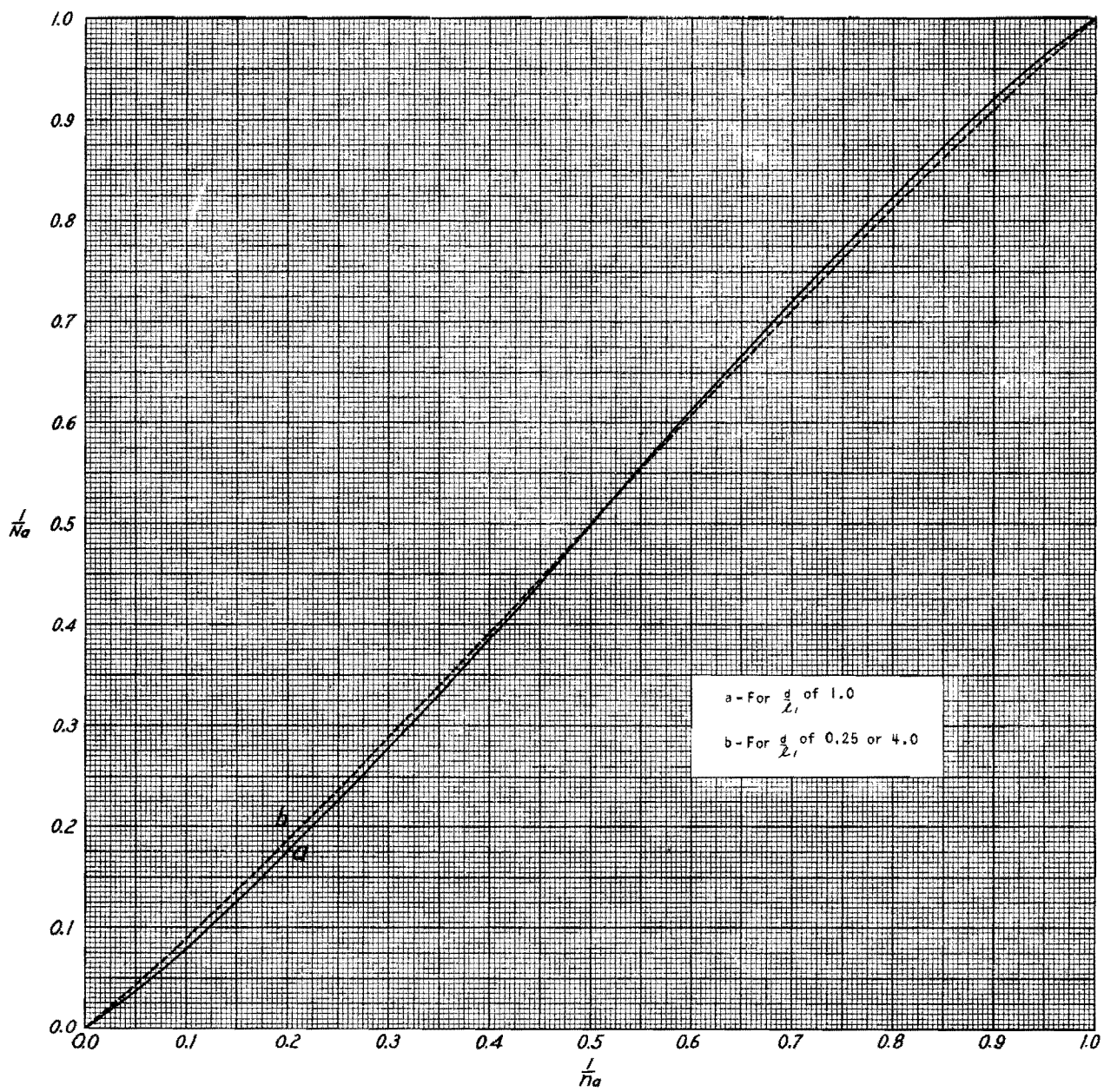


Figure 18.5 Characteristics of a Single Layer Solenoid as an Autotransformer.

particular attention should be given to minimizing parasitic losses. The coil forms selected should have low dielectric losses along with good dimensional stability, and the coil windings should be secured to the coil in such a manner that the stability of the inductance approaches that of the coil form. This end is most elegantly achieved by plating the windings directly on a highly stable form. Because the interests of this project were confined to the causes of "short term" frequency variations, no attempt was made to design highly stable inductors. Simple single-layer solenoids of P.E. wire wound on ceramic forms were found to be quite satisfactory. Extensive use was made of the Cambridge Thermionic Corporation types LS-5, LS-6, and LS-T slug-tuned forms equipped with high frequency slugs. These were found to be adequate for most purposes.

The design procedures for obtaining a specified impedance ratio are based on the assumption that the core of the transformer has a uniform permeability. Such is not the case when a powdered iron slug is used for incremental tuning. However, by positioning the slug so that it affects only the inductance of the end turns of the winding, tuning may be accomplished without seriously altering the impedance ratio of the transformer.

The high-frequency slugs used in the aforementioned coil forms have performed satisfactorily in the frequency range of interest when used in low impedance circuits. However, excessive slug heating was observed in oscillators where the impedance levels and power output were high. More efficient operation was obtained by removing the slugs and tuning with a small variable ceramic capacitor.

Transformers for use at frequencies above 100 Mc must be physically small, the number of turns in the primary winding is low, and it is difficult to obtain large impedance ratios with the autotransformer configuration. However, suitably large impedance ratios may be obtained by using the two-winding transformer. Due to the shortness of the transformer winding the terminals are in close proximity, and if the usual terminal clips are used, the distributed capacity of the winding will be considerably increased. It has been found expedient to dispense with the terminal clips and to use coil dope to hold the windings in place. While the resulting assembly is not

mechanically strong, it is satisfactory for experimental purposes.

C. Layout.

Components which are suitable for use in high frequency oscillators are inherently small, and it is probable that the ultimate compactness of a given circuit is limited by undesirable parasitic couplings and thermal radiation. It is particularly important to avoid overheating the crystal; because short leads are desirable, this is difficult to accomplish when tubes are operated with high bulb temperatures.

Because of the moderate to low impedance levels encountered in series-mode oscillators, little trouble is caused by coupling due to stray capacity provided the tube is well shielded. However, care must be exercised to avoid stray magnetic coupling. At frequencies near 50 Mc the transformers may be separated sufficiently to avoid excessive coupling; above 100 Mc, however, the requirements on lead lengths are so severe that close spacings must be used. Here one must depend on correct orientation of the transformers to minimize undesired coupling.

Troubles which are often experienced from RF currents in ground leads may be minimized by the use of a single-point ground. Good results have been obtained by using the center part of the miniature tube sockets for this purpose.

D. Adjustment Procedures.

Because of manufacturing variations and the approximate nature of most design procedures, some final adjustments must be made to insure proper circuit performance.

In some parallel-mode oscillators final adjustment may be accomplished by varying a single element, the requirements on the other elements being either lenient or compensated for by this adjustment. When this is true, the procedure is simple and the values of tube currents may be used as an indication of correct tuning. Most series-mode oscillators, however, require at least two tuning adjustments; and the transformer-coupled oscillator with a compensated crystal requires five. Because the tube currents are a function of the tuning of all these elements a more complex procedure is required.

In the early stages of this project approximate tuning was accomplished

by adjusting critical elements to the design values prior to their assembly in the circuit. A high frequency Q meter was used for this purpose. Because the circuit environment of the element differs from that in which it was measured, this method was not highly successful, and procedures based on the use of a grid-dip meter were developed. These procedures have been used with good success, and are best described with reference to specific circuits. Both the Millen Type 90661 Grid-Dip Meter, and Measurements Corporation Model 59 Megacycle Meter have been used, the latter being preferred because of its greater frequency range and sensitivity.

1. Simple Antiresonance.

The network used in the output circuit of electron coupled oscillators, in the plate circuit of the cathode-coupled oscillator, and for compensating the crystal holder capacity may be represented as in Figure 18.6.

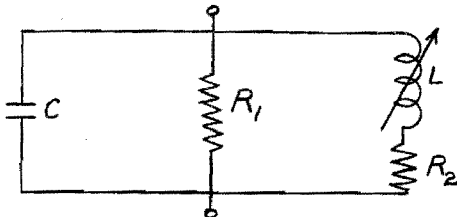


Figure 18.6 - Antiresonant Network

In this figure, R_1 represents the load or damping resistance and R_2 represents the coil losses.

It is desired to adjust the circuit to antiresonance at some specified frequency. This may be accomplished by adjusting the grid dip meter to the specified frequency (ω_0), coupling its output to L , and adjusting the value of L to obtain the meter dip which indicates resonance. Then

$$\omega_0 L = 1/\omega_0 C , \quad (18.26)$$

and if R_2 is small the difference between this condition and true antiresonance is negligible. If the value of R_1 is low, the circuit Q may be insufficient to give a sharp indication of resonance. In this case R_1 must be removed and the adjustments made with the circuit undamped. This results in little error provided the shunt capacity of R_1 is small compared to C .

When this network is used for crystal compensation, the crystal must be

replaced by a capacitor equal to the holder capacitance. This is necessary because of the crystal's low resistance near ω_0 as well as its rapidly varying reactance characteristic in this region. Specifically, the grid-dip meter locks to the crystal frequency, and no useful indication is obtained.

2. Impedance-Inverting Networks.

The properties of the network in Figure 18.7 have been discussed in Chapter II and examples of its use in oscillator circuits were presented in Chapter XIII. In its simplest form the network corresponds to the equations

$$\omega_0 L = 1/\omega_0 C_0 = 1/\omega_0 C_n, \quad (18.27)$$

and is equivalent to a lumped-constant quarter-wave line.

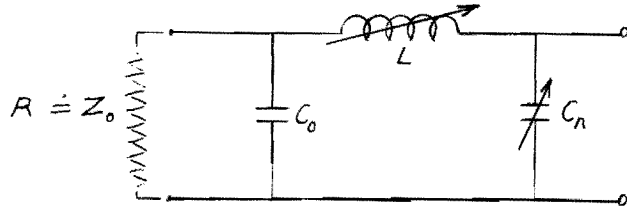


Figure 18.7 - Impedance Inverting Network

The correct value of L may be obtained by removing the damping resistor and crystal, replacing the crystal with a capacitor equal to the holder capacity, short circuiting C_n and adjusting L to obtain resonance as indicated by the grid dip meter.

The adjustment is completed by obtaining the correct value of C_n . In the Pierce circuit, C_n is varied by adjusting a variable capacitor connected from plate to ground, in the Miller circuit, the plate inductance is varied, while in the impedance inverting transitron the capacity from screen to ground is varied. In all of these circuits the correct value of C_n may be obtained by removing the plate and filament voltages, short-circuiting the crystal socket and adjusting the variable element to obtain resonance as indicated by a grid-dip meter.

In the event that the network has a configuration other than that of the quarter-wave line, i.e. $\omega_0 L \neq 1/\omega_0 C_0 \neq 1/\omega_0 C_n$, appropriate resonant frequencies may be computed and the adjustments made at these frequencies.

3. Transformer Networks.

In order to obtain the correct transfer phase and impedance ratio, two adjustments must be performed on each transformer in the circuit. The high-side inductance must be adjusted to antiresonate its shunt capacity, and the total leakage inductance must be resonated with the low-side series capacity.

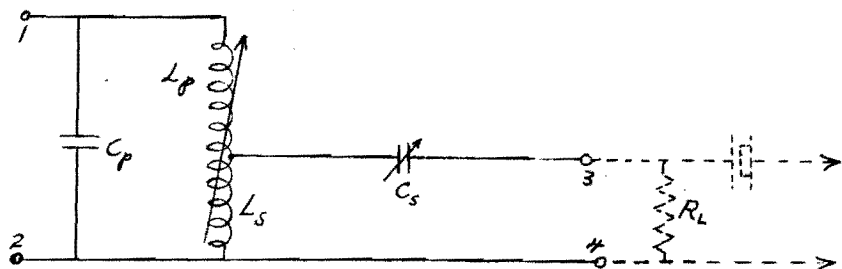


Figure 18.8 - Transformer Network

To obtain these adjustments the low-side terminals of the transformer (3,4) are open-circuited and L_p is adjusted to antiresonate C_p at the crystal frequency. Then with both high- and low-side terminals shorted, C_s is adjusted to resonance. Under these conditions, C_s is resonant with an inductance equal to $(1 - k^2)L_s$. Because the position of the tuning slug affects the coefficient of coupling, these adjustments must be performed in the foregoing order.

At high frequencies the inductance of the transformer leads may be appreciable when compared to the total inductance L_p ; therefore, the short-circuits used in making these adjustments should be applied at the ends of the leads. Moreover, excessively large leakage inductance due to long leads will result in impedance ratios that differ greatly from those computed by the methods described in paragraph B of this chapter.

BIBLIOGRAPHY

- (1) Massaut, P. H., "Distributed Capacitance Chart," *Electronics*, March, (1938).
- (2) Palermo, A. J., Proc. I.R.E., Vol. 22, July (1934).
- (3) Grover, F. W., Inductance Calculations. D. Van Nostrand and Co., Inc., New York, 1947.

Final Report Project No. 131-45

- (4) Brown, H. A., Radio-Frequency Electrical Measurements. McGraw-Hill Book Co., Inc., New York, 1938.
- (5) Shea, T. E., Transmission Networks and Wave Filters. D. Van Nostrand and Co., Inc., New York, 1929, pp 325 ff.
- (6) Rosa, E. B. and Grover, F. W., "Bureau of Standards Bulletin," 8, p 119, (1912).

XIX CONCLUSIONS AND RECOMMENDATIONS

A. Summary of Results Achieved.

The principal accomplishments of this project may be listed as follows:

1. Design from fundamental considerations of circuits which operate on an untuned basis over wide frequency bands.
2. Development of a new and useful criterion of frequency stability in feedback oscillators (the $R_L D$ product).
3. Development of new and useful relationships expressing the ratio of output power to power dissipated in the resonator.
4. Demonstration that many circuits differing considerably in configuration are subject to the same fundamental limitations and are capable of equivalent performance.
5. Demonstration of certain basic differences of performance in different circuits.
6. Development of useful criteria for the selection of particular circuits to meet specified performance requirements.
7. Presentation of new and useful methods of adjusting oscillator circuits to operate in accordance with design calculations.
8. Demonstration that oscillators may be made to operate in close conformity with calculated designs.

B. State of the Art.

It is now possible to obtain reasonable values of frequency stability and power output in crystal-controlled oscillators up to frequencies of about 150 Mc. However, the last octave of this range presents considerable difficulty, and there is much room for improvement. For both the crystal and associated circuits, the limit of present techniques appears to occur near 150 Mc.

The basic difficulty with the crystal is one of mechanical precision. Whether a low overtone of a very thin crystal or a high overtone of a thicker plate is employed, the mechanical requirements on surface flatness and parallelism are comparable and very severe. Moreover, the problems of applying suitable electrodes and of adjusting to frequency are both difficult.

Circuits are limited by parasitic inductances and capacitances, and by the fact that electron transit-time introduces phase shift, reduces gain, and lowers the input impedance of available tubes. Although disk-seal triodes in

suitable cavities will oscillate at frequencies up to about 3000 Mc, it is difficult to obtain oscillation at frequencies above 500 Mc with conventional miniature tubes. Because the loop phase and gain of the circuits in a crystal oscillator must be rather accurately controlled if good performance is to be obtained, the practical frequency limit is about 150 Mc, as previously stated.

Another intrinsic limitation of the circuits should be mentioned. In all circuits the element values which yield maximum frequency stability lead to a low ratio of output to crystal power, and therefore to a low available power output. However, in the transformer-coupled oscillator and in some other oscillators, the elements may be readjusted in such a way that a considerable power output can be obtained with only a moderate degradation of the frequency stability.

Several circuits, notably the grounded-grid and the transformer-coupled, are capable of untuned operation with good frequency stability and moderate power output over a frequency band at least 15 Mc wide. That is, any frequency in the design range may be obtained merely by plugging-in a suitable crystal, without any other adjustment.

No complete investigation of the secular stability of circuits or crystal was made. However, it was found in typical circuits that replacement of the vacuum tube, or a 10 per cent change in the supply voltages produced a frequency change of only a few parts in a million. These facts support the conclusion that the frequency deviations which may be charged to aging or drift of components other than the tube and crystal are negligible. The secular stability of thin overtone crystals is probably substantially inferior to that of thicker crystals, whether operated in the fundamental or overtone mode. This difficult problem was not pursued further because it was beyond the scope of this project.

C. Preferred Circuits and Their Properties.

A great variety of oscillator circuits (including some originated on this project) have been analyzed and tested during the course of this work. Consistent with the experience of other workers in the oscillator field, the performance of the various circuits was found to be much more similar than one might anticipate from the variety of circuit arrangements. However,

several important differences in performance and convenience do exist. This section summarizes the characteristics of some of the more important oscillator circuits.

1. The Cathode-Coupled Oscillator.

The cathode-coupled oscillator, which requires two triodes for its operation, has as its principal advantages simplicity and reasonably good frequency stability. However, the power output is relatively low, the bandwidth of untuned operation is only moderate, and this oscillator requires two triodes having relatively high transconductance. With suitable precautions, output at a harmonic of the operating frequency may be obtained from a suitable tuned circuit; however, one of the triodes must be replaced with a pentode if the full advantages of electron coupling are to be realized. The arrangement has features in common with both the grounded-grid and grounded-plate single-tube oscillators. One may think of the added tube as replacing the transformer in one of the latter circuits. Only in rather exceptional circumstances is the use of the extra tube justifiable in operating equipment.

2. The Transformer-Coupled Oscillator.

This arrangement employs a grounded-cathode pentode with physical input and output transformers to produce the required phase reversal and impedance transformations. Because the impedance levels and phase characteristics of this circuit may be controlled with considerable ease, the arrangement is very flexible in application. A properly adjusted transformer-coupled oscillator can equal or surpass every feature of the performance of any other circuit employing an equivalent tube and crystal. It is therefore regarded as a very desirable arrangement.

A transformer-coupled oscillator designed for broad-band untuned operation will operate over a band of 15 or 20 Mc with a relatively uniform power output of 200 mw and a crystal dissipation of 50 mw. An oscillator of this sort operating near 100 Mc with a plate voltage of 150 volts will have a frequency stability of about 0.1 ppm/v.

A similar oscillator adjusted for greater power output will have an untuned bandwidth of only a few Mc and a frequency stability of about 0.2 ppm/volt. However, with a crystal dissipation of 50 mw, the power output

will approach one watt.

3. The Grounded-Grid Oscillator.

The grounded-grid arrangement may employ either a triode or a pentode, and either one or two transformers. Crystal compensation is ordinarily desirable, but may be achieved economically by winding the cathode choke or transformer on the same form with the plate transformer.

The broad-band untuned form of this oscillator is capable of results closely comparable with those achieved with the transformer-coupled arrangement. Moreover, the plate transformer need not produce a phase reversal, and the cathode transformer reduces to a simple choke in most cases. Therefore the arrangement is very simple and compact.

The power output of the grounded-grid oscillator is markedly inferior to that of the transformer coupled circuit, especially at the lower frequencies where transit time loading is not serious. Therefore, this circuit is most useful where simplicity or broad-band operation is the principal requirement.

4. Impedance-Inverting Oscillators.

The circuits of this group employ a loss-free network having a 90° phase shift in conjunction with a series-mode crystal to produce an equivalent antiresonance. Such circuits are suitable for operation with a vacuum tube connected as a Pierce, Miller, or Transitron oscillator. The effective Q degradation, D, is quite small, and the impedance levels required for operation with typical tubes are comparable with those required in the transformer-coupled oscillator; therefore, the frequency stability which may be realized with this circuit is very good. In fact, the best frequency stability observed on this project was produced by a transitron impedance-inverting circuit. The power output of such oscillators is generally rather low, although the Miller arrangement is capable of a reasonable power output with tolerable crystal power. Probably the greatest disadvantage of these oscillators is the narrow frequency band of untuned operation.

5. Grounded-Plate Oscillator.

The grounded-plate circuit is similar in several respects to the grounded-grid arrangement. It requires but one transformer, which need have no phase reversal, and offers a simple means of crystal capacitance

compensation; however, the circuit does not have a favorable ratio of output to crystal power, and is difficult to adjust in class C operation. The principal importance of the grounded-plate arrangement is as the basis for electron-coupled oscillators in which the screen of a pentode is bypassed to ground. Such oscillators are useful because the load does not affect the frequency of operation, and because an appreciable output may be obtained at a harmonic of the operating frequency. At the present time the usefulness of frequency-multiplying oscillators is seriously restricted by the losses which are inherent in the construction of miniature pentodes; however, some relatively simple changes in these tubes would greatly improve this feature.

6. Other Circuits.

Multiple feedback-loop oscillators have been studied rather carefully, and are capable of excellent performance. However, they are difficult to adjust, and generally require more circuit elements than other circuits having comparable performance. They are therefore of very limited practical importance.

The transitron oscillator in which the suppressor and screen are coupled by a series-mode crystal may be regarded as a special case of the transformer-coupled oscillator. However, no phase reversal is required, and the transformers may be replaced by simple chokes if the crystal has a suitable high impedance. The resulting circuit, although quite simple, is capable of good frequency stability. It is analyzed in some detail in Chapter 16 because it illustrates one way of eliminating the effect of crystal holder capacitance.

D. Choice of Circuit.

The circumstances of use greatly affect the decision as to which circuit is best for a given situation. In particular, a considerable amount of design effort can be justified in a circuit which is to be reproduced in large numbers, particularly where economy of space and power consumption are important. On the other hand, an oscillator designed for a single special test should yield the desired operation with a minimum investment of engineering time; and economy of parts or power is of minor importance.

In situations where good frequency stability and moderate power output are desired, and maximum economy of space and components is required, the

grounded-grid oscillator is quite suitable. Where more power output is required or the grounded-grid arrangement leads to inconvenient element values, the transformer-coupled circuit is favored. It too affords a compact arrangement with few parts. Moreover, tubes which are suitable for this circuit are usually quite economical of plate and heater power.

The cathode-coupled oscillator is quite versatile and employs no mutual inductance. Because it is very simple to set up and adjust, it is particularly suitable for experimental work or in situations where a minimum amount of engineering is desirable. It has been widely used for measuring the resistance of crystal units.

Impedance-inverting oscillators are capable of excellent frequency stability and require a very small number of elements. However, the power output is low, the untuned bandwidth is small, and the upper frequency limit is about 100 Mc.

The electron-coupled grounded-plate oscillator is appropriate if output at a harmonic of the operating frequency is desired or if extreme isolation from the load is required. However, the power output which may be obtained at harmonic frequencies is low because of losses inherent in presently available tubes.

E. Remaining Problems.

Although the state of the art has advanced considerably since the beginning of this project, there are a number of remaining problems. Additional work is needed in connection with the improvement of units, tubes, other components, and circuits. Moreover, much work remains to be done in the measurement, and standardization specification of the properties of both circuits and crystals.

Among the remaining circuit problems is additional work on the control of a free-running oscillator by means of a crystal discriminator. Although some work was devoted to this problem during the project, no really promising approaches were discovered until it was too late to exploit them. It now appears that automatic frequency control may be produced in a system consisting of only a single-tube electrically-tuneable oscillator, a single-crystal discriminator and two germanium diodes. Such a system is sufficiently simple

Final Report Project No. 131-45

to warrant use in any situation where its frequency stability or power output is superior to that of a simple crystal oscillator.

Additional work remains to be done in simplifying and improving oscillators for the higher frequencies, particularly with a view to easy manufacture and field maintenance. Although the problems of adjustment and servicing were given serious consideration during this project, it is certain that many problems of this nature must be solved on the basis of actual field experience.

XX IDENTIFICATION OF TECHNICIANS

The personnel who have contributed time to this project are listed in alphabetical order in the following table:

William H. Bradley.	Research Assistant
William T. Clary.	Assistant Professor
Charles E. Durkee	Assistant Professor
William A. Edson.	Project Director
Donald W. Frazer.	Assistant Professor
James C. Hogg, Jr.	Assistant Professor
Stephen L. Johnston	Research Assistant
William B. Jones.	Assistant Professor
Howard L. McKinley.	Associate Professor

The background and qualifications of these men, along with the period of their service, is presented in the following paragraphs:

Mr. Bradley received training in the U. S. Army radar and radio schools, and has had extensive experience as a technician in design, assembly, and testing of electronic circuits. He had previously worked for other projects at this station, and was associated with this project on a full time basis during the period of November 1949 through June 1950.

Mr. Clary holds the M.S. in E. E. degree from the Georgia Institute of Technology. Except for the summer quarters of 1948, 1949 and 1950, he has contributed to this project on a part time basis during its entire duration. He has an excellent working knowledge of electronic circuit design, and has worked for the Naval Research, and Oak Ridge National Laboratories.

Mr. Durkee has served as an assistant project director on another project at this station and has the M.S. in E.E. degree from the Georgia School of Technology. He was employed on a full time basis by this project during the summer quarter of 1949.

Mr. Edson has served as project director during the term of this project, and previously as the director of a project on the Keying Properties of Quartz Crystal Oscillators. He received the degree of Doctor of Science in Electrical Communications at Harvard University in 1937, has been associated

with the Georgia Institute of Technology since 1945. He was formerly associated with the Bell Telephone Laboratories in New York. He is at present a member of the Subpanel On Frequency Control Devices of the RDB, and has an excellent practical and theoretical knowledge of crystal problems and electronic circuit design.

Mr. Frazer, who received the M.S. in E.E. degree from the Georgia Institute of Technology in 1948, has had considerable experience in the field of high frequency electronic circuits. He served for four years with the U. S. Navy as an Electronic Field Engineer, and was employed, on a part-time basis, by this project during the period of June 1948 through April 1950.

Mr. Hogg, who holds the M.S. in E.E. degree from the Georgia Institute of Technology, was associated with this project on a full-time basis during the period of June 1949 through December 1950. He was formerly associated with the Service and Research departments of the Sperry Syroscope Company, Inc., and has had considerable experience with high frequency circuits.

Mr. Johnston, who holds the degree of M.S. in E.E. from the Georgia Institute of Technology, was assigned to this project on a full-time basis during the period of November 1949 through January 1950.

Mr. Jones, who holds a M.S. in E.E. degree from the Georgia Institute of Technology, worked for this project on a part-time basis during the period of September 1948 through August 1949. He has had previous experience in circuit development with R. I. Sarbacher and Associates, then in Atlanta.

Mr. McKinley holds the degrees of Electrical Engineer and M.S. in E.E. In addition, he is licensed by the State of Georgia as a professional electrical engineer. He has considerable electronic circuit experience and served this project on a part-time basis from August 1948 through June 1950.

APPENDIX A

STABILITY OF CRYSTAL-CONTROLLED OSCILLATORS
METHODS OF DETERMINING

A. Introduction.

The frequency stability of a crystal-controlled oscillator is a quantity requiring definition. In the broadest sense, frequency stability is a measure of the deviation from some prescribed frequency, which may arise from any cause whatsoever, such as:

1. effect of temperature changes on crystal,
2. effect of temperature changes on circuit parameters,
3. aging of the crystal,
4. addition of capacitance due to proximity of foreign material,
5. changes in filament or plate voltages, or
6. change of tube parameters.

These items may be subdivided into two groups, (a) "long-term" causes, such as aging of the crystal and slow changes in mean temperature, and (b) "short-term" causes, such as rapid temperature changes, variation of parasitic capacitance, and changes of voltages.

In the present work, emphasis is placed upon the latter, the former being outside the scope of the project. The immediate purpose of this section is to show that the stability with respect to plate voltage has an adequate correlation with other values of stability.

B. Changes in Frequency as a Function of Variations in Plate Voltage.

Intuitive conclusions as to the stability of an oscillator are quickly reached by trained personnel operating the equipment. Factors such as the effect of body capacity produce frequency deviations indicative of the stability, but such factors do not lend themselves readily to measurement.

Fortunately, a convenient tool, which is easily controlled and measured, is available in the plate- (and screen-) voltage supply. Analytic determination of the effect of a change in plate voltage upon tube parameters (in a triode, for example) is difficult, particularly if the oscillator operates in a class C condition. Nonlinearity, inherent in this type of operation,

precludes a meaningful mathematical analysis. However, a number of useful facts are known. A decrease in plate voltage produces a marked change in transconductance and dynamic plate resistance, and tends to bring the operation closer to class A. Changes in density of the electron stream within the tube result in variations of the inter-electrode capacitances. In addition, changing the temperature of the tube may cause a change in the physical spacing of elements. It seems probable, also, that the decreased current flow through the crystal may cause a frequency change by reduction of temperature.

In this report the frequency stability expressed as parts per million per volt (ppm/v) has been consistently used as a criterion of performance. It remains to be shown by experimental procedures that this criterion is meaningful, in that other controllable causes of frequency deviation produce results consistent with predictions established by the criterion ppm/v.

C. Experimental Confirmation of Criterion.

In order to obtain experimental data which might serve to confirm the criterion, three separate oscillators of different basic types were used. Tables A.1, A.2, and A.3 present the results of tests conducted with the following:

1. a double-transformer coupled oscillator, sharply tuned at 70 Mc,
2. a grounded-plate oscillator, sharply tuned at 70 Mc, and
3. a broad-band grounded-grid oscillator, in the 70 Mc region.

TABLE A.1

FREQUENCY DEVIATION IN CYCLES OF A 70-MC TRANSFORMER-COUPLED CRYSTAL OSCILLATOR

Parameter Varied	Crystal No. 40	Crystal No. 270	Crystal No. 271
E_{bb} (30-volt change)	250	350	300
Crystal can shorted to chassis	140	out of oscillation	110
Tube shield added	30	60	45
Crystal shunted with 3 mmf	40	50	25
Plate coil shunted with 0.25 mmf	No oscillation

Final Report Project No. 131-45

TABLE A.2

FREQUENCY DEVIATION IN CYCLES OF A 70-MC
GROUNDED-PLATE CRYSTAL OSCILLATOR

Parameter Varied	Crystal No. 40	Crystal No. 270	Crystal No. 271
E_{bb} (30-volt change)	500	800	1000
Crystal can shorted to chassis	220	300	370
Tube shield added	200	260	600
Crystal shunted with 3 mmf	250	500	375
Plate coil shunted with 0.25 mmf	No oscillations

TABLE A.3

FREQUENCY DEVIATION IN CYCLES OF A 70-MC
GROUNDED-GRID CRYSTAL OSCILLATOR

	Crystal No. 40	Crystal No. 41	Crystal No. 250
Tube No. 1. E_{bb} (30-volt change)	400	500	220
Tube No. 2. E_{bb} (30-volt change)	300	400	160
Tube shield added	15	50	20
Plate coil shunted with 0.5 mmf	300	600	340

D. Conclusions.

With but one or two minor exceptions, the deviation in frequency as a result of variation of parameters was consistent in magnitude with that predicted by the plate-voltage criterion, ppm/volt.

This is important because it shows that the convenient plate-voltage criterion may be relied upon as a significant measure of the frequency stability of these circuits. This fact serves to expedite stability tests, which otherwise might be cumbersome and time consuming.

APPENDIX B

CONSERVATION OF BAND WIDTH AND LOW PASS TO BAND PASS TRANSFORMATION

The low pass to band pass transformation has, among others, a property of importance related to band widths. The bandwidth, in cycles, over which the impedance or admittance of the branch stays within prescribed limits is unchanged. This principle may be illustrated by the following simple example involving a single condenser and its antiresonant analog.

Let b be the susceptance of a capacitor in the low pass structure, and b_o its susceptance at the point ω_o for which $b_o = \omega_o C$. In the anti-resonated band pass, the corresponding susceptance will be:

$$b = \omega C = 1/\omega L \text{ or } \omega b = \omega^2 C = 1/L . \quad (1)$$

b will assume the values $\pm b_o$ at two points on opposite sides of the band. These points may be indicated by ω_2 and ω_1 , then equation (1) becomes

$$\omega_2 b_o = \omega_2^2 C = 1/L \quad (2)$$

$$\omega_1 b_o = \omega_1^2 C = 1/L . \quad (3)$$

Their difference is

$$(\omega_2^2 - \omega_1^2) C = (\omega_2 + \omega_1) b_o = (\omega_2 + \omega_1) \omega_o C , \quad (4)$$

or

$$\omega_2 - \omega_1 = \omega_o . \quad (5)$$

It is thus seen that the frequency interval between corresponding points in the band pass structure is the same as the positive frequency interval in the low pass structure.

Bode¹ on page 213 generalizes this principle to the theorem on the conservation of band width:

"The width of the frequency band, in cycles over which a given response can be maintained in a circuit of given general configuration containing prescribed series inductances and shunt capacitances is independent of the location of the band in the spectrum."

This property and theorem have been applied in the basic consideration of band widths of networks used in oscillators described in this paper. In

most cases a low pass structure of a desired band with was analytically produced; it was then transformed into a band pass structure with corresponding band width. This transformation is made by resonating each inductance of the low pass structure with a series condenser and by antiresonating each capacity of the low pass system with a shunt inductance at the desired center frequency.

BIBLIOGRAPHY

1. Bode, H. W., Network Analysis and Feedback Amplifier Design. D. Van Nostrand and Co., Inc., New York, 1945.